Tidal inlets on littoral drift shores

September 1999 Maurice J. de Haas

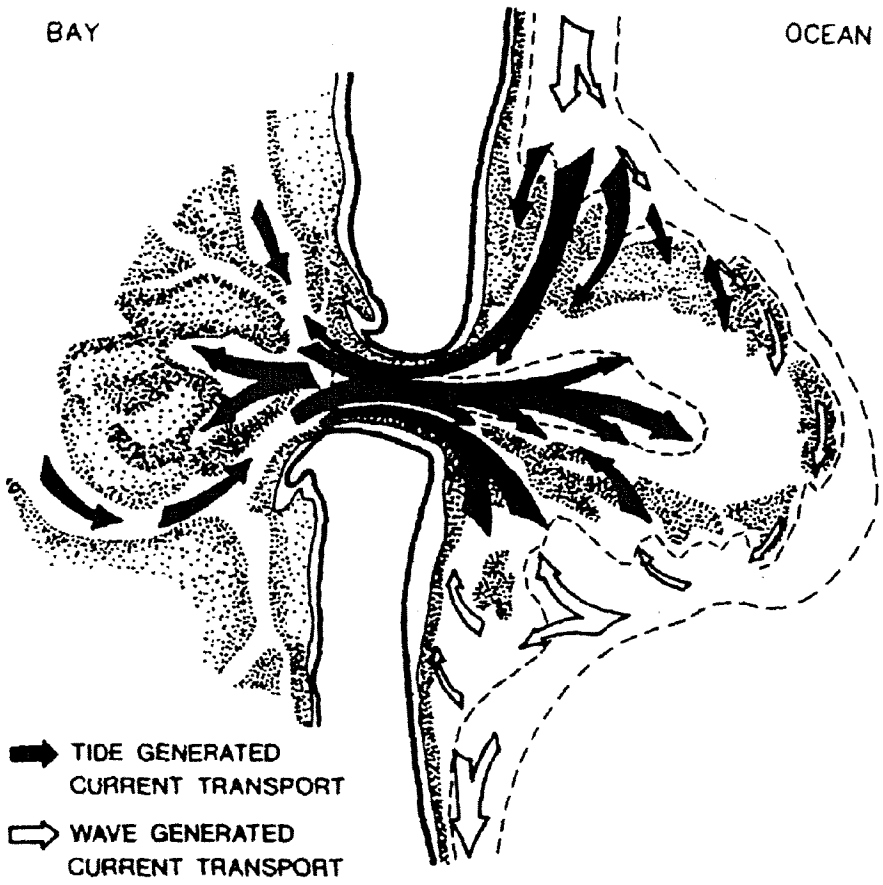

Volume I

TU Delft
Technische Universiteit Delft
Faculteit der Civiele Techniek

Notations

A_b	Surface area of the basin	[m^2]
A_c	Cross-sectional area of tidal inlets	[m^2]
A_d	Deposition area	[m^2]
a_0	Ocean tidal amplitude	[m]
a_{s0}	Spring ocean amplitude	[m]
a_b	Bay tidal amplitude	[m]
b	Cross-sectional width at water level h	[m]
b_c	Mean sea level width of a cross-section	[m]
B	Dimensionless damping coefficient	[-]
C	Chezy Coefficient	[$m^{1/2}/s$]
D_x	Sediment particle grain diameter	[m]
d_a	Average depth in the cross-sectional area of the inlet throat	[m]
d_m	Maximum depth in the cross-section of the inlet throat	[m]
d_c	Shallowest depth in the cross-section of the inlet throat	[m]
E	Phase lag basin tide	[-°]
E_s	Stratification parameter	[-]
f	Darcy-Weisbach friction coefficient coefficient	[-]
f_c	Friction factor due to currents	[-]
f_w	Friction factor due to waves	[-]
f_{cw}	Wave-current friction factor	[-]
F	Friction factor	[-]
Fr	Froude number	[-]
h	Water depth	[m]
h_b	Depth of the inlet basin	[m]
H	Wave height	[m]
H_w	Wave height at breaker line	[m]
H_{rms}	Root mean square value of waves	[m]
H_0	Deep water wave height	[m]
G	Dimensionless tidal frequency	[-]
g	Gravitational acceleration	[m/s^2]
k	Wave number	[rad/m]
k_s	Hydraulic roughness	[m]
k_{sg}	Grain roughness	[m]
$k_{s\Delta}$	Bed-form roughness	[m]
K_{en}	Coefficient for entrance losses	[-]
K_{ex}	Coefficient for exit losses	[-]
K(t)	Repletion coefficient	[-]
K2(t)	Inertia coefficient	[-]
L	Wave length	[m]
L_c	Inlet length	[m]
L_b	Length of the inlet basin	[m]
M_{predom} [m^3/yr]	Predominant annual littoral drift	
M_{total}	Total annual littoral drift	[m^3/yr]
M_s	Total of material transported by the inlet gorge	[m^3]
m	Sum of exit and entrance losses	[-]
N	Tidal amplitude inside basin/ocean tidal amplitude	[-]
P	Spring tidal prism	[m^3/half tidal cycle; ft^3/ half tidal cycle]
p_a	Atmospheric pressure at sea level	[mbar/hpa]

$Q(t)$	Discharge through the inlet	$[m^3]$
Q_{max}	Maximum inlet discharge	$[m^3/s]$
Q_{river}	River discharges	$[m^3/s]$
R	Hydraulic radius	[m]
S	Sedimentation	$[m^3]$
$\partial S(t)$	Annual sedimentation	$[m^3]$
$\partial S(t=0)$	Initial sedimentation	$[m^3]$
s	Side slope at mean sea level	[-]
t	Time	[s]
T	Wave period	[s]
T_{tide}	Tidal period	[sec]
TV	Tidal volume	$[m^3]$
V	Depth average current velocity	[m/s]
V_s	Stratification parameter	[-]
V_t	Combined wave current velocity over the bottom	[m/s]
V_{wb}	Near-bed current velocity	[m/s]
V_{cb}	Near-bed orbital velocity	[m/s]
V_{mean}	Mean velocity over half tidal cycle	[m/s]
$V_{mean\ max}$	Mean velocity over the cross-sectional area and maximum velocity during spring tide conditions	[m/s]
$V`_{max}$	Dimensionless inlet velocity	[-]
V_{max}	Maximum inlet velocity	[m/s]
V_{cr}	Critical velocity	[m/s]
$\partial V(t=0)$	New longterm equilibrium situation	$[m^3]$
W	Width of the entrance	[m]
z_a	Static rise of the mean sea water level	[m]
α	Ratio relative effect of waves and tidal currents	[-]
$\tan\alpha$	Slope nearshore zone	[-]
β	Damping coefficient for the first overtide	[-]
γ_{break}	Breaker index	[-]
τ_s	Shear stress	$[N/m^2]$
τ_{cr}	Critical shear stress	$[N/m^2]$
ω	Frequency of the ocean tide	[rad]
Δ_h	Average bed-form height	[m]
Δ_l	Average bed-form length	[m]
θ	Angle between the current and the wave direction	[-°]
ϕ	Parameter to indicate grain dimensions	[-]
$\eta_0(t)$	Ocean tide	[m]
η_{max}	Wave induced set-up	[m]
$\eta_b(t)$	Basin tide	[m]
ρ_w	Density of water	$[kg/m^3]$
ρ_s	Density of sediment	$[kg/m^3]$
Ω	Helmholz frequency	[Hz]

List of figures

Volume I: Tidal inlets on littoral drift shores

List of figures chapter 1

List of figures chapter 2

List of figures chapter 3

List of figures chapter 4

List of figures chapter 5

Preface *(Volume I and II)*

In order to graduate as a Civil engineer from the Delft University of Technology in the Netherlands, it was necessary to choose a graduation project. By being in close contact with Professor Kamphuis, I was able to acquire general information on a project in Australia. Although the amount of research needed to successfully complete the quantitative analyses for this project, exceeds the mandatory time that stands for graduating, it was only possible to finish up specific parts of the project. After consulting the "Department of Environment" in Australia it was suggested to me to concentrate on the part which qualitatively studies tidal inlets on littoral drift shores along the Gold Coast Seaway.

The final report consists of two parts: Volume I and Volume II.
Volume I is a general study on Tidal inlets and Littoral Drift shores, to attain important theoretical information before part of the analyses can be carried out. By accumulating the information in Volume I, it later (in Volume II) allows us to obtain a better understanding on the hydrodynamic and morphological processes involved around the Nerang River Entrance and the Gold Coast Seaway.

Readers guide *(Volume I and II)*

In Volume I special attention will be paid to Tidal Inlets on Littoral Drift Shores in general. Section 1 gives general information about the appearance and origin of tidal inlets. Also the most important morphodynamic parts of a tidal inlet will be discussed. Section 2 discusses the hydrodynamic impact on tidal inlets due to waves, currents, severe weather conditions and of course astronomical tides. In section 3 some considerations are discussed on the development of tidal inlets. (morphodynamic) These developments are generally a result of the hydrodynamic active forces, discussed in section 2. Section 4 discusses the stability of tidal inlets. In literature, stability of tidal inlets is mostly discussed in terms of empirical relations. The emphasis in Volume I is not on discussing formulas or advanced computation techniques, but on the qualitative description of the very dynamic interaction of tidal inlets with the active hydrodynamic forces. Section 4 gives a few of the most common and most used stability relations. In this section also some background information is given on these specific stability relations. Special attention will be paid to the stability concept originally developed by Escoffier (1940). This theory gives rather good insight in the behaviour and development of tidal inlets. With the use of this theory the reader is able to get a good first impression of the relevant processes at work. Also special attention will be paid on the stability concept developed by Bruun (1978). Section 5 discusses some important methods for improvement of unstable tidal inlets.

Volume II describes the case of the stabilised Nerang River Entrance (Gold Coast Seaway). In section 1 the historical behaviour of the Nerang Entrance is described and partly evaluated with the use of some theory described in Volume I. Section 2 describes the hydrodynamic components active on the Gold Coast area in general. Section 3 discusses the most important conclusions of model tests, which were carried out by the Delft Hydraulics Laboratory. These model tests are used in this report as a reference in order to evaluate some hypotheses about the behaviour of the stabilised Nerang River Entrance (Gold Coast Seaway) over a period of ten years after the commencement of the project. However the most interesting part of this case study is the impact of the sand bypass installation on the morphology of the Gold Coast Seaway over the last ten years. This is discussed in section 4. In this section the available information which was collected over the past ten years is analysed. The emphasis in this

section is the impact of the sand bypass installation on the adjacent beaches and the development of the ebb tidal delta, over the first ten years of operation. And last but not least some considerations are given about the possible morphological developments in the future.

Graduation committee:
Prof.Dr.Ir. J.W. Kamphuis
Dr.Ir. J. van de Graaff
Dr.Ir. J.A.Roelvink
Ir. P. Huisman

The Hague, September 1999

Maurice J. de Haas

Summary

After consulting the "Department of Environment" in Australia it was suggested that an extensive generic study about Tidal Inlets on Littoral drift shores gives them an insight in the processes at work and also the possibilities to improve the stability in order to make tidal inlets suitable for safe navigation. This report describes the most important issues related to tidal inlets on littoral drift shores in general. It is written with the intention to provide some general information to readers who are interested in tidal inlets in general. However this report also provides some specific information to be able to study the stabilisation of the Nerang River Entrance, Queensland Australia.

The term tidal inlet is generally used to describe the narrow waterway that connects a tidal basin with the ocean and through which reversing tidal flows are concentrated. Tidal inlets on littoral drift shores appear all over the world. In most cases they provide a passage from the ocean to a lagoon. For tidal inlets in highly developed areas it is important that safe navigation for vessels is possible. Therefore inlets can be an impulse to harbour activities and/or the tourist industry.

Tidal inlets with a littoral drift origin can be split up in two main groups:

- Breakthrough of a barrier coast
- The non-closure of a spit

Tidal inlets that are created by the non-closure of a spit are in general more favourable for navigation. In these cases the tidal currents through the entrance are strong enough to flush the channel. Inlets who are created by the breakthrough of a barrier coast as a result of a major meteorological event are more likely to close by the littoral drift.

In general a tidal inlet consists of three major morphological units:

- The ebb tidal delta
- The main entrance channel (tidal gorge and entrance channel)
- The flood tidal delta (bay or lagoon section)

The inlets ebb tidal delta is the shallow section on the seaside. Tidal inlets naturally built these ebb deltas in order to create or to re-establish a dynamic equilibrium. These ebb deltas can be seen as a naturally built bridge to bypass littoral drift across the entrance. Ebb deltas can be dangerous for navigation because they locally reduce the depth in front of the inlet. The latter is also true for the main entrance channel. The main entrance channel is the connection between the ebb tidal delta and the flood tidal delta. It is obvious that the main entrance channel must provide sufficient depth for safe passage by vessels. The flood tidal delta can be seen as the interior section of the tidal inlet. Save passage of this part of the inlet is possible when stable channels with sufficient depth are present. The presence, development and stability of these specific morphological sections are highly determined by the hydrodynamic parameters acting on them.

Inlet hydrodynamics must be seen as a combination of water level variations, currents and waves. Inlet hydrodynamic characteristics are the driving forces for sediment transport patterns and depositions. So it is important to have a clear picture of the hydrodynamics near inlets. The most important hydrodynamic forces on tidal inlets delta are the combined effect of astronomical tide and waves. Astronomical tide in general is responsible for the

development and stability of the main entrance channel while waves determine the magnitude of littoral drift and also the dimensions and shape of the ebb tidal delta.

The dynamic behaviour of the three morphological units is defined as inlet stability. Stability must be interpreted as dynamic stability. The morphological sections involved attempt to maintain a situation of relatively small changes for a significant amount of time. If this is the case than the tidal inlet can be called stable. In terms of stability the following distinction can be made.

- Location stability: Stability of tidal channels and inlets with respect to their location.
- Cross-sectional stability: Stability of geographical dimensions of morphologic units, primarily described with empirical relations.

Several investigators have studied the dynamic stability of tidal inlets. Bruun(1978) defined the widely used stability parameter [r]. Escoffier(1940) developed a theory to investigate the cross-sectional stability of tidal inlets.

Man-made structures (jetties) or human interference (dredging) can be used to improve the stability of tidal inlets. A relatively new way of stabilising inlets is a combination of jetties and mechanical bypassing of the littoral drift across the entrance channel. This way of stabilising inlets is used in the case of the Nerang River Entrance. The impact on the inlet morphology is described in Volume II: "Nerang River Entrance Stabilisation (Gold Coast Seaway)".

1. Introduction tidal inlets on littoral drift shores

1.1. Introduction

1.1.1. General description

Tidal inlets on littoral drift shores appear all over the world. Some of these are studied in detail especially those along the USA coast. Reason for this is the increasing importance of tidal inlets. A stable inlet makes safe navigation possible for vessels and can be an impulse to the tourist industry.

There are several definitions for tidal inlets found in literature. Steijn (1991) described the definitions used by Bruun and Gerritsen (1960) and also Escoffier (1940). They define tidal inlets as: "The short waterway connection between the sea and a bay, a lagoon, or a river entrance through which tidal and other currents flow". For the present study the definition described by Huis in `t Veld et al. (1987) is followed: "The term tidal inlet is generally used to describe the narrow waterway that connects a tidal basin with the ocean and through which reversing tidal flows are concentrated". The basic difference between a tidal inlet and estuaries or river mouth deltas is that the width of the tidal inlet entrance is usually small with respect to the typical size of the interior basin and that tidal inlets partly reflect long wave energy (Steijn, 1991). In general tidal inlets can be split up in three main groups (Bruun, 1978):

- Tidal inlets with a geological origin
- Tidal inlets with a hydrological origin
- Tidal inlets with a littoral drift origin

Examples of inlets with a geological origin are the fjords in Norway and San Francisco Bay. Such inlets have rocky entrance channels and a non-alluvial bottom. Inlets with a predominantly hydrological origin are formed where rivers enter the ocean, and the tidal currents can penetrate through the river mouth and make contributions to their geometry. Examples are the Western Scheldt and the river Mersey (Bruun, 1978). In this report only the tidal inlets with a predominant littoral drift origin are discussed. Tidal inlets with a littoral drift origin can be split up in two main groups:

- Breakthrough of a barrier coast
- The non-closure of a spit

After a tidal inlet is formed it starts to develop by the active hydraulic forces. These forces introduce sediment transport in- and outside inlets. Some time after creation of a new inlet, it starts to develop towards a dynamic equilibrium. The dynamic equilibrium of a tidal inlet depends highly on the ability of the inlet to bypass the littoral drift naturally. According Bruun and Gerritsen (1960) some tidal inlets migrate towards a more suitable location where the conditions to bypass sediment naturally are better. This migration of the inlet is dangerous for navigation because of the ever-changing conditions of the inlet entrance. In terms of navigation tidal inlets formed by a spit formation are more favourable for navigation than inlets created by breakthroughs. This is caused by the fact that relatively higher velocities

Figure 1.1: The Virginia barrier islands

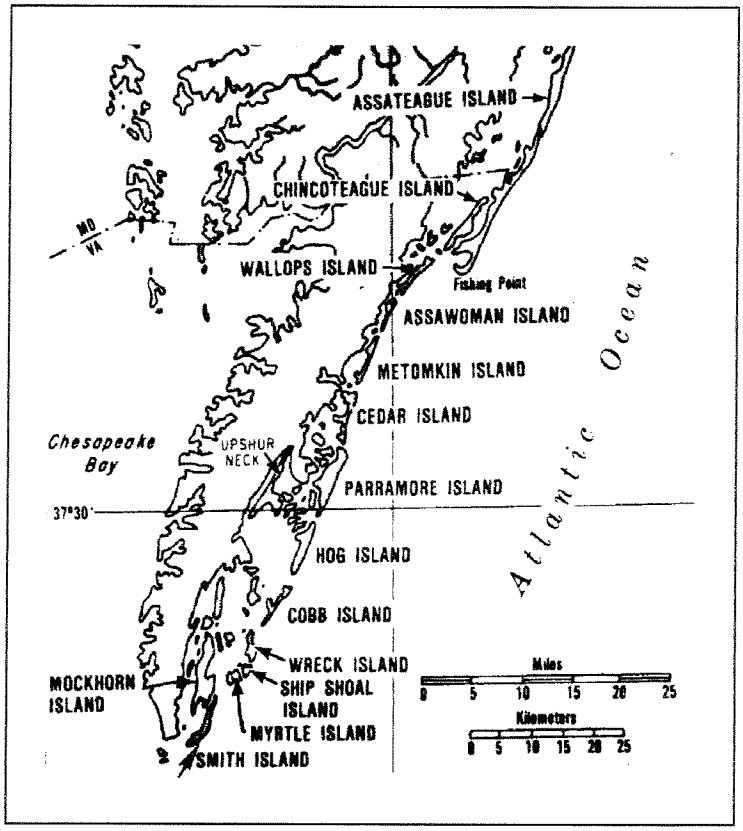

(From: Coastal Stabilization, Silvester and Hsu, 1993)

Figure 1.2: Formation of a barrier system

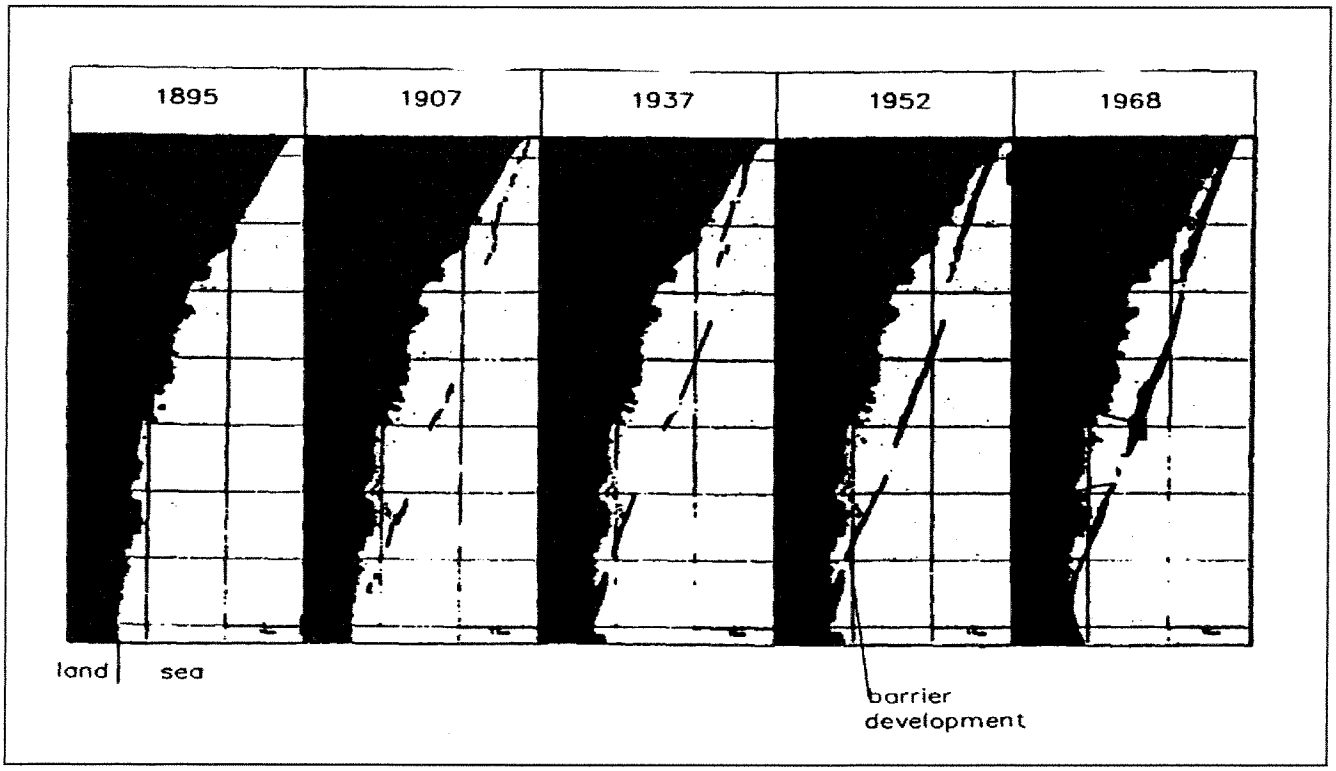

(From: Steijn, 1991 after: Christiansen, e.a., 1985)

occur during the narrowing of the cross-section resulting in a stable and wider cross-section (Bruun, 1978).

In general a tidal inlet consists of three major morphological units:

- The ebb tidal delta (shallow section on the seaside)
- The main entrance channel (tidal gorge and entrance channel)
- The flood tidal delta (bay or lagoon section)

The ebb tidal delta is the morphological unit on the ocean side of a tidal inlet and consists of broad shoals of sediment mainly deposited by the ebb current when it reduces velocity as it spreads out into the sea. The entrance channel is the intermediate section between the ebb tidal delta and the gorge channel. The tidal gorge channel is the most narrow and deepest part of the tidal inlet and connects the entrance channel with the ocean on one side and on the other side a bay or lagoon.

1.1.2. Breakthrough of a barrier coast

Tidal inlets are mostly located on barrier beaches. About ten percent of the total world's coastline consists of barrier coasts; one third of them are located along the North American coasts. Barrier beaches are accumulations of sand of limited width, which stretch lengthwise along the coast. They either partially or fully enclose bodies of water between them and the mainland. During severe storms these barrier islands provide protection for the mainland by absorbing wave attack. Barrier formation is a continuing process and is best described by the "bulldozer mechanism". It means that sediment is transported onshore, by the continued action of waves and tides. Barriers can form when there is sufficient supply of beach material from offshore, and the bottom bathymetry is such that the waves break at some distance from the coast, because of a broad shallow foreshore zone. A barrier will form at the outer edge of this shallow zone where the waves break; the supply of sand will eventually build up a berm, isolated from shore, which becomes the barrier (Van Loo, 1976). An example of a barrier beach formation is shown in Figure 1.1. Figure 1.2 shows the formation of a barrier system along the coast of Denmark over the last century. A barrier coast can also be created by spit formation (section 1.1.3.).

Hydraulic gradients across barrier island occur because water levels at either side of the barrier are determined by separate, but not independent, physical settings. A breakthrough of barrier coasts is caused when these hydraulic gradients become too large. According to Steijn (1991) these hydraulic gradients are induced as follows:

- ***From the seaside*:** Storm surges. Numerous smaller unstable inlets are created while under more average conditions; the littoral drift will close them. The gradients are induced by washovers of breaking waves and sea level changes.
- ***From the lagoon side***: River discharges.
- ***From the barrier side*:** Human interference by dredging an inlet.

Tidal inlets on barrier coasts (as a result of a breakthrough) may appear more or less in groups. This can be explained by the fact that the inlet traps large amounts of littoral drift. When another breakthrough appears on the downdrift side of this inlet, less littoral drift is

Figure 1.3: South shore of Long Island, New York, showing closed, partially closed, and open inlets.

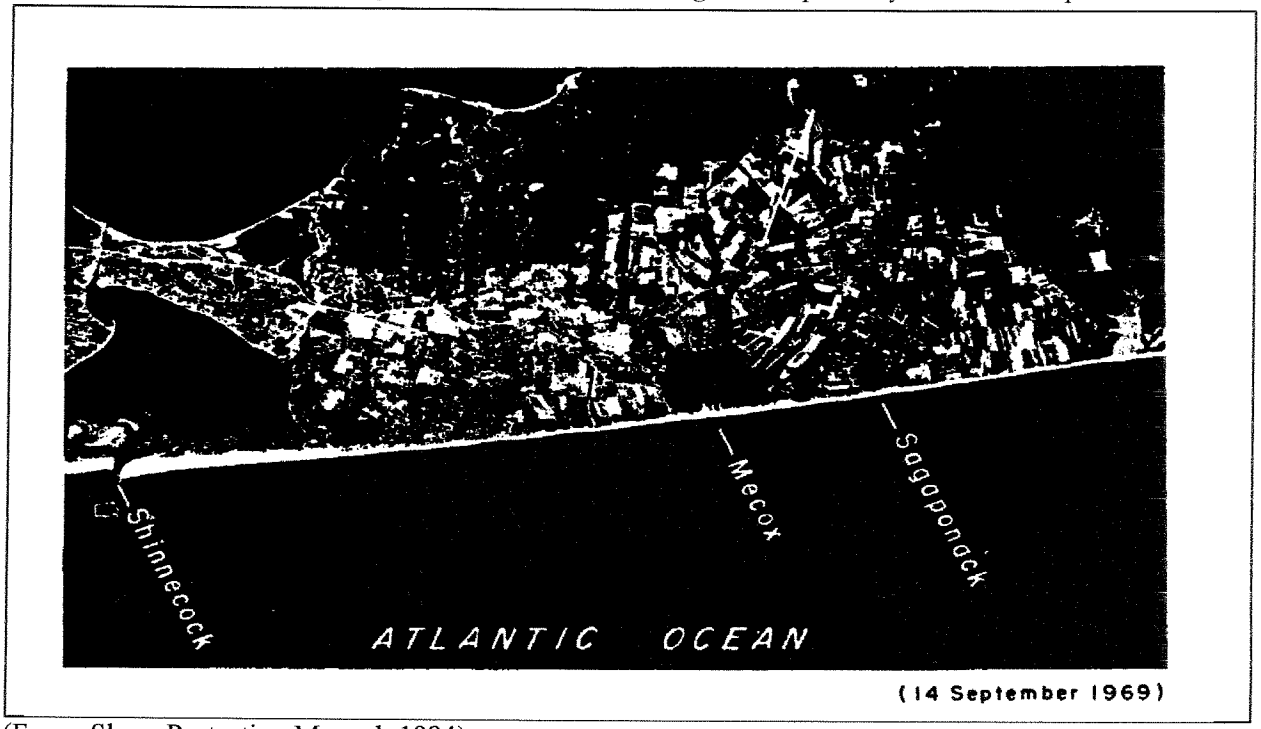

(From: Shore Protection Manual, 1984)

Figure 1.4: Refraction taking place at the end of a spit

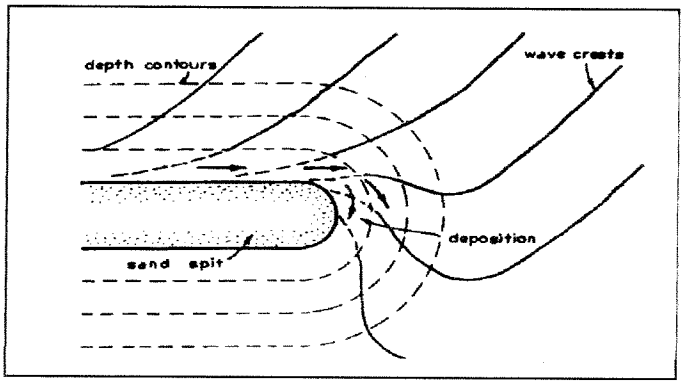

(From: Coastal Stabilization, Silvester and Hsu, 1993)

Figure 1.5: Survey map of Matagorda Bay

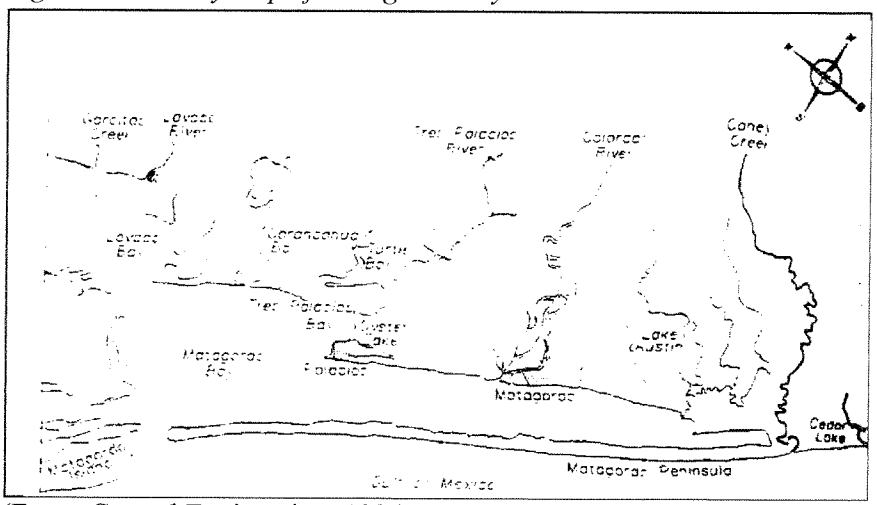

(From: Coastal Engineering, 1996)

available for silting up the new gap. A breakthrough in a barrier beach will stay open when sufficient tidal current keeps the opening from silting up. The smaller more unstable inlets will migrate or be closed by littoral drift. The size of the inlet opening depends mainly on the tidal prism (amount of water that flows through the inlet per half tidal cycle) which on its turn is dependent on the basin area. Assuming a uniformly fluctuating basin water level, the amount of water flowing in per half tidal cycle is smaller when the basin area is smaller. The Shore Protection Manual (1984) shows an excellent example of this. This is shown in Figure 1.3. Along the South shore of Long Island, New York there are three lagoons formed by a breakthrough. The smallest one is fully choked by the littoral drift. (Sagaponack), the second somewhat larger lagoon (Mecox) is partly open. The largest of the three (Shinnecock Bay) is connected to the ocean and sufficient for navigation.

1.1.3. The non-closure of a spit

A barrier coast can also be created by wave induced longshore transport of sediment. A spit migrates under longshore sediment supply mostly in the same direction as the longshore transport. At the end of the spit sedimentation takes place because of a decreasing sediment transport capacity. This is caused by the fact that waves no longer break at the deeper outer parts of the spit (Van Loo, 1976) and the refraction of waves at the spits end which may result in deposition of sediment as shown in Figure 1.4. When a spit grows towards the mainland, narrowing of the entrance takes place. If the tidal currents are strong enough the narrow gap remains open and a tidal inlet is born. Figure 1.5 gives an example of a tidal inlet created by the non-closure of a spit. During the spit formation several small breakthroughs may occur during storm surges, but they will silt up quickly. A severe storm may result in excessive amounts of sand deposited in the (small) entrance channel reducing its cross-section. When flow through the entrance channel is unable to keep it free from deposits, it will shoal very quickly and eventually close.

1.2. Classification of tidal inlets

1.2.1. Introduction

Classification of tidal inlets can give some insight in the present appearance, the behaviour of tidal inlets in the past and can be of use to predict the developments in future. Also the relative importance of the different processes acting on tidal inlets can be estimated. According to Steijn (1991) the classification of tidal inlets provides a tool to:

- Analyse the system and detect the parameters representative to the processes at work.
- Compare a specific situation with similar situations.

By comparing a specific situation to another, it is possible to provide an initial understanding of this new situation and allows a decent first hand estimate to be made, before further analyses can be carried out. This is especially helpful for those locations where little or no data is available.

Steijn (1991) states that tidal inlets can be classified by:

- *Geometric parameters,* which focus primarily on the appearance, or morphology, of an inlet.

Figure 1.6: Four types of inlet configurations

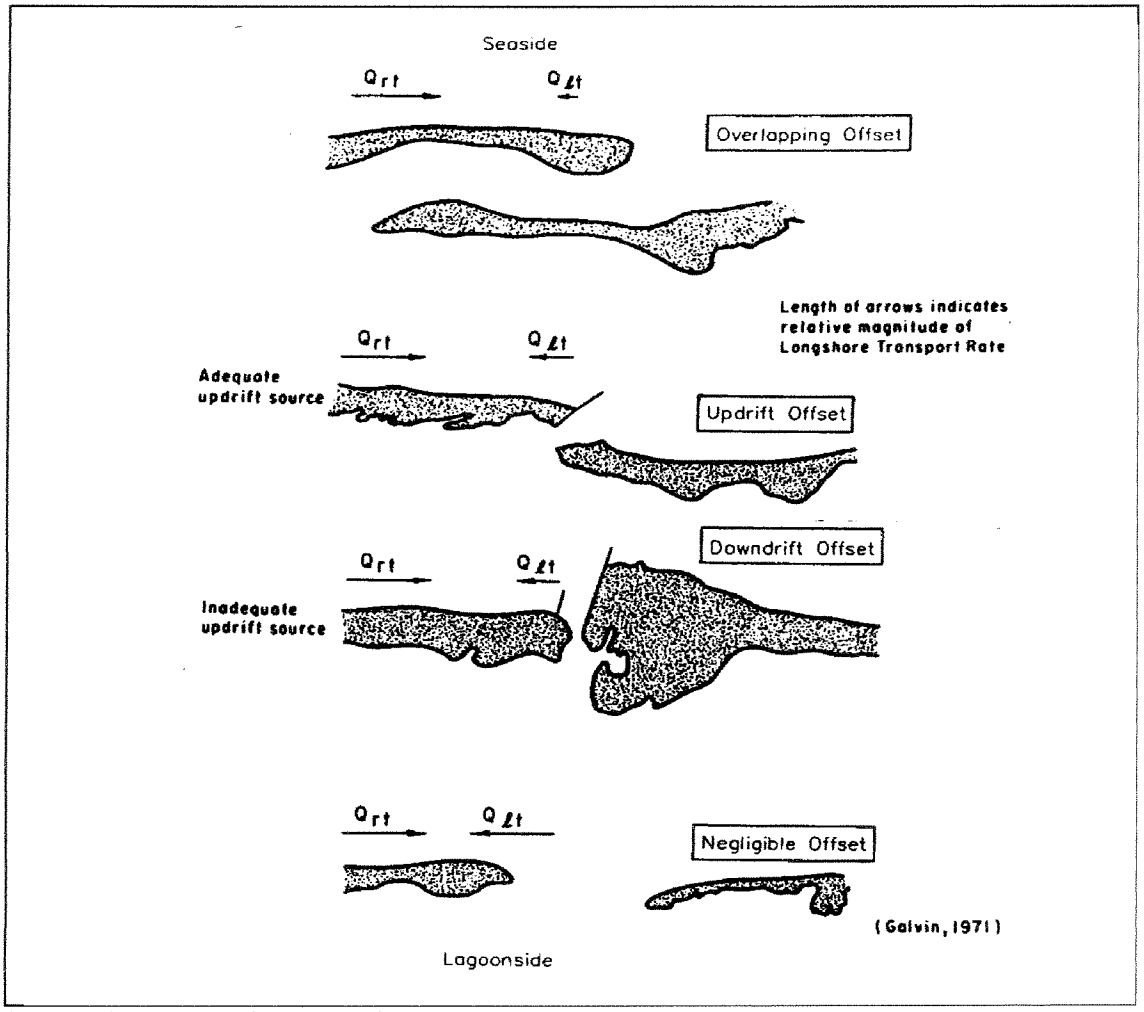

(From: Shore Protection Manual, 1984)

- *Hydraulic parameters,* on the other hand solely focus on the underlying physical processes.

1.2.2. Geometric classification

Geometrical classification seems a questionable way of sorting inlets, because it does not relate the underlying physical processes to the observed general behaviour. If on the other hand little or no information is available, it might be the only way to get some information (Steijn, 1991).

Reference is made to Steijn (1991) for geometric classification by various authors: Bruun and Gerritsen (1960) and Niemeyer (1990). According to Steijn these latter methods of classification are hardly applicable in actual practice and therefore not described here.

The Shore Protection Manual (1984) describes a geometrical classification, which considers the shape of the shoreline configuration of the barrier islands, resulting in detailed studies on inlets along the USA Atlantic and Gulf coasts. Figure 1.6 shows the four types of inlet configurations. Steijn (1991) sorts the offsets as follows:

- *Overlapping offset* where the updrift coast overlaps the inlet due to a seaward and downdrift extension. This configuration can develop where there is a large littoral drift and strong tidal current to maintain the inlet. This is the case for large bays in combination with large vertical tide. According to Bruun (1978) this offset is the most common for inlets with barrier spits.

- *Offset on updrift side:* This is the case when there is a significant littoral drift opposite to the predominant drift.

- *Offset on downdrift side:* In this case the littoral drift is rather small. According to Bruun (1978): "The explanation of this may sometimes be of geological nature, but quite obviously it is mostly the result of a combination of a strong longshore current and the influence of the channel geometry". The ebb currents are interfering with the wave action resulting in a local reversal of the drift causing a shoal on the downdrift side of the inlet.

- *Negligible offset,* where the offset is less than the minimum width of the inlet. These situations occur where the net littoral drift is very small.

Classifying inlets may not be an immediate solution to a numerical problem, but allows a qualitative perspective on a specific unknown situation.

1.2.3. Hydrodynamic classification

The advantage of using hydraulic parameters in classifying tidal inlets is to give information on processes involved regardless of the configuration of tidal inlets. In other words hydraulic parameters can be seen as independent boundary conditions. These conditions are better parameters for classification purposes (Steijn, 1991). The hydraulic parameters used for hydrodynamic classification are tides and waves. Both are independent, in their origin, of the tidal inlet system configuration and therefore suitable for classification. Tidal range outside the tidal inlet depends on the ocean tide, and its interaction with the continental shelf. The waves acting on tidal inlets are generated by a storm on the ocean far away (swell) or locally (local Wind Sea). As will be pointed out later, both tides and waves are essential for the development and stabilisation of tidal inlets.

Figure 1.7: Detailed inlet classification

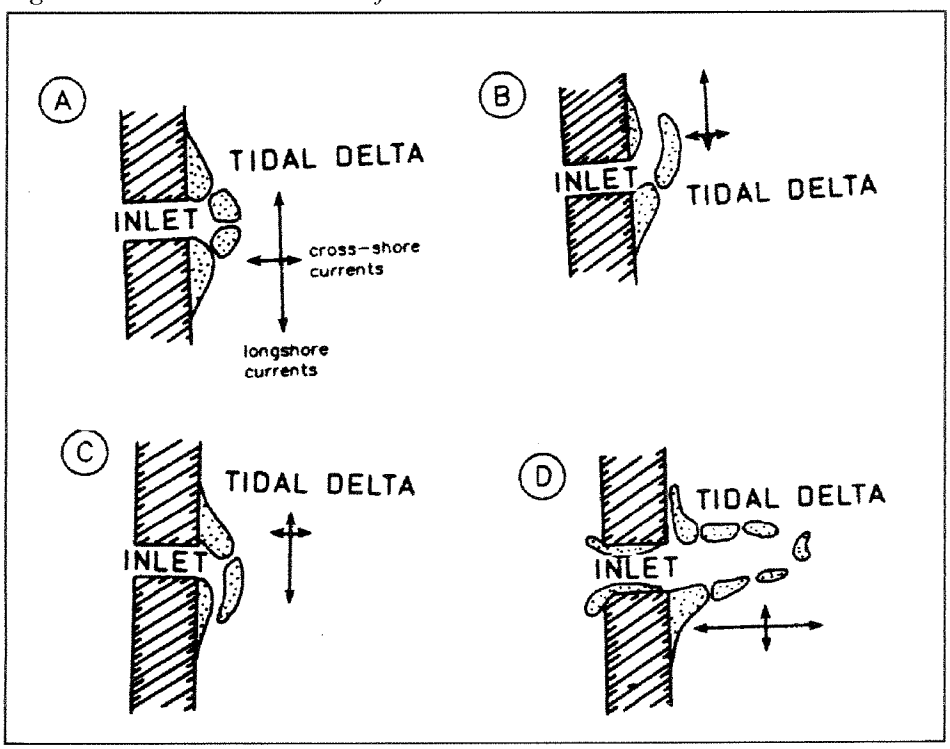

(From: Oertel, 1988)

Water level variations by astronomical tides are mainly responsible for current patterns in- and outside tidal inlets. When water levels fluctuate on the ocean side, they are responsible for hydraulic gradients over the entrance of the channel. This gradient causes a driving force, which is responsible for either a flow from the inside out or a flow from the outside in, depending on the direction of force. This force is an important factor in the development and stability of tidal inlets

Huis in `t Veld et al. (1984) classified the tidal range as follows:

- Micro-tidal, tidal range: < 1,0 m
- Low meso-tidal, tidal range: 1,0 - 2,0 m
- High meso-tidal, tidal range: 2,0 - 3,5 m
- Low macro-tidal, tidal range: 3,5 - 5,5 m
- High macro-tidal, tidal range: > 5,5 m

Waves have a significant influence on the morphology of tidal inlets. In general the action is the limiting factor for the growth of the ebb tidal delta. Waves have a very important influence on the sediment transport patterns. This is especially true for those waves that are capable of penetrating the entrance of the channel into the flood tidal delta. The wave climate is generally characterised by the mean significant wave height H_S which is based on a yearly average:

- Low wave energy: $H_S < 0,6$ m;
- Medium wave energy: $0,6 \text{ m} < H_S < 1,5$ m;
- High wave energy: $H_S > 1,5$ m

The actual development of inlets is based on the combination of the tidal ranges and wave energies. It is therefore important to relate waves to the tides on inlets and classify the parameters in a proper manner.

Oertel (1975) combined the relative impact of these two major components by classifying tidal inlets as tide dominated, wave dominated and transitional. The tide dominated inlet shows a deep main entrance channel which results from the relatively large tidal ranges. Shoals develop along the channel by the blocking of the (low) littoral drift by the ebb tidal flow. The wave dominated tidal inlet shows large amounts of suspended sediment due to the wave action, and several smaller breakthroughs, which will eventually close up by the littoral drift. The transitional tidal inlet develops more channels through the barrier. A significant littoral drift results in shoals on the flood tidal delta, where the sediment is transported into the basin by the flood currents. A submerged bar develops on the ebb tidal delta.

Several other investigators have described a more detailed classification. Classifying in detail is basically looking at specific parts of tidal inlets of for example the ebb tidal delta. A detailed classification based on flood tidal delta development is almost impossible due to the fact that the transport of sediment patterns and morphology inside tidal basins are a very complicated process and differ significantly for each individual tidal inlet even if they are located on the same beach within a few kilometres. Steijn (1991) described the more detailed classifications of tidal inlets given by Oertel (1975, 1988) and Sha (1990). Oertel (1988) gives a detail-classification of ebb tidal deltas of tide dominated inlets as a function of the ratio between the cross-shore flow velocities and the longshore flow velocities as illustrated in Figure 1.7.

Figure 1.8: Qualitative classification of the ebb tidal delta

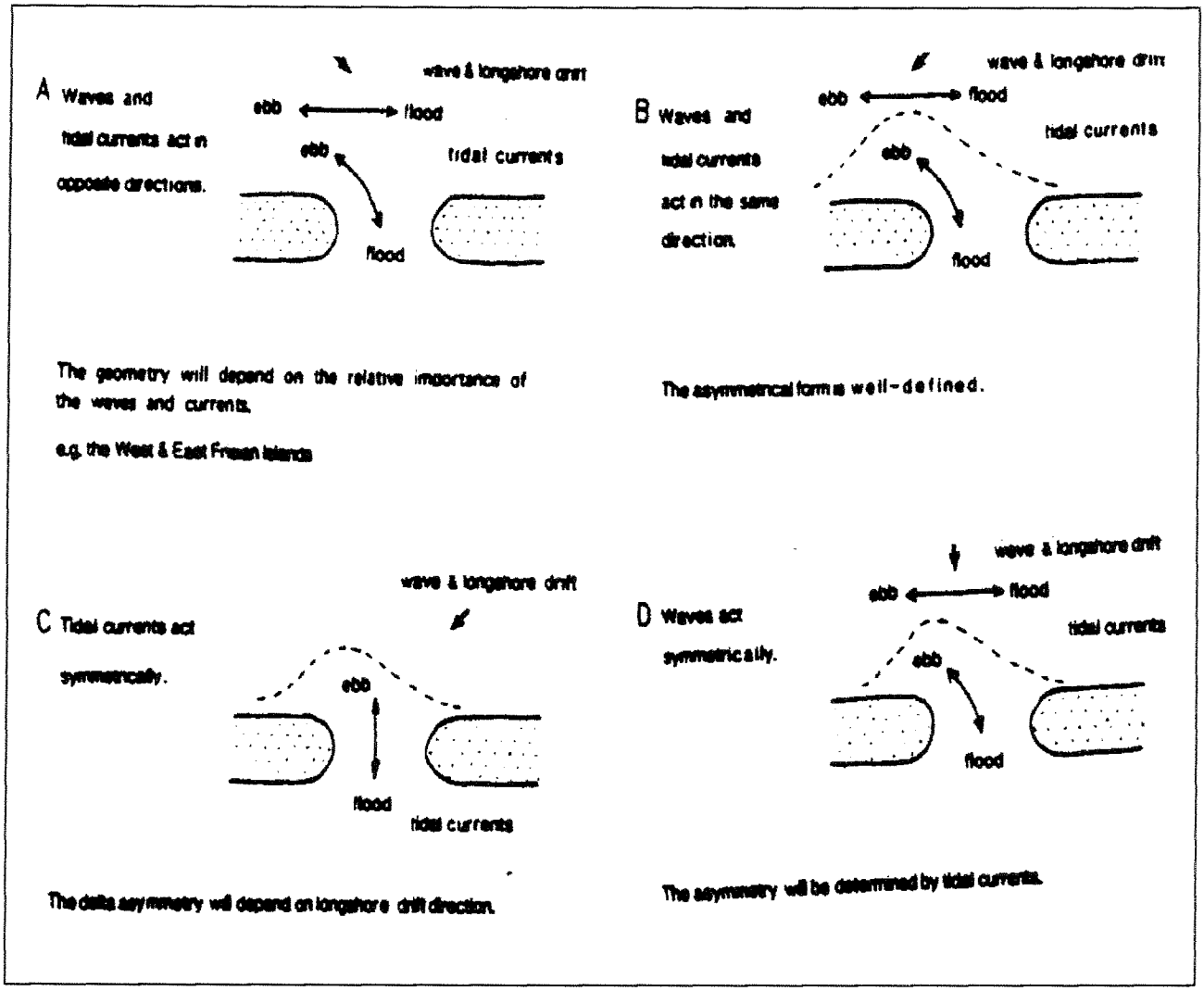

(From: Sha, 1990)

Figure 1.9: Typical Morphologies of tide and wave dominated tidal inlets

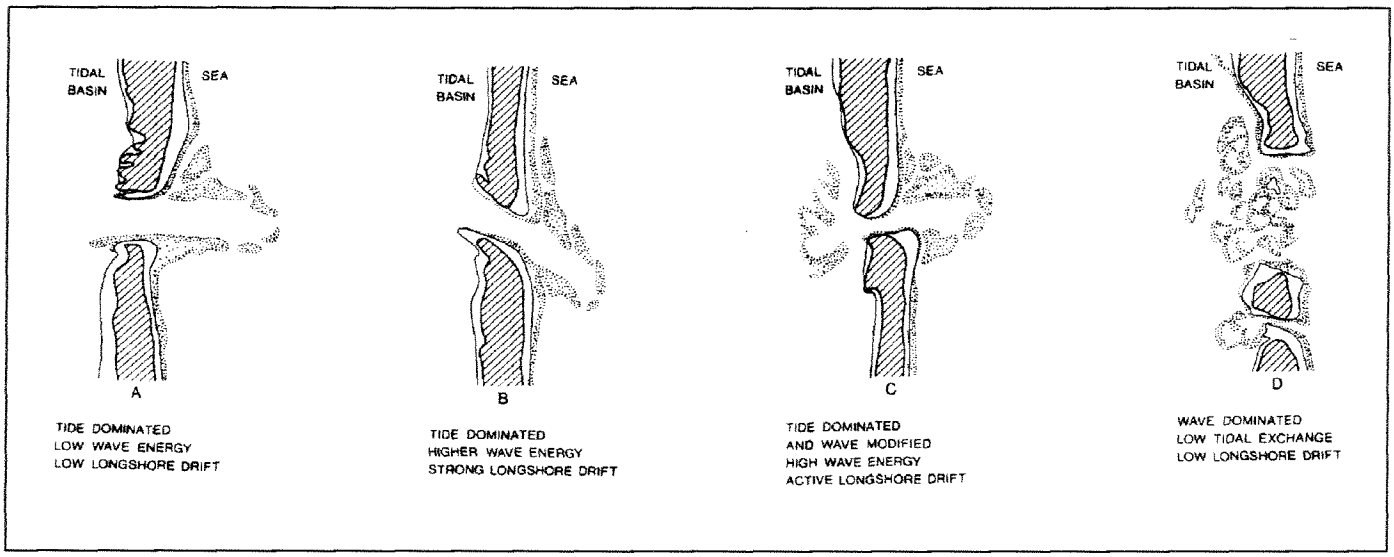

(From: Huis in `t Veld et al, 1987)

- ***Type A:*** The prevailing forces of longshore and onshore (flood) currents are greater than the offshore (ebb) currents.
- ***Type B:*** The prevailing force of the longshore current in one direction is greater than in the other direction.
- ***Type C:*** Like B, but now in the other longshore direction
- ***Type D:*** The prevailing forces of the inlet currents are greater than the forces of the longshore currents.

Oertel`s investigations are qualitative because there are no quantitative values given, also a transition between the different types is not defined (Steijn, 1991).

Steijn (1991) described a qualitative classification of the ebb tidal delta by Sha (1990). He described a model for the ebb tidal delta under influence of tides, waves and littoral drift as shown in Figure 1.8. The possible offset of the ebb tidal delta depends as pointed out before on the relative importance of waves and tidal currents alongshore and in- and outflow through the inlet. ***Sketch A*** shows the case that wave induced longshore drift is directed opposite to the interaction of alongshore and cross-shore directed currents. The asymmetry of the ebb tidal delta depends on the tide- or wave dominance. Tide dominated inlets: the ebb delta tends to updrift asymmetry, where wave dominated inlets tend to downdrift asymmetry. ***Sketch B*** shows the situation where waves and interacted tidal currents act in the same direction. The asymmetrical form is well defined. ***Sketch C*** shows the situation where the longshore tidal currents are absent, the asymmetry is determined by the wave action. ***Sketch D*** shows the case where no wave direction prevails, the asymmetry of the ebb tidal delta depends on the asymmetry of the tidal currents.

Huis in `t Veld et al. (1987) gives typical morphologies of tidal inlets illustrated in Figure 1.9. Where tide dominate or wave activity and longshore drift is weak, the ebb tidal delta develops as a main channel bordered by channel margin linear shoals (A). Much of the sediment carried along the shore in the nearshore zone becomes incorporated into the ebb delta. With increasing wave energy and longshore drift, ebb deltas form closer to shore and become oriented with the dominant incoming waves and longshore drift. In these cases a long transverse bar or a series of marginal shoals develop on the updrift side of the tidal inlet (B). Most of the sediment supplied by the longshore drift is by-passed along the outer shoals by the tide and wave generated currents. Along shorelines where longshore drift is less active, or waves approach more from different directions, ebb deltas form as shoals with a number of diverging main channels (C). Wave and tidal currents carry sediment over the delta as well as into the tidal basin where it accumulates on the flood tidal shoals. Wave dominated inlets typically have wide shallow channels with numerous shoals and a poorly developed or non-existent ebb tidal delta. The inner side of the entrance usually has spillover lobes of sediment radiating inwards from the entrance (D) (Huis in `t Veld et al., 1987).

Steijn (1991) concluded: "The hydrodynamic classification by Oertal (1975) must be seen as illustrative. From maps it can be seen whether an inlet is tide or wave dominated or both. This may improve the insight on the hydrodynamic forces and its effect on the morphology of a specific tidal inlet without actual data in a early stages of investigation". The classifications by Sha (1990) and Huis in `t Veld et al. (1987) are also illustrative, however they can give some specific information on the ebb tidal delta offset as a result of the tidal wave direction and the direction of dominant incoming waves

Figure 2.1: Tidal range versus barrier island length

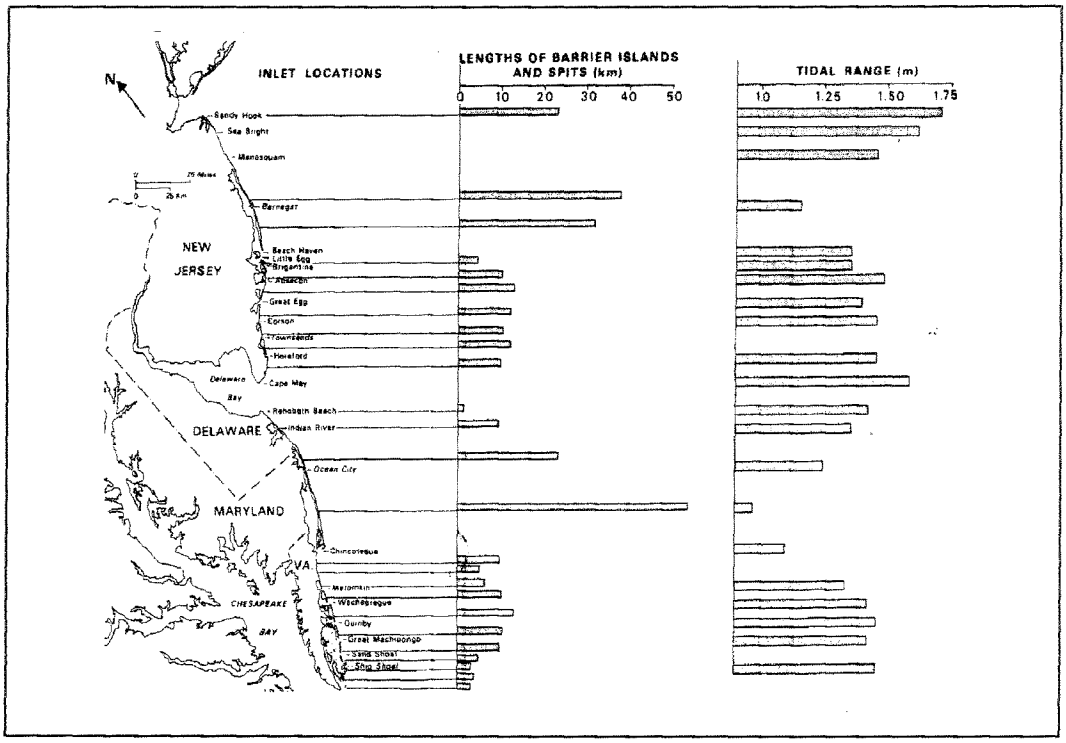

(From: FitzGerald, 1988)

Figure 2.2: Bay area versus tidal inlet width

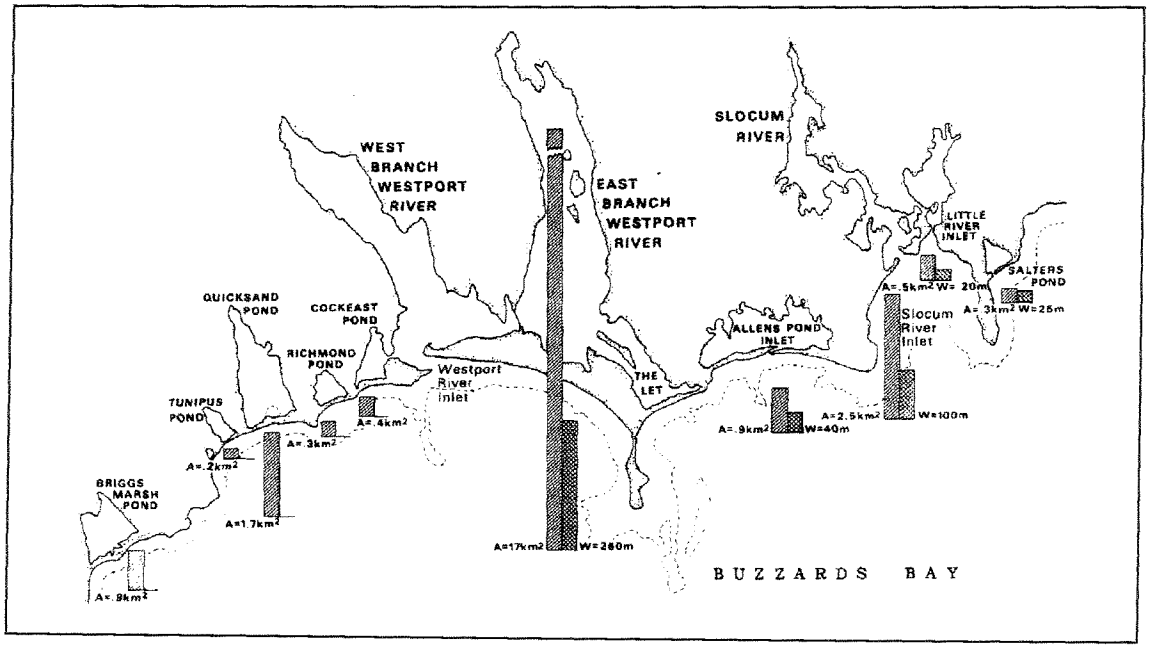

(From: FitzGerald, 1988)

2. Inlet Hydrodynamics

2.1. Introduction

Inlet hydrodynamics must be seen as a combination of water level variations, currents and waves. Inlet hydrodynamic characteristics are the driving forces for sediment transport patterns and depositions, and therefore determine the safety of a tidal inlet for the passage of vessels. So it is important to have a clear picture of the hydrodynamics near inlets. Therefore Authorities measure water level variations, currents and wave data of a certain area during long periods of times. Measuring data gives a much better view on the hydrodynamic impact on tidal inlets in a specific area. However there are situations for which other approaches must be sought for hydrodynamic information. These are according to Mehta and Özsoy (1978):

- Inlets for which data is not available
- Inlets which have been modified since data for prediction purposes were obtained
- Newly opened inlets.

In these situations inlets have to be studied using analytic predictive methods. (Mehta and Özsoy, 1978)

Inlet hydrodynamics are very important for the genesis, development and stability of tidal inlets. There are several important factors that influence the hydrodynamics of tidal inlets according to Mehta and Özsoy (1978):

- Inlet and bay geometry
- Bed roughness characteristics
- Fresh water flow
- Ocean tide characteristics
- Ocean wave characteristics
- Sediment movement

A combination of these factors produces a rather complex situation. In the following sections the different hydrodynamic impacts which have a significant influence on the morphological development of tidal inlets will be briefly discussed. A longterm effect on tidal inlets may be the relative sea level change which will also briefly described here.

2.2. Water level variations

2.2.1. Introduction

The water level variations are an important hydrodynamic parameter for the morphological development of tidal inlets. Figure 2.1 shows the relation between tidal range and the length of barrier islands on the East Coast of the USA. This figure illustrates that an inverse relation exists between the tidal range and the length of barrier islands. Higher tidal ranges induce more tidal power/unit surface area, more inlets and shorter barrier islands. The interaction between water level variations and morphology of tidal inlets is obvious, as they, in combination which the bay area determine the tidal prism, which is a very important parameter for the magnitude of currents inside the inlet gorge and basin (FitzGerald, 1988).

Figure 2.3: Development of time velocity asymmetry in a tidal inlet

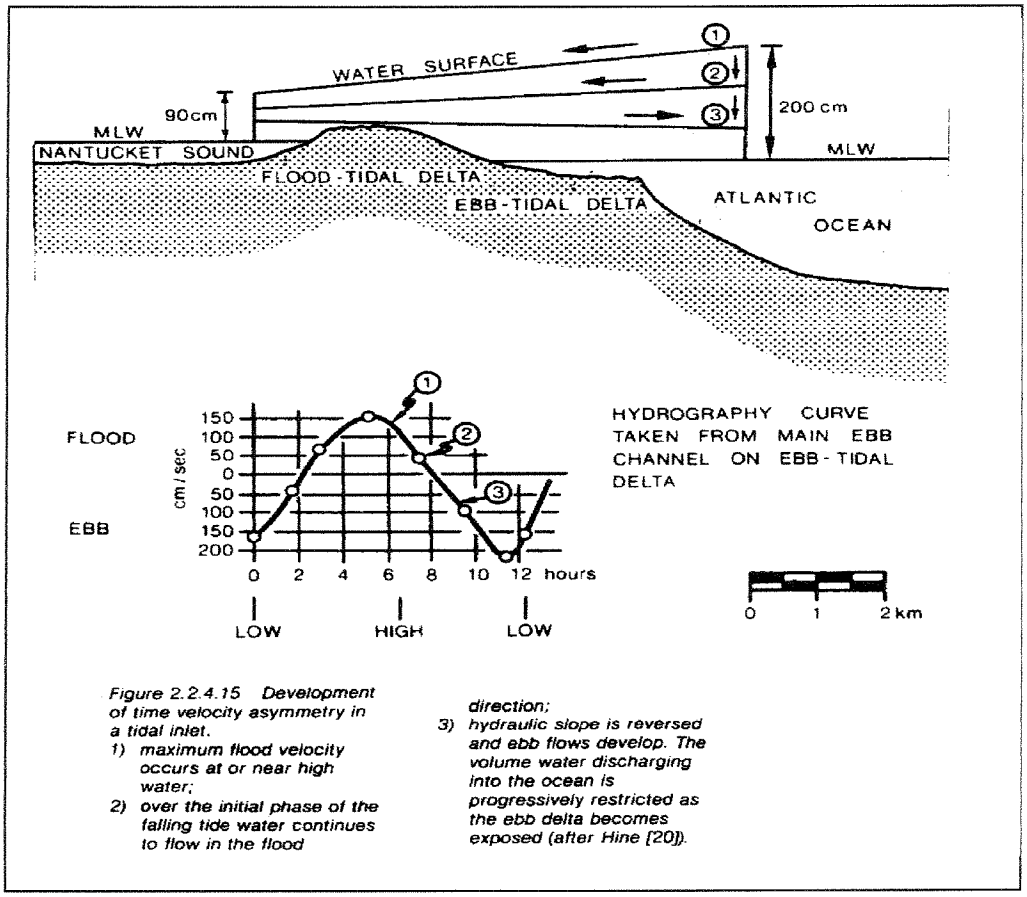

Figure 2.2.4.15 Development of time velocity asymmetry in a tidal inlet.
1) maximum flood velocity occurs at or near high water;
2) over the initial phase of the falling tide water continues to flow in the flood direction;
3) hydraulic slope is reversed and ebb flows develop. The volume water discharging into the ocean is progressively restricted as the ebb delta becomes exposed (after Hine [20]).

(From: Huis in `t Veld et al., 1987)

Figure 2.4: Idealised inlet / bay geometry

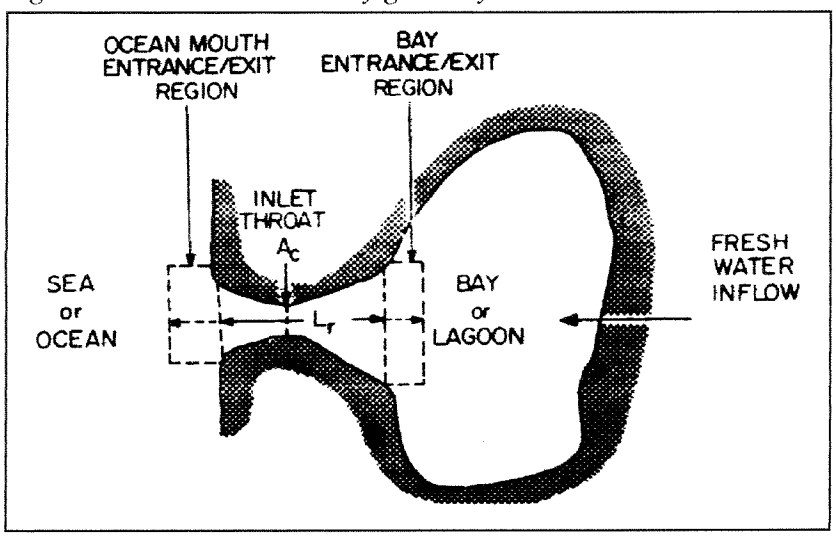

(From: Bruun, 1978)

The latter is clearly illustrated along the western Buzzard Bay, Massachusetts, coastline. Figure 2.2 illustrates the bay area versus tidal inlet width. Large bay area causes large inlet width. West of `West Branch River` (to the left in Figure 2.2) no inlets are present while east of it by the same bay area do have inlets. This is caused by difference in wave exposure. The western part of this coast is less exposed by waves (FitzGerald, 1988).

The changes in water levels are caused by several independent phenomena. Wind - or wave induced set-up and set-down, atmospheric pressure fluctuations (severe weather conditions), and mean sea level rise have an influence on the barrier formation, and the depth of the basin. When inlet basins are large, large amounts of sediment per unit sea level rise are needed to raise the bottom of the basin. This may change the coastline position of the barrier islands or the amounts of sediment stored on the ebb- and flood tidal delta (Steijn, 1991). But the most important component of water level variation is of course the astronomical tide. In general there are three types of astronomical tide. Semi-diurnal and diurnal and mixed. Semi-diurnal tide has generally two governing gravitational force components: the moon wave (M_2) with a period of 12 hours and 25 min and a sun wave (S_2) with a period of approximately 12 hours. In spite of the much greater mass of the sun, the moon component has the biggest influence because its distance to the earth is relatively small compared with the distance of the sun to the earth. The difference between two successive high waters is called inequality. The magnitude of inequality is dependent of the declination of those heavily bodies who influence the tidal movement. On the Dutch coast and the northern parts of the Atlantic Ocean the inequality is small (few percents) of the difference between high and low water. This type of tide is called semi-diurnal. But there are places were the inequality is so big that only one per 24 hours high and low water occur (Nortier, 1989). This type of tides is called diurnal. The transition between semi-diurnal and diurnal tide is called mixed tide. Other important factors that influence the water level variation due to astronomical tide are the tidal wave propagation and its interactions with the continental shelf.

Besides the hydrodynamic condition, the basin geometry in relation to the water levels is important. This is especially true if different tidal inlets are connected with each other, through the same basin. Tidal waves propagating along the coast entering inlets at different times. Due to this the tidal wave is modified when propagating through the basin (Steijn, 1991).

2.2.2. Influence of tidal inlets on water level variations

2.2.2.1. Amplitude - phase difference

Typical for tidal inlets is that the width of the entrance is usually small with respect to the typical size of the interior basin. Tidal currents through the entrance channel therefore have a typical time-velocity asymmetry where maximum flood and ebb currents develop before high or low water. According to Huis in `t Veld et al.(1987), this is caused by a difference in tidal range between the ocean and the basin as a result of the flow restricting effect of the narrow inlet entrance (narrow gorge effect). Figure 2.3 shows this qualitatively. As the crest of a progressive tidal wave passes a tidal inlet, water starts to flow into the basin. This continues until some time after high water. After high water the ocean water level starts to fall until it reaches the basin water level. This causes a relatively long high water period inside the basin. When the trough of the tidal wave passes, low water will be slightly higher in the basin so ebb flows continue during the initial phase of the following flood. As a result of this phenomenon the phase of the tide will increase and the amplitude will decrease with respect to the ocean tide (Huis in `t Veld et al., 1987). The changes in amplitude and phase in the interior basin can result in a duration asymmetry of falling and rising tide as much as three hours (Steijn,

Figure 2.5: Frequency response curves of the fundamental amplitude and the first overtide amplitude (A and B) and the frequency response of the phase lag of the fundamental amplitude (C) and the first basin overtide component (D)

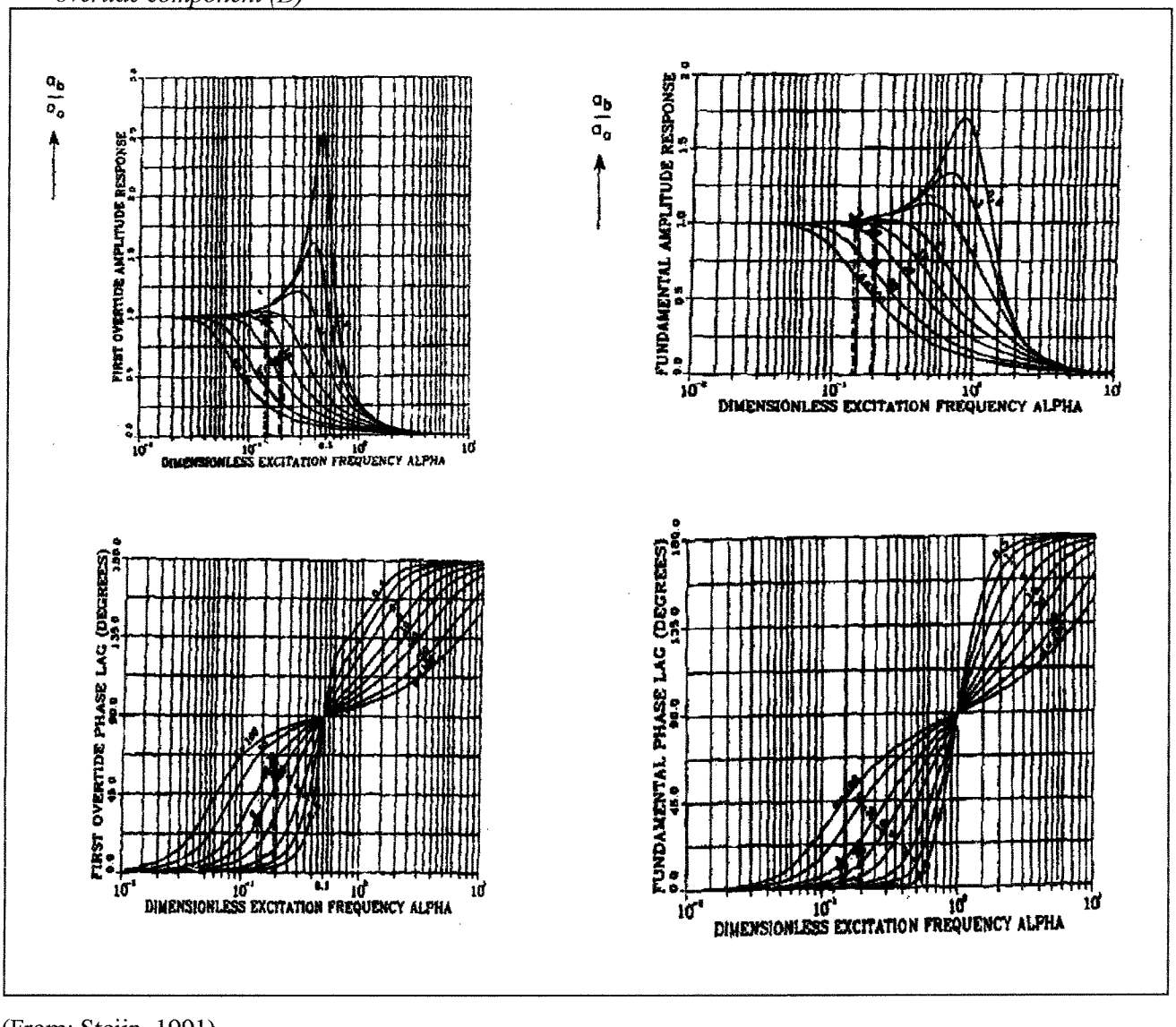

(From: Steijn, 1991)

1991). The effects of this amplitude - phase difference on the tidal currents are described in section 2.3.1.

2.2.2.2. Overtides

When a tidal wave propagates towards the gorge channel energy is transferred from ocean tide components towards higher harmonic components. This higher harmonic response is called overtides (Steijn, 1991). According to Di Lorenzo (1988): "Overtides depend mainly on the local geometry and frictional characteristics of the basin and the ocean tidal forcing. Tidal inlets act as a sort of filter on the penetrating tidal wave: part of the ocean tide will be reflected, part is transmitted and part is dissipated". Many authors have attempted to describe this phenomenon: Mehta and Özsoy (1978) developed a rather simple algorithm for this phenomenon. However they simplified the ocean tide only by the first harmonic and used an idealised inlet / basin system, as illustrated in Figure 2.4, which includes numerous other simplifications as well. The Shore Protection Manual (1984) described a similar method according to O'Brien and Dean (1972). Di Lozenzo (1988) developed an analytical model with the idealised inlet/ basin system. Frequency response curves of the fundamental amplitude and the first overtide amplitude are shown in Figures 2.5A and 2.5B (Figures 2.5C and 2.5D are discussed later). These graphs show the amplitude response of the basin water level for various values of a damping coefficient (β)(see also 2.2.2.3.). The basic assumptions for the analytical model of DiLorenzo (1988) were:

- Small inlet/bay system (2.2.2.3.). This means that no spatial gradients occur inside the basin, or in other words the basin acts as a storage area for the water entering and leaving the inlet.
- Inlet depth is significantly larger than tidal range
- Negligible stratification, fresh water inflow and water storage in the inlet throat.

It may be concluded that the determination of overtides in an analytical way without modern equipment, is very difficult in actual cases because the models as described above work only with rather unrealistic idealised bay / inlet system with numerous simplifications as for instance the ocean tide characteristics as well as the inlet / bay geometry.

2.2.2.3. Inlet-bay system

In spite of the limiting assumptions of a simple inlet-bay system, it may be useful to illustrate specific tidal inlet characteristics. This may be useful when for instance tidal measurements are not available to determine the water level differences and the phase lag between the ocean and lagoon. In such a situation, or in cases where a quick guess of tidal characteristics is sufficient, the rather simple algorithm of Mehta and Özsoy (1978) may be of help. DiLorenzo (1988) also used the idealised inlet-bay system for his development of an analytical model to predict amplitudes and phases of the mainland first overtide, for instance the M2 and M4 component (Steijn, 1991). (See also 2.2.2.2.)

However using this algorithm no spatial gradient are allowed inside the lagoon. There are several theories for the prediction of the occurrence of hydraulic gradients in the interior of tidal inlets. A concept by Mehta and Özsoy (1978) to investigate the occurrence of hydraulic gradients in a tidal basin is when the ratio between the angular ocean tidal frequency (ω) is (much) smaller than the ratio between the tidal celerity inside the basin and its largest length:

Figure 2.6: Head Losses in an Idealised Inlet Channel

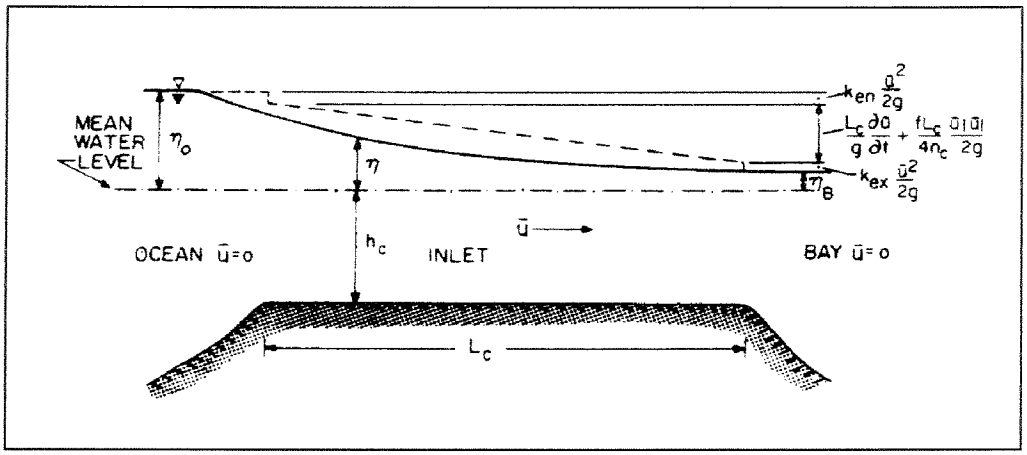

(From: Bruun, 1978)

$$\omega = \frac{2\pi}{T_{tide}} << \frac{\sqrt{gh_b}}{L_b} \quad (1)$$

Where: ω = Angular ocean tidal frequency [rad/s]
T_{tide}= Tidal period [s]
h_b = Water depth inside the basin [m]
L_b = Basin length [m]
g = Gravitational acceleration [m/s^2]

If this is the case no significant hydraulic gradients occur inside the basin. Or in other words the water surface remains nearly horizontal at any time ($\partial h/\partial x \approx 0$). The occurrence of hydraulic gradients inside the basin will be supported when the water depth is small and when the largest distance in the basin is large with respect to the inlet throat dimensions. Small depths give rise to frictional effects and therefore a lower tidal celerity. It is noted that the above criteria for the development of hydraulic gradient are basically developed for more or less closed basins (Mehta et al. 1978).

When no significant hydraulic gradients occur inside the inlet basin, the flow conditions in the tidal inlet gorge are determined by hydraulic gradients across the gorge. With a relatively narrow gorge the basin will not be able to follow the outside water level fluctuations. Therefore significant hydraulic gradients develop across the gorge. These hydraulic gradients (total head) are the driving force for the flow through the gorge. The total difference between the ocean water level and the bay water level across the gorge is the sum of four separate contributions as illustrated by the dashed line in Figure 2.6. This figure illustrates head losses in an idealised inlet channel. These head losses are (1) entrance losses; turbulent losses at the entrance of the channel due to convergence of the flow into the channel. (K_{en}), (2) exit losses; head losses due to loss of kinetic head when the flow separates at it enters the bay. (K_{ex}), (3) head losses due to friction ($fL_c/4R$) and finally (4) the head losses due to inertia (Mehta and Özsoy, 1978). As the corners of the entrance are rounded, no significant energy loss takes place. In these cases a K_{en} value of $K_{en} = 0.05$ may be taken. For the ideal inlet situation the flow entering the basin can be regarded as a separated jet expanding in a basin of infinite width. In that case all kinetic energy is lost and consequently $K_{ex} = 1.0$. (FitzGerald et al, 1988). However in most cases the basin consist of tidal channels, so that the jet-concept is not really satisfied. In these cases a value of $K_{ex} = 0.5$ may be taken (Steijn, 1991).

The friction loss coefficient (F) used in the algorithm of Mehta and Özsoy (1978) is defined as:

$$F = K_{en} + K_{ex} + \frac{f \cdot L_b}{4 \cdot R} \quad (2)$$

Where f is the Darcy-Weisbach coefficient ($8g/C^2$). In most cases the values $K_{en} + K_{ex} = 1.3$ and $f = 0.03$ can be used. In the ideal situation where the flow enters the basin with infinite width like a separated jet, then all kinetic energy is lost and therefore $K_{ex}=1.0$. However if the basin consist of tidal channels the ideal jet concept is no longer valid and therefore the value of K_{ex} must be taken lower (e.g. $K_{ex} = 0.5$). For inlets with rounded corners of the entrance channel, energy loss is not very significant for the flow entering the inlet. In these cases a value of $K_{en} = 0.05$ may be taken. FitzGerald et al. (1988) used the algorithm by Mehta and Özsoy (1978) to determine the water level differences and the phase lag between the Grande-Entrée lagoon and the Gulf of St. Lawrence in Canada.

Mehta and Özsoy (1978) obtained the solution for the ratio between the tidal amplitude in the lagoon and the ocean (Equation (3)), and the angle of the phase lag (Equation (4)) for the tide in the lagoon (E). The solution for the ratio between the tidal amplitude in the lagoon and the ocean:

$$R = \frac{a_b}{a_0} = \sqrt{\left\{\frac{\sqrt{\left((1-G^2)^4 + M^2\right)} - (1-G^2)^2}{0.5M^2}\right\}} \qquad (3)$$

Where: G = Dimensionless tidal frequency [-]
M = Dimensionless Coefficient [-]

The dimensionless tidal frequency (G) is defined as:

$$G = \sqrt{\frac{L_c A_b}{g A_c}} \cdot \frac{2\pi}{T_{tide}} \qquad (3a)$$

Where: L_C = *The tidal inlet length* *[m]*
A_b = *Surface area of the lagoon* *[m²]*
A_C = *The cross-sectional area of the inlet* *[m²]*
T_{tide} = *Tidal period* *[s]*

The dimensionless coefficient (M) is defined as:

$$M = \frac{16BG^2}{3\pi} \qquad (3b)$$

Where: B = Dimensionless damping coefficient(Equation 3c) [-]
G = Dimensionless tidal frequency (Equation 3a) [-]

The dimensionless damping coefficient (B) is defined as:

$$B = \frac{F}{2L_c} \cdot \frac{A_b}{A_c} \cdot H_0 \qquad (3c)$$

Where: F = Friction factor(Equation 2) [-]
L_C = The tidal inlet length [m]
A_b = Surface area of the lagoon [m²]
A_C = The cross-sectional area of the inlet [m²]
H_0 = Ocean tidal amplitude [m]

The angle of phase lag E [radians or degrees] can de determined with the following expression

$$E = TAN^{-1}\left[\frac{MR}{2(1-G^2)}\right] \qquad (4)$$

Where: G = Dimensionless tidal frequency [-]
R = Ratio basin and ocean tidal amplitude (Equation 3) [-]
M = Dimensionless Coefficient [-]

Figure 2.7: Wind set-up

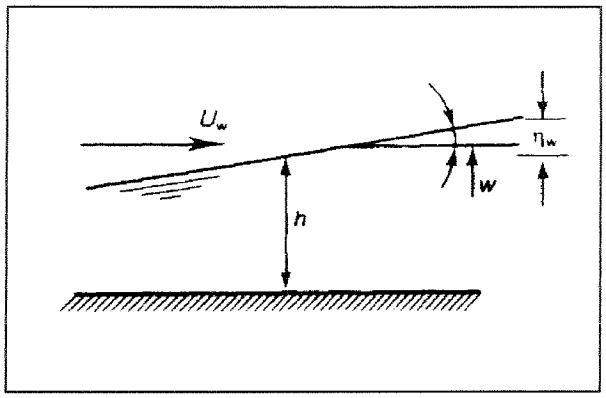

(From: CUR, 1994)

Figure 2.8: Wave set-up

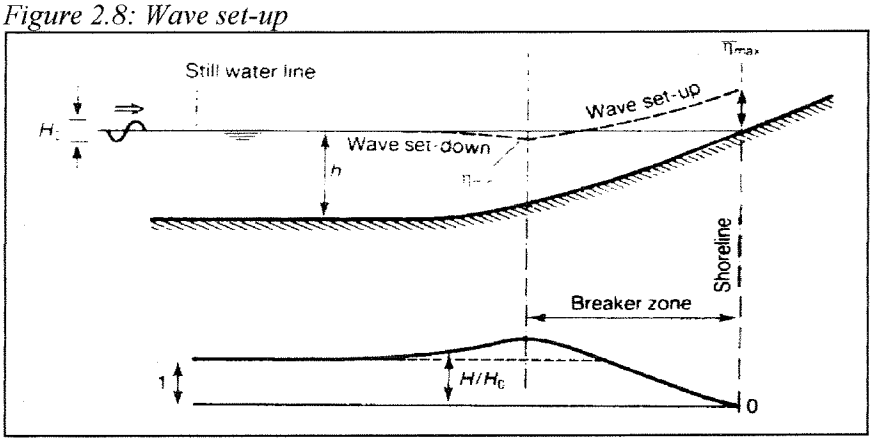

(From: CUR, 1994)

As the value of R is about unity it indicates that the basin water levels easily follows the ocean water levels. Low values of E indicate a limited phase lag between the ocean tide and the basin tide. This is usually the case for tidal inlets with large tidal entrances compared to the basin area.

Frequency response curves for the fundamental amplitude and the first overtide were already shown in Figure 2.5A and 2.5B. The damping coefficient is defined as:

$$\beta = \frac{F \cdot a_o \cdot A_b}{A_c \cdot L_c} \tag{5}$$

And the Helmholtz frequency (Ω [Hz]) which is defined as:

$$\Omega = \sqrt{\frac{g \cdot A_c}{L_c \cdot A_b}} \tag{6}$$

This Helmholtz frequency can be regarded as a resonance frequency of the bay system, in case of no frictional damping". Figure 2.5C and 2.5D are similar plots given for respectively the frequency response of the phase lag of the fundamental amplitude (2.5C) and the first basin overtide component (2.5D). Steijn (1991) states: "Dependent on the specific configuration, the fundamental tidal component can lead over the first overtide (or vice versa). The model indicates that due to non-linear frictional dissipation mechanisms, mean sea level slopes upwards and downwards towards the basin in case of ebb- and flood-dominance, respectively". Verification of the analytical model indicates that the model woks best for inlet/bay systems with low or high Helmholtz frequencies.

2.2.3. Wind and wave set-up

Shear stresses by wind on the water surface causes a slope in the water surface. This results in a wind set-up or set-down near tidal inlets. Wind set-up is most pronounced in relatively shallow waters, like bays, lagoons or estuaries (CUR, 1994). The wind set-up is strongly dependent on the local geometry and bathymetry of the tidal inlets. CUR (1994) gives an expression for the wind set-up for a constant depth, as shown in Figure 2.7. In real practice this is not the case. The fetch which must taken into account is not well defined. The expression should be used as a comparison to local measurements where it might give a useful indication of the wind set-up component distribution.

Wave induced set-up is caused by energy dissipation due to the shoaling of the incoming waves. This results in a gradient of the radiation stress perpendicular to the coast. This results in a wave induces set-down near the breaker line and a wave set-up near the shoreline. Figure 2.8 shows this phenomenon. CUR (1994) gives an expression of the wave set-up using the linear wave theory, which can be used as a first estimate of wave set-up (Battjes, 1974):

$$\eta_{max} = 0.3 \cdot \gamma_{br} \cdot H_b \tag{7}$$

Where: γ_{br} = Breaker index: the $\frac{H}{h}$ ratio;

H_b = Wave height at breaker line (regular waves)

2.2.4. Relative change in sea level

The reason to call changes in sea level relative, that it is difficult to distinguish whether changes in the sea levels are due to actual changes in the sea level, changes in the land level, or both (Shore Protection Manual 1984). Sea levels are generally rising because the atmospheric temperature, which ultimately heats up the surface of the sea, covering 70% of the globe. Due to the rise of temperature, water expands and causes a rise of mean sea level. At present there is a rising trend of 0,10 to 0,15 m per 100 years since 1879 (CUR, 1994). The rise in mean water level due to rising temperatures is increased by human impact, the so-called "greenhouse effect". This is expected to cause a rise in global temperature of about 2°C to 4°C over the next 100 years compared with the 0,5°C increase over the last 100 years (CUR, 1994). Changes in land levels (rise and fall) are caused by tectonic forces or isostatic impound.

What is the effect of relative sea level change on tidal inlets? With sufficient sediment available the shoals on the flood tidal delta will become higher. Steijn (1991) described three scenarios of the tidal inlet reaction on this phenomenon:

- If the interior shoals are able to follow the sea level rise, a huge amount of sediment will be required to fill up the interior basin. This sediment will be eroded from the ebb tidal delta and the barrier islands.

- If the bed of the interior basins are initially not able to follow the sea level rise, the tidal prism (P) will increase, resulting in larger maximum velocities in the tidal channels. As a result the ebb tidal delta growth increases resulting in a decrease of wave energy transferred to the flood tidal delta (sheltering effect) which in turn increases shoaling also on the flood tidal delta. In this case sediment is also needed and therefore extracted from the barrier islands and the nearshore.

- If interior basins do not follow the sea level rise. Tidal prism will increase and therefore increase of the ebb tidal delta, which again causes erosion of the barrier islands.

- A general effect on the beaches due to the relative sea level rise is that waves attack beaches on a higher elevation which can cause massive erosion and the permanent loss of sediment, especially during storm surges.

2.2.5. Severe weather conditions

2.2.5.1. Introduction

Severe weather conditions have a great influence on waves and therefore on the amount of littoral drift. Cyclones and hurricanes can generate waves of great intensity. According to Silvester et al. (1993) these waves occur in regions of low atmospheric pressure. " Low in this sense implies only a reduction of 3,0 % from the normal. A value of twice this amount would result in the severest storm possible". Severe weather conditions may create severe danger in the coastal region as well as the possibility of full closure of a tidal inlet by heavy littoral drift and large suspended sediment exposure. Also the water levels are important, it determines the region that will be exposed to high wave energy. High wave energy in combination with a high water level may increase the penetration of waves into the flood tidal delta; this may cause severe erosion on the landward side of this delta. Tropical cyclones have unique wind structures that can produce some of the highest velocities. The name of such extreme weather

Figure: 2.9: Plan of sea surface wind conditions

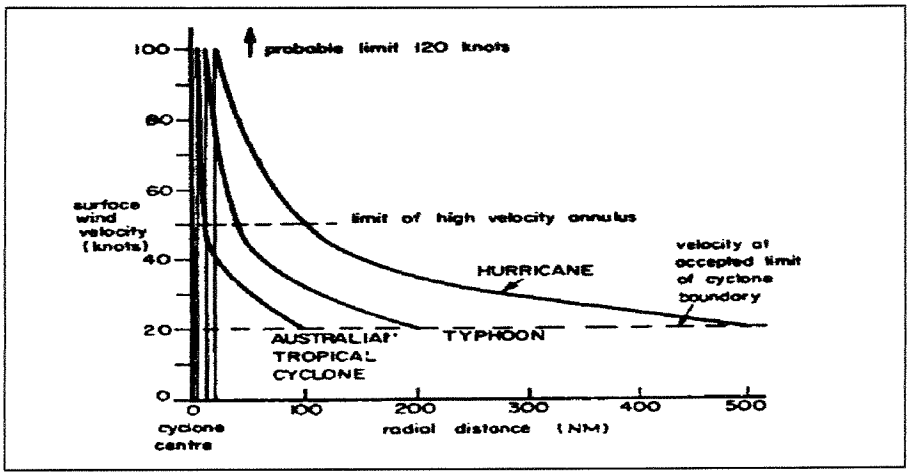

(From: Silvester and Hsu, 1993)

Figure 2.10: Radial wind distributions in tropical cyclones

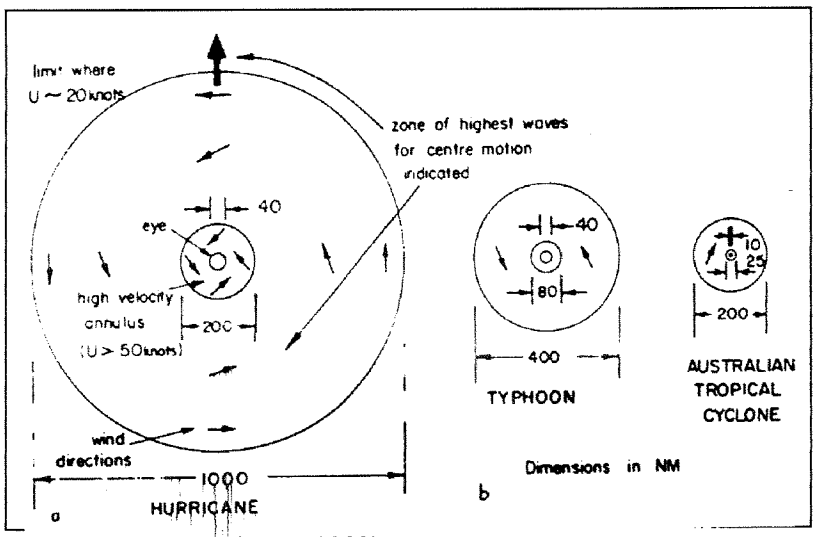

(From: Silvester and Hsu, 1993)

conditions depends on the location. On the East Coast of the USA they are called hurricanes, in the western pacific typhoons, and plane tropical cyclones in Australia. Tropical cyclones have a life cycle of immature, mature and waning (Silvester et al. 1993) Figure 2.9 shows the typical wind profiles for these three major classes. "Radial profiles of wind velocities are illustrated in Figure 2.10, where it is seen that maximum speeds around the eye are of the same order even though the overall radii of wind action differs geographically". Wind directions in (a) and (b) of Figure 2.9 are shown for the Northern Hemisphere were these particular versions occur; that in (c) if for the Southern Hemisphere or more particularly the Australian version Silvester et al. (1993).

2.2.5.2. Storm surges

A storm surge is the result of wind-induced set-up and atmospheric pressure fluctuations. The atmospheric pressure causes a corresponding rise or fall of the mean sea water level. CUR (1994) gives a relation of the static rise (z_a [m]) of the mean sea water level:

$$z_a = 0.01 \cdot (1013 - p_a) \tag{8}$$

Where p_a = Atmospheric pressure at sea level [mbar/hpa]

The value 1013 in this equation gives the mean air pressure at sea level (mbar or hPa). According to CUR (1994) there are storms in zones of higher latitudes (> 40°) in which variations from 960 mbar to 1060 mbar are common. In tropical regions the storm pressure may drop to 900 mbar. (Static rise: 1,13 m!). Due to dynamic effects this rise may be increased significantly. The water levels are changing correspondingly as a storm surge when a depression moves very quickly. A storm surge behaves like a long wave with a wavelength of approximately the width of the depression. The heights of these waves are increased by the shoaling effect near the coast. The actual water levels near tidal inlets are the result of the above-described effects superimposed on the astronomical tide and other meteorological effects. These water levels are generally called: storm surge level (CUR, 1994). The qualitative impact of storm surges on water levels is illustrated in Figure 2.11.

2.2.5.3. Increasing wave action

Wave heights increases significantly during severe weather conditions. An increase in wave action leads to a more than linear increase in sediment transport. This is shown by the general formula for the sediment transport:

$$S_x = K_h \cdot H^b{}_{rms} \tag{9}$$

Where: K_h = A function of the hydraulic and morphological boundary conditions.
H_{rms} = Root-Mean-Square value of the waves in the wave spectrum.
b = A constant for a specific set of boundary conditions (b > 1)

So during and some time after the passage of a cyclone, excessive sediment transport may occur. High sediment loads on tidal inlets results in a decreasing cross-sectional area of the gorge. The massive littoral drift may permanently close unstable inlets.

2.3. Currents

2.3.1. Introduction

On the oceanside in deep water some distance offshore, large-scale currents resulting from the global wind distribution are dominant. Closer to the shore current reversal may take place as a result of eddies generated due to interactions with the coastal formations or by a local wind field. More closer to the shore near tidal inlets currents as a result of the water level variations (astronomical tide), wave driven longshore current, wind driven currents, river discharges and density currents mostly effect the flow patterns on the three morphological units of tidal inlets. The relative importance of these current `sources` determine the morphology of tidal inlets.

The tidal inlet gorge (entrance channel) is the most affected by the in - and outflowing currents, because the whole tidal prism and river discharges in the interior basin, has to pass the relatively narrow gap. Tidal currents through the gorge show an asymmetry in ebb and flood flows (time- velocity asymmetry). This can be explained by looking at the effect of the water level variations on the geometry of tidal inlets. In section 2.3.5. some entrance current computation methods will be described which can be used to get a first estimate of the inlet current magnitude.

As already been described in cases of tidal inlets with rather narrow entrances, the water level variations on the bayside do not follow the ocean water level variations (narrow gorge effect) resulting in a decreasing tidal amplitude and increasing phase (Huis in `t Veld et al., 1987). As a result of decreasing amplitude less water will flow into basins with small cross-sectional areas with respect to inlets with larger cross-sectional areas. The increasing phase and decreasing amplitude of the basin tide with respect to the ocean tide cause longer flood duration because after high water the ocean water level starts to fall (water is still flowing in) until it reaches the basin water level. After this, tidal currents start to flow out until some time after low water. However the tidal prism that entered during flood must be flow out in a shorter period of time and with lower water depths. This causes the higher ebb currents. The hydrography curve in Figure 2.3 shows this current distribution in time. After low water on the ocean side, the low water inside the basin will be slightly higher so ebb flows continue during the initial phase of the following flood. The latter is responsible for the ebb and flood dominance of parts of the tidal inlet ebb tidal delta, which will be discussed later in detail.

Important for the occurrence of flood and ebb dominant currents inside the gorge channel is the relation between the mean inlet depth and the basin water depth. The dominance of ebb currents is favoured in cases of a relative large mean inlet depth and rather flat basins with increasing surface area with rising tide. However if the basin is open and wide with a mean depth larger than the inlet throat, then the dominant current inside the gorge are flood dominant because of the increased flow resistance for ebb (Steijn, 1991). According to Steijn (1991): Niemeyer (1990) relates flood and ebb dominance of the gorge channel, to the tidal inlet classification. Tide dominated inlets will usually be ebb dominant, while wave dominated inlets will show more flood dominance. Transitional inlets often have an ebb dominant gorge channel but also secondary channel(s) where flood currents dominate. Gorge channels which are not flood dominated are called neutral channels (Bruun, 1978).

The current patterns inside tidal inlets may also be significantly influenced by tide driven longshore currents. Steijn (1991) described after van den Berg (1978) the influence of the longshore tidal currents and the cross-shore tidal currents in the inlet gorge and the influence of this on the inlet morphology. The tidal inlets in the Southwest part of the Netherlands and

Figure 2.12: Influence of the longshore tidal currents on the inlet morphology

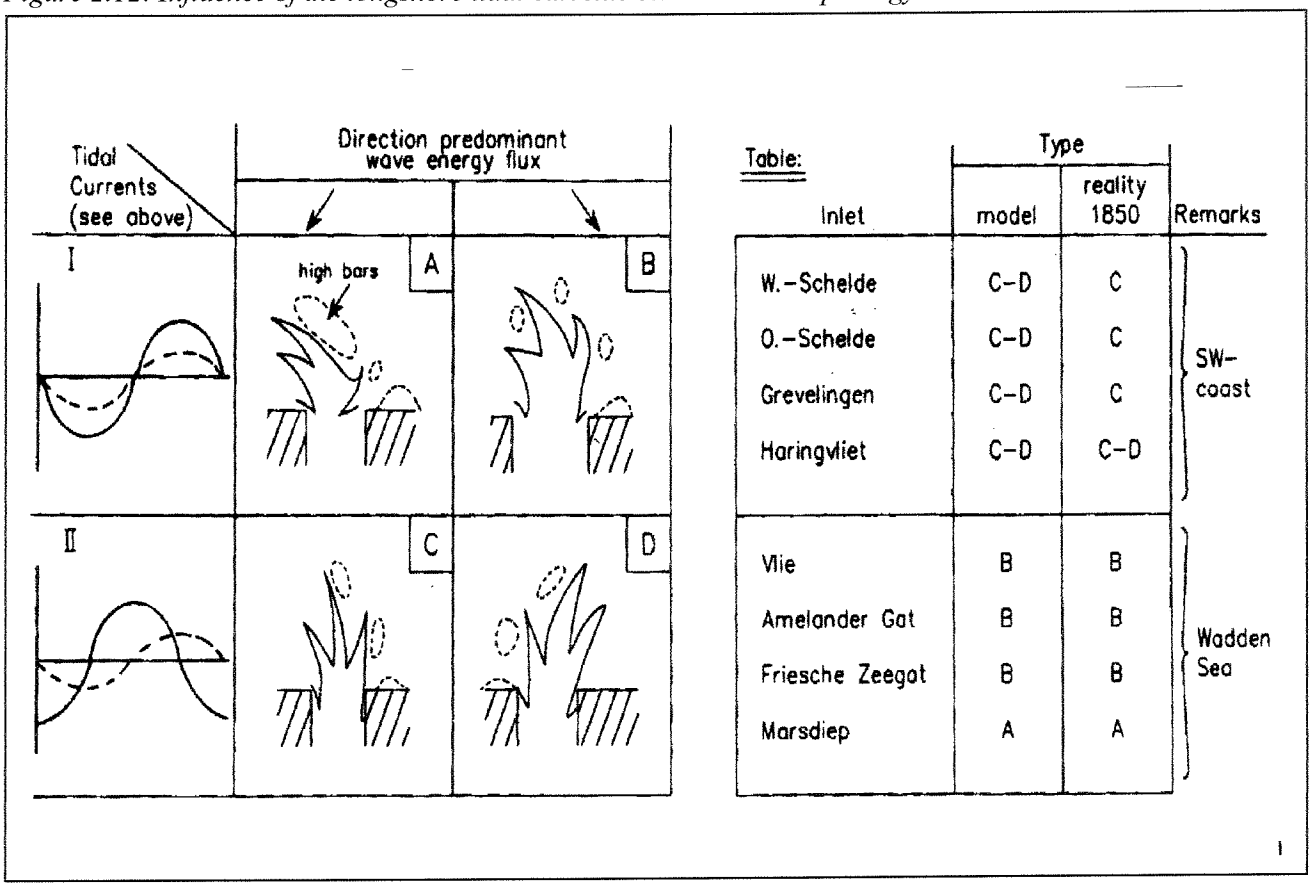

Table:

Inlet	Type: model	Type: reality 1850	Remarks
W.-Schelde	C-D	C	SW-coast
O.-Schelde	C-D	C	SW-coast
Grevelingen	C-D	C	SW-coast
Haringvliet	C-D	C-D	SW-coast
Vlie	B	B	Wadden Sea
Amelander Gat	B	B	Wadden Sea
Friesche Zeegat	B	B	Wadden Sea
Marsdiep	A	A	Wadden Sea

(From: Steijn, 1991)

Figure 2.13 Two basic cases of flow patterns over a tidal cycle

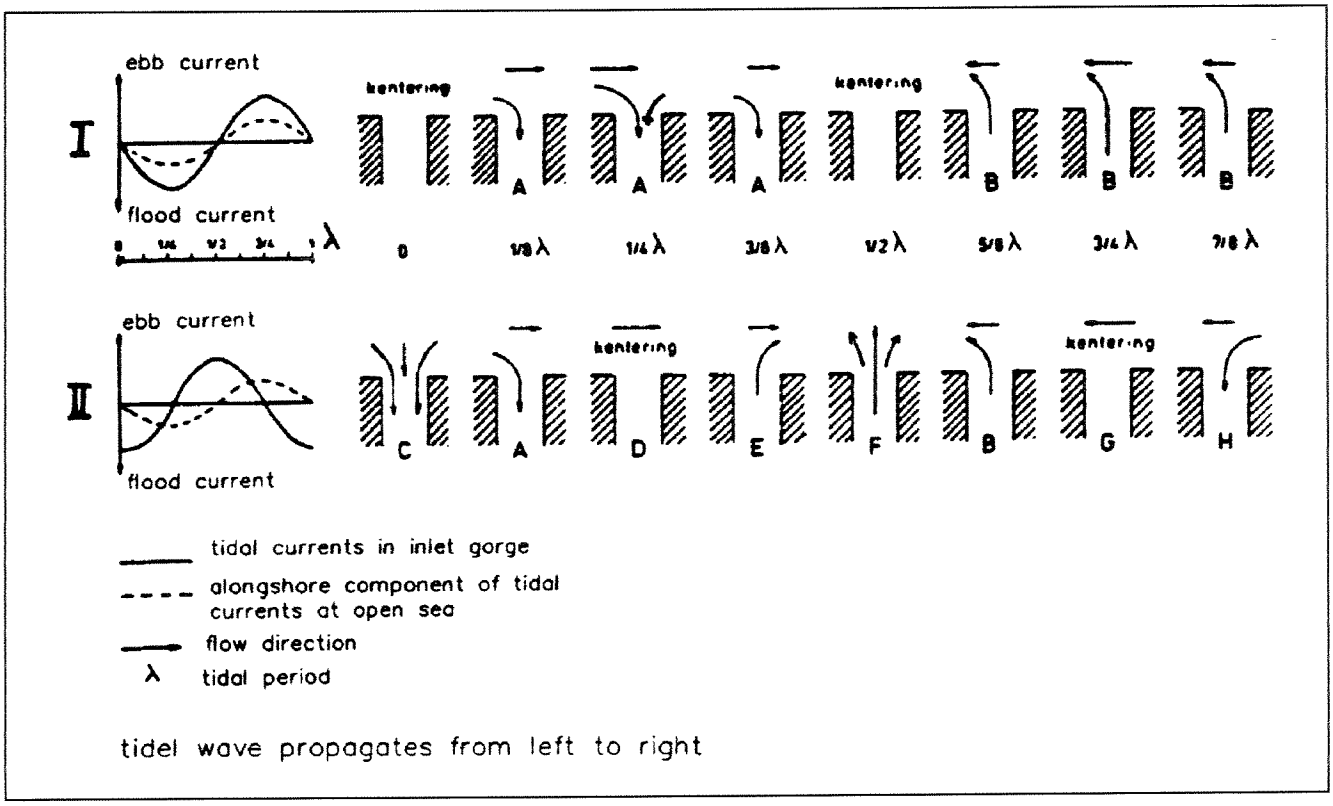

(From: Steijn, 1991)

those at the western Wadden Sea were used as study material (Figure 2.12). "The tidal range along the Dutch Coast decreases from the SW to the northern end of Holland, whereafter it increases in the eastward direction along the Wadden Sea coast. The difference in tidal range results from the tidal wave propagation in the North Sea. It implies that when HW has been reached along the Holland coast, an upward water level slope still exist in northern direction, while this is a downward slope in eastern direction along the Wadden Sea coast. As a consequence of this, the maximum flood currents reach their maximum (at open sea) after and before HW for the Holland coast and the Wadden Sea coast, respectively. Turn of the tide at open sea along the Holland and Wadden coast takes place several hours and shortly after HW, respectively. As the inlet currents turn shortly after HW, this finally results in a remarkable difference along the Dutch coast; in the southern part, the phase difference between the alongshore tidal currents at sea and the cross shore currents in the inlets amounts to about 3 hours, whereas this is nil for the northern part". Steijn (1991) describes the flow patterns over the tidal cycle for these two basic cases. A flat bottom and a tidal wave propagation from the left to the right are assumed.

Case 1: No phase differences are present (Wadden Sea inlets). Two basic flow patterns (marked as A and B) can be recognised. The flow concentrates on the left side of the inlet (Figure 2.13).

Case 2: The phase differences equals a quarter of the tidal period (SW-part of the Netherlands). Now, eight different flow patterns (marked as A to H) can be recognised (Figure 2.13).

Measurements in the Wadden Sea inlets and Oosterschelde (SW-coast) show that for the Wadden Sea inlets, flow patterns A and B are dominant over the tidal cycle. The consequence can be found in the orientation of the main ebb channel, which is located at the western side of the inlet. The flow patterns C and F appeared to dominate in the Oosterschelde inlet, resulting in a much more central location of the main ebb channel.

2.3.2. Currents on the ebb tidal delta

On the ebb tidal delta two separate currents meet: the alongshore wave driven current and the tidal currents which are more or less perpendicular to each other. The diversion of the longshore current by the tidal inlet current is called *dynamic diversion* (Oertel, 1988). The earlier described ebb delta classification by Oertel (1988) was based on the principles of dynamic diversion. The tidal current act as a hydrodynamic shield for the longshore current. The tidal current itself acts as a fully turbulent diverging jet. Figure 2.14 shows for an ideal inlet the flow patterns (so without dynamic diversion) of a turbulent diverging jet. For an ideal inlet the distributions of the streamlines in the zone of flow establishment (ZOFE) depend on the inlet size and are independent of speed. Maximum velocities occur in this near field, with streamlines evenly distributed across the inlet. After this the flow enters the zone of established flow (ZOEF) where the velocity profile gradually transit from a more or less rectangular profile into a more spreaded profile at some distance from the inlet (Bruun, 1978). The erosive potential of this ebb current is proportional to the magnitude of water leaving the inlet during ebb (Oertel, 1988).

Tidal inlets with a significant river discharge can develop a diverging jet that acts according to the idealised model of ebb-jet diffusion. An idealised free ebb-jet is illustrated in Figure 2.15 (A). Ebb-jet diffusion is the result of velocity difference between the edge of the jet and the ambient fluid. This causes a mixing region, which decelerate the jet in lateral direction. The limit of this zone is reached when the mixing region has penetrated to the entire line of

Figure 2.14: Definition Sketch for a shallow water jet

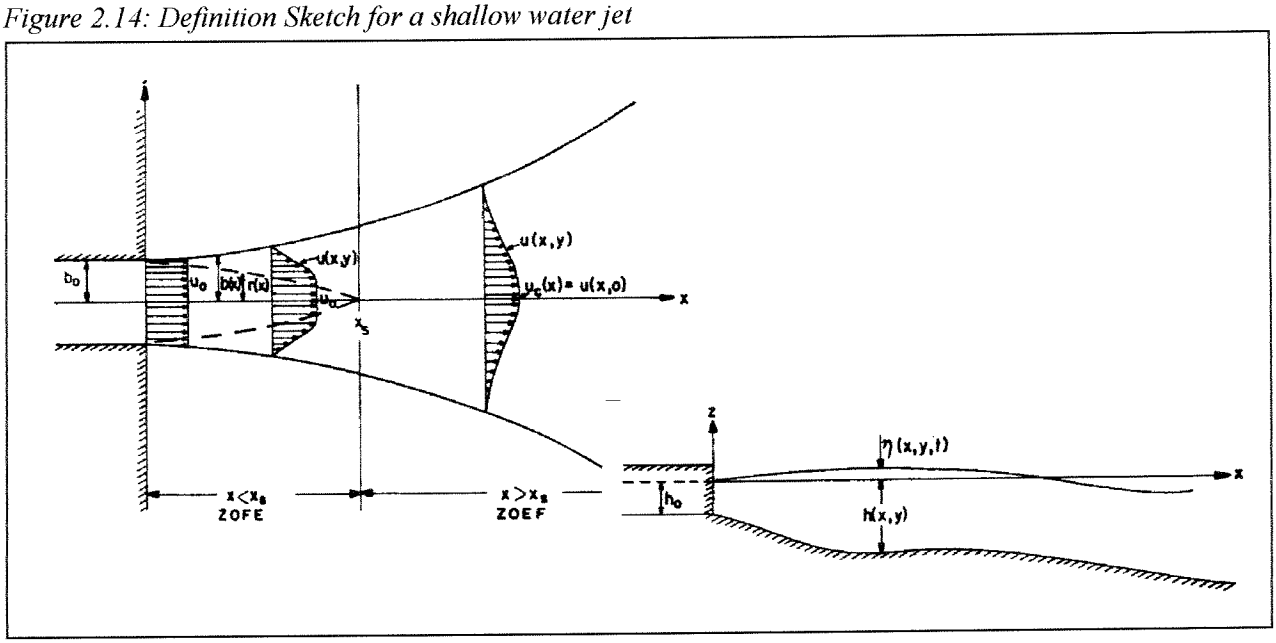

(From: Bruun, 1978)

Figure 2.15: Idealised tidal current patterns on the tidal inlet ebb tidal delta

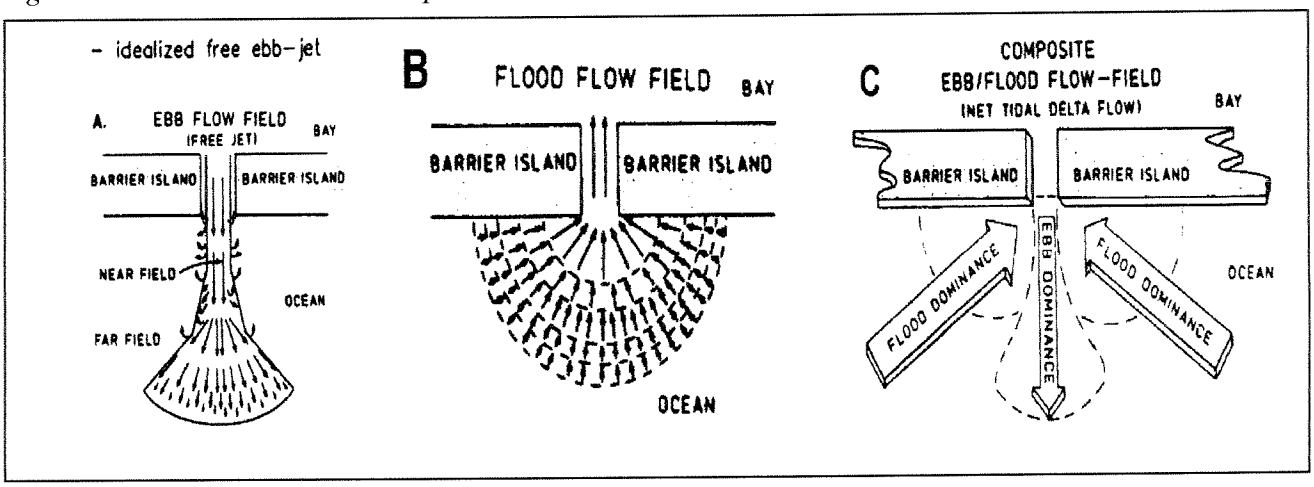

(From: Oertel, 1988)

the jet. Oertel (1988) described the most important phenomenon that influence this jet, they are:

- ***The bottom friction:*** The increasing bottom friction increases the rate of spreading of the jet and thus reducing the total length of the jet. It appeared that the spreading of the jet is exponential as opposed to linear for zero bottom friction.

- ***River discharge*:** Due to a river discharge the flow will have a character of a forced flow. Forced flows spreads more rapidly than non-forced flows with no river discharges.

- ***Waves and littoral current*** divert and compress the natural inlet jets. The most important force causing more (linear) spreading of the jet is the wave momentum-flux.

- ***Bottom slope*:** On a seaward sloping bottom, the jet streamlines tend to converge. If the bottom slope is horizontal the streamlines remain rather straight. The maximum velocity on a slopping bottom remains more or less constant.

The decrease in sediment transport capacity due to the blockage of the longshore transport current and the perpendicular decelerating tidal flow causes sediment depositions (dynamic diversion). The configuration of the shoals on the ebb tidal delta depends on contributions of these different flow patterns and the redistribution by the flood flow because flood flow on the seaward side differs from the ebb flow. Figure 2.15 (B) shows the flood flow distribution which can be described as a sheet flow with section as wide as 180° (Oertel, 1988). These different ebb and flood patterns results in a division of ebb and flood dominated section on the ebb tidal delta as illustrated in Figure 2.15 (C). It must be realised that the current patterns described above are idealised.

In some situations the flow on the ebb tidal delta is reversed in the bayward direction. The ebb tidal jet can cause a counter current nearshore circulation. This is called the *ebb-jet effect*. In Figure 2.16 can be seen that due to the configuration of the nearshore bathymetry of the ebb tidal delta, the ebb flow is forced in the main ebb channel. This may result in current circulation (eddies) near the barrier islands. The circulation can have, although the velocities are rather weak, an important influence on the sediment transport towards the tidal inlet gorge (Oertel, 1988). Refraction of waves on the ebb tidal delta supports this bayward current.

Another very important process that influences the idealised current pattern are the wave driven current caused by shoaling and breaking of waves on the outer edge of the ebb tidal delta, the so called ebb terminal lobe. The wave induced currents act different for ebb and flood flow in the outer edge of the ebb tidal delta. "During flood the wave induced water mass fluxes are in the same direction as the flood flow, during ebb flow this is reversed resulting in a cell-circulation, which causes a complex deposition pattern". (Steijn 1991) Bruun (1978) states that this phenomenon is stronger by lower tidal ranges. However it has not exclusively an influence on the current patterns, but also on the wave penetration through the gorge into the flood tidal delta. This phenomenon is illustrated in Figure 2.17. A more detailed description of the effects of waves and currents is given in section 2.4.4.

2.3.3. Wind driven currents

Due to shear stresses between the water surface and the moving air on the upper parts, waterlayers will start to move more or less in the same direction as the prevailing wind

Figure 2.16: Jet effect on the ebb flow

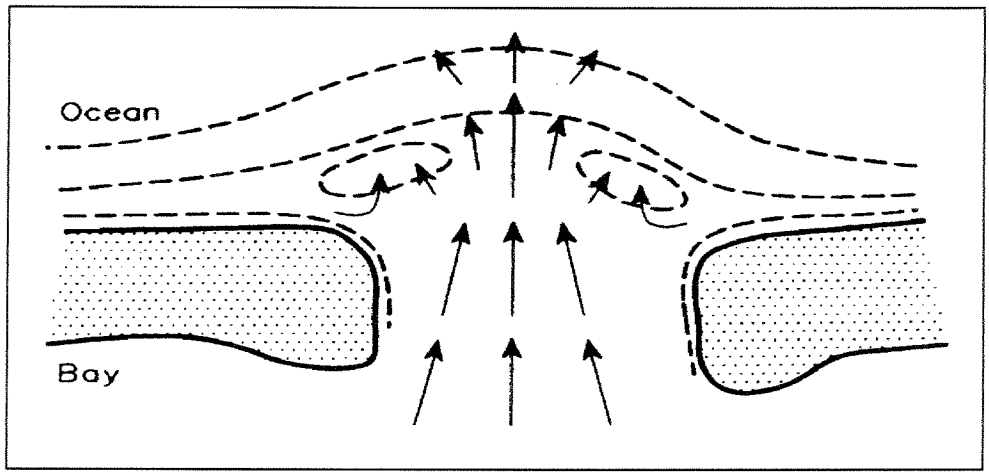

(From: Oertel, 1988)

Figure 2.17: Influence of waves on tidal currents on the tidal inlet terminal lobe

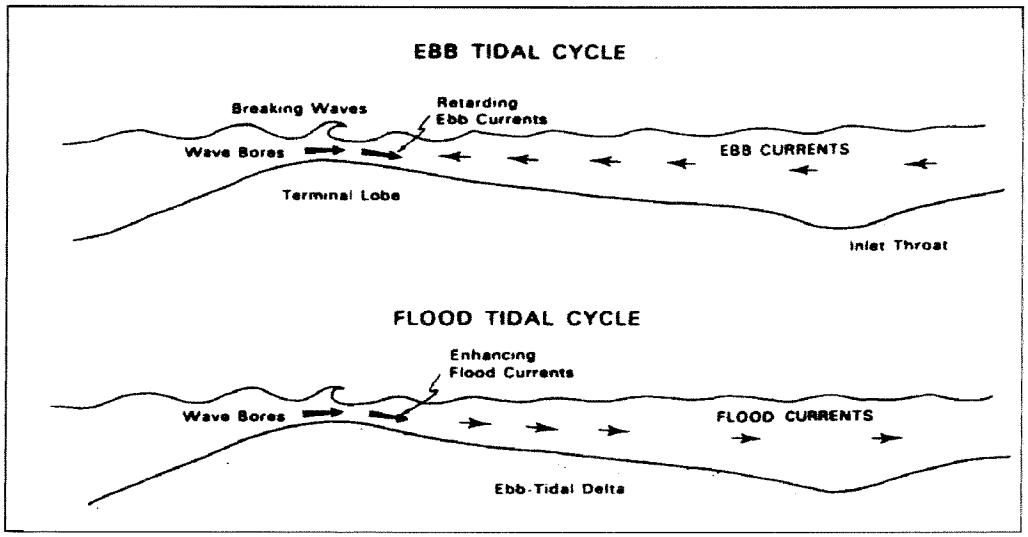

(From: Steijn, 1990)

Figure 2.18: Wind driven currents in the nearshore zone during storm conditions

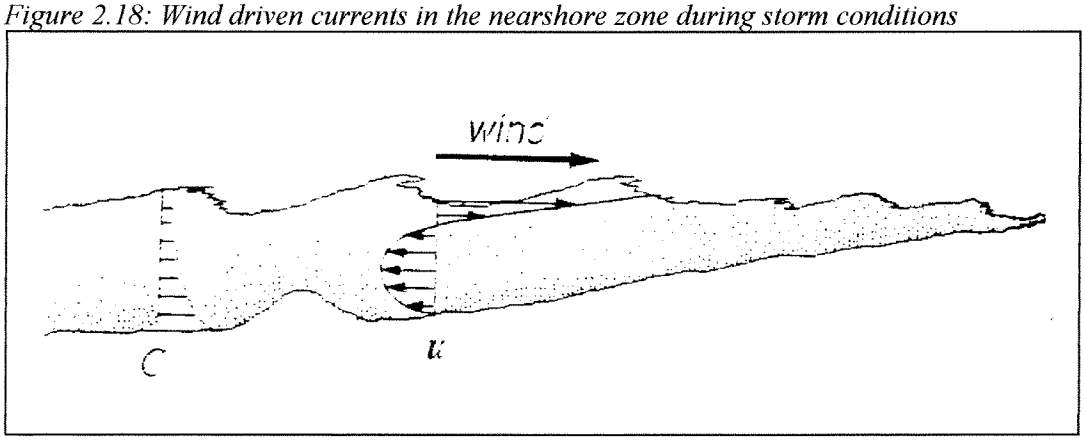

(From: Coastal Engineering, 1996)

direction (Steijn, 1991). In case the wind is shoreward, a strong landward-directed current is induced in a thin layer near the water surface and a compensating current along the bed. This offshore current may transport large amounts of sediment especially during storm conditions because of the presence of much suspended sediment in the nearshore zone. This effect is shown in Figure 2.18. The velocities are determined by the duration of the particular wind condition and its force. Similarly, a seaward wind will induce a seaward current in the thin upper layers and a compensating landward current in the lower water layer. (Matsunaga et al, 1996). In addition to these reverse currents a water level set-up or set-down can be created near the coast to compensate for the respective wind induced shear stress. This process is called upwelling and downwelling (Steijn, 1991).

Another important effect of the wind driven currents can be recognised in the interior basin of the inlet/bay system. Currents over the flood tidal delta flats are greatly influenced by wind forces. These currents can cause a flattening of the interior shoals and may induce a net sediment movement over the shoals. For dominant wind direction, a significant amount of water and sediment can be transported in this direction. This can result in a shift of the drainage divides behind the barrier islands causing a difference in the total amount of water flowing in and out of the tidal inlet changes.

2.3.5. Inlet currents

Looking at the previous sections it is obvious that inlet currents are very complex. However in order to get an impression of inlet currents in a given practical case some simplified methods can be used. The most common used methods are described in Bruun (1978) and Steijn (1990). Here two (easy to handle) simplified expressions are presented.

King (1974) used an analogue computer and applied time-variations in the coefficients resulting from the time variations in A_b (t). The solutions curves are given in Figure 2.19. In these solution curves (Shore Protection Manual, 1984):

$$V'_{max} = \frac{A_c \cdot T_{tide} \cdot V_{max}}{2\pi \cdot H_0 \cdot A_b} \qquad (10)$$

Given the basin and ocean tide characteristics it is possible to calculate the parameters B and G, after which the dimensionless $V`_{max}$ and the bay amplitude response follows (H_0 and H_b) Equation (10) then gives the solution for V_{max}. An estimate of the average flow velocity over the flood and ebb-tide can be obtained by taking $2/\pi$ of V_{max} assuming a sinusoidal sea tide (Bruun, 1978).

Drapeau (1988) gives the following expression, neglecting inertia, for the maximum value of the velocity averaged over the cross sectional area of the inlet:

$$V_{max} = \sqrt{\frac{2 \cdot g \cdot \eta_0 \cdot \sin(E)}{F}} \qquad (11)$$

A more mathematical, and probably more accurate, approach to tidal inlet hydrodynamics is given by van de Kreeke (1988) and is beyond the scope of this report.

Figure 2.19: Solution curves for basin and ocean tide characteristics

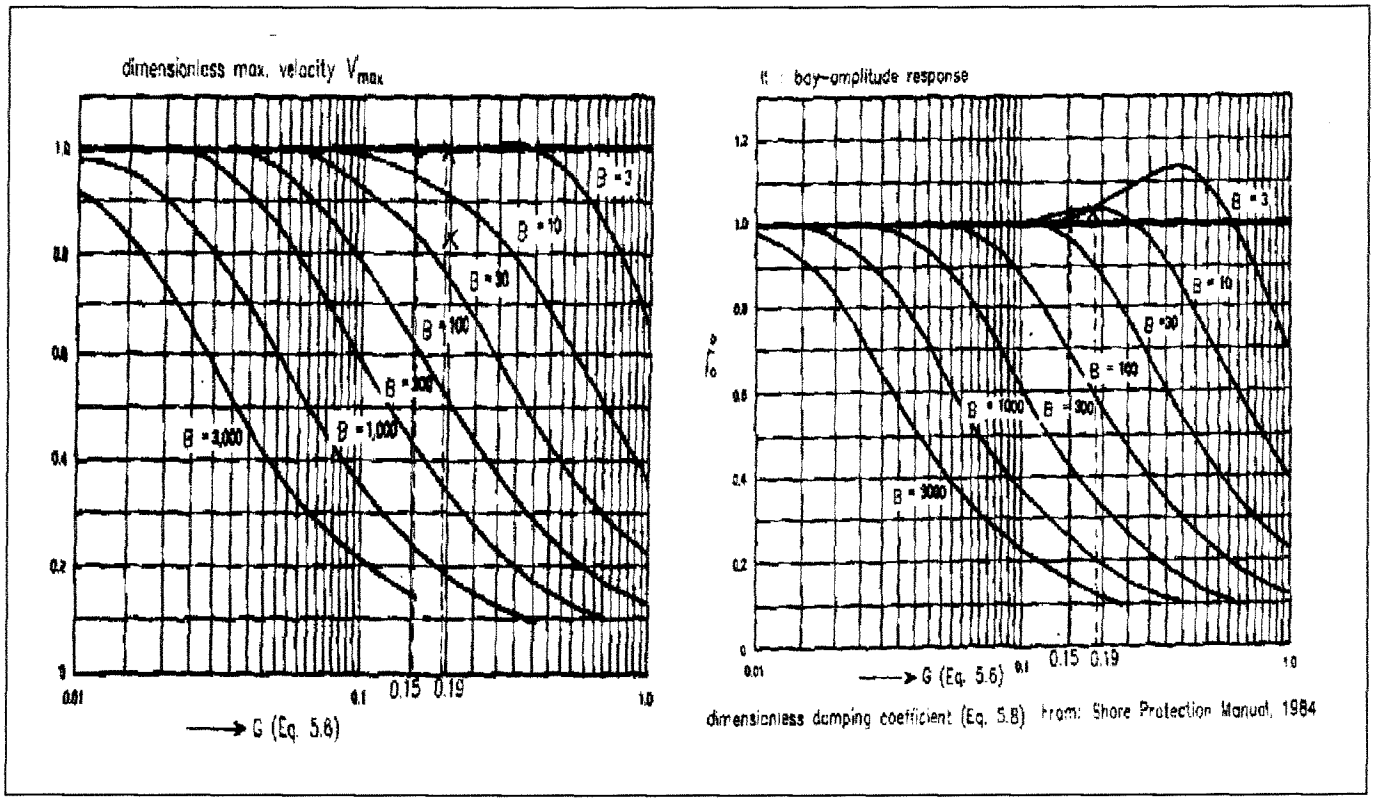

(From: Steijn, 1991)

Figure 2.20: Schematised transport and depth characteristics of an inlet channel with wave action

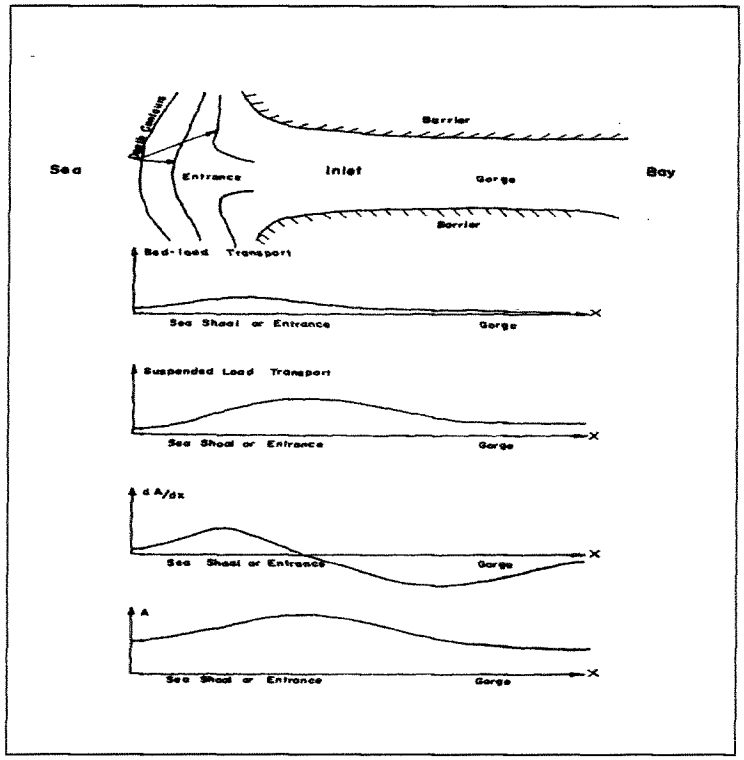

(From: Bruun, 1978)

2.4. Waves

2.4.1. Introduction

Currents are always present in tidal inlets on littoral drift shores. Waves are considered as the second most important active force. The wave height and period are the most important wave parameters for a specific wave climate. The direction of waves is important for the determination of the direction and magnitude of the littoral drift. The frequency of occurrence of a specific wave condition is also of importance because it determines its contribution towards the net annual littoral drift.

As pointed out before the morphology and development of inlets depends mostly on the relative importance of currents and waves. Both wave and currents have a significant effect on tidal inlet sediment transport patterns and therefore its morphology, not only for the three morphological sections but also for the adjacent beaches. A good description of sediment transport and sediment transport patterns in the vicinity of tidal inlets is very difficult but essential for a good understanding of the morphological development of tidal inlets. A pointed out earlier, tidal inlets can be split up into three morphological units: the ebb tidal delta, the flood tidal delta and the main entrance channel (including the gorge channel). Each of these has its own hydraulic exposure and therefore its own sediment transport characteristics (Bruun, 1978). Waves are primarily responsible for the shape and volume of the ebb tidal shoals and flood tidal shoals when significant amount of waves is able to propagate through the entrance gorge. Wave breaking on the ebb tidal delta results in a considerable amount of sediment in suspension, especially in the intermediate zone between the ebb tidal delta and the gorge channel. Moving towards the gorge wave action becomes limited and therefore the bed load increases and becomes predominant (Bruun, 1978). Bruun and Gerritsen (1960) give a schematically transport- and depth characteristics of an inlet channel with wave action as illustrated in Figure 2.20.

2.4.2. Impact of waves on the nearshore zone and the ebb tidal delta

Wave breaking on the adjacent beaches can cause an intensive cross-shore and longshore transport in the breaker zone on the updrift as well as the downdrift adjacent beaches. Sediment is supplied either from deep water or from the adjacent beach sections. The cross-shore sediment transport in into the breaker zone is either transported to the dry beach sections and than transported further by wind, or transported further along the coast by the wave driven longshore current. This mass transport by breaking waves into the breaker zone (onshore water movement near the surface) must be compensated by (near bottom) return currents in seaward direction. These return currents may be concentrated in more or less regular distances along the shore for instance in gaps along the breaker bar or alongside a breakwater. This concentration of this seaward directed cross-shore currents (rip current) might have a significant effect on the sediment transport out of the breaker zone into deeper water. The cross-shore and longshore currents together result in horizontal circulation cells inside the breaker zone. When a rip current is concentrated along a breakwater, significant amount sediment can be transported around the tip of the breakwater and into the entrance channel. This may cause a dangerous situation for navigation.

Wave breaking on the ebb tidal delta decreases the ebb delta growth and increases bed and particularly suspended load. The flood currents transports this sediment towards the flood delta shoals (Bruun, 1978). This has a significant impact on the height and development of the basin shoals, which will be described later in detail. An idealised tidal inlet is shown in Figure 2.21. This figure shows the influence of wave action on the ebb tidal delta. The breaking of

Figure 2.21: Idealised representation of the local drift reversal typically found on the downdrift side of tidal inlets

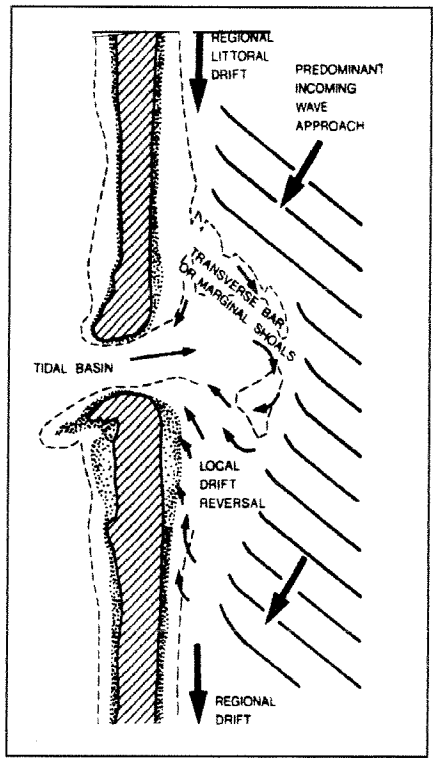

(Huis in `t Veld et al, 1987)

Figure 2.22: Example of reversed flow by wave refraction on the ebb tidal delta

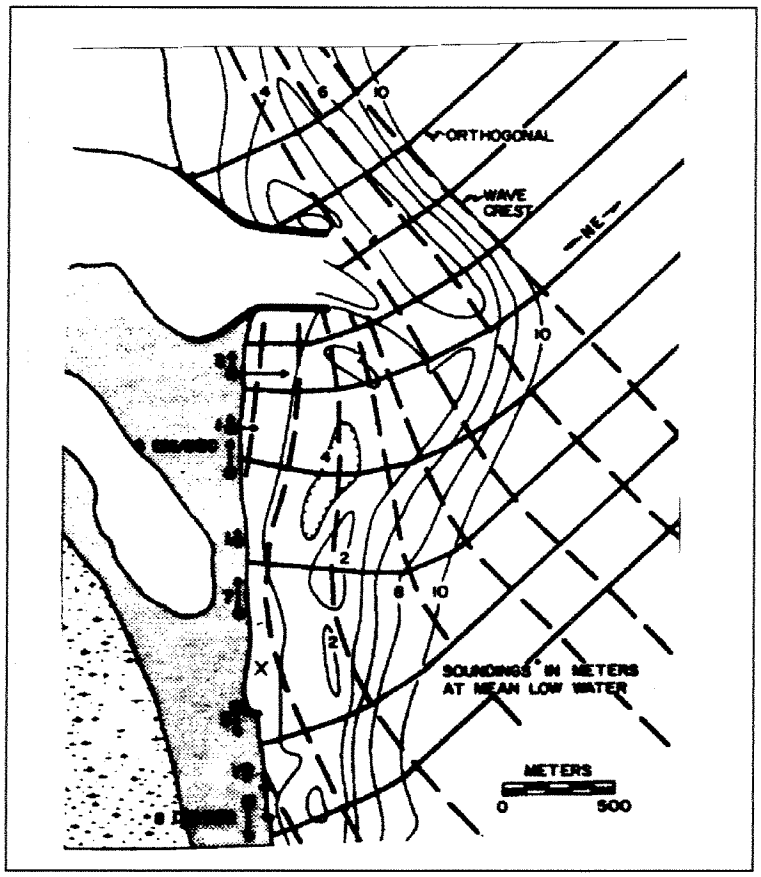

(Huis in `t Veld et al, 1987)

waves in the nearshore zone is the driving force of the littoral drift. Wave breaking in the nearshore zone causes a gradient in the radiation stress perpendicular and alongside the coast. The alongside gradient of the radiation stress is the driving force for the longshore current and determines the net annual sediment transport capacity (Van der Velden, 1995). The perpendicular component results in a slope of the mean water level with on the seaside a wave induced set-down and near the beach in a wave induced set-up (Van der Velden, 1995). When wave action is significantly different on a short distance along to the coast, for example as result of wave diffraction by a breakwater, gradients along the coast in set-up and set-down can cause a reverse current in the breaker zone. Another phenomenon, which may cause a reversed flow, is wave refraction on the ebb tidal delta. This occurs also when wave crests propagating parallel to the shoreline (changes in nearshore bathymetry). An excellent example of reversed flow caused by wave refraction is the Merrimack inlet USA illustrated in Figure 2.22.

Another impact of waves on the sediment transport capacity is the sheltering effect due to swash bars at the ebb tidal delta. The outer bars and shoals dissipate part of the offshore wave energy, creating a zone of reduced wave energy. In these zones the longshore transport capacity decreases and results in deposition of sediment into the flood channels. These two wave-determined mechanisms feed the inlet with sediment from the adjacent coastline, which is redistributed by tidal currents (Steijn 1991).

Figure 2.23 schematically shows the effect of waves on the earlier described two basic cases along the Dutch coast (see 2.2.1.). Four situations are considered: A and B correspond with the Wadden Sea inlets (no phase differences), and C and D correspond with the SW-coast, with a phase difference of a quarter of the tidal cycle. The direction of the wave energy flux is from the right (so opposing the direction of the tidal wave propagation) for situations A and C, and from the left (so in line with the tidal wave propagation) for situations B and D. The table in Figure 2.27 gives the classification of several Dutch inlets according to this scheme. This classification has been compared by with the appearance of these inlets in 1850, well before human interventions in the systems (Bruun, 1978). The agreement is good. It shows that:

- Inlets in the southwestern part of the Netherlands were typically type C inlets (with slight southward-located ebb channel due to wave flux coming from the north).

- The Wadden Sea inlets were typically type B inlets (with a more distinct westward located main ebb channel due to the zero-phase lag of the tidal currents at open sea and in the inlet gorge; predominant wave energy flux reduces this effect)

2.4.2. Impact of waves on the gorge and flood tidal delta

Waves do not have exclusively an effect on the ebb tidal delta but also in the flood tidal delta. Stabilised and trained tidal inlets in general have larger cross-sectional areas because they are less bothered by littoral drift. However larger cross-sectional areas mean in general that more waves propagate towards the flood tidal delta. The wave climate inside the flood tidal delta depends on the entrance geometry and the tidal currents. The uniform spreading of the wave energy in the basin is the most important factor determining the height of the intertidal areas as well as sorting and spreading of material. Combination of waves and currents enhance the wave penetration on the bayward side. This is caused by the interaction of currents on waves. According to Bruun & Jonsson (1978): "When a wave propagates through an area with a variable current, its length and height will change as well as its speed and direction of propagation". The effect of currents on waves is especially noticeable near tidal inlets, where

Figure 2.23: Effects of interaction of tidal currents on inlet morphology

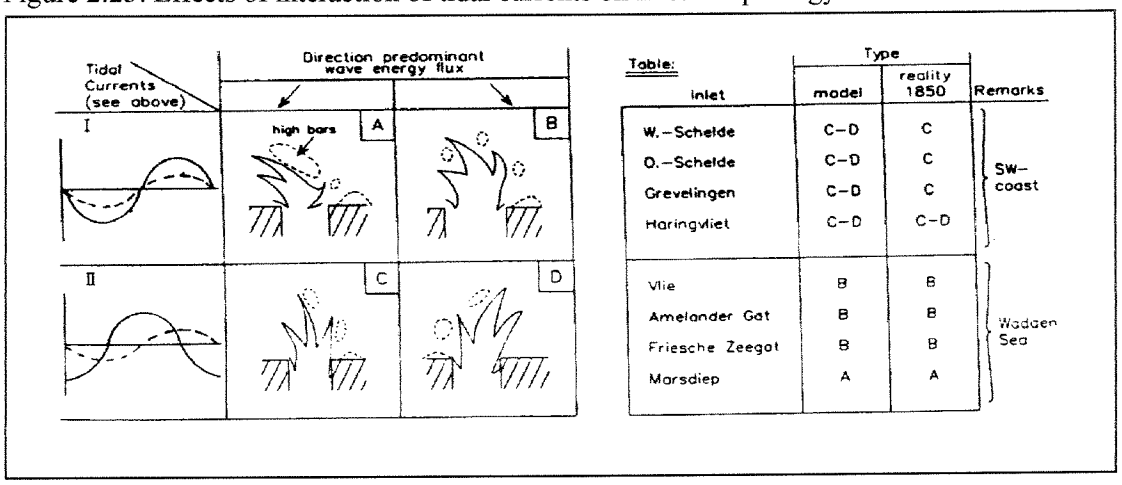

Table:

Inlet	Type: model	Type: reality 1850	Remarks
W.-Schelde	C-D	C	SW-coast
O.-Schelde	C-D	C	
Grevelingen	C-D	C	
Haringvliet	C-D	C-D	
Vlie	B	B	Wadden Sea
Amelander Gat	B	B	
Friesche Zeegat	B	B	
Marsdiep	A	A	

(From: Steijn, 1991)

Figure 2.24A and 2.24B: Wave refraction at a tidal inlet

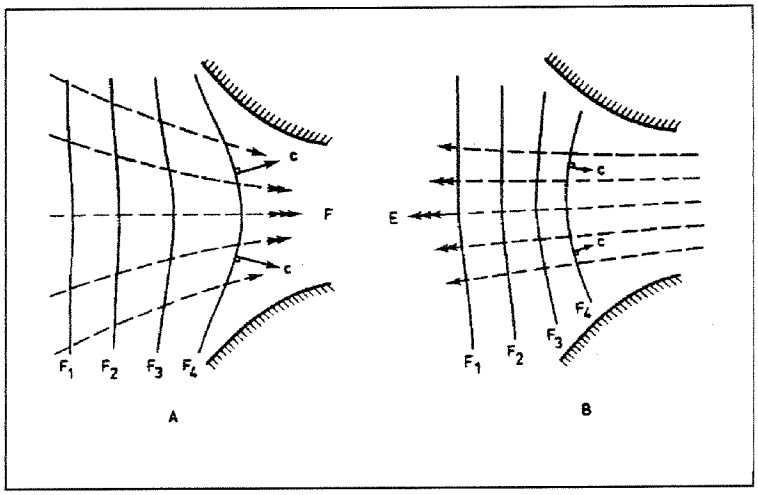

(From: Bruun, 1978)

Figure 2.25: Resultant tide and wave generated currents of an idealised tidal inlet

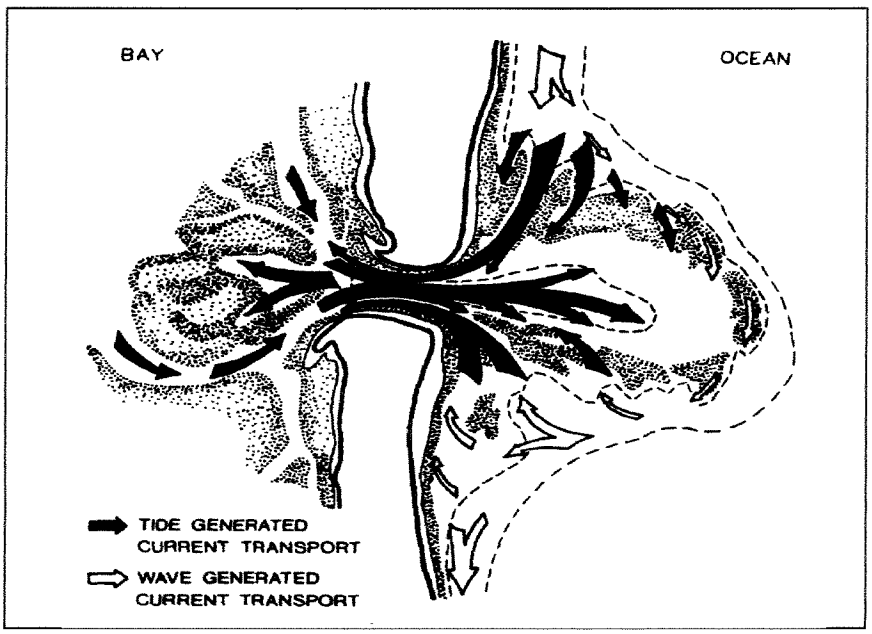

(From: Huis in 't Veld et al., 1987)

ebb and flood currents transform the waves considerably. Ebb currents in opposite direction of the wave propagation increase the wave height and steepness. This may result in wave breaking and a decrease of wave penetration in the inlet basin (Bruun & Jonsson, 1978). The increased wave steepness and possible wave breaking may cause a hazardous condition for navigation. Shoaling on the foreshore is an additional phenomenon increasing the wave steepness. Bruun & Jonsson (1978) described an example of wave steepening due to opposing current is found near South Africa, where sea waves of height 6 m meeting the Agulhas current can be tripled in height (!). Extensive damage to a number of ships has been reported in this area.

During flood the wave propagation and the flood current are in the same direction. The flood current increases the wavelength and decreases the steepness and tend to enhance the wave penetration into the flood tidal delta (Jonsson, 1978). This effect is shown schematically in Figure 2.24. Figure 2.24 (A) illustrates the spread of wave energy by the flood current and Figure 2.24 (B) the concentration of energy in the inlet middle by the ebb current. According to Bruun & Jonsson (1978): "In `A` the `following` flood current increases the wave length. As the current speed and the water depth normally is highest in the middle of the channel, a spread of energy towards the channel sides occurs at the same time. In `B` the `opposing` ebb current augments wave height and reduces wavelength, thus having a double effect on the wave steepness increase. The distinct difference between the structure of ebb and flood current appearance on the ocean side should be brought to light in this connection. While the flood current slowly builds up from a region of very small velocity to a maximum at the inlet throat, the ebb currents has a jet-like structure out from the inlet and can be felt much further offshore".

Another interesting phenomenon described by Steijn (1991) is the so called *tunnelling-effect* and the energy transfer of waves penetrating through the gorge into the flood tidal delta channels. Due to the lower bottom friction as a result of deeper water, waves propagate further in the bayward tidal channels compared to the tidal flats, which result in a wave energy transfer out of the channels. This is reduced by the reflections on the channel boundaries. Wave reflection on the tidal flats to the channels can also take place. This results in a concentration of wave energy at the landward end of such a channel. This concentration of wave energy may cause erosion on the bayward side. Wave breaking and energy dissipation on the ebb tidal delta is of crucial importance to the development of the shallow areas at the bayside of the inlet. Due to breaking and bottom dissipation the wave heights and periods are reduced significantly. Spectral analysis of wave records detects that an energy transfer to higher frequencies occurs when waves are propagating towards the inlet. The higher and longer waves are transferred into a large number less high but steeper waves (Steijn, 1991).

The previous sections discussed the hydrodynamic characteristics that are valid in the vicinity of tidal inlets on littoral drift shores. All these characteristics together form resultant current patterns. Figure 2.25 illustrates the resultant tide- and wave generated currents of an idealised tidal inlet.

Figure 3.1: M_s/pM_t versus τ/τ_s for tidal inlets

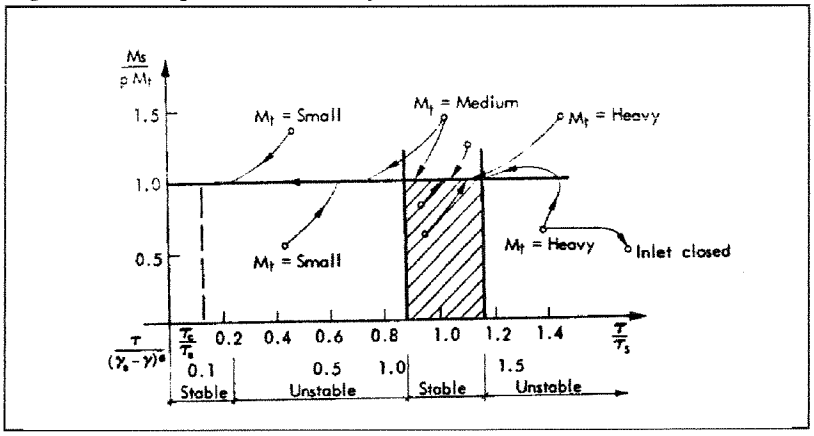

(From: Bruun, 1978)

3. Development and morphology of tidal inlets

3.1. Introduction

The previous sections described the impact of the specific hydrodynamic forces on tidal inlets. The development and the stability of tidal inlets are very much related. It is obvious that unstable tidal inlets induce developments and reverse. The stability of tidal inlets will be described later, in terms of several stability relations. The following sections describe the developments of the separate morphological sections as well as the interactions. The gorge channel plays a crucial role in the development and stability of the inlet because it is the connection and the transport unit that provides and determines the current distribution and sediment transport to both the flood- and ebb tidal delta. Special attention will be paid to the development and equilibrium condition of the ebb tidal delta because it determines the stability and is of crucial importance for navigation. As a result of the development of tidal inlets large amounts of sediment are either naturally bypasses or extracted from the littoral drift. It is obvious that these phenomena have significant influence on the tidal inlet itself, as well as on the adjacent beaches (Figure 3.1).

3.2. Bottom shear stress and stability shear stress

An important parameter for the development and stability of tidal inlets on littoral drift shores is the bottom shear stress. Bruun (1978) describes the development of tidal inlets after breakthrough by the ratio between the bottom shear stress and the stability shear stress (or critical shear stress). This development is described in the next section. Waves and current affect both the gorge channel and ebb tidal delta. Wave action is more pronounced on the ebb tidal delta and decreases when moving towards the relatively narrow and shallow gorge channel. For stable and relatively deep trained entrances wave action inside the entrance channel have significant influence on the bottom shear stress. The bottom shear stress (τ_b) depends mainly on the bottom roughness, cross-sectional area and the maximum (spring tide) flow conditions. For steady flow the current induced shear stress acting on the gorge channel bed can be calculated as:

$$\tau_{bc} = \frac{1}{2} \cdot f_c \cdot \rho_w \cdot V^2 \qquad (12)$$

In which : $f = 8g/C^2 = 4\, f_c \leftrightarrow f_c = 2g/C^2$ (*Darcy-Weisbach friction factor*)
V = Depth average current velocity [m/s]
C = Chezy coefficient [$m^{1/2}/s$]

Grant and Madsen (1978) prescribed the following relation for the shear stress due to both waves and currents as:

$$\tau_{cw} = \frac{1}{2} \cdot f_{cw} \cdot \rho_w \cdot V_t^2 \qquad (13)$$

In which: f_{cw} = Wave-current friction factor
V_t = Combined wave-current velocity over the bottom

The stability shear stress or critical shear stress (τ_{cr}) is defined as the average shear stress along the bottom, of an inlet-cross-sectional area which is stable under maximum flow conditions. Or in other words, when the stability shear stress is exceeded, the particle moves from the bottom and will be transported by water movement. The larger τ_{cr} the better are the

conditions for cross-sectional stability. The τ_{cr} value depends on the following factors (Bruun, 1978):

- *Soil conditions of the bottom*, coarser bottom material will usually give higher values for τ_{cr} than finer material.
- *Suspended sediment load.* Increase of the amount of suspended sediment load (stirred up by wave action, turbulent flow, or silt load from rivers) decreases the resistance of a channel due to reduced turbulence. Consequently, the value for τ_{cr} will increase.
- *Wave action*; will decrease the stability shear stress τ_{cr} as it may considerably increase the bed load transport by tidal currents.
- *Littoral drift* influences the shape of the inlet, but also supplies the inlet currents with sediment. Increase in littoral drift will raise the value for τ_{cr} relatively. Karssen and Wang (1991) stated that the τ_{cr} value varies from 3.5 N/m^2 for small littoral drift to 5.5 N/m^2 for large littoral drift and subsequent sediment load.

3.3. Development and morphology of the main entrance channel

3.3.1. General

The tidal gorge and the intermediate section form the main entrance channel that connects the ebb tidal delta and the flood tidal delta, so it is obvious that these two morphological units are highly influenced by the behaviour of the gorge channel. The three morphological units together form the tidal inlet system so it's not hard to imagine that the overall stability and development depends on the behaviour of the entrance channel. The tidal gorge the narrowest and deepest section of the total tidal inlet. Both ebb- and flood currents are concentrated in this gorge. The following sections describe in general the development of inlet gorge section. In addition, some attention will be paid to the `equilibrium` condition and the non-scouring condition.

The developments of a newly born inlet, resulting from a severe overwash during a hurricane, typhoon or severe storm has in the initial state of development, a relatively short gorge and its cross-section will be increased by the tidal flow. In the inlet gorge the sediment is mostly transported as bed load. This bedload movement of sediment may be compared to "rolling carpets" on the bottom of the gorge. Parts of this carpet are lost to the shoals at both sides of the tidal inlet. Figure 3.1 gives a relation between currents flushing ability and the littoral drift to the gorge. Assuming that the total littoral drift from both sides to the gorge is pM_{total}, where p indicates the percentage of material from the total littoral drift, which interferes with the gorge. The quantity of material transported by the gorge current is M_S (flushing ability). Due to tidal water movement on a bottom, shear stresses will be generated. These bottom shear stresses influencing the cross-sectional area for flow are τ. Figure 3.1 illustrates the inlet developments in different cases by the ratio τ/τ_S, where τ_S is the determining shear stress for bottom stability (stability shear stress) (Bruun, 1978):

- $M_S \geq pM_{total}$, which means that the inlet currents are able to flush the material supplied from the littoral drift.
- $M_S \leq pM_{total}$, which means that the inlet currents are not able to flush the material supplied from the littoral drift.

After creation of a new inlet by a breakthrough, development starts, because more material is flushed out than deposited in, which scours the new entrance channel. The situation is as follows: $M_S / M_{total} > 1$. The entrance channel cross-section will increase and the τ/τ_S will decrease. If M_{total} is rather small the channel will be develop towards a non-scouring channel. If M_{total} is relatively large, the inlet may develop a stable channel with a τ_S value in accordance with the outside input of sediment load. In case $M_S/M_{total} < 1$, which means that the entrance currents are not able to flush all the material brought in by the littoral drift, therefore the ratio τ/τ_S increases; the cross-section decreases and the inlet narrows. If Mtotal is relatively small a stable situation may not be reached, but the gorge may also gradually deepen and widen and develop slowly towards a non-scouring condition. If M_{total} is very large, the channel may or may not develop towards stability. If the inlet has large tidal prism, the first possibility is most likely to happen. If the tidal prism is smaller, the inlet most likely closes. (Bruun, 1978)

The equilibrium condition is reached when the inlet channel currents develop a bottom shear stress, which is able to keep the channel free from deposits without scouring the channel considerably. ($\tau = \tau_S$) This situation occurs if the total transport of material from the ocean into the gorge equals the bed load movement through the gorge by ebb and by flood, or in other words, the flushing ability of the tidal inlet equals the amount of littoral drift to the inlets from the sides ($M_S = pM_{total}$). If a state of equilibrium is reached it may not be everlasting because deposits at both ends, increase the length of the channel. When the inlet reaches a certain length, depending on the tidal prism and the littoral drift, currents have gradually weakened which results in a decreased cross-sectional area. This sedimentation of the gorge decreases the tidal prism, which may finally result in less ability of the gorge channel to flush the material brought in by the littoral drift, which may finally close up the inlet. It may be concluded that, as a result of a severe storm, large and particularly irregular littoral drift combined with small tidal flows due to low tidal ranges and perhaps a modest lagoon area, may result in shoaling and finally close up of the inlet (Bruun, 1978).

Non-scouring entrance channels are not bothered by scouring currents inside the entrance channel. Consequently littoral drift or other sediment supply, apart from suspended material must not bother it. From this follows that it either has to be located on the immediate downdrift side of a complete littoral drift barrier, or it must be protected by breakwaters on either side. These structures in this case must extend oceanward beyond the active littoral drift zone. A third possibility is that the inlet is located in a very definite littoral drift nodal area for instance on a protruding headland from which material leaves towards either side. A fourth possibility is at the downdrift of another `complete` littoral drift barrier, for instance a detached breakwater. Non-scouring channels may also develop in cases where a tidal inlet is stabilised with relatively short breakwaters and a bypass-installation on the updrift side of the inlet. In these cases the net littoral drift is directly bypassed into the downdrift active littoral zone. The entrance channel in the most favourable cases not bothered by littoral drift. Tidal currents are able to scour the entrance channel. With increasing cross-sectional area, results in decreasing tidal currents. This continues until the tidal currents are decreased below the threshold of grain motion.

As described above, the development of an inlet gorge towards non-scouring results in a gradually deepen and widen of the gorge cross-sectional area. This is important because the gorge must have sufficient depth to prevent bottom creep (see also 3.3.2) of material into the gorge, and tidal velocities must be reduced to where there is no movement of bottom sediments within the gorge.

Development towards non-scouring entrance channels the following adverse effects have to be considered:

- Possibility of such low tidal velocities as to fail to create adequate flushing action and cause pollution problems;
- A wide entrance channel may permit excessive wave energy to be delivered to the inner basins. Measures must be taken to properly dispose of this wave energy by either absorption or reflection.
- Breakwaters have to be designed without large voids in the tide and wave zone. In the case of Mission Bay the breakwater design had to be corrected because of the use of cap rock only in the tide and wave zone above mean lower low water level. The large voids (35 to 40 %) inherent in cap rock permitted an excessive amount of littoral sand to pass through the jetty into the channel. Sealing of portions of the jetties effectively reduced this shoaling factor". The impact of jetty design on the tidal inlet morphology was also investigated in model experiment by Wang et al. (1996).

Bruun (1978) concluded that Non-scouring channels are favourable for navigation but have high initial costs and requires special conditions such as availability of a comparatively small open bay or lagoon. The more important the inlet is from an economical point of view, the more justifiable the development of a non-scouring channel.

3.3.2. Factors influencing tidal throat geometry and orientation

Bruun (1978) described the factors influencing the cross-sectional area. FitzGerald (1976) studied tidal inlets in North and South Carolina (USA). He concluded that the size and depth of the entrance channel depends on the relative importance of tides and waves. On microtidal coasts, where inlets are wave dominated, the gorge is relatively shallow and small, unless their bay areas are substantial. Tide dominated coasts indicate large tidal prisms resulting in relatively large and deep cross-sections (Bruun, 1978). The relatively small and shallow gorge, on microtidal inlets, results from a difference in wave action on the ebb tidal delta and the gorge. Wave breaking over the bars and shoals on the ebb tidal delta causes a strong increase of bed and particularly suspension load. Due to the lag of sufficient tidal currents, the gorge is not able to flush this high sediment load and the cross-sectional area of the gorge decreases (Bruun, 1978). FitzGerald (1976) also investigated the factors influencing the throat section symmetry. He found three main factors that influence the throat symmetry on mesotidal inlets. "They are, in order of their importance, the meandering of the channel thalweg, the inlet shoreline configuration and the dominant longshore transport direction. The sedimentological nature of the channel banks and bottom also have an influence on throat configuration".

Tidal inlets particularly on tide dominated coasts show water level variations inside the flood tidal delta with a typical time-velocity asymmetry which results in longer flood duration, and with the same tidal prism, a stronger ebb flow through the gorge. This phenomenon was already described in Section 2.3.1. In addition significant wave action over the offshore bar may influence the time velocity asymmetry by increasing flood flows over the ocean bar. It is obvious that this time-velocity asymmetry has a significant impact on the throat geometry. Assuming that the rate of sediment transport through the inlet is proportional to the current velocities, ebb currents are able to transport far more sediment than flood currents. This ebb current dominance in bed load capacity (net outward transport) at the inlet results in a natural flushing ability. The latter is very important because it naturally keeps the inlet from silting

Figure 3.2: Price inlet in South Carolina

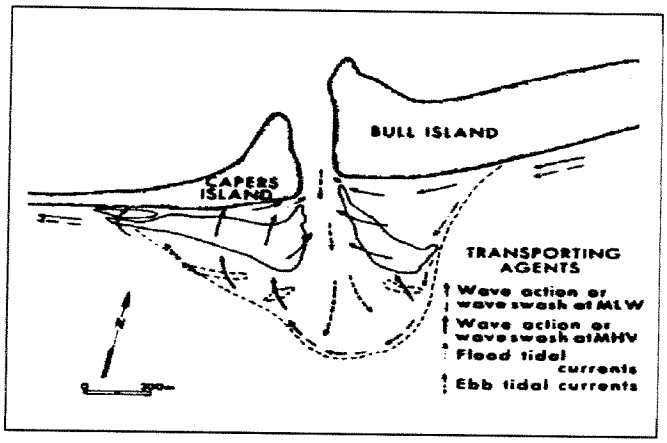

(From: Bruun, 1978)

Figure 3.3: Inlet channel orientations

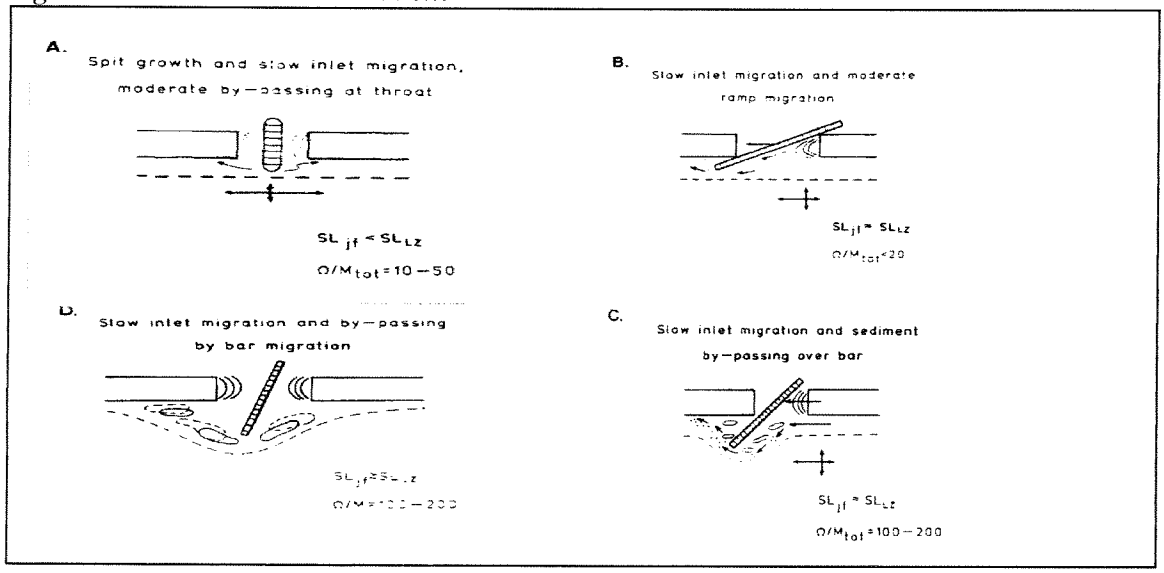

(From: From: FitzGerald, 1982)

up, especially during severe weather conditions, by flushing the relatively high bed and suspended load entering the inlet during flood (Bruun, 1978).

The stronger ebb currents are also responsible for long term adjustments of the throat geometry (Bruun, 1978). FitzGerald studied the tidal throat geometry of the central South Carolina inlets over the last century. These inlets have constricted due to spit accretion at both sides of the inlet throat. In order to maintain their flow areas, the inlets have scoured their channel bottoms and deepened. FitzGerald studied the Price Inlet in South Carolina, illustrated in Figure 3.2. FitzGerald (1976) concluded that the gorge responds rapidly to the changing flow conditions, "as evidenced by a good correlation between throat cross-sectional area and tidal range for the half tidal cycle directly preceding the recordings of the individual cross-sections". He also concluded, by looking at these particular cases, that changes on the ebb tidal delta can have a significant influence on the inlet gorge geometry. When the shoals on the ebb tidal delta reaching a certain depth, natural bypassing of sediment across the inlet becomes significant. If the offshore bar increases in volume, it is be able to bypass more material across the gorge. Because less material is entering the gorge the cross-sectional area may increase slightly. However the ebb flow may decrease somewhat at the same time because of the increased length and therefore increased resistance of the flow. On the other hand, increased bar volume means also more wave breaking, especially during storms, which causes more material stirred up outside the entrance and therefore more sediment transport towards the entrance decreasing its cross-sectional area. As mentioned earlier this section, the amount of littoral drift has a crucial impact on the cross-sectional area of tidal inlets. Inlets exposed to heavy littoral drift generally have smaller gorges with respect to other inlets with less littoral drift and the same tidal prism. Despite of this heavy littoral drift, the cross-sectional area may increase due to increasing bottom shear stresses by storm waves. This increasing shear stress on the bottom increases the mobility of the grains and the transport of material.

Another interesting phenomenon causing cross-sectional asymmetry is sediment movement towards the side of the gorge channel because of the higher sediment concentrations in the middle of the channel. These higher sediment concentrations are the result of the locally higher velocities in the channel. Therefore, deposits of material on the banks will occur, causing an increased channel slope, which will cause bed load movement towards the middle of the channel by the combined action of gravity, current shear and uplift forces. At a certain slope an equilibrium condition will be established (Karssen and Wang, 1991).

The orientation of the entrance channel is determined by the hydraulic conditions. In section 2.3.2 the jet-effect was already discussed. Littoral and coastal currents may divert these jets. The littoral currents are the most important agents of inlet current division. Coastal currents play a limited role seaward of the littoral zone. Oertel (1988) illustrated potential morphodynamic relations for several different conditions. He defined the Seaward Limit of a natural inlet jet field (SLjf) and the Seaward Limit of the littoral zone (SLlz) and vectors of current diversion. Oertel estimated the (Sljf) as the section from the inlet gorge to the distal end of the ebb tidal delta, and the (SLlz) by the mean line of breakers as the seaward limit of the littoral zone. (Oertel, 1988) When the net effect of the longshore current is diversion of the jet, a reorientation of the inlet channel is required.

Figure 3.3 illustrates channel orientations caused by different magnitudes of inlet migration and sediment bypassing. Type A deltas represent a condition where the extent of the jet field is approximately equal to or less than the seaward limit of the littoral zone. Diversion of the inlet jet by the littoral current is significant with almost complete inclusion of the inlet flow into the littoral zone. In this case most of the littoral zone is active in sand bypassing across the inlet. The associated P/M_{total} ratio may range from 10 to 50. For a description of the

Figure: 3.4A and 3.4B: Idealised typical delta formations for tidal inlet on littoral drift shores

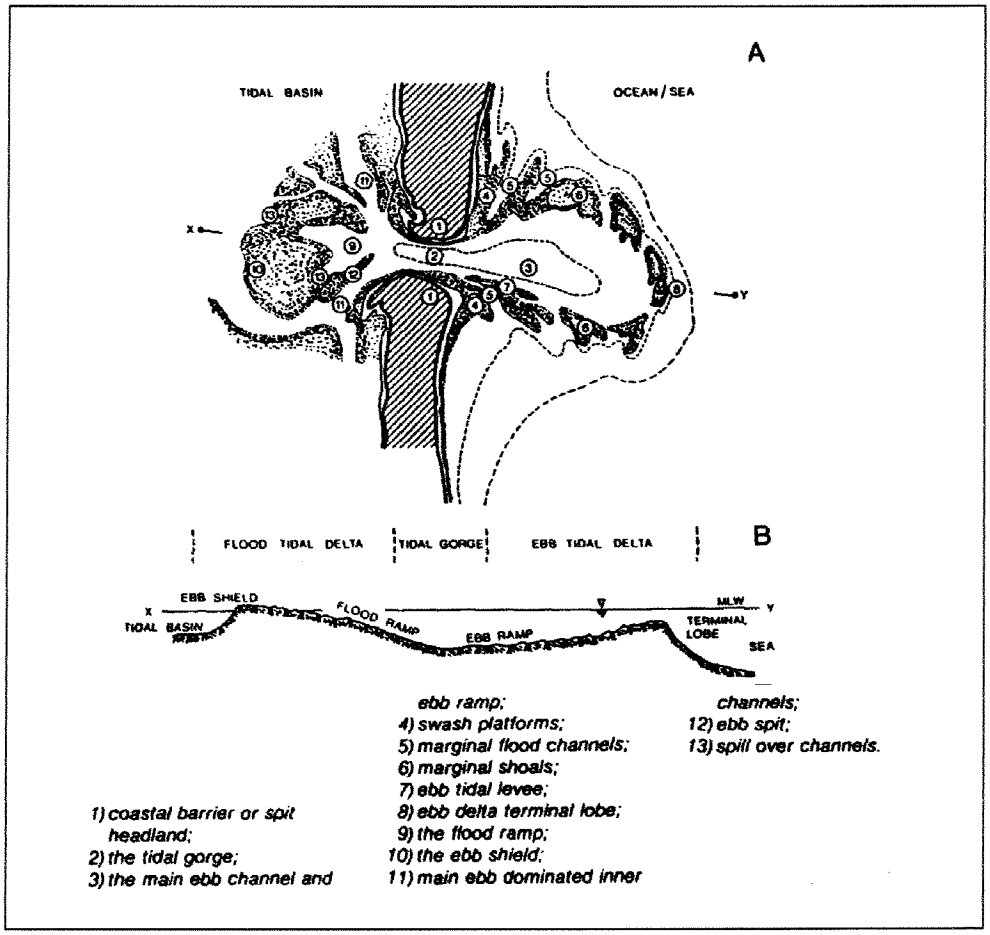

(From: Huis in `t Veld et al, 1987)

meaning of the P/M_{total} ratio reference is made to section 3.7.1. In cases where the ratio P/M_{total} ranges from 10 to 50, almost complete littoral bypassing of the inlet is accomplished, and little or no material is diverted to the shoreface. The slow migration of the inlet is dependent on the small amount of material that does not bypass the inlet but is deposited on proximal spits and shores on the updrift side of the channel. Type B and Types C deltas are variations of deltas that fall between the Type A and Type D categories. Type B shows the deposition occurs at the proximal end of the inlet (in spits) sand bypassing occurs at the end of the inlet at the edge of the littoral zone. Type C shows slow sediment bypassing occurs over the bars at the distal end of the inlet channel and Type D shows a slow sediment bypassing takes place by bar migration over the shoals at the distal ends of the inlet channel. For these cases diversion of the inlet flow is partial and the seawards limit of the littoral zone. When the P/M_{total} is relatively low then bypassing and channel margin accretion may occur entirely within the littoral zone. (Type B) With a downdrift orientation of the resultant jet, the proximal end of the gorge migrates in response to sediment accumulation on the updrift shore of the inlet. Distal ends of the gorge migrate in response to rates and characteristics of bar bypassing in relative close proximity to the littoral zone. If P/M_{total} is relatively large, then bypassing is relatively slow and it may be accomplished by littoral sediment transport directly across the bar system. Bar bypassing occurs where sediment is transported directly across the bar by the diverted littoral current (Type C). The decease in the rate of bypassing, with respect to the case described by Type B, generally results in an oblique orientation of the ebb delta and channel. Bar migration bypassing occurs where the primary means of bypassing is governed by bars migrating over the surface of the ebb tidal delta. These deltas produce pronounced seaward inflections in the shoreface contour lines. The slow migration rate of bars is similar in magnitude to the rate of inlet throat migration (Type D). When the orientation of the inlet channel is approximately normal to the shoreline, then the rate of filling along the throat margins at the distal end of the ebb channel. This type of inlet appears to migrate slowly and thus its migration may be inhibited by pre-Holocene topographic depressions.

3.4. Development and morphology of the ebb tidal delta

3.4.1. General

The ebb tidal delta is the seaward bulge of sand formed just seaward of the tidal inlet. Figure 3.4 illustrates an idealised, typical ebb delta morphology. The ebb current scours the main ebb channel, flanked by channel margin linear bars and wide swash platforms. The channel margin linear bars are formed by sedimentation caused by the laterally decreased current from the gorge along the edge of the jet. Swash bars on either side of the inlet can form sand shoals, which can be attached to the barrier beaches by wave action. Continued accretion due to this phenomenon eventually may result in a downdrift offset (Huis in `t Veld et al., 1987). Swash bars are essentially sediment masses taken from the longshore drift. They are formed at the inlets because of a combination of the influence of: (1) the ebb tidal currents, which deposit the main lobe of the ebb tidal delta, and (2) wave refraction around the lobe, which tends to slow down, or halt, the transport of sand past the inlet. The marginal flood channels separate the channel margin linear bars from the adjacent beaches. (Shore Protection Manual, 1984).

The dynamic diversion of the ebb jet causes the longshore current to bend in seaward direction. On the transition of the two flow patterns the sediment transport capacity will decrease resulting in a sediment deposition (marginal shoals) (Huis in `t Veld et al., 1987). Ebb tidal delta acts like a bridge for sediment to bypass the tidal inlet in order to prevent massive downdrift erosion. The bypassed sediment may be returned to the tidal basin by a

complex combination of currents and waves on the ebb tidal delta. Refracting waves and the ebb-jet effect over the ebb tidal delta causes a partly local reversal of the littoral drift immediately on the downdrift side of the tidal inlet entrance. This local reversal causes some sediment bypassed along the outer shoals to accumulate on the swash bars downdrift of the inlet entrance. (Huis in `t Veld at al., 1987)

Most of the ebb tidal deltas are ringed by a complex system of marginal shoals. These shoals are very dynamic because of continuous exposure of waves and currents. In most cases shallow channels separate the ebb delta marginal shoals. These channels are deeper on the outer parts of the ebb tidal delta because the flow in this region is ebb dominated. Near the barrier islands the channels are flood dominated (Huis in `t Veld et al., 1984). The occurrence of flood and ebb dominant channels on the ebb tidal delta can be explained as follows. Due to the time - velocity asymmetry the following situation exist: maximum ebb velocity occur at about low water, so during the first stages of the flood tide, the ebb-jet maintains some inertia (ebb-currents are still flowing out blocking the flood currents). Steijn (1991) states that the turning of the tide in the tidal channels and on the top of the tidal flats depends on the ration of inertia and friction. Inertia forces are strongest in the tidal channels, and consequently, the flow direction will not instantly change as the water level slope changes. Friction forces are strongest on the top of the tidal flats. This will result in relatively low flow velocities. Because the inertia forces are relatively small on the top of the tidal flats, the flow direction will follow more or less the water level slopes. The turn of the tide (slack water) thus comes a little later in the channels than on the top of the tidal flats. Due to the inertia forces, the flood currents initially cannot flow towards flood tidal delta trough the whole cross section of the entrance channel. As a result of this, the flood current is forced along the barrier coasts. In a later stage of the flood flow, the currents use the whole entrance channel cross sectional area (Huis in `t Veld et al, 1984) The ebb delta morphology and sediment transport patterns reflect all the above mentioned processes.

Resent investigations by Dombrowski and Mehta (1996) on the ebb tidal delta evolution show that also some other parameters than pointed out before play a role in the ebb delta development as well as the equilibrium bar shape. Previous investigations have established the dependence of the ebb delta volumes on wave energy and tidal energy at tidal inlets on littoral drift shores. Dombrowski and Mehta (1996) examined this with respect to the rate off delta growth and the final equilibrium delta volume starting with the opening of a new inlet when no ebb delta is present. Dombrowski and Mehta (1996) developed a diagnostic model for examining the influence of the ratio of wave energy to tidal energy on delta growth by solving a derived differential equation by numeric integration. The model was applied to five Florida inlets. The overall conclusion was that the ebb delta may never attain a true equilibrium volume. The actual volume fluctuates about a `quasi-equilibrium` volume consistent a wave energy to tidal energy ratio representative of the long term wave and tidal conditions at the entrance. For more information on the wave energy to tidal energy reference is made to Dombrowski and Mehta (1996).

Dombrowski and Metha (1996) investigated the effect of following parameters on the ebb tidal growth:

1. Suspended sediment concentration: It was evident that the with an increasing sediment concentration the time of sedimentation becomes more rapid. Increasing the suspended sediment concentration in the littoral zone caused increased delta growth equilibrium, but it did not influence the equilibrium volume.

2. Median sediment grain size: The increase in sediment diameter increases the rate of deposition, due to the dependence of particle fall velocity on the sediment size. An increasing

Figure 3.6: Ebb tidal delta of Boca Grande Inlet

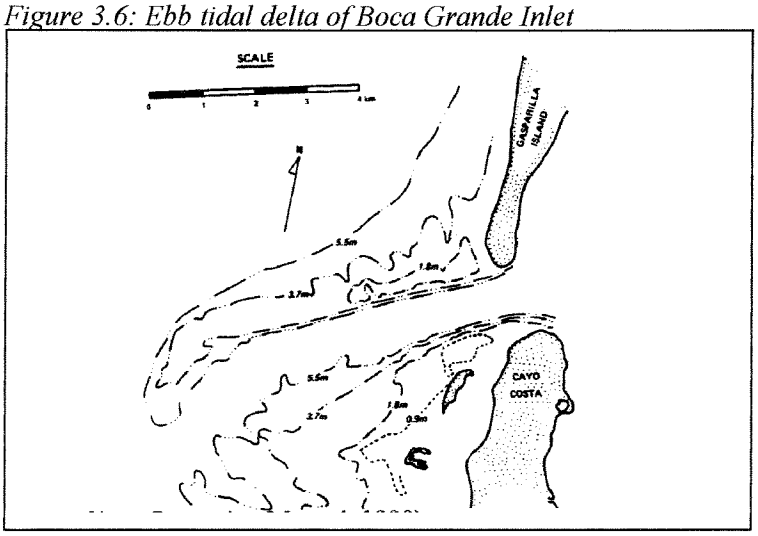

(From: Shore Protection Manual, 1990)

Figure 3.7: Bathymetry of San Francisco Bar, Circa 1900

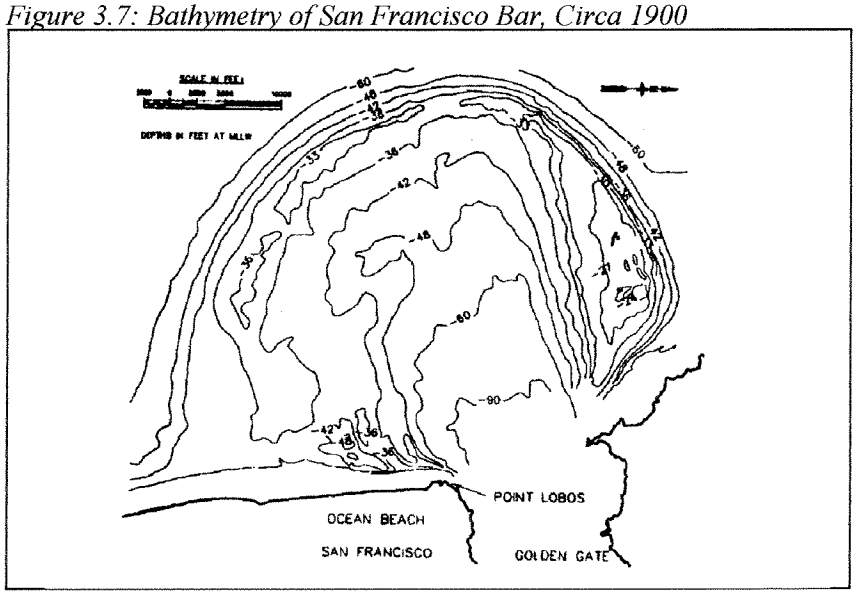

(From: Coastal Engineering, 1996)

Figure 3.8: Flood and ebb channel characteristics and sediment circulation currents

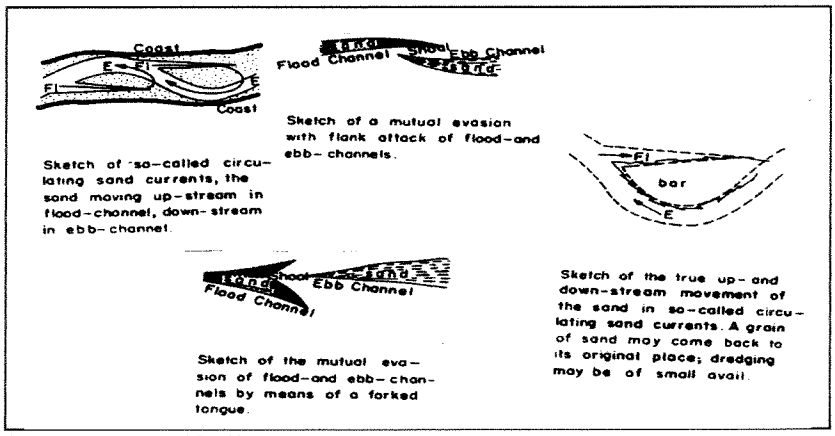

(From: Bruun, 1978)

sediment size increases also the critical shear stress, allowing the sediment bed to remain more stable as compared to the bed composed of smaller grain size under the same flow conditions. This effect results in an increase in the equilibrium volume for increasing grain diameters. The increase of sand particle size increased the growth rate as well as the equilibrium volume.

3. The deep water wave height, H_0: Increasing the wave height increased the time of approach to equilibrium but decreases the equilibrium volume.

3.4.2. Factors influencing the ebb tidal delta

Tidal inlets tend to develop towards a dynamic equilibrium. Sediment bypassing plays an important role. The ability for the sediment to bypass tidal inlets depends in particular situations on the ebb tidal delta. Important parameters of the ebb tidal delta are the depth and the equilibrium bar shape (Bruun, 1978). The natural sand bypass mechanism will be described later in detail.

Local wave and current action determines the depth and width of the ebb tidal delta. Another phenomenon that influences the dimensions of the ocean bar is the tidal prism. In situations were there is little wave action and large tidal prism, sediment tend to build up larger ocean shoals thereby increasing the resistance against this tidal flow. An example of an ebb tidal delta with low average wave activity is given in Figure 3.6. The ebb tidal delta of the Boca Grande Inlet, USA extents a considerable distance of 6,4 kilometres offshore. However, it is not necessarily true that large tidal prisms cause large ocean shoals. When tidal inlets are exposed to rather heavy wave conditions, the suspended sediment may exceed the bed load. As a result of the large tidal prism much material will be sucked into the bay and deposited on the bay shoals. This development can only continue until a certain point when the bay shoals become so large that the tidal prism decreases. At this point the ebb tidal delta becomes more exposed by sediment and starts to grow (Shore Protection Manual, 1984).

The above described formation and development of the ebb tidal delta does not include however the sediment load coming from river discharges. When there is very little or no wave action present, the river mouth develops extensive ebb tidal deltas containing river sediments. The enormous mud banks in the river entrances at the amazons, the San Francisco Entrance, which is shown in Figure 3.7, and the Maracaibo Entrance in Venezuela are examples of gigantic ebb tidal deltas. In these cases it indicates that there is low wave energy present. This can also be concluded at the fact that navigation channels are dredged through this ocean bar. With high or moderate wave energy input the navigation channel will be closed as fast as its been dredged. (Bruun, 1978)

Another interesting phenomenon of sand supply to the ebb delta or into non-scouring channels is *bottom creep*. Bottom creep is basically onshore transport of sand by waves. The basic components of onshore transport of material were already briefly described in section 2.4.3. According to Bruun (1978) mass transport by non-breaking waves is the basic component involved in the bottom creep phenomenon. Bottom slope and grain size are the most important parameters. A gentle bottom slope and swell favour this onshore transport. Finer grain sizes generally create flatter bottom slopes for a given wave condition. Significant bottom creep towards tidal inlets outside the breaker zone and ebb tidal delta contributes to the formation of an ebb tidal delta with rather steep slopes. However, compared with the longshore transport, the quantity of material reaching tidal inlets from the offshore areas is relatively small (Bruun, 1978).

3.5. Morphology of the flood tidal delta

The flood ramp (Figure 3.4B) is a gradually shallowing part of the flood delta and begins at the end of the gorge. Landward of this point the flood delta becomes shallower and is divided by the typical, relatively shallow and unstable, flood dominated channels. The broad shoal on the outer section of the flood tidal delta frequently dries at low water. This is called the "ebb shield". On the landward side of this ebb shield a steep slope separates the ebb shield and the main ebb channels. From these channels the flows directly into the gorge back into the sea. (Huis in 't Veld, 1987)

Inside the flood tidal delta, flood dominated and ebb dominated channels are separated by bars between them, over which sand migrates (Bruun, 1978). Figure 3.8 shows ebb and flood channel characteristics as well as sediment circulation currents. During falling tide, water from the shallow areas on the bayside is flowing into the surrounding tidal channels, causing relatively higher ebb velocities, which results in more stable relatively deep ebb channels. The above described situation is called ebb dominant. Ebb dominance occur when the basin area is rather flat, with increasing surface area with rising tide (Bruun, 1978). Generally it can be said that during falling tide the average water depths are somewhat lower than during rising tide, with an significantly decreasing surface area during falling tide, the tidal prism must leave the flood tidal delta through ebb tidal channels which results in higher velocities in these channels. During rising tide the flow velocities decrease because of the increased surface area and the resistance of the flow by the tidal flats, causing relatively shallow unstable flood channels with a "dead end" (shoal on the end of the channel at the bayward side) (Bruun, 1978). After most tidal flats are flooded the velocities may increase because of the lower resistance of the flood currents. This results in an additional asymmetric flow velocity distribution over a tidal cycle, giving rise to the ebb- dominance in large parts of the basins (Steijn, 1991). The separation of flood and ebb flows is reflected in the typical dune bed-form developed over the flood tidal delta, as illustrated in Figure 3.5A. (Huis in 't Veld et al., 1987). From this figure can also be concluded that the ebb and flood channels are more pronounced on the flood tidal delta. This is caused by the fact that wave action on the flood tidal delta is much less that on the ebb tidal delta were the channels are much less pronounced.

3.6. Selective sedimentation

The relatively coarse particles in suspension by wave action on the ebb tidal delta will not be travelling very long distances. It will soon reach the bottom of the gorge and travel as bed load. Bruun (1978) states that the bottom material that travel as bed load inside the inlet gorges is derived from the shores and beaches on either side of the inlet. This means that in most cases sand material of: 0,1 - 0,3 mm. The sedimentation of individual particles depends on the fall velocity. If the suspended sediment particles have a low fall velocity (small particle diameter) they can travel up to several kilometres before settling, reaching the flood tidal delta. On the flood tidal delta these finer particles, still in suspension, will settle down reaching calm water on the flood delta shoals.

For a tidal inlet on littoral drift shores, in most cases material will travel as bed load in the gorge, unless the entrance is very short. On very short entrances there will be significant wave action and also significant suspended sediment with respect to the bed load. Sediment found on the bay shoals on the flood tidal delta is mostly the finer sand. Coarser to medium sand is found on the ebb tidal delta offshore bar. In the gorge medium to fine sediment can be found (Bruun, 1978). The coarser material settles closer to the actual inlet area. The lagoonward directed sediment transport may be induced by (Steijn, 1991):

Figure 3.9: Normal profile of cross-shore distribution of longshore littoral drift

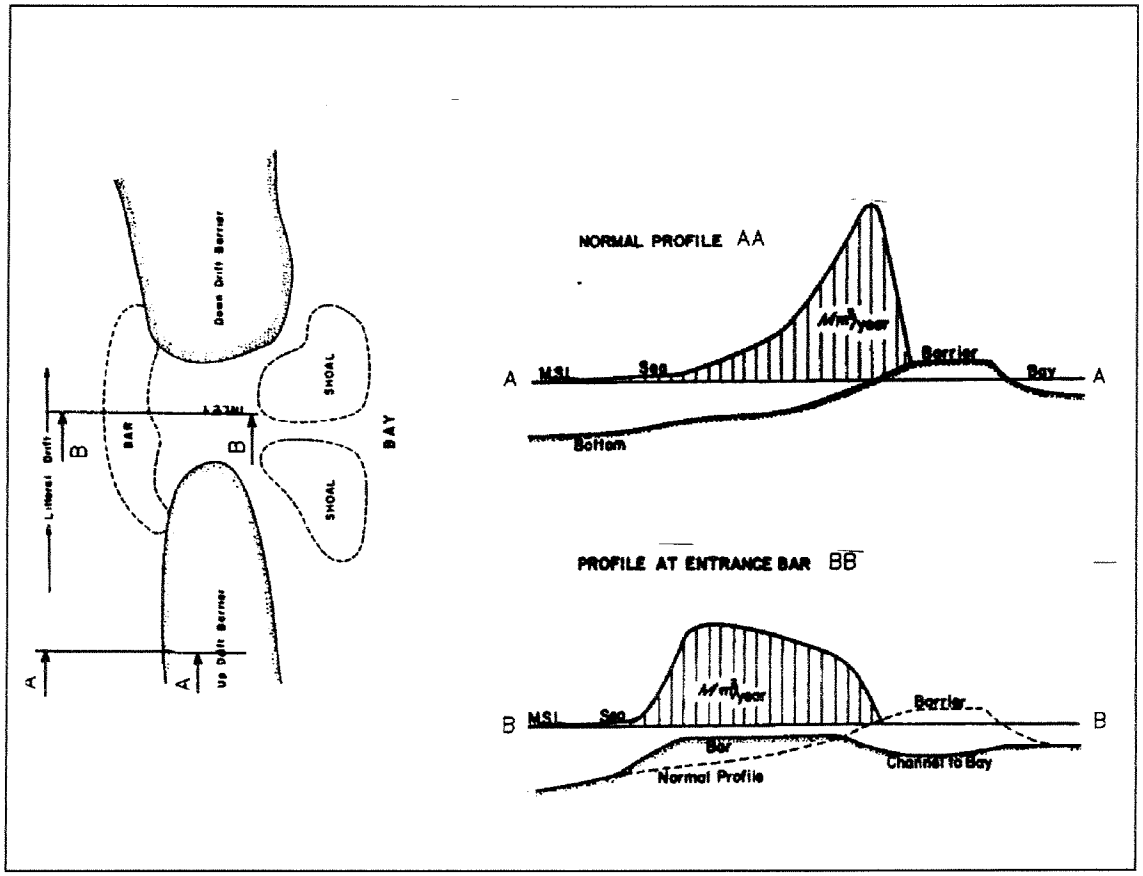

(From: Steijn, 1991)

Figure 3.10: Sediment transport by tidal flow in the channels

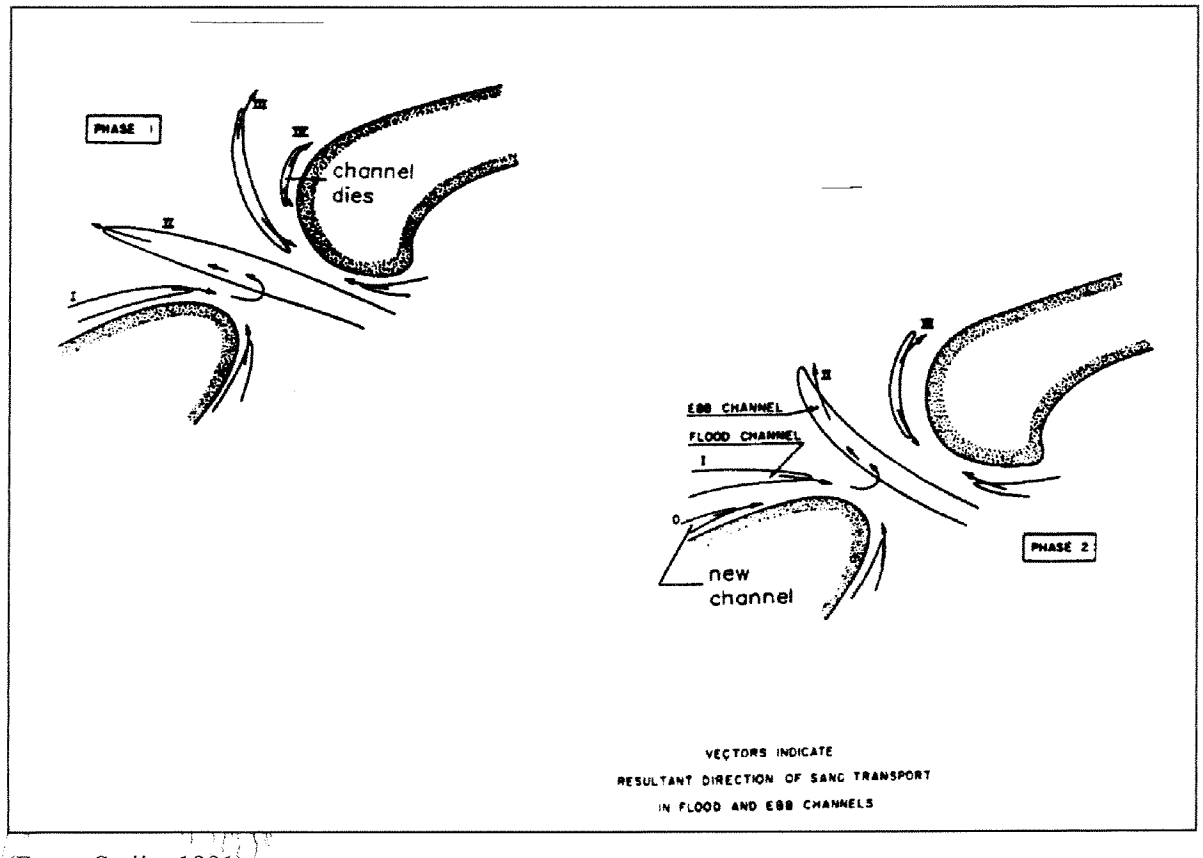

(From: Steijn, 1991)

- ***Density currents*** due to salinity differences.

- ***Tidal distortion:*** Due to the longer flood duration and low flood velocities near HW slack, the finer particles may stay longer in suspension an have more time to settle inside the lagoon. This means that during HW slack the finer particles settle more inside the lagoon that with LW slack.

- ***`Settling lag` and `Scour lag` effects:*** *Scour lag* is the phenomenon that a sediment particle tends more towards settling then towards eroding for a particular shear stress. The settling velocity of sediment particles is somewhat smaller then the erosion velocity. Settling lag is the phenomenon that a particle needs some time to reach the bottom after the flow velocity has reduced below the critical settling velocity.

3.7. Natural sediment bypassing of tidal inlets

3.7.1. General

Sediment bypassing is the process which allows material to become part again of the normal littoral drift a short distance downdrift from the littoral barrier (inlet, channel etc.)

Bruun (1978), stated that two main principles of natural bypassing by natural action occur:

1. Bypassing via offshore bars: A submerged bar in front of the inlet may act as a "bridge" via which sediment is carried to the downdrift area.

2. Bypassing by tidal flow: This takes place when deposits taken into the inlet by flood currents and taken to the downdrift area by the ebb currents.

Bruun (1978) defined parameter r. Value of parameter r determines which type of natural bypassing most likely occurs at a specific tidal inlet. This parameter is also used to get a first impression about the inlet stability:

$$r = \frac{P}{M_{total}} \tag{14}$$

in which P is the tidal prism (m^3 per half-tidal cycle) and M_{total} the total littoral drift (m^3 per year).

The stability of tidal inlets in terms of bypass capacity expressed in this latter expression of r is as follows:

- $r < 20$: Inlets become unstable non- permanent "overflow channels"

- $20 < r < 50$: The tidal inlets are typical "bar-bypassers".

- $50 < r < 150$: Combination of bar-bypassing and flow bypassing: the entrance bars are still pronounced.

- $r > 150$: The tidal inlets are predominant tidal flow bypassers: little bar and good flushing.

Figure 3.11: Models of inlet sediment bypassing for mixed energy coasts

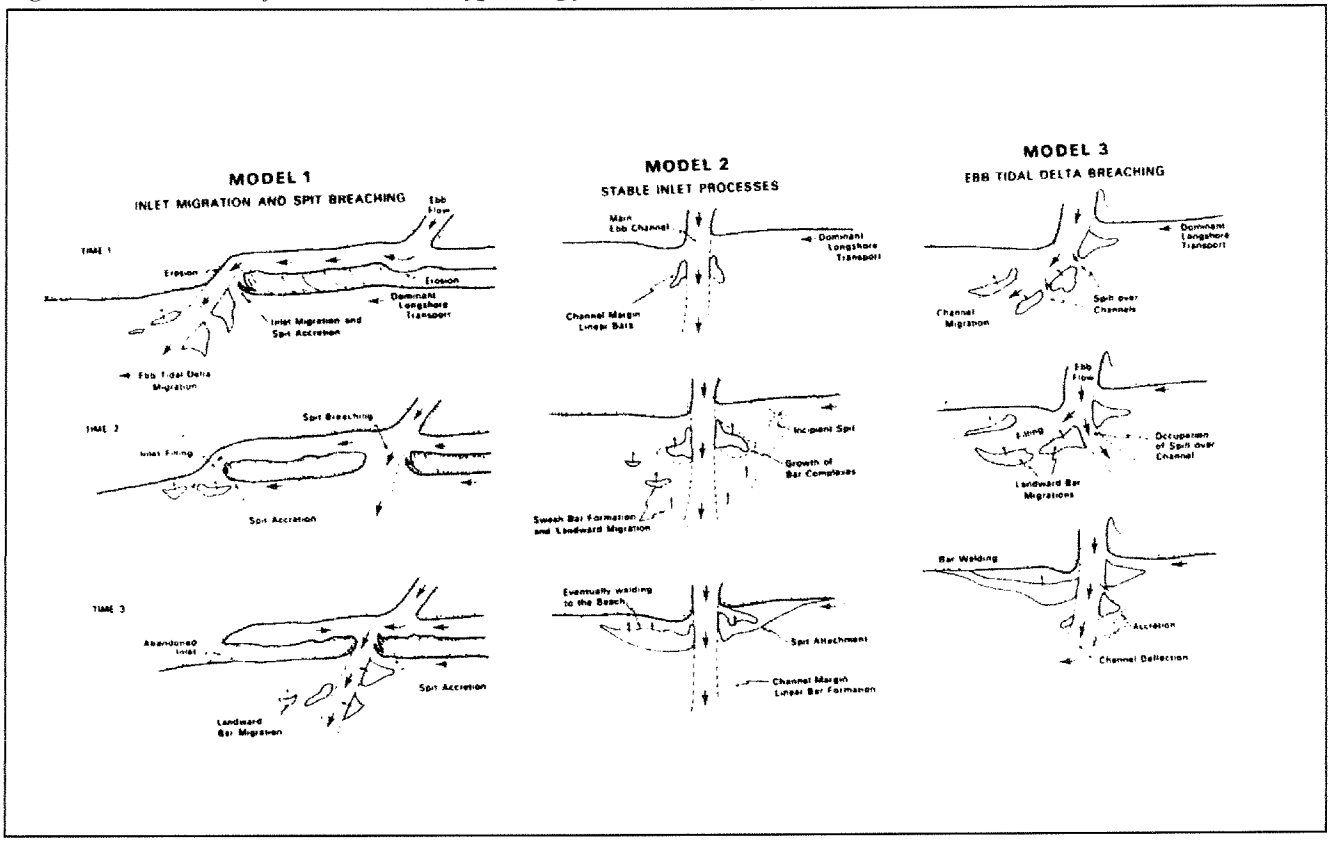

(From FitzGerald, 1982)

Figure 3.12: Example of inlet migration and spit breaching (Kiawah inlet)

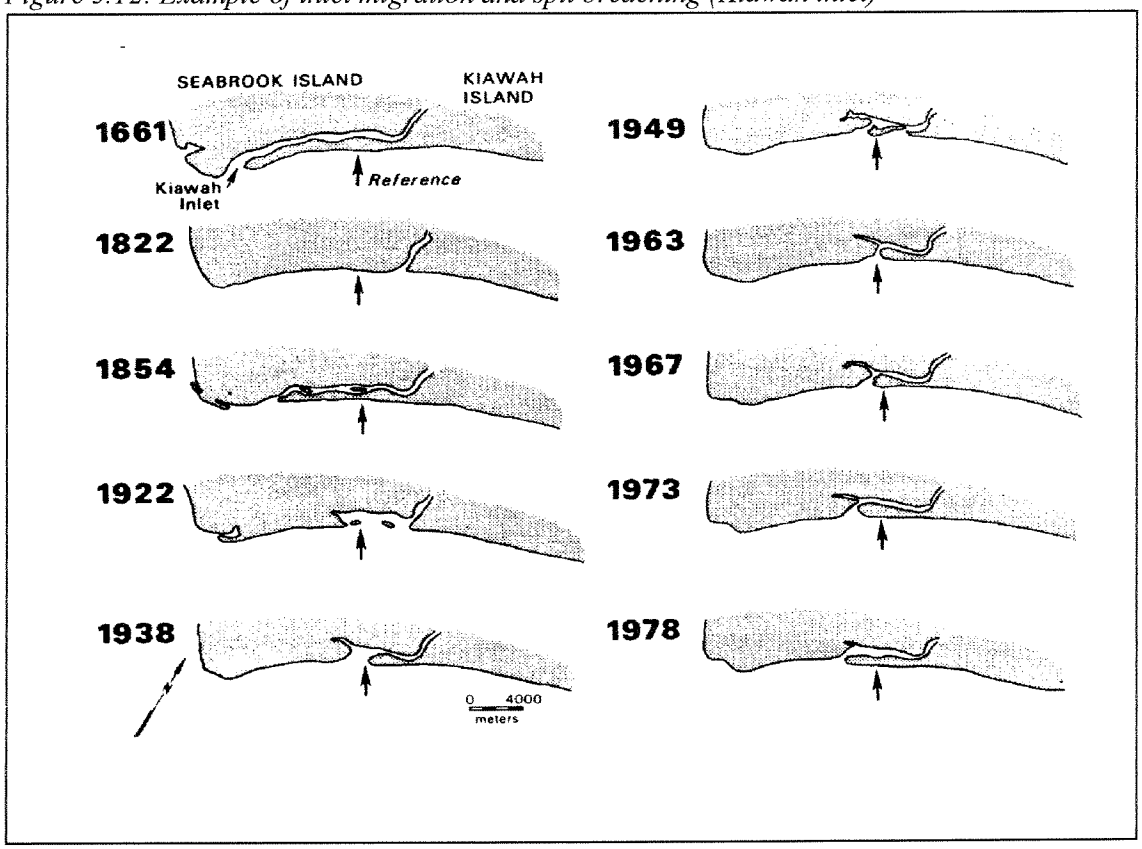

(From FitzGerald, 1982)

3.7.2. Bar bypassing

The bar bypass mechanism becomes important in cases were significant wave action is present. In these cases the littoral drift continues over the submerged bar to the downdrift barrier island in order to re-establish the equilibrium condition before the inlet was created. It is possible to estimate the required dimensions like with and depth of the submerged bar by examine the littoral drift capacity and the normal profile cross-shore distribution of it, illustrated in Figure 3.9. The integrated longshore drift capacity is kept at the same level (no gradients in the longshore transport capacity).

Increasing amounts of littoral drift, the depth of the bar will decrease and its width will increase. The breaker depth of the storm waves usually determines the depth over the bar. The bar-bypassing mechanism is rather dangerous for the navigation, because sandbars are limiting the depth of the entrance to the tidal inlet as well as the deposition of sediment in the (dredged) entrance channels. Inlet with bar bypass mechanisms is usually improved by jetty structures. However these improvements are temporal because the bypassing mechanism is causing sedimentation after some time in front of the jetty structure, especially when the offshore beach profile depth is limited (Bruun, 1978).

3.7.3. Tidal flow bypassing

Tidal flow plays an important role in bypassing of material for large values of "r". Bypassing can take place in different ways. According to FitzGerald (1991):

- ***Migration of channels and bars***. Tidal channels can migrate over the inlet trough. Figure 3.10 shows two phases of an inlet/channel system. New channel has developed as another has disappeared. These tidal channels migrate in downdrift direction. One of the reasons for this may be that littoral material is deposited on the updrift banks of the channels forcing the shift downdrift. Another process forcing curved channels to migrate is the meandering capacity. The bars between the channels may follow this migration and occasionally join the downdrift barrier coast.

- ***Transport by tidal flow in the channels***. The vectors in Figure 3.10 indicate the resultant direction of sediment transport in the flood- and ebb channels.

3.8. Explanatory models for tidal inlet bypassing

Fitzgerald (1988) proposed three models, illustrated in Figure 3.11, for inlet sediment bypassing along mixed energy coasts. Note that Model 1 agrees rather well with the `dynamic diversion` concept of Oertel (1988).

Model 1. Inlet migration and spit breaching:

Littoral material transported to a tidal inlet can cause constriction of the inlet throat. The decrease in cross-sectional area will cause increased currents and therefore scours the inlet throat. The longshore transport of sediment causes an accumulation on the updrift side of the entrance. The opposite side of the inlet will erode. This cases the inlet to migrate in the direction of the predominant littoral drift. The rate of migration depends on sediment supply, wave energy, tidal currents and the composition of the channel bank (FitzGerald, 1988). The inlet channel in this way is elongated, which results in an increased flow resistance and therefore lower discharge efficiency. The entrance will eventually deteriorate as a result of a new breakthrough near the original entrance. The old and the new entrance together usually have the same tidal prism as the original entrance. This means that the original entrance

Figure 3.13: Conceptual model of bar migration on the ebb tidal delta

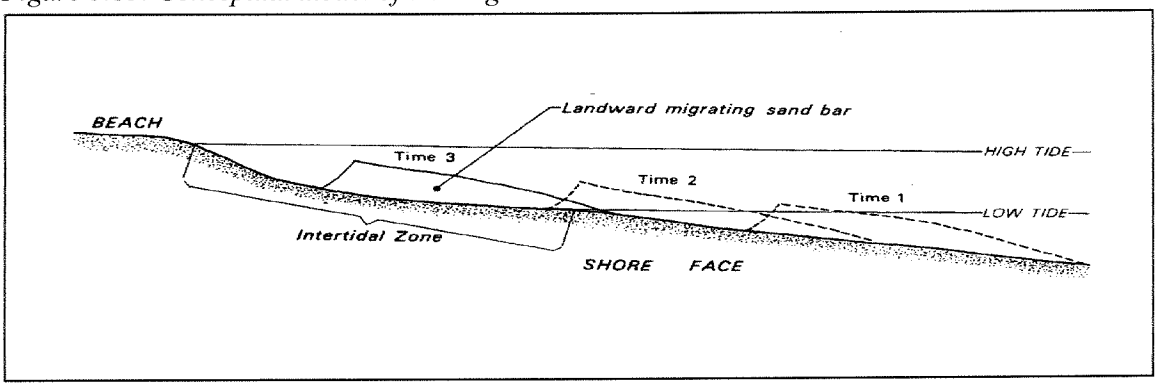

(From: FitzGerald, 1982)

Figure 3.14: Sequential sketches of the ebb tidal delta at Price Inlet

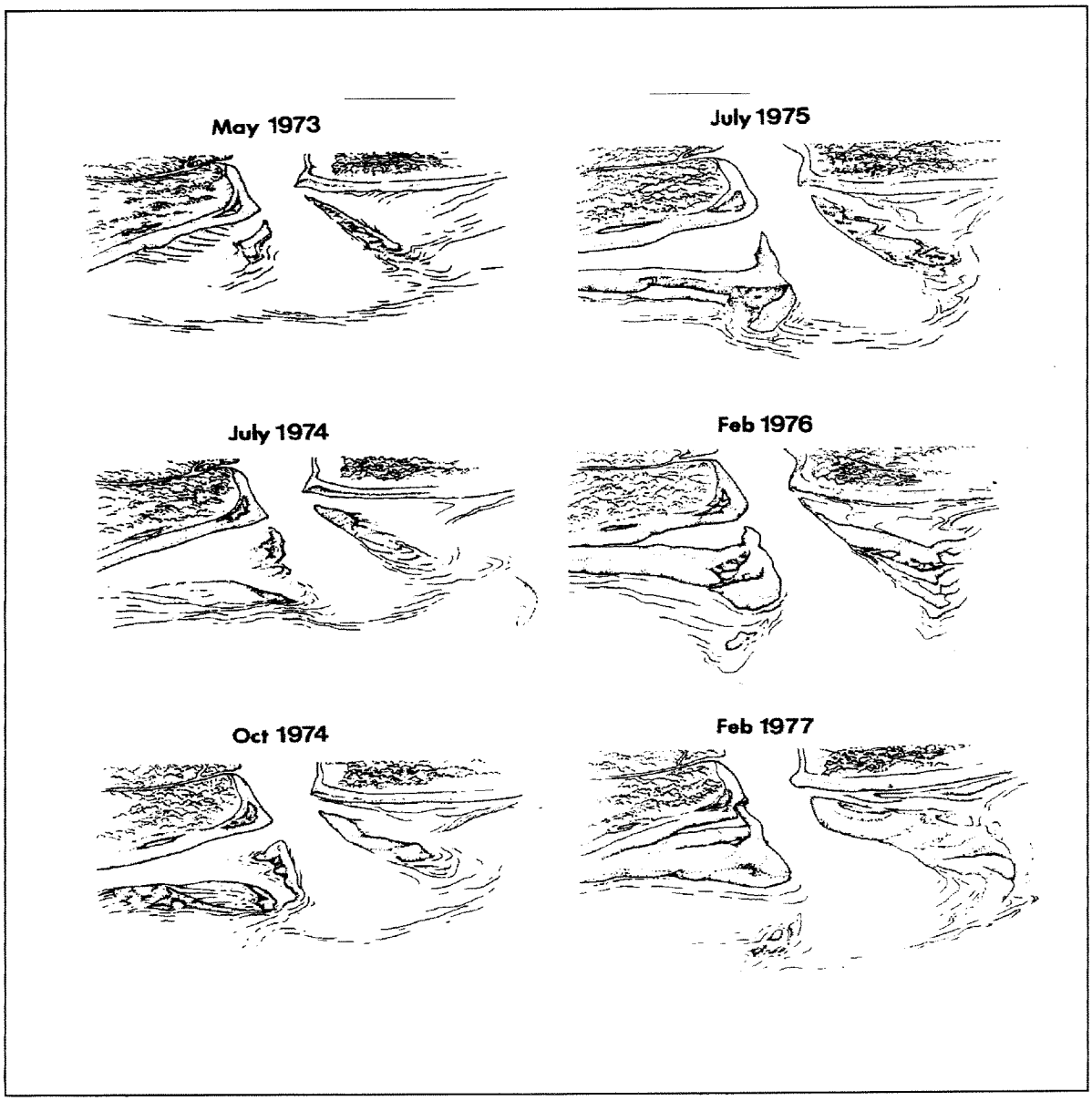

(From: FitzGerald, 1982)

cross-sectional area decreases which ultimately results in closure because of a combination of small tidal prism and large littoral drift. The result of spit breaching is bypassing of a large bulge of sand to the downdrift side of the entrance (FitzGerald, 1988). The new location of such an inlet is rather difficult to predict, but it is quit often located just in front of the ebb channel. FitzGerald (1988) gives an example of bypassing sand by spit breaching. "Since 1661 Kiawah Inlet has experienced at least three episodes of south-easterly migration followed by an updrift relocation of the inlet through spit breaching. As illustrated in Figure 3.12, the breaching process and closure of the old inlet results in the formation of an elongated pond that parallels the shoreline. The spit breaching resulted from large magnitude storms breaching the spit back toward Kiawah Island, bypassing large quantities of sediment."
Most inlets migrate downdrift; however, some examples exist of updrift migration.

Model 2. Stable inlet processes

Stable inlets have a stable throat position and a non-migrating main ebb channel. Sand by-passing at these inlets occur through the formation of bars which migrate and attach to the downdrift coast. These large bars have been formed by the stacking and coalescing of wave built accumulation of sand (swash bars) on the ebb tidal delta platform. Due to flood dominance at these parts of the ebb tidal delta in combination with the breaking and shoaling waves, the swash bars move onshore. As mentioned earlier the breaking and shoaling waves over the ebb tidal delta creates bores of water which augment the flood flow, but which retard the ebb flow. Due to this phenomenon a net landward sediment transport occurs at both sides of the entrance. The net movement of sediment onshore also has been attributed to greater wave suspension during the flood cycle than during the ebb cycle (FitzGerald, 1988). New bars will constantly develop due to a more or less continuous sand delivery by the ebb tidal channel. Thus sediment bypassing in this model depends on sand deliveries through the channel system. The rate of migration of the swash bars decreases when they reach the coast. FitzGerald (1988) explains this as swash bars gain a greater intertidal exposure when they migrate up the shoreface. Thus, wave swash, which causes the bar's movement, operates over an increasingly shorter period of the tidal cycle. The decelerating of the migration of swash bars results in the stacking and coalescing of individual bars to large complexes. These bars can be 1 - 2 km long and 100 - 250 m wide! FitzGerald (1988) exemplified the sequential development of the bar complex of the Price Inlet between 1973 and 1977. Figure 3.13 illustrates a conceptual model of bar migration on the ebb tidal delta. It has been shown that when the bar complexes are in mid-stage development, wave refraction processes, described before, produce a reversal in the longshore transport direction along the downdrift shoreline (FitzGerald, 1984). During this time little sand escapes the confines of the ebb tidal delta. This situation changes as the bar complex migrates closer to the beach and wave action is able to transport sand from the bar to the downdrift shoreline. The size of the bar complexes and the time required for the bars to migrate onshore decreases as the size of the inlet decreases (FitzGerald, 1988). Figure 3.14 shows sequential sketches of the ebb tidal delta at Price Inlet, drawn from oblique aerial photographs (FitzGerald, 1991).

Model 3. Ebb tidal delta breaching

Tidal inlets that bypass sediments by ebb tidal delta breaching have a stable inlet throat position, but a variable position of the main ebb tidal channel. The main ebb tidal channel will be pushed towards the downdrift coast by the predominant littoral drift. In a similar way as described for Model 1 and the earlier described ebb delta development caused by 'dynamic diversion' by Oertel (1988). The migration of the main ebb channel in some cases continuos until it impinges against the downdrift shoreline. This condition causes erosion on the updrift Barrier Island. (FitzGerald, 1988) The flow efficiency of the elongated channel decreases and hydraulic gradients over the bars steadily increase (Steijn, 1991). The inlet will divert its flow

Figure 3.15: Sequential bathymetric maps of Absecon Inlet, showing the beaching of the ebb tidal delta and onshore bar migration

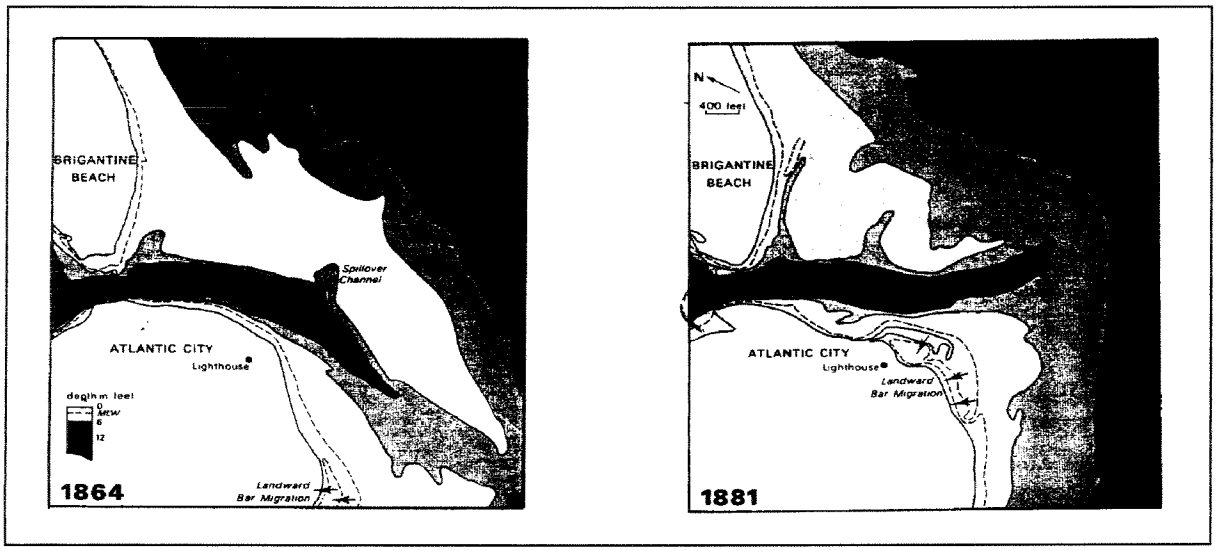

(From: FitzGerald, 1982)

Figure 3.16: Model of tidal inlet processes operating during the flood cycle of a major storm

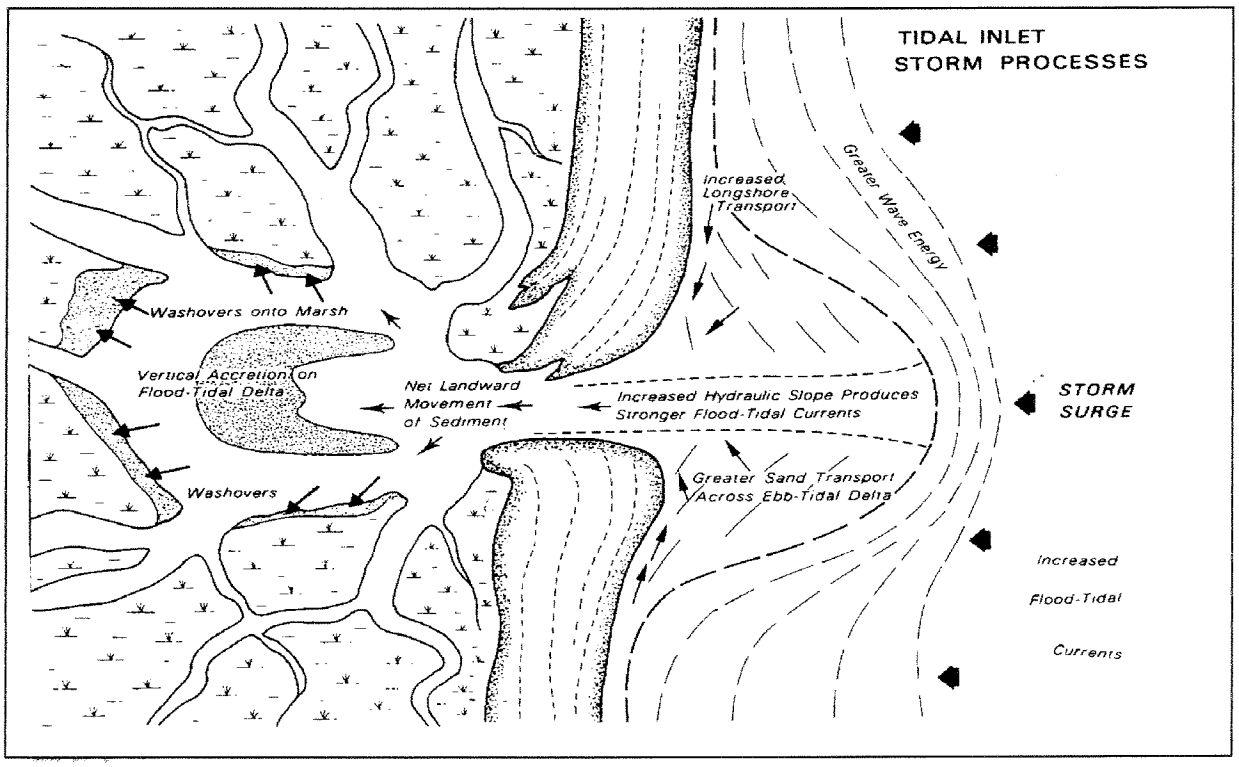

(From: FitzGerald, 1982)

to a more seaward direction via so-called spillover lobe channels. Consequently, the discharge through the old ebb channel decreases and fill up with sediment. This filling occurs due to sand deposition by tidal currents, wave induced sediment transport on the swash platform, and swash bar migration (FitzGerald, 1988). The result is that a large portion of the ebb tidal delta sand bodies is bypassed. According to FitzGerald (1988), this process occur either gradually over a period of 6 to 12 months or catastrophically during a single storm when flood waters increase the scouring ability of the ebb jet. Figure 3.15 illustrates the breaching of an ebb tidal delta and the onshore migration of the bar complex by sequential bathymetric maps of Absecon Inlet, NJ, USA.

Of course in real situations combinations of the later described models may occur simultaneously, or may be dominated by one of the models (FitzGerald 1988). The movement of sediment along the terminal lobe by wave action is almost always present at mixed energy coast.

3.9. Tidal inlets as sediment traps

Dean and Walton (Shore Protection Manual, 1984) indicated that sediment would be trapped inside the flood tidal delta until it reaches an equilibrium shoaling volume. Flood tidal deltas are in general trapping more material than the ebb tidal delta because the wave action inside the flood tidal delta is in most cases little with respect to the ebb tidal delta. Also the stir up of sediment inside the inlet is lower and this results in a lower contribution of sediment to the ebb tidal channel. In general it can be said that the ebb tidal delta not increases a certain dimension, as the flood tidal delta is able to trap continuously sediment. Dean and Walton (1973) show the shoaling of the interior basin of St. Lucie Inlet, Florida. It showed that shoaling continuously took place over a period of about 70 years at a reduced rate of time. Due to the shoaling of the flood tidal delta the frictional channel characteristics are changed such that the inlet becomes hydraulically unstable and resulted in a complete closure. (Shore Protection Manual, 1984). In general the extraction of sediment from the littoral drift will take place during the formation of the ebb and flood delta. Because of this, regression of the shoreline may take place depending on the ultimate sand balance.

FitzGerald (1988) states that tidal inlets not only trap sand temporarily on their ebb tidal deltas, but are also responsible for the longer-term loss of sediment due to sand transport into the flood tidal delta. Figure 3.16 shows a model of tidal inlet processes operating during the flood cycle of a major storm. (FitzGerald, 1988). During storm surges the increased wave energy produces more onshore sediment transport on the ebb tidal delta and higher rates of littoral drift discharges to the inlet gorge. Storm surges also cause an increase hydraulic gradient of the flood tide in the inlet channel. This results in stronger flood currents. The combination of increased onshore sediment transport and sediment transport due to a higher hydraulic gradient, more sediment will be transported to the flood tidal delta (FitzGerald, 1988). Parts of this sediment will be transported to the ebb tidal delta by the ebb current, but part of the sediment has been transported far enough into the flood tidal delta and remains there because the ebb tidal current is not strong enough in this part of the flood tidal delta to flush this sediment back into the inlet system. This process is the possible reason for sand loss into tidal inlets. In more moderate conditions where ebb currents are stronger than flood currents, sediment is jetted sufficiently far offshore to be deposited outside the littoral zone. It appears that the rate at which an inlet traps sediment is higher immediately after the inlet opens than it is later in its history. Another process responsible for sand losses can be the formation of spits into the basin by the combined processes of flood tidal currents and refracted waves (FitzGerald, 1988). FitzGerald (1988) mentions two another major process responsible for possible sand losses in tidal inlets. Tidal inlets may building a recurved spit

into the backbarrier by the combined transport processes of flood and tidal current and refracting waves. And migration of inlets where the inlet throat erodes into the base of the barrier islands sands. In this situation the beach sediments that are transported into the inlet and deposited on the accretionary side of the migrating channel are not replaced entirely by the deposits that are excavated on the eroding portion of the channel. This is because the deposits that underlie the barrier island sands are commonly fine-grained (clay, silt) and when reworked do not become part of the morphological elements of the inlet system (FitzGerald, 1988). If a tidal inlet shows a migrating character, the flood tidal delta continuously extract sand from the littoral system. The ebb tidal delta more or less migrates together with the inlet, without significantly changing its amount of sediment (FitzGerald, 1988)

It is obvious that the ebb tidal delta is also an important sink for sediment coming from littoral drift. As mentioned earlier sediment flushed by strong ebb jets are brought to this offshore area and deposited on the offshore slopes. But there are also some other phenomena that favour transport to the offshore area (Steijn, 1991):

- ***Storm waves & wind***: These waves stir up sediment, and in particular when landward directed wind creates seaward counteracting near bottom flow (return flow).

- ***Turbulent mixing*** along the sediment concentration gradient which exist between the sediment-water mixture of the surfzone and the clear water offshore

- ***Offshore component of gravity*** which act on both the individual sediment particle and on the sediment-water mixture.

The extraction of sediment may be the cause of a new breakthrough. As a result of an decreasing littoral drift new breakthroughs have more change of surviving because it is less exposed to the choking effect of the decreased littoral drift (Bruun, 1978).

4. Stability of tidal inlets

4.1. Introduction

The dynamic behaviour of the earlier described three morphological units is defined as stabilisation. Stability must be interpreted as dynamic stability by which the elements involved attempt to maintain a situation of relatively small changes in the inlet geometry including location, form and cross-sectional areas and shape and the time depend phenomena like the seasonal changes in wave conditions and variations in tidal ranges (Bruun, 1978). Tidal inlets are called stable when severe climatological events of relatively low frequency (large storms) are not able to cause very radical changes. The inlet will return to its "normal" state after a while. The term stability should be understood in the relative sense of the word. Stability does not absolutely exist on tidal inlets on littoral drift shores; the active hydraulic forces are continuously changing the geometry and appearance of the inner and sea shoals as well as the cross-section of the gorge. In general tidal inlets are exposed too extremely variable forces each trying to change the inlet. This is also true for the separate morphological units. In terms of stability conditions the following distinction can be made (Steijn, 1991):

- *Location stability*: Stability of tidal channels and inlets with respect to their location.
- *Cross-sectional stability*: Stability of geographical dimensions of morphologic units, primarily described with empirical relations.

The most important parameters for the stability of tidal inlets are the tidal prism and the littoral drift. They determine the cross-sectional area of the inlet gorge and the shape and volume of the ebb tidal delta. The littoral drift may be considered as the main balancing force, which carry sediment to the entrance by flood currents for deposits on the inner and outer shoals trying to close the inlet. However most tidal inlets on littoral drift shores try to `stay alive` by building up ebb tidal deltas which acts like a bridge for the sediment to be bypassed across the inlet. This in turn means a better flushing of the entrance because it is less bothered by littoral drift. However, as pointed out earlier, this ebb delta formation itself has also an adverse effect on the entrance stability because the increased friction reduces flows through the gorge which in turn results in a decreasing flushing capability and therefore less stability.

4.2. Stability relations

4.2.1. Introduction

The morphological processes acting on tidal inlets are very complex. In spite of this complexity there are a number of investigators who tried to develop some basic equilibrium relations. They found some correlations among certain inlet parameters, such as inlet cross-sectional minimum area, ebb tidal delta area, channel length, maximum channel depth in minimum width cross section, ebb delta area, and controlling depth over the outer bar. In the next sections several well-known widely used stability relations of tidal inlets will be described.

Figure 4.1: Tidal Prism versus cross sectional area

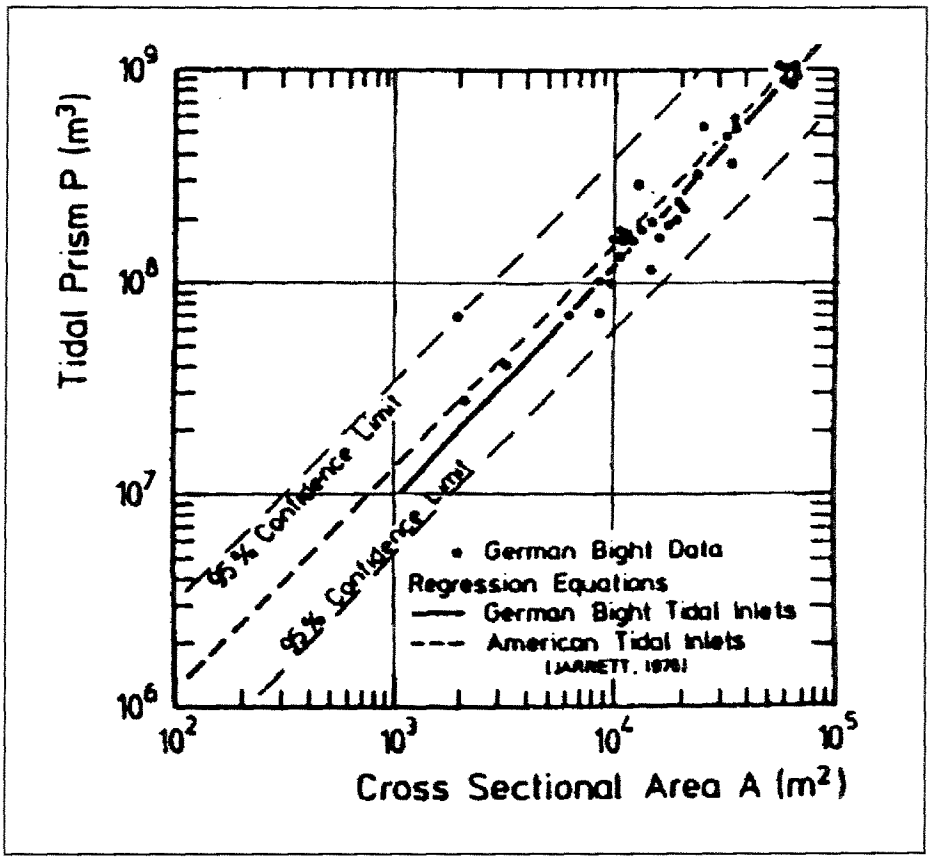

(From: Steijn, 1991)

4.2.2. Empirical stability relations

4.2.2.1. Cross-sectional area stability relations

Karssen and Wang (1991) described the first relation published by O`Brien (1931) assumed an exponential relation between the cross-sectional area (A_c in ft^2) at mean sea level (MSL) and the tidal prism (P in ft^3) at spring tide.

$$A_c = a\ P^b \text{ with: } a = 4.69 \cdot 10^{-4} \text{ and } b = 0.85 \quad (15)$$

In a later article O`Brien (1969) used an improved linear relation (ft^2):

$$A_c = 2.0 \cdot 10^{-5}\ P \quad (16)$$

According to Karssen and Wang (1991): A linear relation between the equilibrium cross sectional area of the entrance channel and the tidal prism can be expected in cases without large ranges in channel depth. In cases with large depth ranges among the channels the following relations by Jarrett (1976) are generally valid. Jarrett (1984, Shore Protection Manual) reanalysed the first relations by O`Brien based on data from a large number of North American inlets. He was able to evaluate (a) and (b) in Equation (30) through regression analysis, thereby categorising the inlets according to the number of jetties and the coastal location. Table 2 gives the (a) and (b) values. This table is derived from Bruun (1978):

Table 2: Cross-sectional stability relations

Coast	Number of Jetties	a	b
All	0, 1 or 2	$5.74 \cdot 10^{-5}$	0.95
All	0 or 1	$1.04 \cdot 10^{-5}$	1.03
All	2	$3.76 \cdot 10^{-4}$	0.86
Atlantic	0, 1 or 2	$7.75 \cdot 10^{-6}$	1.05
Atlantic	0 or 1	$5.37 \cdot 10^{-6}$	1.07
Atlantic	2	$5.77 \cdot 10^{-5}$	0.95
Gulf of Mexico	0, 1 or 2	$5.02 \cdot 10^{-4}$	0.84
Gulf of Mexico	0 or 1	$3.51 \cdot 10^{-4}$	0.86
Pacific	0, 1 or 2	$1.19 \cdot 10^{-4}$	0.91
Pacific	0 or 1	$1.91 \cdot 10^{-6}$	1.10
Pacific	2	$5.28 \cdot 10^{-4}$	0.85

These empirical relations must be seen as a long term average, neglecting the short term variations that occur in the cross-sectional area of the gorge and they also give rather uncertain results in case of moderate or high wave action (Bruun, 1978). So for microtidal wave dominated inlets these relations should not be used. Steijn (1990) compared the results obtained by Jarrett (1976) for the American inlets with those for inlets in the German Bight. It showed that both data fitted rather well as illustrated in Figure 4.1.

Van de Kreeke (1992) describe in his paper the empirical relation originally developed by Yanak (1988) [m^2]:

$$A_c = 2.41 \cdot 10^{-5}\ W^{0.2}\ P \quad (17)$$

In which: W = Width of the entrance [m]

Figure 4.2: Definitions of parameters of relation I

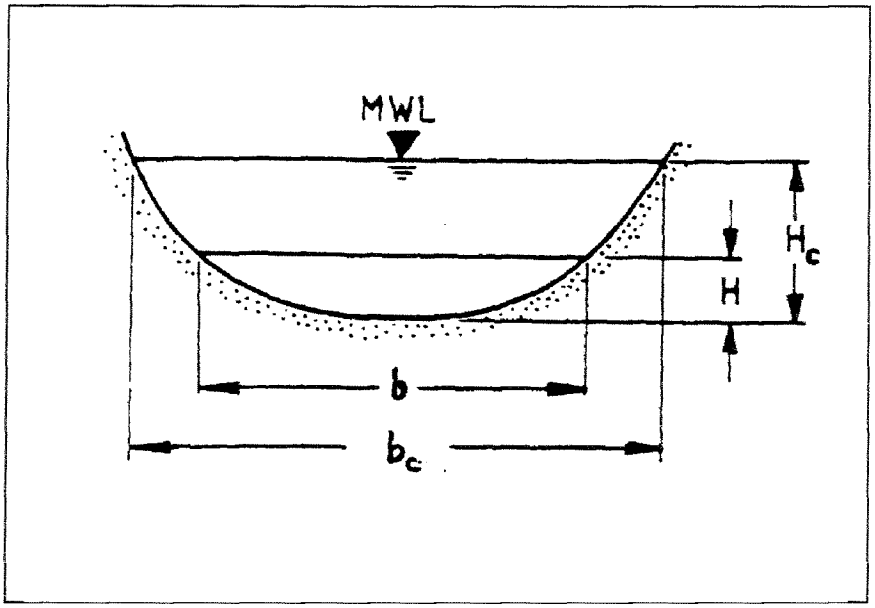

(From: Karssen and Wang, 1991)

Figure 4.3: Definitions of parameters of relation II

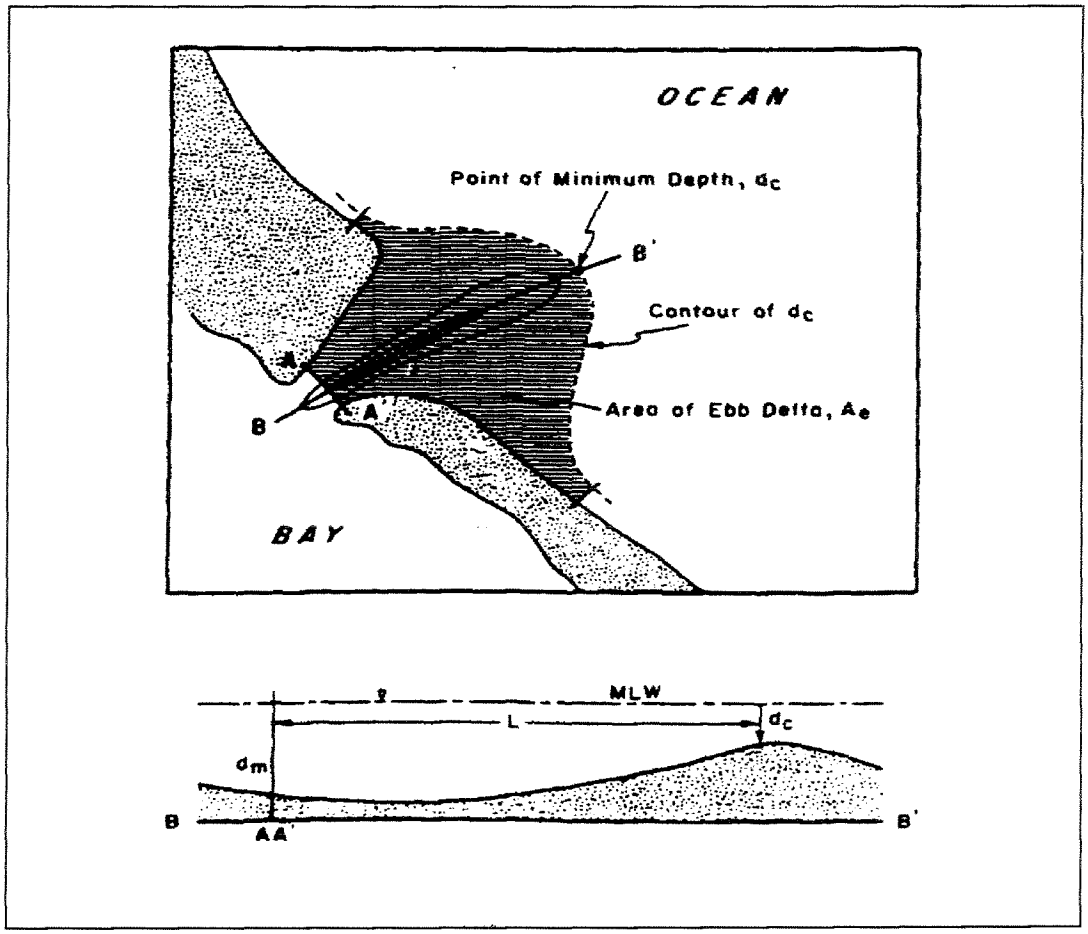

(From: Karssen and Wang, 1991)

Yanak (1988) applied this empirical relation to data set pertaining to twenty stable tidal inlets located on the Southwest Coast of Florida.

Karssen and Wang (1991) proved for the Western Scheldt and the Wadden Sea inlets (Netherlands) that the hydraulic radius of the inlet channel influences the dependency of the cross-sectional area (A_c) and the tidal prism (P) (metrical units):

$$A_c = 1.269 \cdot 10^{-4} P/R^{0.25} \qquad (18a)$$

Note: P is defined in this relation as mean tidal prism

Tidal inlet in general have wide and shallow channels which means that the hydraulic radius is almost equal to the mean depth (Bruun, 1978), so Equation. (18a) develop into:

$$A_c = 1.269 \cdot 10^{-4} P/h^{0.25} \qquad (18b)$$

h = mean depth in metres

Using $R = A_c/A_0$, with A_0 the wetted perimeter, and $A_0 \approx W$, with W the width of the channel, it follows for shallow channels from equation (18b) that (Karssen and Wang, 1991):

$$A_c = 7.64 \cdot 10^{-4} W^{0.2} p^{0.8} \qquad (18c)$$

A_c in m^2

Karssen and Wang (1991) describe also some other empirical relations between the equilibrium cross-sectional area and several other parameters.

4.2.2.2. Some other relations valid for tidal inlets

Eysink (1990) suggests a relation between the mean depth of the tidal channel (h [m]) and the tidal volume. The tidal volume (TV) is defined as the summation of the ebb volume (P_{ebb}) and the flood tidal volume (P_{flood}) or: $TV = P_{ebb} + P_{flood}$.

$$h = 0.35((TV) \cdot 10^{-6})^{0.65} \qquad (19)$$

Karssen and Wang (1991) describe a relation between the equilibrium cross-sectional width and the water level. (Figure 4.2)

$$\frac{b}{b_c} \cdot \left(\frac{h}{h_c}\right)^s \qquad (20)$$

Where: b = Cross-sectional width at water level h [m]
b_c = Mean sea level width of a cross-section [m]
h = Water level above centre line bottom [m]
s = Side slope at mean sea level

Vincent and Corson (Shore Protection Manual, 1984) investigated 67 inlets on the Atlantic and Pacific coasts of the USA and on the Gulf of Mexico; (most of them did not have engineering structures like jetties, etc.). They relate the area of the cross-section with minimum width (A_c) to the length of a channel from the minimum width line to the shallowest depth in the channel as it passes across the edge of the ebb shoal (L) and the shallowest depth in the channel (d_c). Furthermore they relate the average depth (d_a) and maximum depth (d_m) in the cross-section of the inlet throat at minimum inlet width.

- $L = 23.92 \cdot A_c^{0.55}$ (21)
- $d_m = 0.5479 \cdot A_c^{0.38}$ (22)
- $d_c = 0.23369 \cdot A_c^{0.34}$ (23)
- $d_a = 1.42 - 0.347 \cdot d_m$ (24)

Stive and Eysink have developed a conceptual model using the empirical relations to detect and to quantify disturbances of the long-term equilibrium between tidal flow and morphological parameters due to human intervention in the inlet/bay system (Karssen and Wang, 1991). Usually, the morphological response to (sudden) changes of tidal volume and drainage area of the basin shows a certain time lag. The process of morphological response will be fast at first and decelerates the more the new equilibrium situation is reached. The morphological adjustments seem to fit well to an exponential decay function.

$$\frac{\partial S}{\partial t} = -\tau \cdot (S - S_e) \Leftrightarrow \frac{\partial S}{S - S_e} = \frac{dt}{-\tau} \Leftrightarrow \partial \ln(S - S_e) = \frac{dt}{-\tau} \Leftrightarrow \ln(S - S_e) = -\frac{t}{\tau} + C \Leftrightarrow$$

$$S - S_e = C \cdot e^{\frac{-t}{\tau}} \quad (25)$$

For $t = 0 \Leftrightarrow S = 0 \Leftrightarrow C = -S_e \Leftrightarrow S = S_e \cdot \left(1 - e^{\frac{-t}{\tau}}\right)$

Or:

$$S(t) = S(t=0) + S(t=0) \cdot \left(1 - \exp\left(\frac{-t}{\tau}\right)\right) \quad (26)$$

In which:

$$\tau = \frac{\partial V(t=0)}{\partial S(t=0)} \quad (27)$$

The τ-value can be regarded, as the time required obtaining the new equilibrium situation in case the initial adjustments remain constant in time.

∂V (t=0) = new longterm equilibrium situation.

∂S (t = 0) = initial sedimentation

∂S (t) = annual morphological response after time t.

S (t = 0) = initial morphological response

S (t) = total morphological response after time t

Figure 4.4 A: Maximum velocity versus inlet cross sectional area according to Escoffier

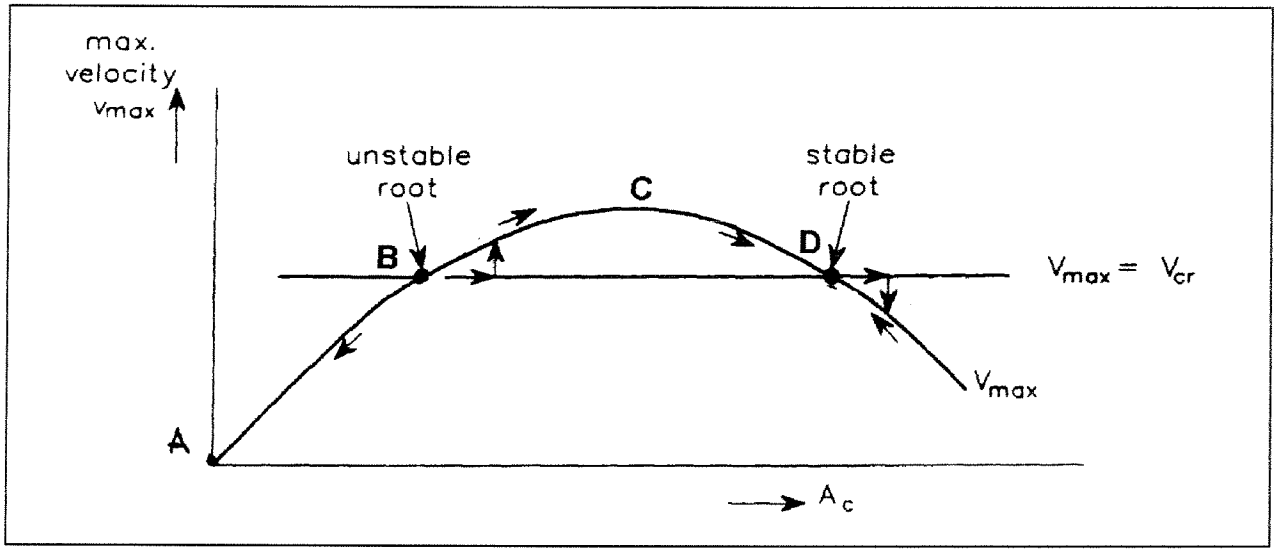

(From: Steijn, after Escoffier, 1940)

Figure 4.4 B: Possible locations of the inlet curve

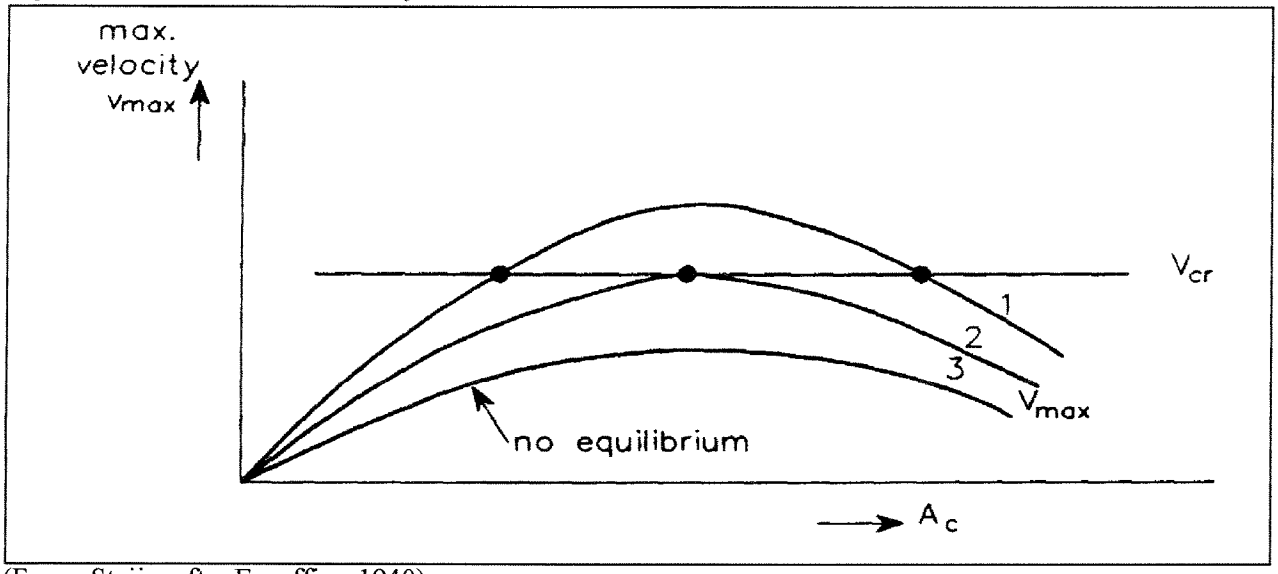

(From: Steijn, after Escoffier, 1940)

4.2.3. Escoffier inlet stability analysis

4.2.3.1. Description of the theory

Escoffier (1940) developed relations where the inlet size (A_c) is controlled by the maximum inlet velocities (V_{max}). The theory of Escoffier (1940) can be used to:

- Determine inlet stability and development.
- Determine what action is needed to assure the permanence of a new inlet formed by a breakthrough as a result of a severe storm or by dredging through the Barrier Island.

Escoffier (1940) defined a critical flow velocity ($V_{cr.}$) in inlets, which is just sufficient to pick up and transport sediment on the bottom of the inlet channel. This critical velocity depends on the amount of sediment carried into the inlet, the sediment characteristics, the wave climate and the Tidal period (van de Kreeke, 1992).

The curve V_{max} versus A_c is plotted in a graphic (Figure 4.4A) as well as the line $V_{max} = V_{cr.}$ By comparing the computed (V_{max}) with the critical velocity (V_{cr}) it is possible to determine if an inlet is 'self-filling', 'self-eroding' or stationary in size. The word stationary must not be confused with inlet stability. A tidal inlet, which is stationary in size, may be stable or not stable. Intersections of V_{max} with the line $V_{max}=V_{cr}$ are points which represent inlet entrance channels who are stationary in size (Escoffier, 1940). For these cross-sectional areas the maximum velocity is just large enough to remove the sediment carried into the inlet by the littoral drift. If the line and curve intersect, there are two points (or roots), an unstable one at (B) and a stable (D). Point (B) represents an unstable equilibrium flow area and point (D) represents a stable equilibrium flow area (van de Kreeke, 1992). If the deviation at point (B) is an increase in cross-sectional area (A_c) than the flow velocities will increase and this results in a further increase of the cross-sectional area. Or in other words: any deviation from point (B) sets into action forces, which tend to further increase the deviation. However if the deviation at point (D) is an increased cross-sectional area the flow velocities will decrease. Consequently, the sediment transport capacity is too small to take care of the sediment carried into the inlet by the littoral drift, which results in a decreasing cross-sectional area and therefore move back to the initial equilibrium condition (D). The sediment transport capacity in the segment (BCD) is larger than that required to remove sediment carried into the inlet by the littoral drift and the inlet will increase its cross-sectional area until it reaches the value (D). A decrease of cross-sectional area at point (B) means that the cross-sectional area approaches zero. "The maximum velocity will decrease as a result of the bottom friction force per unit mass in the inlet being inversely proportional to the cross-sectional area" (van de Kreeke, 1992). Or in terms of sediment transport capacity: the sediment capacity is smaller than the littoral drift carried into the inlet, which results in a decreasing cross-sectional area. The consequent accretion will cause the entrance to ultimately close (A) (Escoffier, 1940). For large values of A_c the tidal prism reaches a maximum value and therefore for increasing values of A_c, the inlet velocity decreases as A^{-1} (van de Kreeke, 1992). Van de Kreeke (1992) defined the equilibrium interval for the stable equilibrium flow area (D), from point (B) to infinity. "Inlets with cross-sectional areas located in the equilibrium interval are *stable inlets*. When the cross-section has an area smaller than (B) the inlet is *unstable*".

A stable inlet does not necessarily imply that the cross-sectional area of that inlet is constant in time and remains equal to the equilibrium flow area (D). Van de Kreeke (1992) states: "When neglecting short term variations associated with the spring-neap tide cycle, these

changes can be divided in seasonal changes and a longterm trend. Seasonal changes are associated with storm activity and are characterised by oscillations of the value of the cross-sectional area about the equilibrium value (D). It seems reasonable to assume that the magnitude of the seasonal changes increases with a decrease in the resistance of the inlet against changes. In case the value of the cross-sectional area remains in the neighbourhood of (D), a measure for the resistance against change (or restoring force) is the slope of the V_{max} curve at (D). In addition to the seasonal variations, during the early stages of their existence many tidal inlets have a tendency to become longer as a result of deposition of sediment at the bay- and ocean side of the inlet channel. The elongation of the inlet channel reduces the hydraulic efficiency of the inlet, resulting in a gradual decrease in cross-sectional area".

Figure 4.4B shows three possible locations of the inlet curve. The highest curve (1) allows for a good stable condition. The lowest curve (3) has no intersections with the $V_{max} = V_{cr}$ line and consequently stability is not possible and the tidal inlet will eventually be closed. If the curve (2) is tangent to the line $V_{max}= V_{cr}$ gives rise to a single unstable root. If the V_{max} curve has two roots (1), the actual dimensions of the channel placing the tidal inlet somewhere on the segment (AB). In this case it will only be necessary to dredge the channel sufficiently to place the cross sectional area somewhere on the segment (BCD) after it will continue to erode itself until it reaches the stable condition represented by point (D).

In general it can be said that higher tidal prisms and lower littoral drift towards the inlet probably combined with low wave energy, gives rise to a higher curve which gives relatively good conditions for inlet stability. In cases of one unstable or no roots at all, it may be possible to raise the whole V_{max} curve sufficiently to cause it to intersect the $V_{max}=V_{cr}$ line at two separate points. The V_{max} curve can be raised in two ways by (Escoffier, 1940):

- Diminishing the effective length (L) of the channel via re-alignments or the construction of inlet jetties, which reduce the hydraulic resistance of the inlet.

- Increasing the hydraulic radius via deepening and narrowing the inlet channel.

The effective length can also be diminished by dredging the ebb tidal delta (Escoffier, 1940). However dredging of the ebb tidal delta seems no solution because sediment will fill the ebb delta very rapidly especially on coasts with high littoral drift. The increase in hydraulic radius is limited by the natural angle of response. Escoffier (1940) states that the inlet geometry will not permit the hydraulic radius to accede in value the quantity:

$$R = \sqrt{2\pi A_c} \tag{28}$$

4.2.3.2. Application of the Escoffier stability theory

Van de Kreeke (1990) applied the Escoffier stability analysis to a single and double inlet bay system: Big Marco Pass and Capri Pass on the lower West Coast of Florida. He used the Escoffier stability analysis on the single Big Marco Pass, prior to the opening of Capri Pass. In this section only the single bay inlet stability analysis will be discussed. For more information on two bay inlet systems reference is made to Van de Kreeke (1990).

Van de Kreeke (1990) calculated the maximum tidal velocities as a function of the gorge cross-sectional area using a lumped-parameter model to describe the hydrodynamics of the flow. In this model, described earlier, is assumed that the bay level fluctuates uniformly and the bay surface area remains constant. Furthermore Van de Kreeke assumed a balance between pressure gradient and bottom friction and accounting for inlet entrance and exit

Figure 4.5: Functions C (K) and sinγ(K) according to van de Kreeke

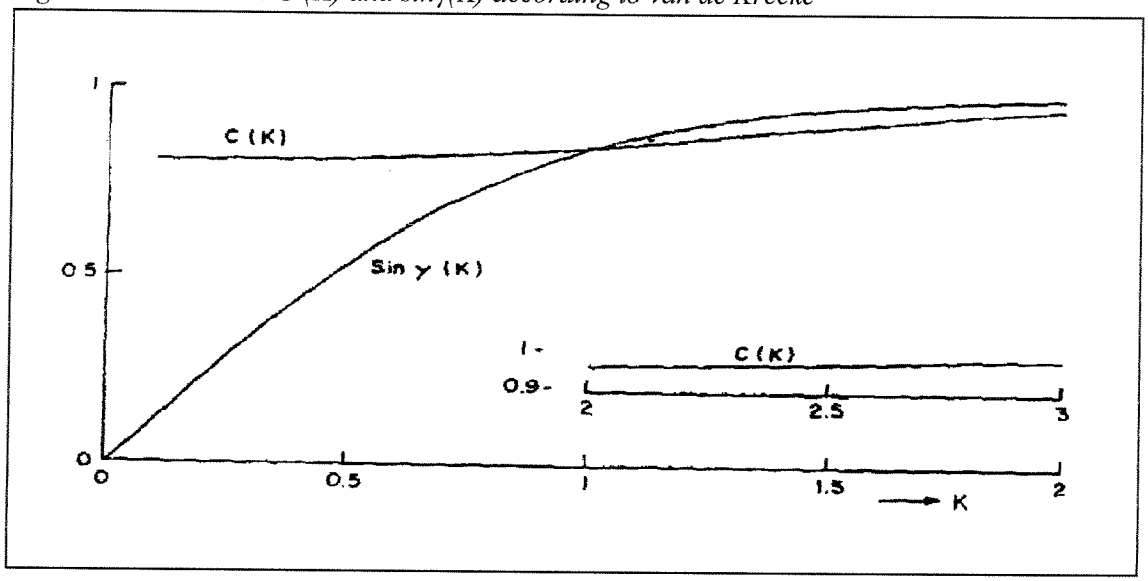

(From: van de Kreeke, 1988)

losses. The velocities are used to calculate the tidal maximum of the bottom shear stress as a function of the gorge cross-sectional area and tidal prism (repletion coefficient K):

$$\tau_s = \rho \cdot F \cdot V|V| \tag{29}$$

In which V is the cross-sectional averaged velocity. Values of the equilibrium shear stress are derived from earlier described empirical relations between the cross-sectional area and the tidal prism for stable inlets.

The cross-sectional averaged inlet velocities in terms of the head difference across the inlet can be expresses as (Van de Keeke, 1988):

$$V(t) = \pm\sqrt{\frac{2 \cdot g \cdot R}{m \cdot R + 2 \cdot F \cdot L_c}} \cdot \sqrt{|\eta_0(t) - \eta_b(t)|} \tag{30}$$

In which: R = Hydraulic radius
m= sum of exit and entrance losses
F = Friction coefficient
L = Inlet length
$\eta_0(t)$ = Ocean tide
$\eta_b(t)$ = Bay tide

For a uniformly fluctuating bay level continuity can be expressed as:

$$Q = A_c \cdot V = A_b \cdot \frac{d\eta_b}{dt} \tag{31}$$

Keulegan (1951) investigated the tidal maximum of the cross-sectional averaged velocity and the amplitude of the bay tide from equation (30) and (31). The resulting expressions are:

$$V = C \cdot \sin\gamma \cdot \frac{2\pi A_b a_0}{A \cdot T} \tag{32}$$

And:

$$\hat{\eta}_b = a_0 \sin\gamma \tag{33}$$

Parameters C and sinγ are functions of the coefficient of repletion "K".

$$K = \frac{T}{2 \cdot \pi \cdot \eta_0} \cdot \frac{A_c}{A_b} \cdot \sqrt{\frac{2 \cdot g \cdot R \cdot \eta_0}{m \cdot R + 2 \cdot F \cdot L}} \tag{34}$$

The functions C (K) and sinγ(K) are illustrated in Figure 4.5 From equation (33) and the assumption of an uniformly fluctuating bay level it follows that the tidal prism is:

$$P = 2A_b a_0 \sin\gamma \tag{35}$$

The closure curve can be calculated from equation (32), (34) and (29). The equilibrium shear stress curve follows by making use of equation (32), (35) and an empirical relation between the tidal prism and the cross-sectional area for stable inlets, which are already discussed in section 4.2.2.1. This results in an expression for the equilibrium shear stress in terms of the cross-sectional area A_c:

$$\tau_{cr} = B \cdot F\left[C(K) \cdot A_c^{\,D}\right]^2 \tag{32}$$

Note: parameter B and D are dependent on the used empirical relation between the cross-sectional area and the tidal prism.

4.2.4. The stability criterion by Bruun

The P/M_{total} ratio was introduced by Bruun and Gerritsen in 1960 and was elaborated on by Bruun (until 1991). The most important factors determining the development of the entrance are the area of the bay and its geometry, the width of the barrier, the length of the gorge and the bay channels, the offshore bottom slope, the tidal range and the magnitude of the wave exposure. These factors may be combined to the tidal prism (P) in m^3 M_{total} is the total quantity of sediment, which drift to the inlet channels. This M_{total} is not the same as the predominant drift (M_{predom}). The predominant drift (or net littoral drift) is the balance between the drift moving in either direction at the entrance (Bruun, 1978). This stability ratio has been used on numerous tidal inlets all over the world, and appeared to be useful to describe overall stability conditions.

Bruun (1978) defined the tidal prism as the volume of water which flows into the flood tidal delta, between low water slack and the next high water slack, during flood, or the total amount of water leaving the entrance between high water slack and low water slack, during ebb:

$$P = \int_0^{T_{ebb} \text{ or } T_{flood}} Q(t)dt \qquad (33)$$

Where: Q (t) = the discharge through the inlet as function of time (t) and T_{flood} or T_{ebb} are the flood and ebb periods. The total tidal period becomes: $T_{tide} = T_{flood} + T_{ebb}$

Tidal prism can be measured. If not, it may be easier to measure the cross-sectional area (A_c) of the gorge. According to Bruun (1978) the $\frac{P}{M_{total}}$ ratio can be described as:

$$\frac{P}{M_{totaal}} = \frac{A_c \cdot V_{mean} \cdot T_{tide} / 2}{M_{total}} \qquad (34)$$

Where: V_{mean} = mean velocity over half tidal cycle = $(\frac{V_{max} \cdot 2}{\pi})$

T_{tide} = tidal period

According to Keulegan (1967) the tidal prism can also be approximated, given a sinusoidal ocean tide and a quadratic head loss due to friction, by the relation:

$$P = \frac{Q_{max} \cdot T_{tide}}{\pi \cdot C(K)} \qquad (35)$$

Where: Q_{max} = maximum discharge (= $A_c \cdot V_{max}$);
$T_{tide} = T_{flood} + T_{ebb}$
C (K) = factor for the non-linearity in the variation of the discharge with time as the result of the quadratic head loss. Keulegan (1950) determined an average C (K) = 0.86 based on measured discharges at four inlets (Bruun, 1978). C (K) can also be determined using Figure 4.5

According to Bruun (1978) the following inlet stability conditions occur:

Figure 4.6: Development of inlet channel under various assumptions according to Bruun

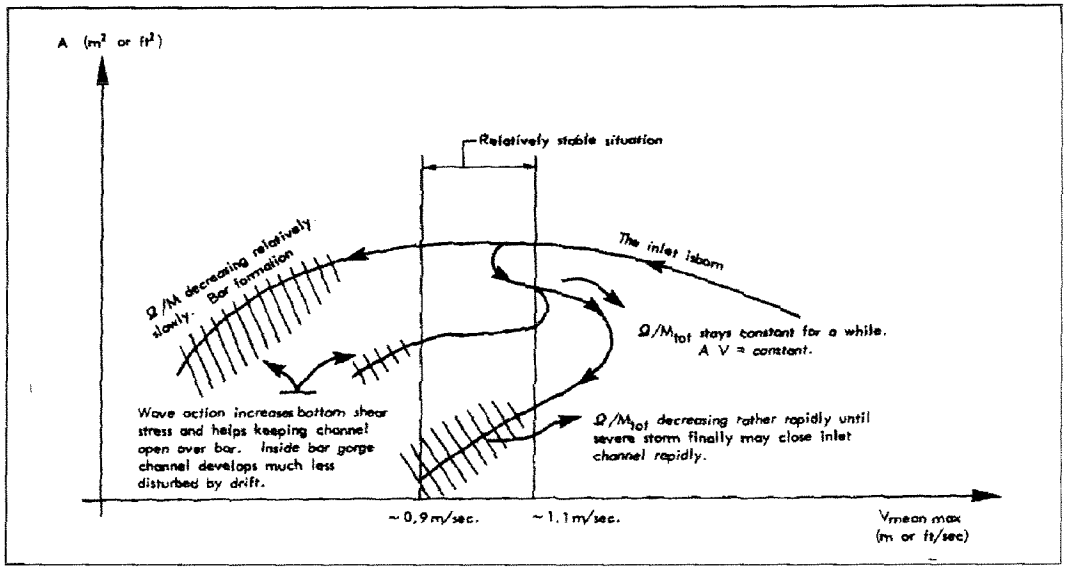

(From: Bruun, 1978)

- $\frac{P}{M_{total}} > 150$: Conditions are relatively good, little bar and good flushing

- $100 < \frac{P}{M_{total}} < 150$: Conditions become less satisfactory, and offshore bar formation becomes more pronounced.

- $50 < \frac{P}{M_{total}} < 100$: Entrance bar may be rather large, but there is usually a channel though the bar.

- $20 < \frac{P}{M_{total}} < 50$: All inlets are typical `bar-bypassers`. Waves break over the bar during storms and the reason why the inlets `stay alive` at all is often that they during a stormy season like the monsoon get `a shot in the arm` from fresh water flows. For navigation they present "wild cases", unreliable and dangerous.

- $20 < \frac{P}{M_{total}}$: Are descriptive of case where the entrances become unstable `overflow channels` rather then permanent inlets.

Evaluating the above described stability ratio it is obvious that the stability of tidal inlets depend mainly on the inlet entrance, the development of offshore bars or ocean shoals and the ability of an tidal inlet to bypass the sediment. (Bruun, 1978). As already mentioned earlier the ratio P/M_{total} can also be used to determine *the way* of sediment bypassing. This relation seems rather reliable according to Bruun (1978). Bruun (1978) investigated numerous inlets all over the world in order to evaluate his stability criterion. The results are listed in Table 3.

Bruun (1978) developed an `equilibrium` concept based on the P/M_{total} ratio, the gorge cross-sectional area and the velocities inside the gorge. Figure 4.6 shows the development of an inlet channel, under various assumptions, after it was born for instance as a result of a severe storm or hurricane. The development towards a `stable` condition depends upon the `gradients`, so that the inlet passing through the `relatively stable situation` gradually may develop less stability, under more violent conditions, suddenly close up. The latter may happen where large fluctuations in the P/M_{total} ratio take place, which in particular refers to relatively small tidal inlets. The concept of equilibrium therefore should always be considered in the relative sense of the word there are many conditions of equilibrium, all referring to particular P/M_{total} ratios, therefore different transfer mechanisms. This approach in fact `cancels` the grouping in `stable and `unstable`. We only have different types or degrees of `stability` (Bruun, 1978).

In Figure 4.6 the stability of inlets refers to the velocities in the gorge. The velocity in the gorge is represented by the $V_{mean\ max}$. The term `mean` refers to the mean over the cross-section and the max refers to the spring tide condition. The $V_{mean\ max}$ = the mean max velocity in the gorge for spring tide conditions. Bruun (1978) found the following empirical relations for $V_{mean\ max}$ based on the experiments from a relatively few inlets:

$$V_{mean\ max} = R^{1/8} - 0.2 \text{ m/s} \quad \text{for: } R \geq 5 \text{ m and,} \tag{36}$$
$$V_{mean\ max} = R^{1/8} - 0.1 \text{ m/s} \quad \text{for: } R \leq 5 \text{ m} \tag{37}$$

Figure 4.7: Relationships between equilibrium volume of sand stored in the ebb tidal shoal and tidal prism

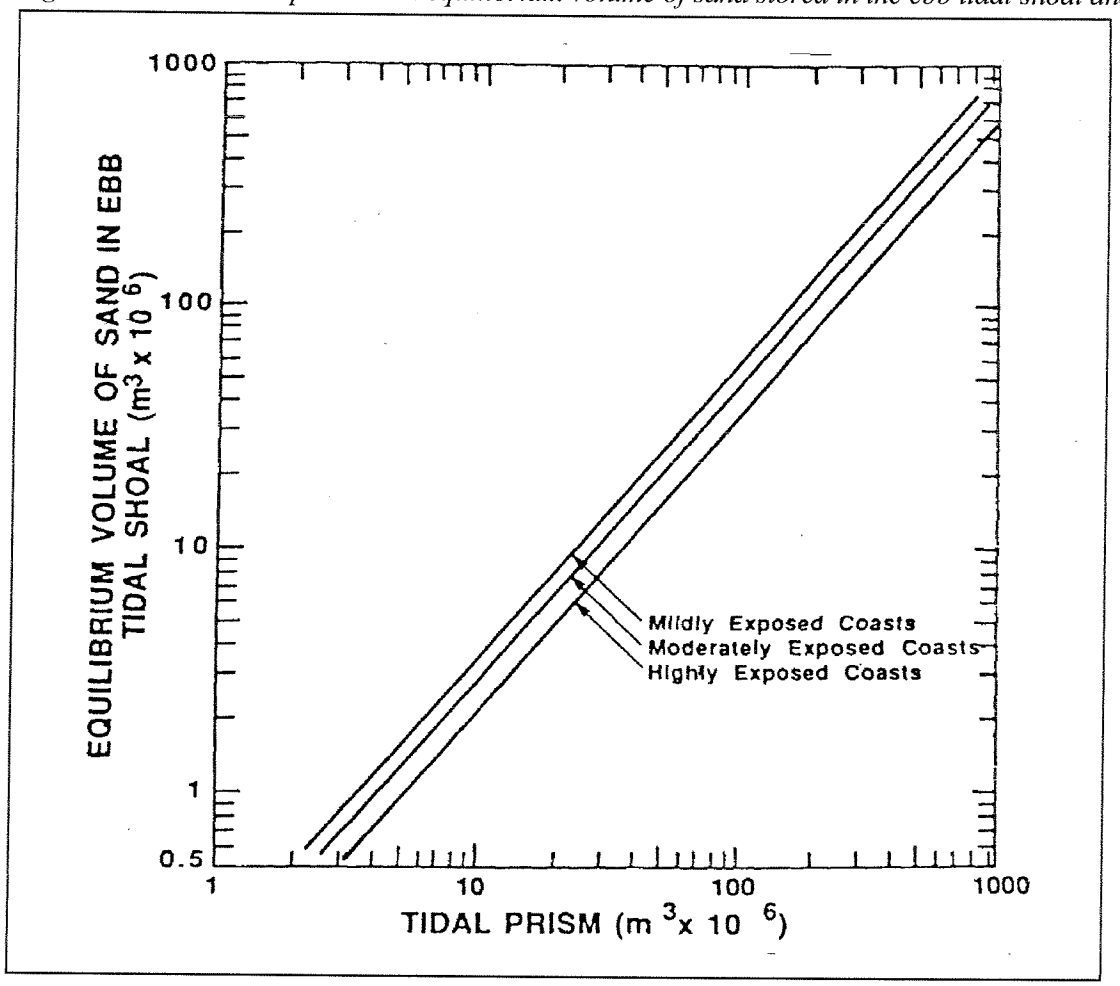

(From: Walton and Adams, 1976)

When discharges and cross-sections are measured the mean max velocity may be approximated by:

$$V_{\text{mean max}} = \frac{Q_{max}}{A_c} \tag{38}$$

Bruun (1978) evaluated the $V_{\text{mean max}}$ to actual cases. In all cases the $V_{\text{mean max}}$ value fit within a narrow range: $V_{\text{mean max}} = 1.0$ m/s ± 0.1 to 0.2 m/s depending mainly on the littoral drift and the tidal prism. The slight difference is probably related to the fact that relatively shallow inlets usually are bothered by littoral drift and there $V_{\text{mean max}}$ velocity therefore has to increase relatively more than in the deeper entrances which on the other hand usually have better cross-sectional geometry than the shallow inlets (Bruun, 1978). With velocities around 1,0 m/s in the gorge channel causes ripples to gradually disappear, and low dunes develop. Or in other words the sand bottom becomes `smooth` for these velocities. With increasing velocities the dunes become lower until finally antidunes develop. According to Bruun (1978) the value of $V_{\text{mean max}} = 1,0$ m/s is located inside the entrance where the ripples have disappeared, and dunes become smoother with increasing velocities. Stable tidal inlets that are subjected, in a relative short period of time, to this $V_{\text{mean max}}$ velocity are able to flush the material brought in during periods of slack water. Therefore the $V_{\text{mean max}}$ velocity is considered to be an important flow parameter in describing the inlet equilibrium condition between the flow and sediment movement (Bruun, 1978). "If $V_{\text{mean max}}$ is dropping below 0,9 m/s, the channel may be in process of decreasing its cross-section and develop towards a new equilibrium condition with a mean max velocity in the gorge of about 1,0 m/s. But it is also possible that the inlet is being choked by an voluminous input of material from for instance a hurricane, or the tidal inlet is building up by an ocean bar which has an flow restricting effect on the gorge velocities. The equilibrium condition, which finally results, depends upon the P/M_{total} ratio. The P/M_{total} ratio in this situation may decrease slowly, in the case of the gradually decreasing cross-sectional area, or in steps in the case of a hurricane. However, if $V_{\text{mean max}} > 1,2$ m/s the channel may also be in trouble, so it has to develop even larger shear stresses for flushing the channel. Such a situation is not lasting, however. It must either result in an increase of the cross-sectional area or in an increase in $V_{\text{mean max}}$ and a simultaneous decrease in cross-section". Also in this case a strong increase of the littoral drift may close the entrance (Bruun, 1978).

4.2.5. Empirical relations for the equilibrium ebb delta

4.2.5.1. Equilibrium ebb delta volume

Walton and Adams (Shore protection Manual, 1984) have presented equations for the volume of sand stored in the ebb tidal delta as a function of the tidal prism for different wave activities on the USA coasts. Measurement `mildly`- `moderately` and `highly` exposed coasts (Figure 4.7).

Table 4: Equilibrium ebb delta volumes

Location	Equilibrium ebb delta volume [m^3]
Mildly exposed coasts	$3.133 \cdot 10^{-4} P^{1.23}$
Moderately exposed coasts	$2.384 \cdot 10^{-4} P^{1.23}$
Highly exposed coasts	$1.975 \cdot 10^{-4} P^{1.23}$
All data	$10.7 \cdot 10^{-5} P^{1.23}$ [ft^3]

Kana and Mason (1988) stated that inlets, which fall below the regression line, could be interpreted as efficient bar bypassers because of the relatively small volume of sand trapped in the delta. On the other hand, inlets falling above the regression line might be considered poor bypassers, but efficient sediment sinks (Kana and Mason, 1988).

Bruun (1978) stated that these relations must referred to a relatively short term base only, and cannot be in agreement with the experience from long term development. The best result of the relation was given for the relatively large jetty protected inlets with highly exposed shores along the Pacific Coast. The reason for the differences from these empirical relations and real cases lie in the importance of the wave action on the ebb tidal delta. Generally wave action causes stunned ebb tidal deltas with limited volumes, and wave action has no clear relation to the tidal prism (Bruun, 1978).

FitzGerald (1988) published a study (Kana and Mason, 1988) of the ebb delta evolution of the migratory Captain Sams Inlet, South Carolina. It appeared that in this particular case the ebb tidal delta volume was approximately 35% less than predicted. They summarised some other factors that may account for the differences between this actual case and the Walton and Adams (Shore Protection Manual, 1984) relation.

- The ebb tidal delta has not jet reached equilibrium after 2.2 years (although its channel appeared to have reached equilibrium quickly).
- Small mesotidal may not follow the same models as the larger inlets with microtidal settings, which dominate Walton and Adams (Shore Protection Manual, 1984) analysis. Also migrating inlets may not follow these models: "The majority of inlets analysed along `mildly` exposed coasts are believed to exhibit more location stability."
- Walton and Adams (Shore Protection Manual, 1984) stated that there relations are more problematic in areas of low wave energy; there are more scatters in the model compared with high-energy settings.

4.2.5.2. Equilibrium ebb delta depositional area

FitzGerald et al. (1988) presented an empirical relation for the ebb delta depositional area using measurement of 21 ebb delta areas of Florida's lower Gulf Coast inlets. The depositional area (A_d [m]) of the ebb tidal delta can be calculated with the following expression:

$$A_d = 2.34 \cdot \left(\frac{P}{2 \cdot a_{so}} \right)^{0.81} \qquad (39)$$

In which: P = Spring tidal prism
a_{SO} = Spring sea tidal amplitude [m]

4.3. Location stability of tidal inlets

Tidal inlets located on sandy beaches in particular cases show a tendency of migration in the direction of the predominant littoral drift. The rate of movement of migrating tidal inlets depends on the magnitude of littoral drift, longshore tidal and other currents and of course the tidal currents in the inlet (Bruun, 1978). On the seaward part of tidal inlet jets act like a sort of hydrodynamic obstacle to the longshore current. As a result of this sediment deposition will

be greater at the updrift side than the downdrift side causing continuing erosion of the downdrift Barrier Island.

Although most migrating inlets are moving downdrift, there are known examples in which the inlets migrate in the opposite direction of the littoral drift. FitzGerald (1988) mentions three possible reasons for such an updrift migration:

1. Attachment of swash bars to the downdrift inlet.

2. Breaching of a spit updrift of the inlet.

3. Cutbank erosion of the updrift inlet shoreline produced by oblique approaching backbarrier tidal channels at the inlet throat. (See also the ebb tidal delta breaching sediment bypass phenomenon)

Spit breaching is the most common means of relocation an inlet updrift, but cutbank erosion of the updrift inlet shoreline also is a major cause of this process, particularly on shallow mixed energy tidal inlets (FitzGerald, 1988). "If the dominant tidal channel of the backbarrier system parallels or semi-parallels the downdrift barrier, then the ebb currents in this channel, and to a lesser extent the flood flow, are directed against the updrift inlet shoreline causing erosion". Steijn (1991) states that meandering - effects of tidal channels may also play a role in updrift migration. "Approaching the gorge the channels in the flood tidal delta locally bend towards the inlet axis causing a erosion on the updrift barrier, and accretion on the downdrift side by the formation of shoals at the innersides of the channel. This phenomenon is similar to what is experienced by meandering rivers". According to Kassen and Wang (1990) Coriolis effects also may play a role in the tidal currents asymmetry.

Examples of inlet migration are the East and West -Friesian Islands (Wadden Sea inlets). Over a period of several centuries the barriers migrated eastward, the inlets narrowed and recurved spits have been build into the backbarrier. FitzGerald (1988) described an interesting hypothesis for inlet migration. Through analysis of an extensive set of current data obtained during four weeks behind the islands Just and Norderney, they found a significant net easterly movement of water and fine-grained sediment across the drainage divides of the interconnected drainage areas. This transport is most pronounced during periods of moderate to strong (dominant) westerly wind, which produces important velocity asymmetries and wave-induced sediment suspension. This caused headward erosion of the tidal channels in the eastern part of the drainage areas, while the eroded material that is transported over the drainage divide is deposited in the heads of the tidal channels in the western part of the adjacent drainage area. The process of eastward, mainly wind-stress-induced, sediment movement contributes to the observed eastward migration of the drainage divides and the resulting asymmetric location of the drainage systems behind the (downdrift) barrier islands. Due to this asymmetric drainage pattern, the main inlet channel approaches the inlet under rather sharp angles, which play a role in inlet migration.

Figure 5.1: Schematic of a jetty improved tidal inlet

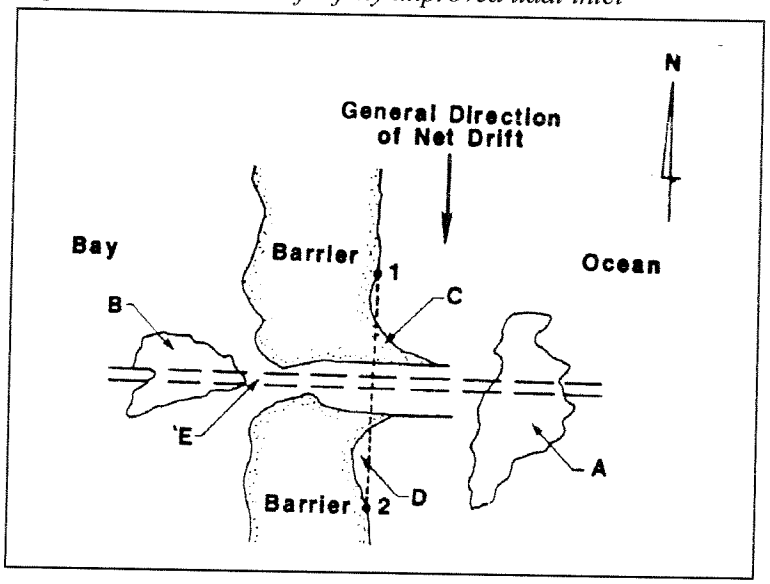

(From: Marina and Metha, 1988)

5. Improvement by structures

5.1. Introduction

As mentioned before, the stability of tidal inlets mainly depends on the behaviour of the tidal entrance and the offshore bar. So for a good stability of tidal inlets improvements are most effective when the entrance channel improves and the natural bypassing mechanism maintains. Many improvements of tidal inlets in the past show that the entrance channel is jetted and sometimes specific methods are used to improve the bypass of sediment. In order to improve the stability of tidal inlet and its navigation, several options are possible (Bruun, 1978).

- Jetties or training walls possibly provided with spurs.
- Breakwater built parallel to the shore.
- Weirs in breakwaters with traps inside for periodic dredging.
- Dredging of navigation channels.
- Mechanical sand bypassing

The above described ways to improve tidal inlets must not be seen as independent methods, mostly a combination of these methods is applied, depending on the actual situation.

5.2. Jetties

5.2.1. Introduction

Jetties or training walls are dams built more or less perpendicular to the coast at one or two sides of a tidal inlet. Figure 5.1 shows a schematic of a jetty improved tidal inlet, which may be considered representative for numerous improved tidal inlets along the East Coast of Florida, USA (Marino and Mehta, 1988). The significant features of improved tidal inlets are the ebb tidal delta, A; the flood tidal delta, B; updrift and downdrift beaches, C and D; and the navigation channel, E. Among these features, in general; the flood tidal delta is the most poorly defined area. The updrift and downdrift beaches (1 and 2) define the alongshore distances of jetty influence of the tidal inlet. The dashed line between 1 and 2 indicates the shoreline position in the absence of the inlet (Marino and Mehta. 1988).

The major goal of jetty improved tidal inlets is to push the sediment so far offshore that it will not threaten the navigation in the entrance channel, and that sediment is able to reach the downdrift coast, to prevent it from erosion (Bruun, 1978). To meet this major goal jetty structures have:

- To increase the currents to cause sand deposited near the tip to be jetted out into deeper water by the ebb currents.
- To block (parts of) the littoral drift in order to reduce sedimentation of the entrance channel.
- To stabilise the position of the inlet. (navigation channel)
- To serve as a breakwater to reduce the wave action in the channel.

Figure 5.2: Schematic ebb shoal development untrained versus trained inlets

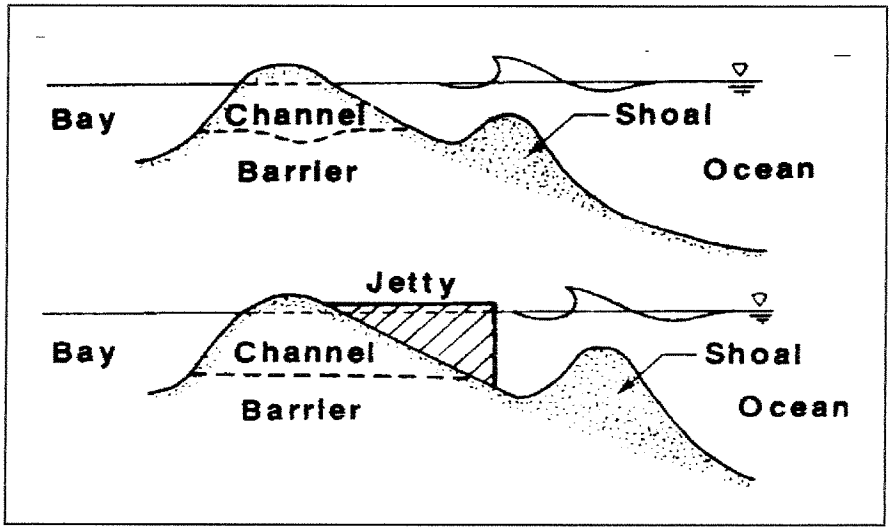

(From: Marino and Metha, 1986)

When an tidal inlet is improved by jetties, the associated sedimentary volumes change until the bottom morphology reaches a new configuration, which can be considered to be approximately in equilibrium with the prevalent currents and wave climate (Shore Protection Manual, 1984). In most cases the net accretion on the updrift side of the inlet is of the same magnitude as the corresponding erosion downdrift. The flood tidal delta experience in most cases relatively minor changes in shoal volume. However the ebb tidal delta shows the most dramatic effect which contains a significant amount of sediment. (Marino and Mehta, 1986) The increased ebb flow associated with jetty improved tidal inlets causes the ebb tidal delta to move into deeper water. This effect is schematically illustrated in Figure 5.2. The length and the configuration of the jetties are the influential factors in determining the distance over which the ebb tidal delta shoal move offshore. After training of a natural inlet or opening of a new (relocated) inlet, the rate of growth of the ebb tidal delta is mainly determined by the rate of supply of sediment from the littoral drift. The larger the drift, the faster the rate at which the ebb tidal delta will develop to its new equilibrium size. However it is noteworthy that when a new inlet is dredged or a natural inlet is trained, sediment trapping usually occurs rapidly initially, followed by much slower shoaling rate (Shore Protection Manual, 1984). The length of the jetties, however, does not necessarily determine the ability of the jetty to cut the littoral drift. Tidal currents and wave action related to the length and depth at the extreme end of the jetties determine the extent up to which the jetties will be able to block the littoral drift (Bruun, 1978). The latter is an important consideration because according to Marino and Mehta (1988) the governing forces (tides and waves) determine the equilibrium size of the ebb tidal delta. The variability in the littoral drift does not correlate with the variability in ebb shoal volumes. From this may be concluded that the length of the jetties determine the distance over which the ebb tidal delta moves offshore, however they do not determine the ebb delta equilibrium size. Marino and Mehta (1988) did not further evaluate this hypothesis.

The cross-sectional area of improved inlets is usually larger with respect to untrained entrances (see also 5.2.3.). The more concentrated ebb currents between the jetties cause this but also wave action plays an important role in this process. Heavy wave action causes high suspended sediment produced on the ocean shoals as well as on the beaches on either side of the inlet. Because of the (partial) blocking of the littoral drift on a jetty protected inlet, it will choke less material for flood flow and flushes more effectively outside the entrance for ebb flow increasing its cross-sectional area. However due to the increased cross-sectional area and probably wider improved entrance more wave penetration may have an adverse effect on the bayward side. This is the case when the inlet is exposed by heavy wave action. The situation for (very) light wave action results in a significantly lower suspended transport rate and probably a low littoral drift. This kind of inlet will in general not be stabilised by jetties. A dredged channel will probably suffice in most cases, as maintenance will be rather small (See also the Escoffier stability analyses). This does not mean that there is no sediment transport, some material may gradually enter the entrance by bottom creep. Also combinations of dredging channel and a trap is possible (Bruun, 1978).

The constructions of jetties to improve tidal inlets with a significant littoral drift have serious consequences for the coastlines of the barrier islands. On tide dominated inlets, with a rather deep entrance channels the transport capacity of waves will be rather low, so the re-establishment of the natural bypass mechanism will be difficult because large amounts of sediment will be needed to build an ocean shoal, which is able to fully bypass the littoral drift. Ebb delta formation on unstable (migrating or newly born) inlets has the consequence that the updrift coast will accrete and the downdrift coast will erode. Usually, the water depth at the tip of the jetties will coincide more or less with the depth of the navigation channel. Therefore, the volume of sediment to be stored in this relatively deep offshore region can quite significant in term of beach erosion. Until the moment that waves are capable to re-establish natural bypassing via the offshore shoal, the downdrift coastline will erode (Steijn, 1991).

Figure 5.3a: Example of a protection with one jetty (Marsonbore Inlet, North Carolina)

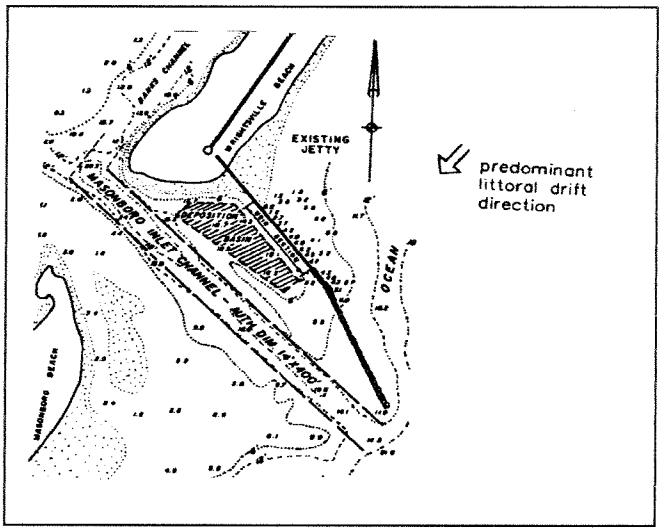

Figure 5.3b: Improved situation (Marsonbore Inlet, North Carolina)

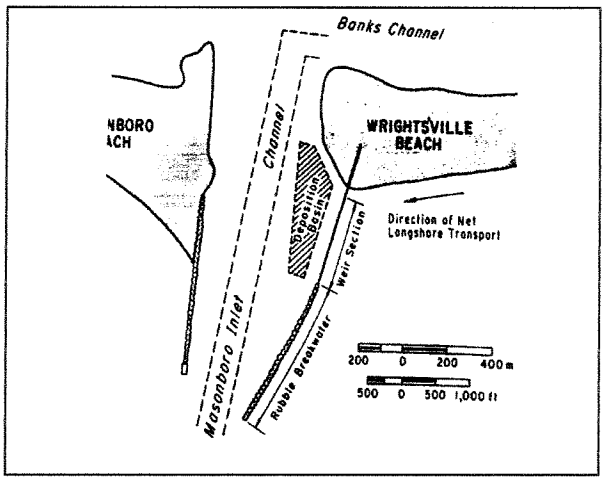

(From: Bruun, 1978)

Figure 5.4: Natural sand bypassing

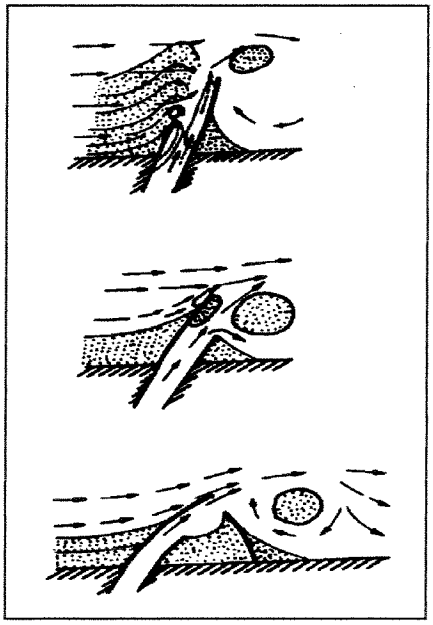

(Bruun, 1978)

Mostly two jetties are used to protect inlets, because one jetty creates problems on its downdrift side. Diffraction of waves can cause current reverse, and therefore sediment transports towards the entrance channel. So to protect a tidal inlet properly two jetties are necessary. An example of a protection with one weir jetty is the Masonboro Inlet, North Carolina, shown in Figure 5.3a. Bruun (1978) described the investigations of Kieslich and Mason (1975) who documented the response of several tidal inlets with a single jetty in the USA including the Masonbore Inlet. "Bathymetric surveys showed that after the construction of a single jetty in 1966, the entrance channel starts to migrate towards the jetty. Two years later 1968 the position of the entrance channel was directly adjacent to the jetty. A number of other single jetty protected inlets show the same development. Also from navigation point of view single inlets are not desirable because of the narrowing entrance channels. Dredging has usually required within a few years after construction" (Bruun, 1978). Later a second jetty was build to improve the situation. This is illustrated in Figure 5.3b.

5.2.2. Efficiency and jetty extension

The efficiency of jetties depends primarily on their length in relation to the bottom slope, wave exposure and the littoral drift. The length of the jetties is often determined in the area of undisturbed littoral drift, in other words, extending through the whole breaker zone. In this case jetties are acting like a total or partial barrier for the littoral drift. In most cases only part of the drift is cut of, and a certain percentage of drift bypasses at the same time as accumulation takes place updrift. The presence of jetties causes a diversion of the littoral drift, which results in bypassing. Bruun and Gerritsen (1960) give various principles of natural sand bypassing across jetty improved tidal inlet, as illustrated in Figure 5.4. To what extent the jetties are going to interfere with the entrance channel depends upon the ability of the tidal currents to flush the channel and maintain the desired depth. The latter is favoured in case strong ebb tidal currents are present, so that the material is lost either in the deep ocean if the offshore bottom is very steep, or drift longshore if the currents outside the navigation channel are strong enough to bring the material downdrift (Bruun, 1978). However in some cases strong ebb current are causing adverse effects. This was the case at the Fort Pierce Entrance in Florida (Figure 5.5) The strong ebb currents flushed the material out which drifted southward on a long shoal. This caused significant downdrift erosion. The strong ebb currents transported sediments too far offshore. The flushed sediments do not easily come back by wave action because of the relatively deep water. To solve this problem the sediment has to bring back to the shore by temporarily nourishment. There are several ways to improve this situation. Asymmetric entrance with a longer jetty on the updrift side makes it possible for the sediment to enter into the littoral drift again. Another more effective way is the use of curved jetties (Bruun, 1978). A negative aspect of curved jetties is that they are longer than straight jetties, which increases the costs significantly. For the layout of the improved tidal inlet with jetty protection there is no universal design approach possible because of the differences between various inlets.

The length of the jetties must be determined taking all cost into account from non- protected with much dredging to fully protected extending across the whole breaker zone. It is obvious that jetties that are extending through the whole breaker zone accumulate large amounts of the littoral drift and cause extensive erosion on the downdrift side. If jetties have a limited length, with their end positions located within the zone of normal littoral drift. Than the depths outside the jetties will have to be maintained by regular dredging. It may be concluded that the length of the jetties is fully determined by the bypassing of sediment across the inlet or: "How short can the jetties be without involving too much risk of sudden shoaling which may be difficult to cope with in time? *Thus the layout of an improved tidal inlet requires consideration on navigational safety as well as to littoral drift and bypassing by nature and/or by man or by combined efforts*". (Bruun, 1978)

Figure 5.5: Possible adverse effects

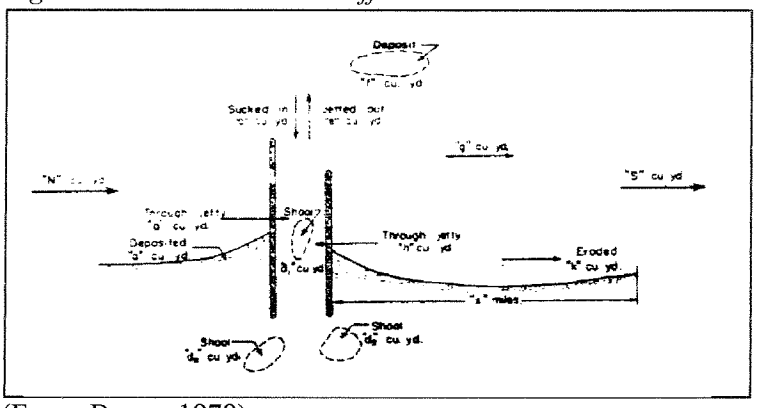

(From: Bruun, 1978)

Figure 5.6: Inlet throat depth without jetty improvement

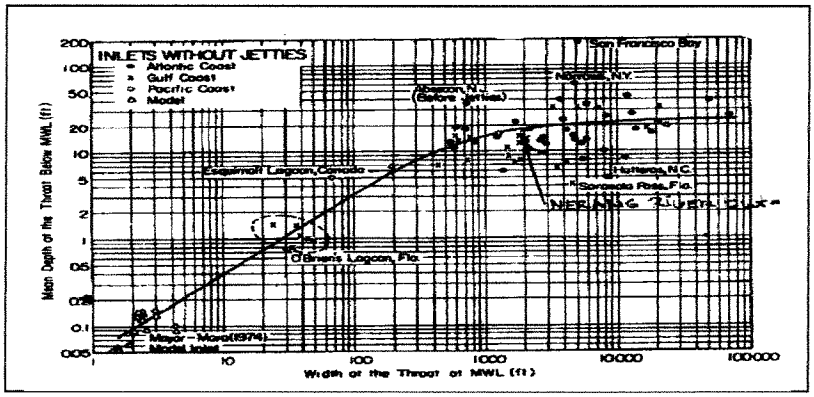

(From: Bruun, 1978)

Figure 5.7: Inlet throat depth with jetty improvement

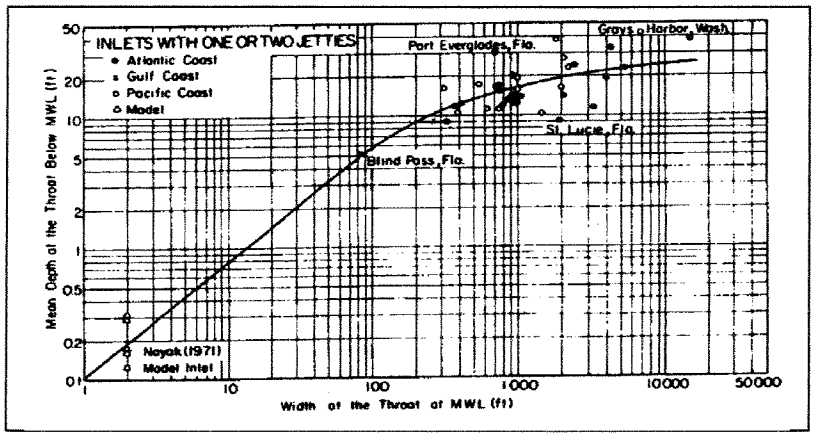

(From: Bruun, 1978)

Figure 5.8: Cross-sectional areas for some improved inlets

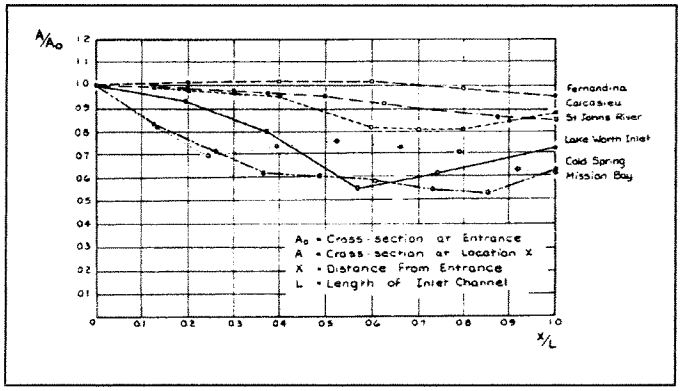

(From: Bruun, 1978)

5.2.3. Effects of jetties on the entrance cross-sectional area

It is obvious that jetties have effects on the inlet cross-sectional area. Bruun and Gerritsen (1960) and Bruun (1978) presented data that show that on the average the ratio between the cross-sectional areas of trained and untrained entrances is approximately 0,88. The reason for the difference in cross-sectional areas must be sought in the velocity distribution in the entrance. In an untrained entrance the velocity varies across the entrance due to variation in water depth. In a trained entrance the velocity is much more evenly distributed. (Delft Hydraulics, 1976)

According to Delft Hydraulics (1976) the differences in cross-sectional areas between trained and untrained entrances can be verified theoretically by assuming that the transport capacity through the two entrances must be the same. Delft Hydraulics (1976) used the following expression to compute the ratio between the cross-sectional area of the trained and untrained entrance:

$$\frac{A_{trained}}{A_{untrained}} = \frac{V_{average}}{V_r} = 0.88 \qquad (40)$$

V_r = uniform current velocity that gives the same transport rates as the average velocity transport rate.

Bruun (1978) showed the validity of the assumption that a typical tidal inlet is wide, with respect to the inlet depth (hydraulic radius ≈ depth) with the data given in Figure 5.6 and Figure 5.7. These figures show the width-depth relation for several North American Inlets and a model inlet, with and without jetties. They show clearly a trend that trained entrances have larger depths at the same width with respect to untrained entrances.

On jetty improved tidal inlets, cross-sectional areas increase when moving oceanward from the gorge. This can be explained by the combining shear stresses of waves and currents. Figure 5.8 shows the cross sectional areas, below MLW, for some jetty improved tidal inlets. The cross-section has been plotted along the length of the inlet channel a dimensionless diagram. From this figure can be seen that the entrance channel cross-sectional area generally are greater than the cross-sections in other parts of the channel. The presence of wave actions has decreased the stability shear stress for the tidal currents because the orbital velocities of the wave action along the bottom of the channel increase the actual shear stress values, resulting in greater cross-sections near the entrance of the channel (Bruun and Gerritsen, 1960) In the case of parallel jetties contraction of the flood flow often occurs at the entrance of the channel. Bruun and Gerritsen (1960) referred to some French investigations on the streamline pattern in tidal entrances. "Contraction of the flood flow means higher flood velocities locally, which cause depth to increase and furthermore may result in a cross-section with a rather marked channel carrying the main part of the flood flow as well as the ebb flow. The entrance cross-section may, therefore develop `uneconomical` with shoaling sections along the jetties particularly the updrift jetty".

5.2.4 Weir jetties

Weir jetties have been developed to prevent the formation of a large offshore shoal, which is dangerous for navigation. This is achieved by building a lower section close to the shore in the updrift jetty. Ideally, the net littoral drifts pass over the weir and settles in the protected inter-jetty deposition basin, which is located near, but separate from, the navigational channel. The deposition area, of course, has to be dredged regularly. Weir jetties work best in areas of low tidal range and a strong predominant drift. The weir jetty bypassing concept has been shown to be an effective means of bypassing a part of the littoral drift. Although the performance of the

Figure 5.9: Sand bypassing, Little River Inlet, South Carolina

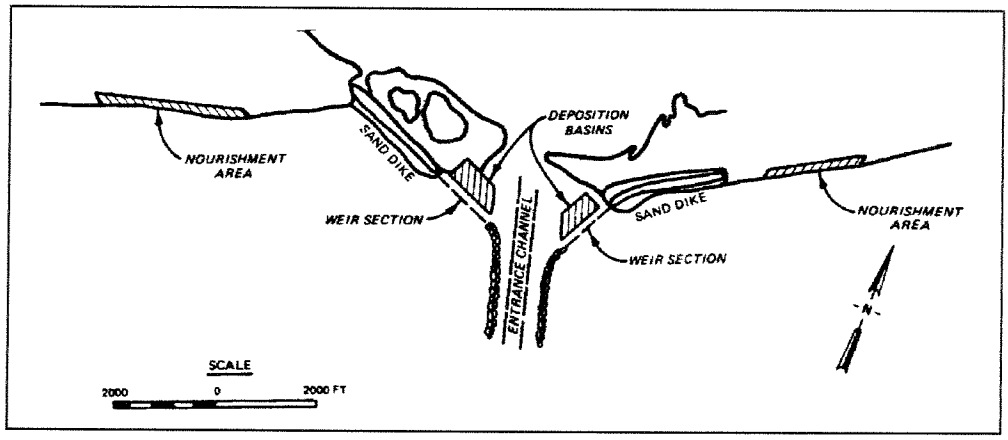

(From: Shore Protection Manual, 1982)

Figure 5.10: Response of the ebb tidal delta on three weired inlets

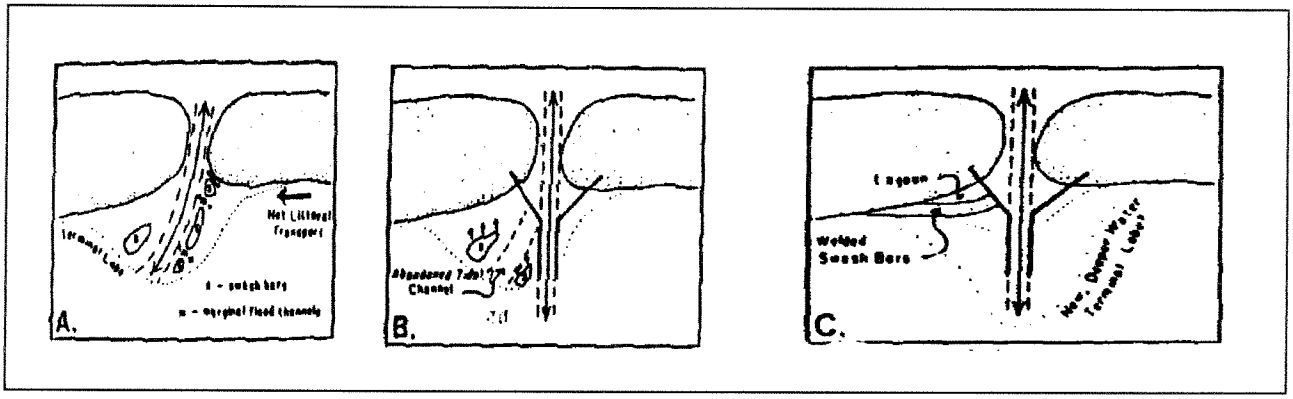

(FitzGerald, 1986)

first weir jetty systems, like any new concept, was not always as expected, recent advancements in their design criteria and in the understanding of their functional behaviour have transformed the weir jetty concept into one of the most feasible methods of bypassing littoral drift (Shore Protection Manual, 1984). Examples of improved tidal inlets with weir jetties are the Murrels Inlet, South Carolina, and the Little River Inlet (Figure 5.9), South Carolina. However weir jetties are not always effective. The East Pass and Ponce de Leon inlets both in Florida were judged to be ineffective and the weirs later deactivated by filling with rubble (FitzGerald et al., 1988). FitzGerald et al. (1988) states that in areas of high tidal range, weir jetty sections constructed at a fixed elevation tend to be less effective since at high tide considerable flow and wave energy can enter the inlet over the weir. In such cases, the use of loose permeable rubble for the weir section will probably be much more effective. An additional significant advantage of a rubble weir section is that, through the addition or removal of rocks, the permeability can be decreased or increased, respectively, thereby allowing `fine-tuning` at relatively low cost. The need for an degree of fine-tuning could be based on profile monitoring results and could be carried out annually or when deemed appropriate (FitzGerald et al., 1988).

FitzGerald et al. (1988) investigated the response of the ebb tidal delta on these three weired inlets at South Carolina, illustrated in Figure 5.10. (A) Shows the configuration before construction of the jetties. (B) Shows that the jetty construction confined tidal flow between the jetties, resulting in a disappearance of natural flood and ebb segregation. This `tidal abandonment` causes wave dominance in the former ebb tidal deltas, which caused a landward sediment transport in these areas. (C) Shows beach ridge welding and formation of a lagoon on the downdrift side of the inlets, while a new ebb tidal delta terminal lobe developed.

5.3. Improvements by dredging of traps or navigation channels.

Dredging of the ocean side (ebb tidal delta) is useless because the littoral drift fills it rapidly. Therefore dredging of the bayside (flood tidal delta) is better, it increases the tidal prism and the sediment transported to the bay side is not returned by the ebb currents and so lost for the ocean side causing a decrease in bar volume. This is true for rather heavily exposed shores and therefore limited offshore bar development (Bruun, 1978).

On shores where the littoral drift is weak and wave action rather low the navigation channels are not or very low subjected to siltation. In these particular cases dredging of channels to improve navigation is an option. The improvement of tidal inlets by dredging was done for numerous port entrances. But in most of the cases, tidal inlets form too many disturbances to the natural situation that it has to cope with shoaling problems. When significant tidal currents in combination with river discharges are present the siltation problems increases, especially in those areas where the currents decreases, introducing potential sedimentation. (Bruun, 1978) To improve these situation sand traps has been developed. A trap is simply a locally deepen area in which the larger particles (sand) will be deposited because of the decreasing transport capacity of the currents. The smaller particles (silt) are flushed by the tidal currents to be deposited in the ocean. So these traps are accumulation areas for material which would otherwise settles down in the dredged navigation channel. The location of these traps must be at those places where accumulation of sand appears. Figure 5.11A and 5.11B shows two examples of sand traps. When the littoral drift is significant the threat is from both sides so traps have to be designed accordingly. In these cases dredging is a continuous process (Bruun, 1978).

Figure 5.11A: Sand bypassing, Sebatian Inlet, Florida

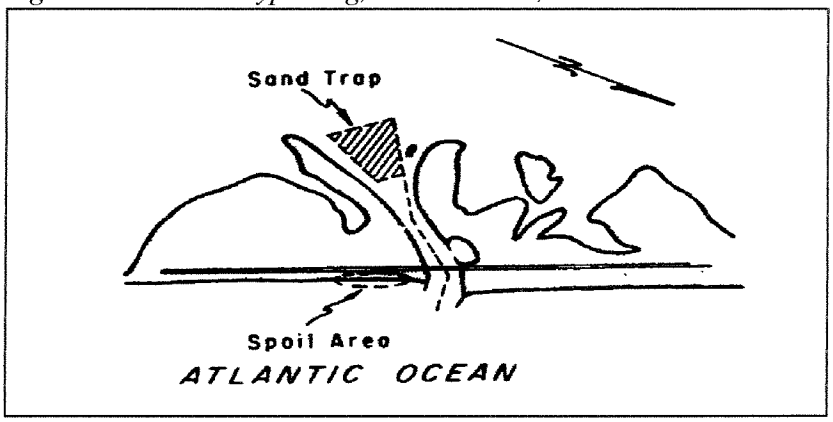

(From: Shore Protection Manual, 1986)

Figure 5.11B: Sand bypassing, Jupiter Inlet, Florida

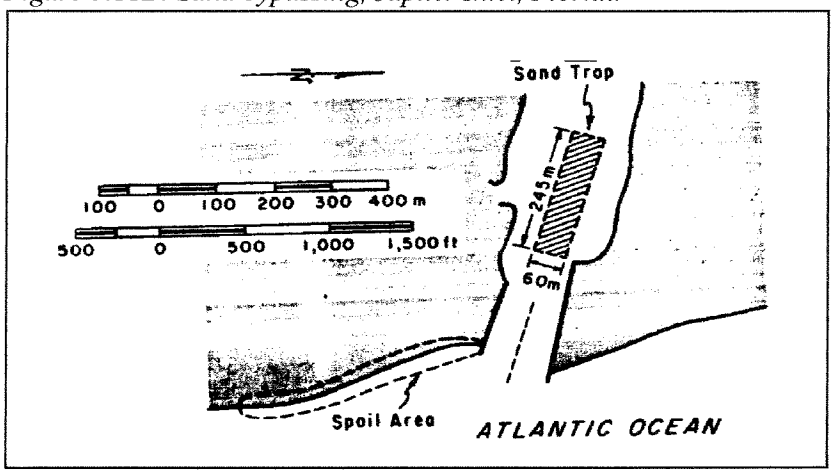

(From: Shore Protection Manual, 1986)

Figure 5.12: Bypass System

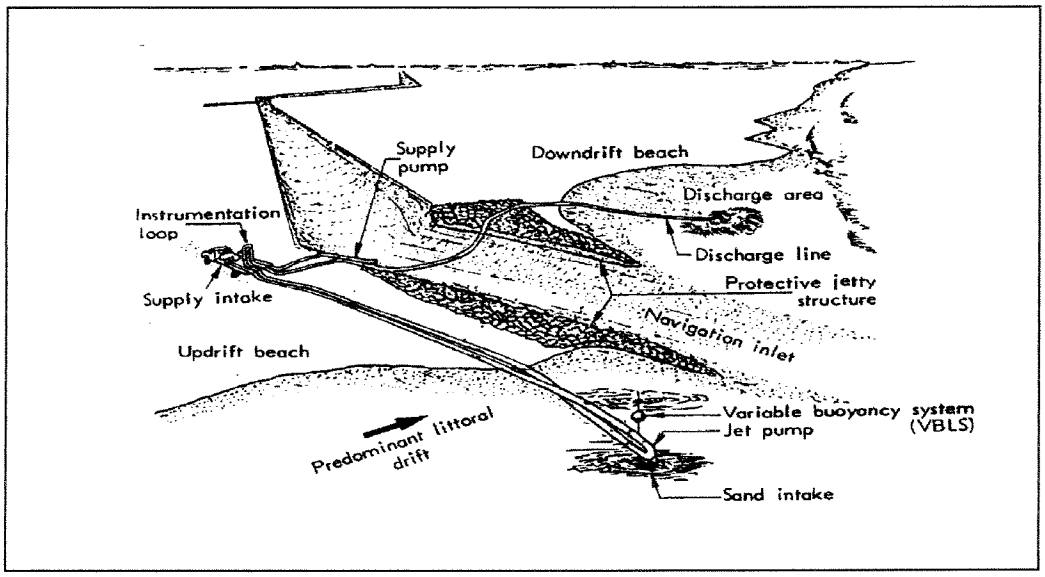

(From: Bruun, 1978)

5.4. Mechanical inlet sand bypassing

5.4.1. Introduction

When nature is unable to bypass sediment across tidal inlets by currents (tidal flow bypassing) and wave action (bar bypassing), and regularly dredging is not wanted, than mechanical bypassing must be undertaken. As any groin or jetty protection of an tidal inlet entrance represents a partial or complete littoral drift barrier it will be necessary to create a bypassing system (Bruun, 1978). Figure 5.12 gives a sketch of a mechanical bypassing installation. Mechanical bypassing serves three main purposes:

- Protection of navigation channels against deposits by longshore littoral drift materials.
- Protection of the downdrift side beaches against erosion caused by the littoral drift barrier.
- Preventing or reducing ocean bar building in order to create a safe entrance for navigation.

There are in general three basic methods for mechanical bypassing of sediment. (Shore Protection Manual, 1984).

- Fixed land-based dredging plants
- Floating bypass plants
- Land-based vehicles or draglines

However in most cases a combination of these methods appeared to be the most economical choice. Example of a combination of fixed land-based dredging plants and a floating bypass plant is given in Figure 5.13 of the Rudee Inlet, Virginia. (Sand bypassing of the weir jetty impoundment zone).

5.4.2. Fixed land-based dredging plants

5.4.2.1. Introduction

Fixed land-based dredging plants have three important parts: the updrift intake, the discharge line who brings the sediment trapped on the updrift side to the downdrift side and the downdrift point of discharge. Example of a fixed bypassing plant, Lake Worth Inlet, Florida, is given in Figure 5.14. These plants consist of a dredge pump located in a building and an intake with limited movement both horizontally and vertically.

5.4.2.2. Updrift intake

The updrift intake is basically an ordinary suction dredge that is in fixed position near the beach intercepting littoral drift to be transported downdrift. Protection Manual (1984) states: "Plants are positioned on an existing structure supported by a independent foundation. Some moveable plants have been located on jetties with the capability of dredging along the length on both sides. Such plants have a much larger reservoir or deposition basin to accumulate the littoral drift during storm periods when the rate of transport exceeds the pumping capacity. To be effective, the design and position of the artificial fixed bypassing plant (updrift intake) depends on the variation in longshore transport and has to be studied critically. The average amount of accreted sediment on the jetty is equal to the minimum quantity of material that has

Figure 5.13: Fixed bypassing plant, Rudee Inlet , Virginia

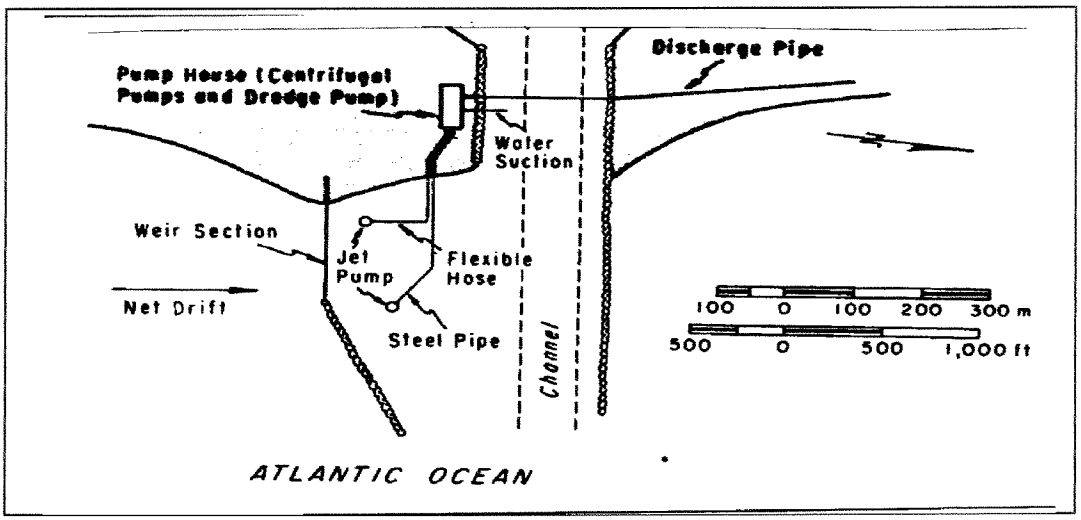

(From: Shore Protection Manual, 1986)

Figure 5.14: Fixed bypassing plant, Lake Worth Inlet , Florida

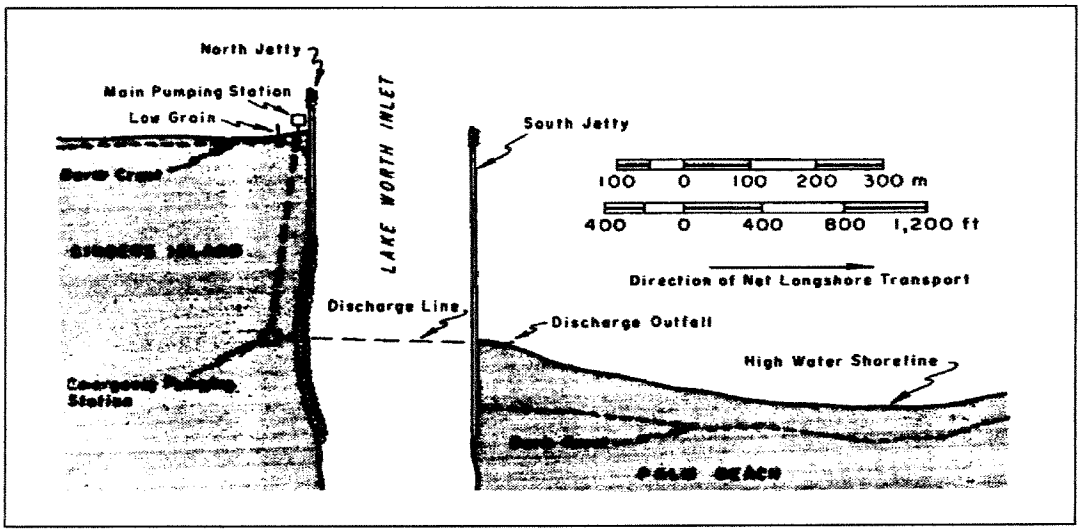

(From: Shore Protection Manual, 1986)

Figure 5.15: Sand bypassing, Santa Barbara, California

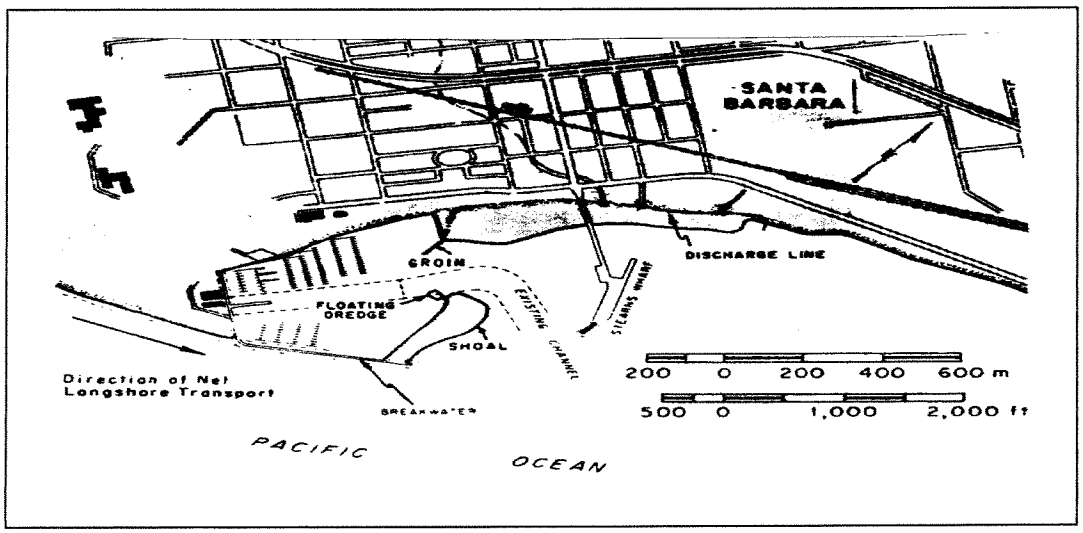

(From: Shore Protection Manual, 1986)

to be bypassed. During a year the fluctuation of the quantity of material causes the plant to operate below or above its capacity. For an effective operation the position of the bypass plant is crucial. When a bypassing plant is located to close to the shore it may result in a landlocked plant when the rate of material reaching the barrier within a short time interval exceeds the pumping capacity. Another result of a landlocked bypassing plant is the large losses of material around the barrier. On the other hand if the location is to far seaward it will take a while until sufficient sediment has impounded to be effectively bypassed. The latter raised the idea of a mobile bypass plant on a trestle with the capability of dredging a long deposition reservoir on both sides. This increases the capacity of the littoral reservoir and reduces the possibility of landlocking".

FitzGerald et al. (1988) states that the effectiveness of the bypass installations at Lake Worth Inlet and Port of Palm Beach Entrance in Florida are not very high, not because of technical deficiencies but rather because of human interference in the system's design/operation.

5.4.2.3. Discharge line

Its obvious that this discharge line has to be secured from damage by (pitching) ships crossing the entrance channel and maintenance dredging operations. Its position is fully dependent on the local circumstances. Also a flushing system must be present to keep the discharge line free from clogging when the pumps are shut down. (Shore Protection Manual, 1984)

5.4.2.4. Downdrift discharge point

Probably the most important part of land-based dredging plants is the point of discharge. The location of this part is important for the effectiveness of the whole bypassing plant. This point is not critical if there is a unidirectional longshore drift present (Shore Protection Manual, 1984). In previous chapters is pointed out that currents can be reversed by refraction of waves or diffraction by the downdrift barrier. Also the tidal current pattern must not be forgotten. Due to this reversal transport some of the material is transported back to the downdrift barrier or in the entrance channel. This reverse transport should be kept to a minimum to reduce the channel maintenance. Tidal currents towards the inlet may frequently predominate over other forces and produces a strong movement of material towards the downdrift jetty or into the inlet. Situations with no downdrift jetty is asking for trouble particularly when the discharge point is located inside the influence zone of the updrift jetty. According to the Shore Protection Manual (1984), the optimum location for the discharge point requires wave data, refraction and diffraction diagrams and (nearshore) tidal current data. Another approach to keep the discharge point near the downdrift barrier is to use groins to block the updrift movement of sediment. This alternative consideration is valued in determining the most economical discharge point (Shore Protection Manual, 1984).

5.4.3. Floating bypass plants

This method is known as jet pump sand bypassing. The pumps are able to reposition within the impoundment zone and therefore able to dredge a large area. Richardson and McNair (1981) describe the jet pump system and outline the necessary planning and hydraulic design of such an installation (Shore Protection Manual, 1984). Examples are the Rundee Inlet, Virginia, the floating dredge in the harbour of Santa Barbara shown in Figure 5.15, California, and the pipeline dredge shown in Figure 5.16, on the bayward side of the reef-natural sand spillway at the Hillsboro Inlet Florida.

Figure 5.16: Sand bypassing, Hillboro Inlet, Florida

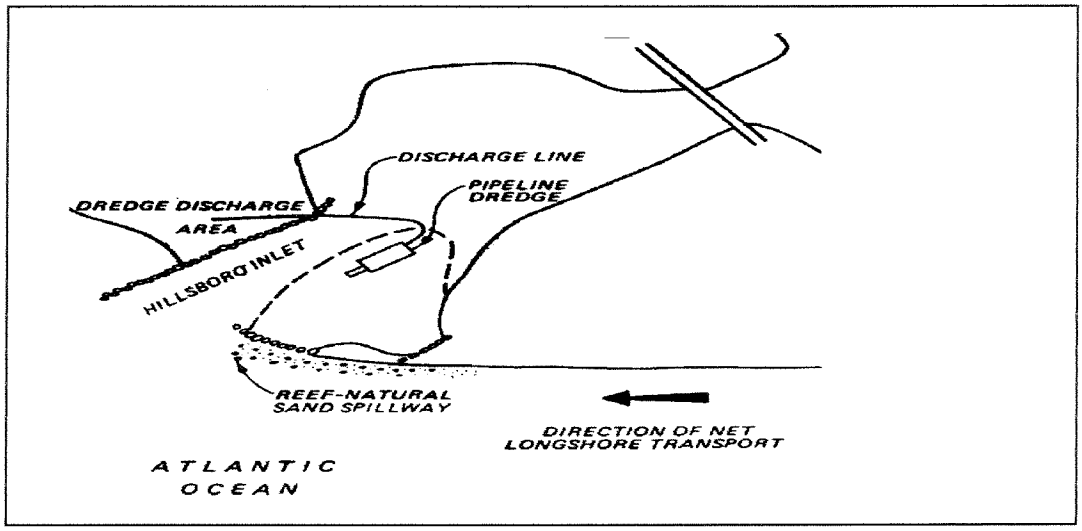

(From: Shore Protection Manual, 1986)

Figure 5.17A: Types of littoral barriers where sand transfer systems have been used

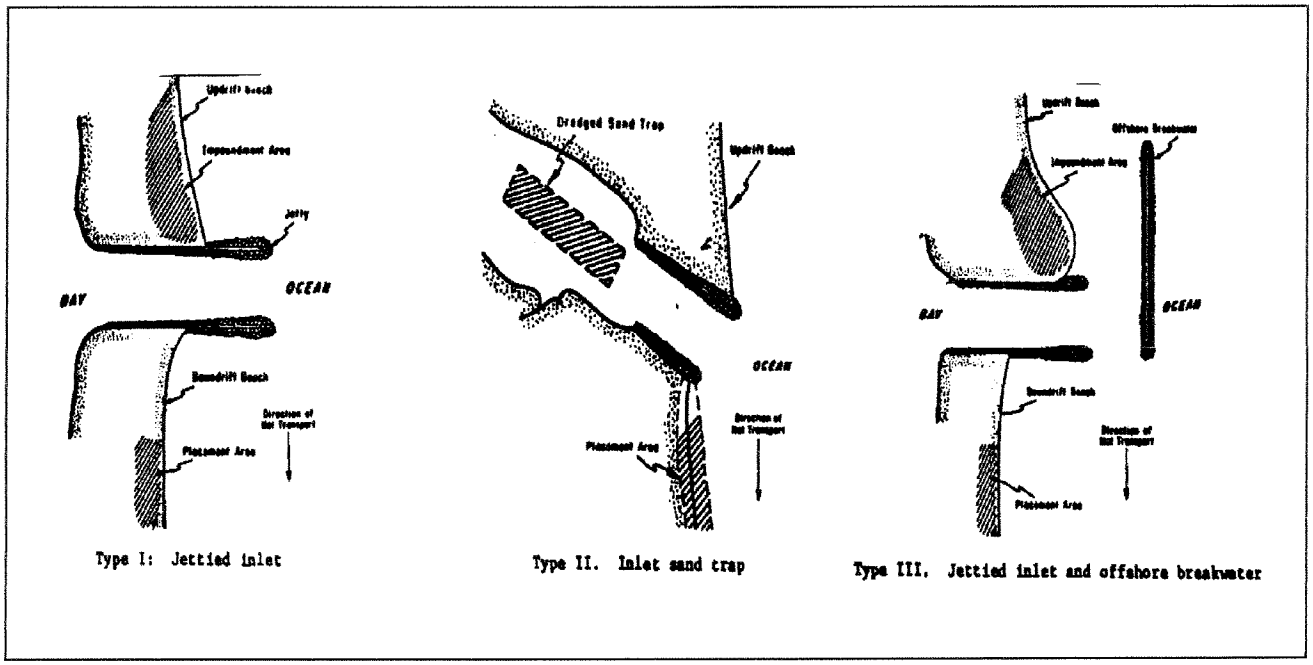

(From Shore Protection Manual, 1986)

5.5. Examples of inlet improvements

The improvement of tidal inlets on littoral drift shores with types of littoral barriers, like jetties and breakwaters that have been used in the past are shown in Figure 5.17. This figure shows clearly that inlets in general are improved by at least one littoral barrier. However proper sand bypassing across the inlet is necessary to prevent the downdrift coast from severe erosion. All types of improvement show an updrift impoundment- and downdrift displacement zone. For more detailed information is referred to the Shore Protection Manual (1984).

Type I show a jetted inlet, bypassing of littoral drift can be done by land-based dredging plants or by a floating plant when there is no severe wave action present on the impoundment area. In any type of operation at such a jetted inlet, it is likely that some bypassing material will pass around the updrift jetty into the channel, especially after the accretion capacity of the jetty has been reached. Example: Port Hueneme, California. (Shore Protection Manual, 1984).

Type II shows a sand-bypassing technique of dredging a sand trap in the protective area of the tidal inlet entrance. This is particularly useful when river discharges carry high sediment loads and in cases were there is a sufficient tidal current available to move the sediment into the inlet where it is deposited into the sand trap. Periodic dredging of the trap and depositing of the dredged material on the downdrift beach completes the bypass operation. Because of the sheltered area of the sand trap it is possible for the dredging equipment to serve also during severe weather conditions. Examples are Jupiter Inlet and the Sebastian Inlet, Florida (Shore Protection Manual, 1984).

Type III shows an attempt to bypass the littoral drift by a combination of jetties and an offshore breakwater. The deposition area is created by the offshore breakwater parallel to the shore. The offshore breakwater creates a shadow zone behind the breakwater, reducing the sediment transport capacity and therefore induces sedimentation. The offshore breakwater must be located far enough in order to keep the sedimentation capacity sufficient. Also maintenance of the offshore breakwater is difficult because it is inaccessible from the land (Delft Hydraulics, 1976). In this design, a floating plant works effectively, completely protected by the breakwater and most of the sand moving inshore of the offshore breakwater be bypassed. Practically no shoaling of the channel would be expected. Although this type is considered the most effective type of improvement for both navigation and sand bypassing, its on the other hand normally the most costly. Example at the Channel Island Harbour, California (Shore Protection Manual, 1984).

Type IV is also been used effectively. The shore connected breakwater with impoundment at its seaward end. Bypassing is performed by a floating plat, but heavy wave action could cause delays during the removal of the outer part of the impoundment. Most of the sand transported alongshore would be bypassed, either naturally or mechanically, but some shoaling of the navigation channel is likely between the dredging operations. Examples are at Santa Barbara California and at Fire Island Inlet, New York (Shore Protection Manual, 1984).

Type V is a shore connected weir jetty with a low crest near the shore. Behind the weir section there is a deposition zone or impoundment basin located. This design is to provide bypassing of the littoral drift moving inshore of the seaward end of the weir by a floating plant, thus not permitting any of that part of the littoral drift to shoal the navigation channel. A successful bypassing operation at Hillsboro Inlet, Florida where a basin behind a natural rock ledge is dredged periodically, formed the basis of this design. Examples: Perdido Pass, Alabama, Little River Inlet, South Carolina. (Shore Protection Manual, 1984).

Figure 5.17B: Types of littoral barriers where sand transfer systems have been used

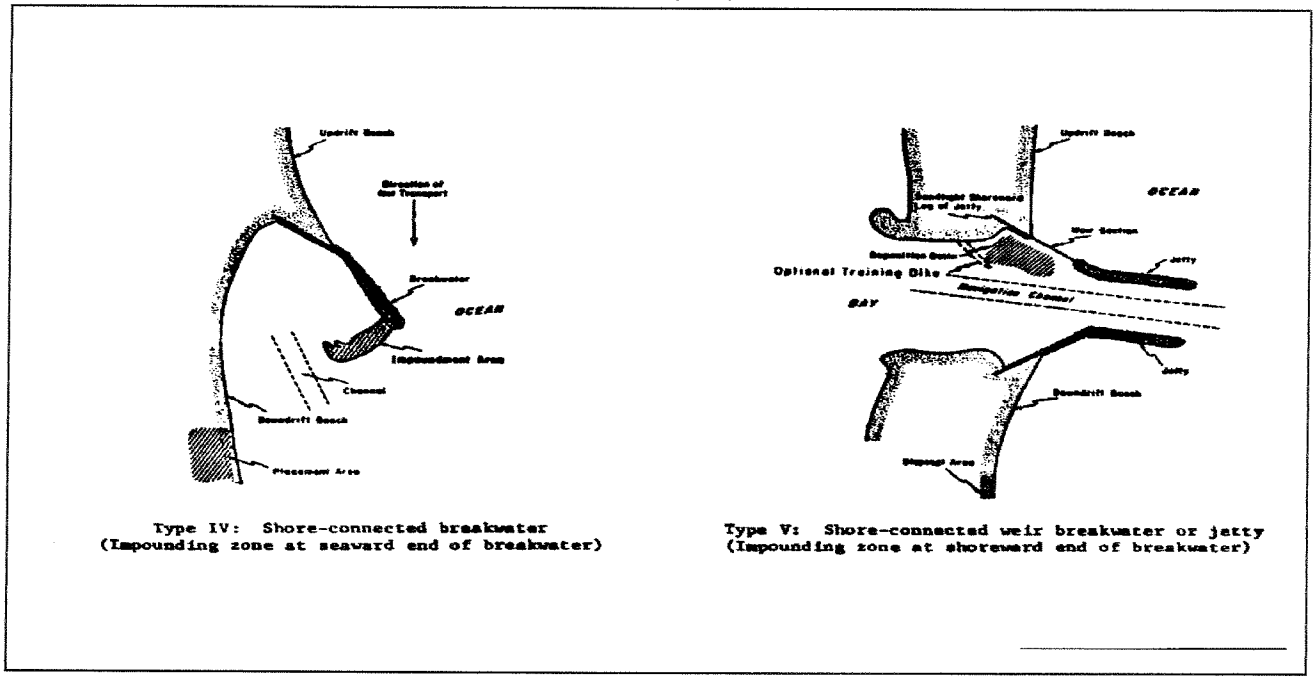

(From Shore Protection Manual, 1986)

References (Volume I and II)

Aubrey , David G. , Weishar, Lee (Editors) , 1988, Hydrodynamics and sediment Dynamics of Tidal Inlets
Section: "Shoreline erosional-depositional processes associated with tidal inlets"
Springer-Verlag, New York, USA

Beach Protection Authority Queensland, Australia
Nerang River Entrance Stabilization, 1986

Bruun, Per , 1978
Stability of tidal inlets (Theory and Engineering)
Development in geotechnical engineering; volume 23
Elsevier scientific publishing company, Amsterdam -The Netherlands.

Bruun, Per , 1978, Gerritsen, F. , 1960
Stability of Coastal inlets
Coastal Engineering Laboratory, University of Florida, Gainsville
North-Holland Publishing Company, Amsterdam -The Netherlands.

Coughlan, P.M. ; Robinson, D.A. ; 1988
Gold Coast Seaway-Its impact on the Adjacent Coast
Second Australian Port, Harbour and Offshore Engineering Conference 1988
Brisbane, 25-27 October 1988.
Brisbane Australia.

Delft Hydraulics Laboratory, 1970.
Gold Coast, Queensland, Australia
Coastal erosion and related problems
Volume I ; Conclusions and recommendations, I - R 257 (I)
Delft; The Netherlands.

Delft Hydraulics Laboratory, 1970.
Gold Coast, Queensland, Australia
Coastal erosion and related problems
Volume II , part I, Investigations (Text and Tables) , I - R 257 (IIa)
Delft; The Netherlands.

Delft Hydraulics Laboratory, 1970.
Gold Coast, Queensland, Australia
Coastal erosion and related problems
Volume II , part II, Investigations (Figures) , I - R 257 (IIb)
Delft; The Netherlands.

Delft Hydraulics Laboratory, 1976.
Nerang River Entrance Stabilization
Report on model investigations ; M 1259
Delft; The Netherlands.

Delft Hydraulics Laboratory, 1992.
Gold Coast, Queensland, Australia
Southern Gold Coast littoral sand supply

Final Report, Volume II
Delft; The Netherlands.

Department of Harbours and Marine and the Gold Coast Waterways Authority, Australia
Water level monitoring report the Broadwater/Nerang River Entrance 1987
Tide section, Department of Harbours & Marine August 1987

Di Lorenzo, J.L., 1988
The overtide and filtering Responce of Small Inlet Bay Systems
Aubrey, D.G. and Weishar, L. , 1988; pp 24 - 53

Dombrowski, Michael R. , Mehta, Ashish J. , 1996
Ebb delta evolution of coastal inlets
Coastal Engineering 1996 Volume 3 ; chapter 253 (Edited by Billy L. Edge)
Proceedings of the twenty-fifth international conference ; American Society of Civil Engineering - New York

Drapeau, Georges, 1988
University of Quebec, Canada
Lecture notes on Coastal and Estuarine Studies, Volume 29.

Escoffier, Francis F. , 1940
United States Engineer Office. Mobile, Alabama
Stability of Tidal Inlets
Shore and Beach, October 1940 pag.114-115

FitzGerald, Duncan M. , 1988
Department of Geology, Boston University
Lecture notes on Coastal and Estuarine Studies, Volume 29.

Huis in `t Veld, J.C. ; Stuip, J. ; Walther, A.W. ; van Westen, J.M. , 1987
The Closure of Tidal Basins; part: Environmental Conditions; D. Smith
Delft University Press, Delft - The Netherlands.

Jonsson, I.G., 1978
Stability of tidal inlets (Theory and Engineering); part: Combinations of waves and currents
Development in geotechnical engineering; volume 23
Elsevier scientific publishing company, Amsterdam -The Netherlands.

Karssen, B and Wang, Z.B. , 1991
Morphological modelling in estuaries and tidal inlets
Part: I A literature survey Z473
Delft Hydraulic Laboratory ; Delft - The Netherlands

Kana and Mason, 1988
Department of Geology, Boston University
Lecture notes on Coastal and Estuarine Studies, Volume 29.

King, D.B. (1974)
The dynamics of inlets and bays
Tech. Rep. 2, Coast. and Ocean. Eng. Lab. ; University of Florida

Keulegan, G., 1950

Tidal flow in entrances. Water level fluctuations of basins in communication with seas.
Techn. Bull. Nr. 4 , Committee on tidal hydraulics, USCE, Waterways Experiment Station, Vicksburg, Miss.

Kreeke, J. van de , 1990
Stability analysis of a two-inlet bay system
Coastal Engineering Nr. 14 pp 481-497
University of Miami

Loo, van L.E. , 1976
Coastal Engineering Vol. I Introduction ; part Coastal Formations
Faculty of Civil Engineering , Delft University of Technology ; Delft - The Netherlands

Matsunaga, N.; Hashida, M. ; Kawakami, H. , 1996
Wind Induced Waves and Currents in a Nearshore Zone
Coastal Engineering 1996 Volume 3 ; chapter 260 (Edited by Billy L. Edge)
Proceedings of the twenty-fifth international conference ; American Society of Civil Engineering - New York

Manual on the use of Rock in Hydraulic Engineering, CUR Report 169, 1994
Centre of Civil Engineering Research and Codes; Rijkswaterstaat/ Department of Public Works
Gouda - The Netherlands.

Marino, James N., (Coastal Engineering Research Centre) and Mehta, Ashish J. (Coastal and Oceanographic Engineering Department, University of Florida), 1988
Lecture notes on Coastal and Estuarine Studies, Volume 29.

Mehta, A.J. and Özsoy , 1978
Stability of tidal inlets (Theory and Engineering), Per Bruun, Chapter 3 , Inlet Hydraulics
Development in geotechnical engineering; volume 23
Elsevier scientific publishing company, Amsterdam -The Netherlands.

Niemeyer, H.D. , 1990
CM5 Morphodynamics of Tidal Inlets
Course: Coastal morphology; Stichting Postak. Onderwijs Civiele Techniek en bouwtechniek, Delft

Nortier, I.W., 1989
Toegepaste vloeistof mechanica. hydraulica voor waterbouwkundigen
Educaboek BV, Culemborg - The Netherlands.

O`Brian, M.P. 1969
Equilibrium Flow areas of inlets on sandy coasts
Journal of the waterways and harbours Div. , ASCE, Nr. WWI; pp 43 - 52

O`Brian, M.P. and Dean, R.G. , 1972
Hydraulics and sedimentary stability of coastal inlets
Proc. 13th. Coastal Engineering Conf., ASCE, New York; pp 761-780

Oertel, G.F., 1975
Ebb tidal deltas o9f Georgia estuaries
Cronin, L.E.

Oertel, G.F., 1988
Processes of Sediment Exchange Between Tidal Inlets, Ebb deltas and Barrier Islands
Aubrey, D.G. and Weishar, L.

Sha, L.P., 1990
Sedimentological studies of the ebb tidal deltas along the West Frisian islands, The Netherlands
Ph.D. thesis; publication nr. 64, Geologica Ultraiectina, University of Utrecht, Utrecht, the Netherlands

Shore Protection Manual, Volume I and II (Second Printing, Fourth Edition), 1984
Coastal Engineering Research Centre
US Army Corps of Engineers, Washington DC - USA.

Silvester, Richard , Hsu, John R.C. , 1993
Coastal Stabilization Innovative Concepts
Department of Civil and Environmental Engineering , The University of Western Australia
New Jersey USA.

Steijn, R.C. , 1991
Some considerations on tidal inlets; Literature Survey H 840.45
Delft Hydraulics ; Delft - The Netherlands

Technische Adviescommissie voor de Waterkeringen, 1995
Basisrapport Zandige Kust (Behorend bij de Leidraad Zandige Kust)

Velden, E.T.J.M. van der; 1995
Coastal Engineering
Faculty of Civil Engineering , Delft University of Technology
Delft - The Netherlands

Wang, Xu , Lin, Lihwa , Wang , Hsiang, 1996
Laboratory Mobile Bed Studies on Ebb Tidal Shoal Evolution
Coastal Engineering 1996 Volume 3 ; chapter 255 (Edited by Billy L. Edge)
Proceedings of the twenty-fifth international conference
American Society of Civil Engineering - New York

Nerang River Entrance Stabilisation
(Gold Coast Seaway, Queensland Australia)

September 1999 Maurice J. de Haas

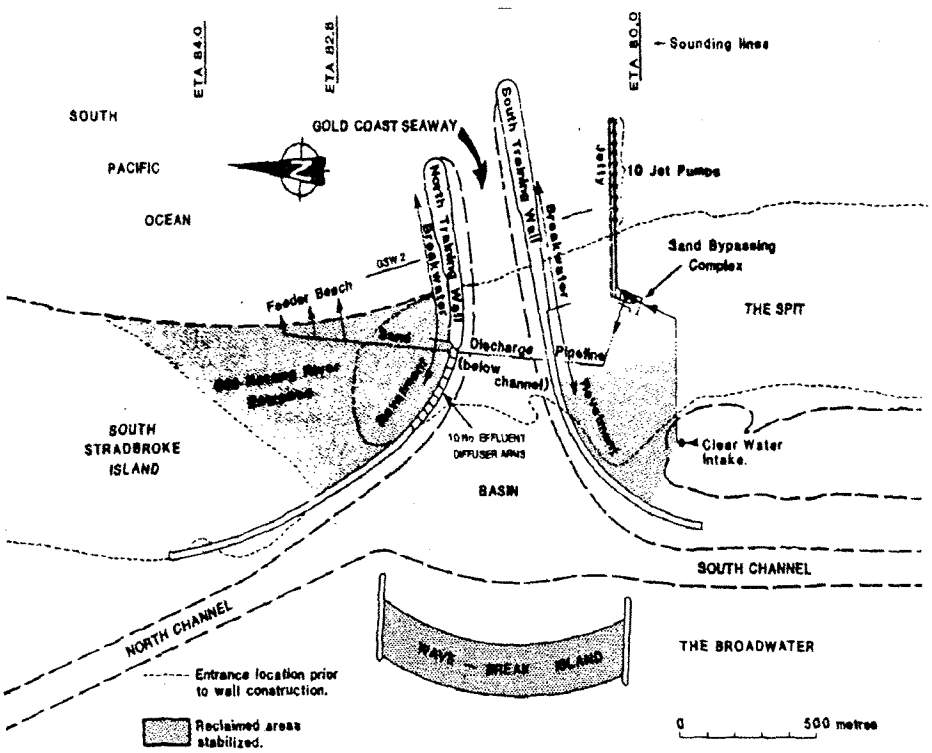

Volume II

TU Delft
Technische Universiteit Delft
Faculteit der Civiele Techniek

Notations

A_b	Surface area of the basin	[m^2]
A_c	Cross-sectional area of tidal inlets	[m^2]
A_d	Deposition area	[m^2]
a_0	Ocean tidal amplitude	[m]
a_{s0}	Spring ocean amplitude	[m]
a_b	Bay tidal amplitude	[m]
b	Cross-sectional width at water level h	[m]
b_c	Mean sea level width of a cross-section	[m]
B	Dimensionless damping coefficient	[-]
C	Chezy Coefficient	[$m^{1/2}/s$]
D_x	Sediment particle grain diameter	[m]
d_a	Average depth in the cross-sectional area of the inlet throat	[m]
d_m	Maximum depth in the cross-section of the inlet throat	[m]
d_c	Shallowest depth in the cross-section of the inlet throat	[m]
E	Phase lag basin tide	[-°]
E_s	Stratification parameter	[-]
f	Darcy-Weisbach friction coefficient coefficient	[-]
f_c	Friction factor due to currents	[-]
f_w	Friction factor due to waves	[-]
f_{cw}	Wave-current friction factor	[-]
F	Friction factor	[-]
Fr	Froude number	[-]
h	Water depth	[m]
h_b	Depth of the inlet basin	[m]
H	Wave height	[m]
H_w	Wave height at breaker line	[m]
H_{rms}	Root mean square value of waves	[m]
H_0	Deep water wave height	[m]
G	Dimensionless tidal frequency	[-]
g	Gravitational acceleration	[m/s^2]
k	Wave number	[rad/m]
k_s	Hydraulic roughness	[m]
k_{sg}	Grain roughness	[m]
$k_{s\Delta}$	Bed-form roughness	[m]
K_{en}	Coefficient for entrance losses	[-]
K_{ex}	Coefficient for exit losses	[-]
K(t)	Repletion coefficient	[-]
K2(t)	Inertia coefficient	[-]
L	Wave length	[m]
L_c	Inlet length	[m]
L_b	Length of the inlet basin	[m]
M_{predom}	Predominant annual littoral drift	[m^3/yr]
M_{total}	Total annual littoral drift	[m^3/yr]
M_s	Total of material transported by the inlet gorge	[m^3]
m	Sum of exit and entrance losses	[-]
N	Tidal amplitude inside basin/ocean tidal amplitude	[-]
P	Spring tidal prism	[m^3/half tidal cycle; ft^3/ half tidal cycle]
p_a	Atmospheric pressure at sea level	[mbar/hpa]
Q(t)	Discharge through the inlet	[m^3]

Q_{max}	Maximum inlet discharge	[m^3/s]
Q_{river}	River discharges	[m^3/s]
R	Hydraulic radius	[m]
S	Sedimentation	[m^3]
$\partial S(t)$	Annual sedimentation	[m^3]
$\partial S(t=0)$	Initial sedimentation	[m^3]
s	Side slope at mean sea level	[-]
t	Time	[s]
T	Wave period	[s]
T_{tide}	Tidal period	[sec]
TV	Tidal volume	[m^3]
V	Depth average current velocity	[m/s]
V_s	Stratification parameter	[-]
V_t	Combined wave current velocity over the bottom	[m/s]
V_{wb}	Near-bed current velocity	[m/s]
V_{cb}	Near-bed orbital velocity	[m/s]
V_{mean}	Mean velocity over half tidal cycle	[m/s]
$V_{mean\ max}$	Mean velocity over the cross-sectional area and maximum velocity during spring tide conditions	[m/s]
$V`_{max}$	Dimensionless inlet velocity	[-]
V_{max}	Maximum inlet velocity	[m/s]
V_{cr}	Critical velocity	[m/s]
$\partial V(t=0)$	New longterm equilibrium situation	[m^3]
W	Width of the entrance	[m]
z_a	Static rise of the mean sea water level	[m]
α	Ratio relative effect of waves and tidal currents	[-]
$\tan\alpha$	Slope nearshore zone	[-]
β	Damping coefficient for the first overtide	[-]
γ_{break}	Breaker index	[-]
τ_s	Shear stress	[N/m^2]
τ_{cr}	Critical shear stress	[N/m^2]
ω	Frequency of the ocean tide	[rad]
Δ_h	Average bed-form height	[m]
Δ_l	Average bed-form length	[m]
θ	Angle between the current and the wave direction	[-°]
ϕ	Parameter to indicate grain dimensions	[-]
$\eta_0(t)$	Ocean tide	[m]
η_{max}	Wave induced set-up	[m]
$\eta_b(t)$	Basin tide	[m]
ρ_w	Density of water	[kg/m^3]
ρ_s	Density of sediment	[kg/m^3]
Ω	Helmholz frequency	[Hz]

List of figures

Volume II: Nerang River Entrance stabilisation

List of figures chapter 1

List of figures chapter 2

List of figures chapter 3

Preface *(Volume I and II)*

In order to graduate as a Civil engineer from the Delft University of Technology in the Netherlands, it was necessary to choose a graduation project. By being in close contact with Professor Kamphuis, I was able to acquire general information on a project in Australia. Although the amount of research needed to successfully complete the quantitative analyses for this project, exceeds the mandatory time that stands for graduating, it was only possible to finish up specific parts of the project. After consulting the "Department of Environment" in Australia it was suggested to me to concentrate on the part which qualitatively studies tidal inlets on littoral drift shores along the Gold Coast Seaway.

The final report consists of two parts: Volume I and Volume II.
Volume I is a general study on Tidal inlets and Littoral Drift shores, to attain important theoretical information before part of the analyses can be carried out. By accumulating the information in Volume I, it later (in Volume II) allows us to obtain a better understanding on the hydrodynamic and morphological processes involved around the Nerang River Entrance and the Gold Coast Seaway.

Readers guide *(Volume I and II)*

In Volume I special attention will be paid to Tidal Inlets on Littoral Drift Shores in general. Section 1 gives general information about the appearance and origin of tidal inlets. Also the most important morphodynamic parts of a tidal inlet will be discussed. Section 2 discusses the hydrodynamic impact on tidal inlets due to waves, currents, severe weather conditions and of course astronomical tides. In section 3 some considerations are discussed on the development of tidal inlets. (morphodynamic) These developments are generally a result of the hydrodynamic active forces, discussed in section 2. Section 4 discusses the stability of tidal inlets. In literature, stability of tidal inlets is mostly discussed in terms of empirical relations. The emphasis in Volume I is not on discussing formulas or advanced computation techniques, but on the qualitative description of the very dynamic interaction of tidal inlets with the active hydrodynamic forces. Section 4 gives a few of the most common and most used stability relations. In this section also some background information is given on these specific stability relations. Special attention will be paid to the stability concept originally developed by Escoffier (1940). This theory gives rather good insight in the behaviour and development of tidal inlets. With the use of this theory the reader is able to get a good first impression of the relevant processes at work. Also special attention will be paid on the stability concept developed by Bruun (1978). Section 5 discusses some important methods for improvement of unstable tidal inlets.

Volume II describes the case of the stabilised Nerang River Entrance (Gold Coast Seaway). In section 1 the historical behaviour of the Nerang Entrance is described and partly evaluated with the use of some theory described in Volume I. Section 2 describes the hydrodynamic components active on the Gold Coast area in general. Section 3 discusses the most important conclusions of model tests, which were carried out by the Delft Hydraulics Laboratory. These model tests are used in this report as a reference in order to evaluate some hypotheses about the behaviour of the stabilised Nerang River Entrance (Gold Coast Seaway) over a period of ten years after the commencement of the project. However the most interesting part of this case study is the impact of the sand bypass installation on the morphology of the Gold Coast Seaway over the last ten years. This is discussed in section 4. In this section the available information which was collected over the past ten years is analysed. The emphasis in this

section is the impact of the sand bypass installation on the adjacent beaches and the development of the ebb tidal delta, over the first ten years of operation. And last but not least some considerations are given about the possible morphological developments in the future.

Graduation committee:
Prof.Dr.Ir. J.W. Kamphuis
Dr.Ir. J. van de Graaff
Dr.Ir. J.A.Roelvink
Ir. P. Huisman

The Hague, September 1999

Maurice J. de Haas

Summary

After consulting the "Department of Environment" in Australia it was suggested that after an extensive generic study about "Tidal inlets on littoral drift shores" the "Nerang River Entrance stabilisation" could be used as a case. The Nerang River is an important river in the Gold Coast region. It is roughly the northern border of the Gold Coast beaches where the Nerang River enters the ocean through a broad shallow estuary known as the Broadwater. The "Department of Environment" is very interested in the impact of the stabilisation works and its effectiveness.

The Nerang river Entrance was prior to training a very unstable tidal inlet and therefore dangerous for vessels. The continuous changes of the navigation channels, both in location and depth resulted in a significant number of boating accidents over the years. Because the entrance is of importance for recreational and commercial reasons the Australian Authorities declared that the Nerang River Entrance must provide a safe navigation and anchorage for recreational craft, as well as numerous fishing vessels. Not only the improved stability of the entrance was an important issue but also the possible adverse effects of the improved entrance works on the adjacent beaches and the nearshore bathymetry.

The Delft Hydraulics Laboratory in the Netherlands was commissioned by the Queensland Government to investigate the problems at the Nerang River Entrance. The Nerang River Entrance investigations by Delft Hydraulics resulted in a report (1976). In this report some recommendations were done to solve this problem. This report by Delft Hydraulics also described the model investigations of the Nerang River Entrance in order to get a impression of the effects of the improvement with and without mechanical sand bypassing. In literature very little is known about the effect of this bypass installation on the morphology of tidal inlets. Therefore the most important results of model investigations are described in this report. In the case of the Nerang River Entrance the mechanical bypass installation was necessary to prevent extensive erosion of South Stradbroke Island. The most important conclusions and recommendations from the Delft (1976) report were followed. The above described studies and recommendations resulted the stabilisation of the Nerang River Entrance with jetties and mechanical sand bypass installation. This resulted in the officially opening of the Gold Coast Seaway in May 1984.

In this report also some calculations based upon the model "simple bay/inlet system" were carried out for the Nerang River Entrance. The (in)stability of the Nerang River entrance was investigated with the theory of Escoffier(1940) The results of these calculations show that the cross-sectional area of the Nerang River Entrance is located at a point some distance from the point of dynamic equilibrium. According to the theory of Escoffier(1940) the cross-sectional area has the intention to increase until it reaches the stable point. However this is not likely to happen because of the unstable character of the Nerang River Entrance.

An important question for the Department of Environment was the evolution of the ebb tidal delta in front of the Gold Coast Seaway. From the period after the commencement of the training works and the bypass installation until now the Gold Coast ebb delta grows and increased in volume. The Department of Environment is interested in the equilibrium delta volume and depth and also the time needed to reach this dynamic equilibrium.

This problem is solved by calculation of the volumetric changes over the past ten years. With the results of these calculations it was possible to give a qualitative view of the ebb delta evolution over the first ten years of operation and the most realistic future developments. It is obvious that bypass installation also caused changes on the southern and northern beaches of

the Gold Coast Seaway. In spite of the limited available data of the northern and southern beaches only some hypothetical conclusion could be drawn. Last but not leased the changes of some representative bottom profiles are studied. Combined with the results of the volumetric changes and the changes in bottom profiles gives an idea how the bypass installation affects the Gold Coast Seaway bathymetry over the last ten years and in the future.

Figure 1.1: Locality plan Gold Coast region

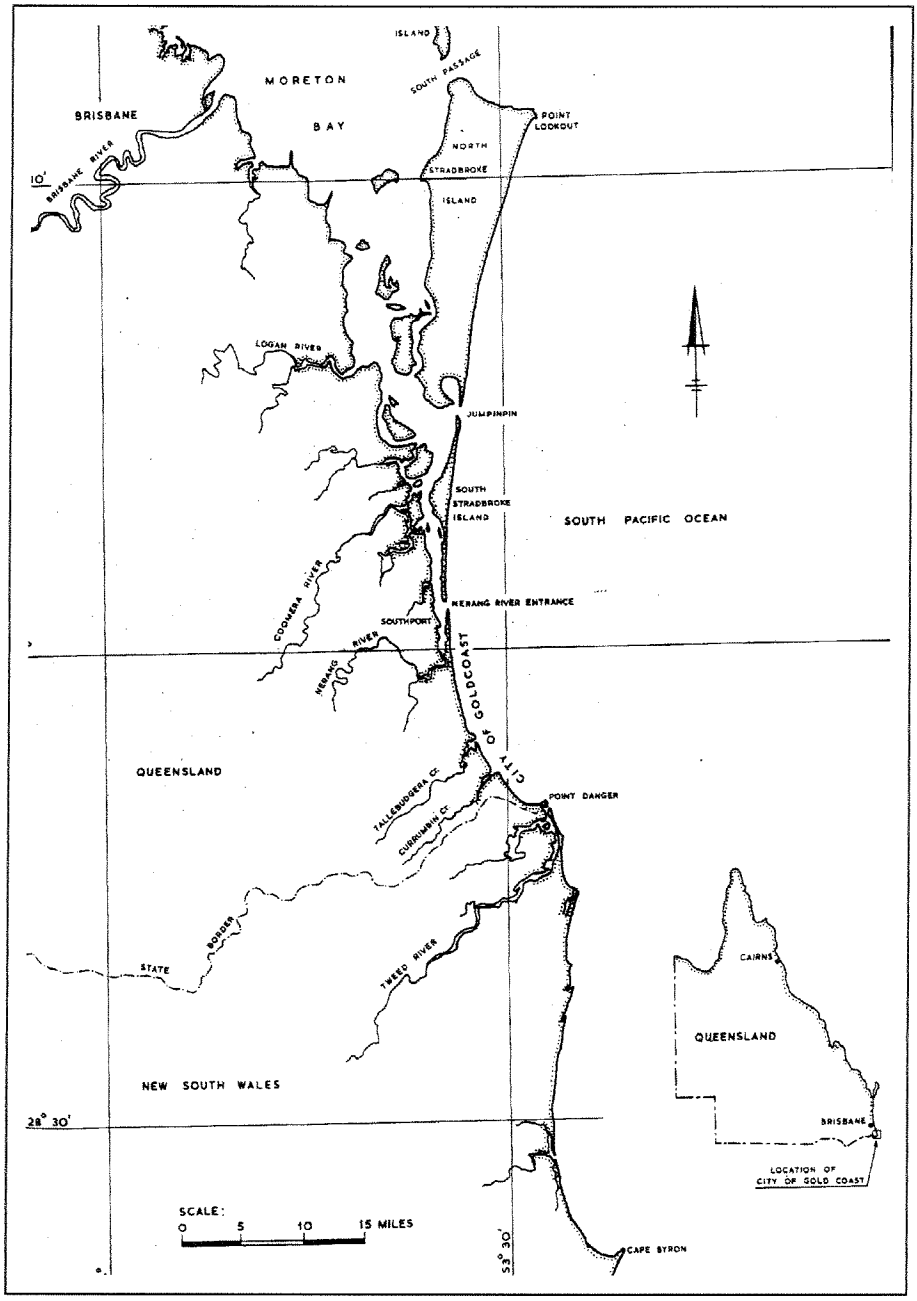

(From: Delft, 1970)

Figure 1.2: Nerang River Entrance in the year 1915

(From: Coastal Management homepage 1998)

1. Nerang River Entrance

1.1. Introduction

1.1.1. General description

On the eastern coast of Australia, approximately 60 kilometres southeast of Brisbane in Southern Queensland the City of Gold Coast is situated. The Gold Coast's 52 kilometres of sandy beaches and good surfing waves provide an important recreational area with many hotels and tourist facilities. However, due to the high wave energy, erosion has become an ongoing problem. From 1968 until now, and probably in the future, much investigation has been done to stabilize the very dynamic beaches of Gold Coast in order to protect the heavily developed coastal region.

The Delft Hydraulics Laboratory in the Netherlands was commissioned by the Queensland Government in the late 1964 to investigate the beach erosion problems at the Gold Coast and to recommend a Programme of Investigations. This was done by a report in 1965. In 1968 the Delft Hydraulic Laboratory was requested to assist in the evaluation of the data being collected consequent to the recommendation of the earlier rapport, and to put forward recommended solutions for the coastal problems of the City of Gold Coast. The conclusions and recommendations of this study were given in the 1970-report of the Delft Hydraulics Laboratory.

This report also examined the instability of the Nerang River Entrance. The Nerang River Entrance is an important river in the Gold Coast region and is roughly the northern border of the Gold Coast beaches where the Nerang River enters the ocean through a broad shallow estuary known as the Broadwater. Interruptions on beaches like the Nerang River Entrance are called tidal inlets. The term tidal inlet is generally used to describe the narrow waterway that connects a tidal basin with the ocean and through which reversing tidal flows are concentrated. South Stradbroke Island borders the river mouth to the north. To the south by The Spit. Figure 1.1 shows a locality plan of the Gold Coast region.

The Department of Harbours and Marine requested the Delft Hydraulics Laboratory in 1973 to further investigate the ways for stabilizing the Entrance. Due to its complexity, the Delft Hydraulic Laboratory strongly recommended, in Delft (1970), a model study for the design of a final layout for the Nerang River Entrance. The model investigations were performed in the Laboratory "De Voorst" of the Delft Hydraulic Laboratory from January 1974 till November 1975 and resulted in a report in 1976. The Department of Harbours and Marine, Australia advised on the training works to the Gold Coast Waterways Authorities who were responsible for the management of the Broadwater and the Nerang River Entrance. The Department undertook fixed bed modelling of the design of the breakwater heads as well as wave penetration into the Broadwater at the Queensland Government Hydraulics Laboratory.

The result of these investigations was an improved tidal inlet by training-walls and artificially bypassing of the littoral drift. The new tidal inlet was opened on May 31, 1986 and named officially the "Gold Coast Seaway".

1.1.2. The Spit

The Spit is the southern Barrier Island of the Nerang River Entrance. During the 1970 investigations of this area, The Spit was approximately 4270 m long and had an average

width of approximately 400 m. The rate of growth, average over the last years of the 1970 investigation, was approximately 26 m in length per year. The average volumetric growth was 120,000 m^3/year. The southern part of The Spit was occupied with a variety of enterprises. The remaining part consisted mainly of sparsely vegetated, wind-formed dune ridges, with swampy areas between. The height of the dune formation decreased in northward direction with some low saddles through which water passes during storm periods threatening to cut a new channel. According to the 1970-report indeed a channel formed during stormy weather in 1936 and again 1951 which was filled in by bulldozer. The location of this breakthrough was just north of Main Beach. Washover by breaking waves occurred in 1967, but did not cut through the whole Spit. Mining took place at some areas of the Spit in periods before 1970. The 1970 situation can be characterised as non-stable, because of the poor system of frontal dunes, and the continuing northward movement of The Spit's end.

1.1.3. South Stradbroke Island

South Stradbroke Island is the northern Barrier Island of the former Nerang River Entrance. The frontal dunes are somewhat higher than those on The Spit. Also on South Stradbroke Island mining took place in the past. According to Delft (1970), stabilising of the Nerang River Entrance and stabilising of the frontal dunes, would offer an attractive area for future developments. Because South Stradbroke Island is isolated from the mainland a connection has to be made for this purpose. If the frontal dunes are not stabilised, South Stradbroke Island may vanish in the long term due to wind erosion.

1.1.4. The Broadwater

The Broadwater is the lagoon in which the Nerang River discharges. This part of the inlet system is called the flood tidal delta. Navigation in this part of the Nerang River Entrance was very difficult because of the dynamic behaviour of the numerous shoals and gullies. An advantage of the numerous shoals, is the breaking of incoming waves on these shoals before reaching the heavily developed landward side of the Broadwater.

1.2. What was the problem?

Like the rest of the Gold Coast beaches the Nerang River Entrance was unstable and therefore dangerous for navigation. The continuous changes of the navigation channels, both in location and depth resulted in a significant number of boating accidents over the years. Because the entrance is of importance for recreational and commercial reasons the Australian Authorities declared that the Nerang River Entrance must provide a safe navigation and anchorage for recreational craft, as well as numerous fishing vessels. Not only the improved stability of the entrance was an important issue but also the possible adverse effects of the improved entrance works on the adjacent beaches and the nearshore bathymetry.

1.3. History of the Nerang River Entrance

1.3.1. Introduction

Monitoring since 1840 showed that the Nerang River Entrance has a notorious history of instability. Figure 1.2 shows the Nerang River Entrance in 1915. Compare this with the present location of the improved Nerang River Entrance (Gold Coast Seaway), it shows that the Entrance migrated to the north. In the last half of the nineteenth century many ships crossed the Nerang River Entrance. From chronicles of the time, evidence was found that

* (All Figures from Delft 1970)

*Figure 1.3: The untrained Nerang River Entrance**

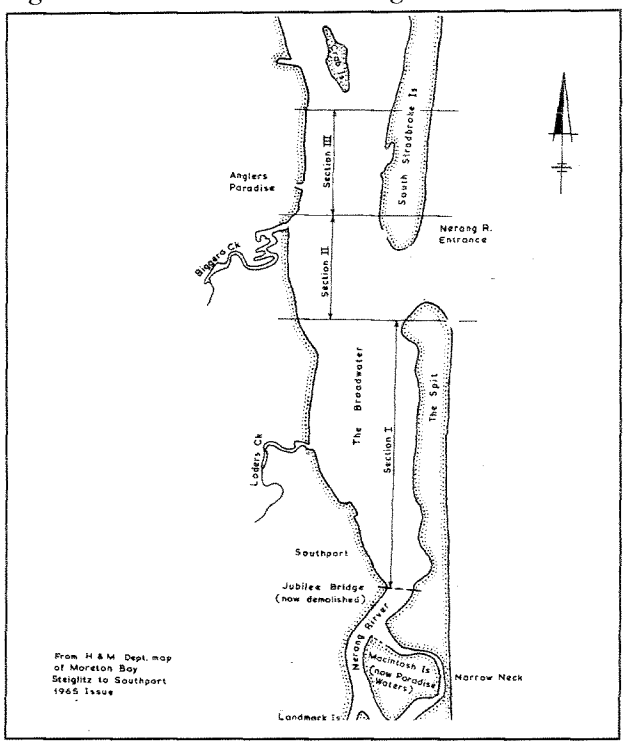

*Figure 1.4: Nerang River Entrance Migration**

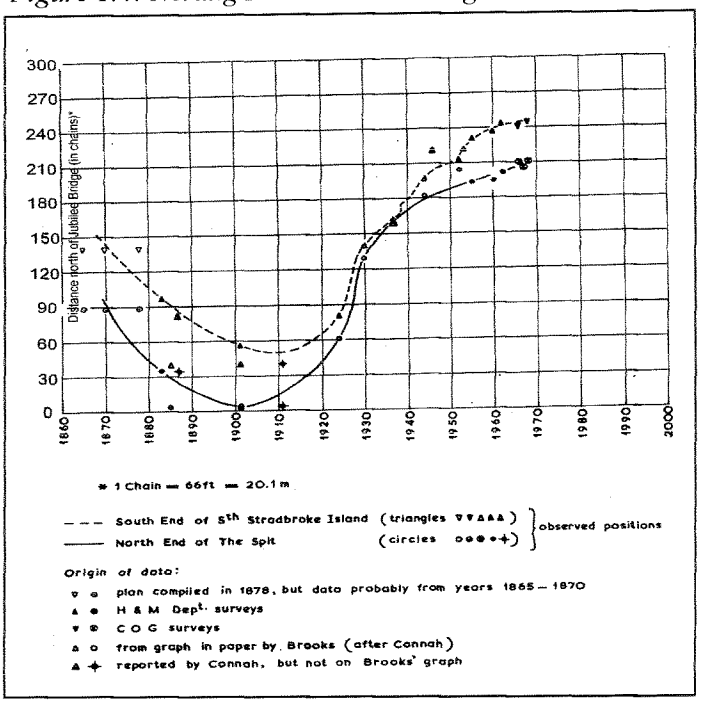

*Figure 1.5: Rate of linear growth of the Spit**

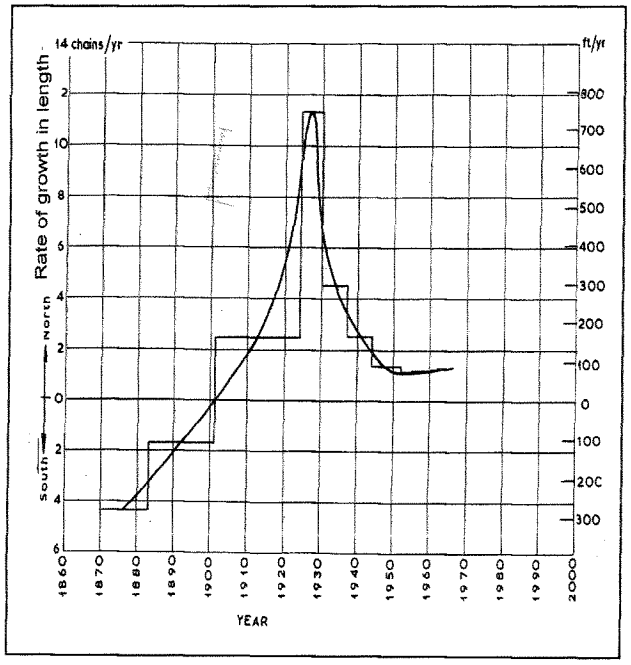

*Figure 1.6: Discharges of some Gold Coast streams *.*

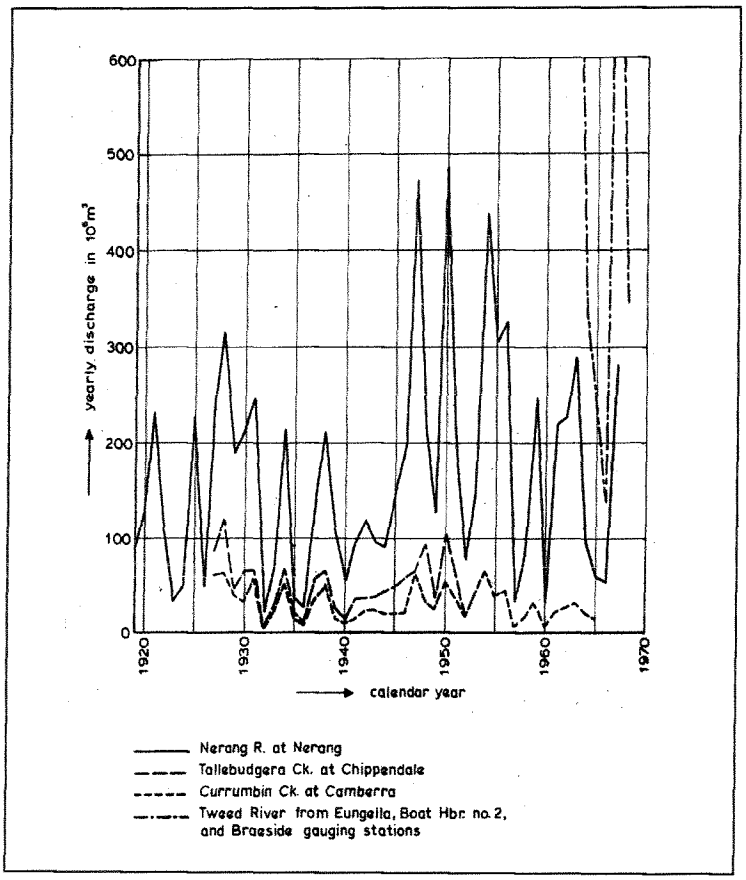

Figure 1.7 a and 1.7 b: Number of cyclones per year in Gold Coast region

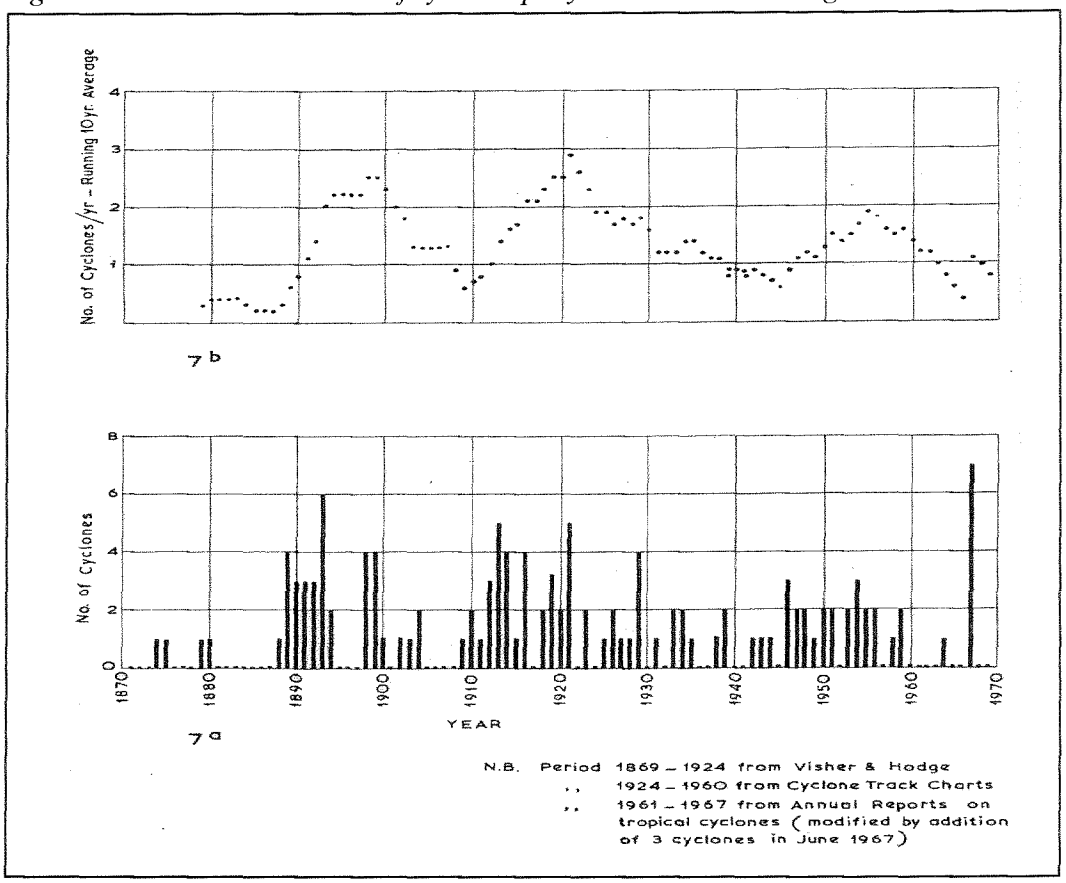

(From: Delft 1971)

suggests that amounts of timber was transported to Brisbane from the northern New South Wales via the Tweed River, Pacific Ocean and across the Nerang River Entrance (Figure 1.1). Before the breakthrough of Jumpinpin (1896) it is possible that flows through the Nerang River Entrance and the southern part of South Stradbroke Island were greater, and therefore maintained greater depth for navigation. From a map dated 1817 it is seen that a large township was located on the southern end of South Stradbroke Island. It has disappeared as the Nerang River Entrance migrated in northward direction. Figure 1.3 shows the untrained situation of the Nerang River Entrance in 1965.

1.3.2. Migration of the Nerang River Entrance

Nerang River Entrance migrated in northward direction. This northward migration is a result of combined effects of the predominant southeasterly wind and wave climate, and a large net longshore sediment transport rate to the north. The northward migration of the entrance developed The Spit by accretion on the updrift side of the entrance. In order to re-establish a dynamic equilibrium, erosion took place on the southern end of South Stradbroke Island. From studying aerial photographs, Delft (1976) concluded that erosion from the southern point of South Stradbroke Island followed after the cross-sectional area decreased by a growth of The Spit by deposition of littoral drift near the entrance.

Delft (1970) investigated the migration of the Nerang River Entrance. Figure 1.4 shows a graph of the migration, in the period 1860-1970, of the Nerang River mouth. According to Delft (1970), it is fairly sure that about the year 1900 The Spit was reaching some distance north of the Jubilee Bridge. This was also shown in Figure 1.2. The situation before 1900 is not quite sure because there are no reliable measurements or charts available. However some data show a southward migration in the period 1860-1900. From about 1900 a northward migration of the mouth has been measured. The reverse of migration direction of the Nerang River Entrance occurred after the breakthrough of Jumpinpin in the year 1896. The location of Jumpinpin is at the northern point of South Stradbroke Island (see Figure 1.1). This breakthrough resulted in a decrease of the discharges through the entrance and therefore decreased the cross-section and channel depth. Figure 1.5 shows that during the years 1901-1968 The Spit has moved to the north over a distance of approximately (210·20.1 =) 4250 m. The graph shows a more or less linear growth of about 63 m/year in this period. Figure 1.5 shows the rate of linear growth of The Spit. Figure 1.4 and 1.5 show a strong increased growth in the years 1920 to 1940. Delft (1970) explained this by looking at the connection between the migration rate and the discharges through the Nerang River Entrance. The yearly discharges in the period 1920-1970 of the Nerang River Entrance, and some other Gold Coast streams, are shown in Figure 1.6. During the period 1920-1940 the average yearly discharges through the Nerang River was less than during 1946-1965. In the period 1944-1968 the rate of migration decreased to a fairly constant rate of 26 m per year. Delft (1970) concluded that relatively low discharges through the Nerang River to the entrance were the possible reason for the increasing migration rate. However it must be noted that the annual Nerang River discharges are rather low compared with the spring tidal prism (water through the Nerang River entrance/ half tidal cycle). The maximum Nerang River discharge ever measured in the period 1920-1970 was approximately $490*10^6$ m^3 (1950) compared with a spring tidal prism of approximately by $30*10^6$ m^3 /half tidal cycle, shows that the Nerang River discharges relatively low.

Delft (1970) also concluded that the influence of the breakthrough of Jumpinpin (1896) on the early stages of migration (1900) is `very doubtful`. This may not be true looking at the correlation between the number of cyclones in the Gold Coast region and the rate of migration, which were shown in the Figures 1.7 and 1.5. Cyclones in the Gold Coast region

are in general responsible for the peak discharges in the Nerang River and through the entrance and probably for very large longshore transport rates to the north during a short period of time. The breakthrough of Jumpinpin was recorded in the year 1896. In this period 6 cyclones occurred in one year! In spite of the very few reliable records available of the Nerang River discharges during the early stages of the migration (1900), it may be concluded the discharges through the Nerang River Entrance decreased, because of the decreased ebb tidal prism after breakthrough of Jumpinpin. The decreased discharges result in less stability of the Nerang River Entrance and therefor favour the migration rate.
Figure 1.5 shows also a strong migration rate in the period 1920-1930. Figure 1.7b shows in this same period a strong increase in numbers of cyclones per year. The constant rate of growth in the period 1950-1960 with very irregular, somewhat lower, Nerang River discharges and a relative constant number of cyclones in this period suggest a stronger correlation between rate of migration and the number of cyclones rather than a correlation between the Nerang River discharges as suggested in Delft (1970). However peak discharges in the Nerang River entrance after passage of a cyclone probably kept the Nerang River Entrance from silting up. Delft (1970) makes also reference to some old records from local residents. They claim a stable position of the Nerang River Entrance in the years between 1885-1900, and according to Delft (1970), a plan prepared by the Harbours and Marine Department shows some older information in which there was a southward migration of the entrance during the years 1865-1900. The reported stable position of the entrance during the years between 1885-1900 compared with the few cyclones during these years suggests that this assumption is right.

1.4. Nerang River Entrance boundary conditions

1.4.1. Introduction

A general description and the influence of inlet hydrodynamics on the morphology of tidal inlets were already described in Section 2 in Volume I. In the following sections the available hydraulic and morphologic boundary conditions of the Nerang River Entrance will be described.

Delft Hydraulics prepared a report in 1992 on the littoral sand supply in the southern Gold Coast region. This report includes also recent measurements of waves, currents, and predictions of littoral drift which are representative for the Gold Coast Seaway region. The Department of Harbours and Marine and the Gold Coast Waterways Authority did evaluation of any changes in tidal levels within the Broadwater caused by the Gold Coast Seaway project. They started a programme for measuring water level variations inside the Entrance, the Broadwater and 20 km up the Nerang River. The recordings started in November 1984.

1.4.2. Waves

1.4.2.1. Introduction

Wave height, period and wave refraction are the most important parameters of a specific wave climate. The direction of waves is important for the determination of the direction and magnitude of the longshore transport. The frequency of occurrence for a specific wave condition is of importance because it determines the directional contribution towards the net annual longshore transport.

Wave recordings from the data collected from ocean going vessels by the KNMI (Netherlands) were used in the model experiments. The data listed by the KNMI was used to compute the weighted significant wave height and period for separately southeastern, eastern and northeastern waves. Waves coming from the east are considered to have not much contribution to the net annual longshore transport rate, and therefore not used in the model experiments.

Delft Hydraulics (1992) compared the KNMI-data with Waverider data described by the Beach Protection Authority (1981). It appeared that the KNMI-data was not reliable but at that time the only available source of information during the 1970 and 1976 investigations. Waverider measurements are more reliable for determining the wave climate. Delft (1992) describes also the results of a new hindcast model. Waverider measurements have been recorded at several locations along the southeast coast of Queensland. The measurement started in 1968 until present. The wave directions were determined from synoptic charts provided by the Bureau of Meteorology, by using a hindcasting technique. Waves are affected differently by refraction and diffraction when reaching the Waverider stations. Delft (1992) compared data from different Waverider locations along the Gold Coast using the directions by The British Meteorological Office. The conclusion was that some Waverider data agreed rather well for several locations but also some significant differences occurred.

The British Meteorological Office primarily prepared a numerical model used for weather predictions. They also developed a Global Hindcast Model for the calculation and prediction of wave conditions. This Hindcast model considers wave generation, propagation and decay, and produces wave height, period and directional information for sea and swell conditions. The Delft Hydraulic Laboratory evaluated the quality of these investigations against the Waverider data from Brisbane (Point Lookout). It showed that some wave heights and directions agreed rather well for both recordings but other show a poor correlation. Delft (1992) compared the Beach Protection Authority (1981) wave climate with the British Meteorological Office Hindcast Model and concluded that more waves from the north-east sector and fewer waves from the east sector were assigned by the BMO climate. For the determination of the directional wave climate both data sets were used. For the computation of the net annual longshore transport near The Spit also both wave climates were used.

1.4.2.2. Wave Refraction

Delft Hydraulic Laboratory (1992) carried out wave refraction analysis using the program REFRAC. This was done to determine the refraction coefficients and wave angles at the -10 m depth contour from Point Danger to the Gold Coast Seaway. Wave height and directions at this contour were used in the computations of the longshore transport rate for The Spit.

1.4.2.3. Directional wave climate

Delft (1992) concluded that according to the Beach Protection Authority (1981) not much difference exist between the different sites of Waveriders and that for the determination of the offshore wave climate at the Gold Coast use can be made of the Point Lookout data (10 years of continuous measurement available). Delft (1992) described the directional wave climate according to the Beach Protection Authority (1981) They presented the directional wave climate as a single representative wave height and period for each section. The wave conditions were transformed to the -10 m depth contour using the refraction results in Delft (1992). The results were (Location Spit):

Table 1: Directional wave climate at 10 m depth contour

H_{rep} [m]	K_2 [-]	H_{mod} [m]	T_{peak} [s]	Angle [degrees]	Angle to normal, 10 m depth [m]	Duration [days]
1.26	0.90	1.13	8.70	54	-26	45.09
1.58	0.97	1.53	8.55	94	+2	148.40
1.53	0.88	1.35	9.20	135	+27	171.50

(From: Delft, 1992)

The directional wave climate was also determined by Delft Hydraulics using both data from the Brisbane Waverider measurements combined with the British Meteorological Office Hindcast Model data. Delft (1992) determined the directional wave climate in 30° sectors by assigning the British Meteorological Office directions to the Brisbane wave height and period data. The wave heights were multiplied with a factor 0,88 to make them representative for the entire recording period. Also these data was transformed to the -10 m depth contour using the refraction results in Delft (1992). The result of this analysis is shown in Appendix A.

1.4.3. Water level variations

1.4.3.1. Introduction

The main source of water level variations are astronomical tides. In general vertical tides determine the level up to which the beaches will be attacked by wave action and horizontal tide can lead to an additional sediment transport in the longshore direction. The horizontal tide in the Gold Coast region is of little importance because the tidal wave approaches the shore at a more or less right angle generating little water movement alongshore. This is not true for the Gold Coast Seaway. Vertical tides outside the entrance are the driving force for tidal currents through the entrance. The prevailing tidal cycle in the Gold Coast region is *semi-diurnal* with a strong *inequality*.

In the following sections water level recordings are compared with some calculations. For a full description of the method of calculation reference is made to section 2 of Volume I.

1.4.3.2. Level Datum

Throughout the previous investigations: Delft (1970, 1976) and in this report, the height of a point is given relative to Queensland State Datum (S.D.). The zero of State Datum was set as equivalent to Mean Sea Level as determined many years ago from the Port of Brisbane tide gauge at the Pile Light. The later reports use the Australian Height Datum (A.H.D.) which is equivalent with Queensland State Datum. Low Water Datum (L.W.D) is approximately -0.7 m relative to A.H.D.

1.4.3.3. Vertical tides

Figure 1.8 shows tidal gauge recordings of the water level variations at some locations in the Gold Coast region. It must be noticed that the water level variations in this figure are drawn backwards in time. The water level variations near Nerang River Entrance were measured inside the Broadwater before improvement of the entrance. From this figure can be concluded that the Nerang River Entrance and the Broadwater geometry have a significant effect on the water level variations inside the Broadwater. The tidal range is decreased while the phase difference increases. This can be explained as follows. Difference in tidal range between the water levels outside the Nerang River Entrance and the Broadwater are a result of the flow restricting effect of the narrow inlet entrance. As the tidal wave approaches the Nerang River

Figure 1.8: Tidal gauge records

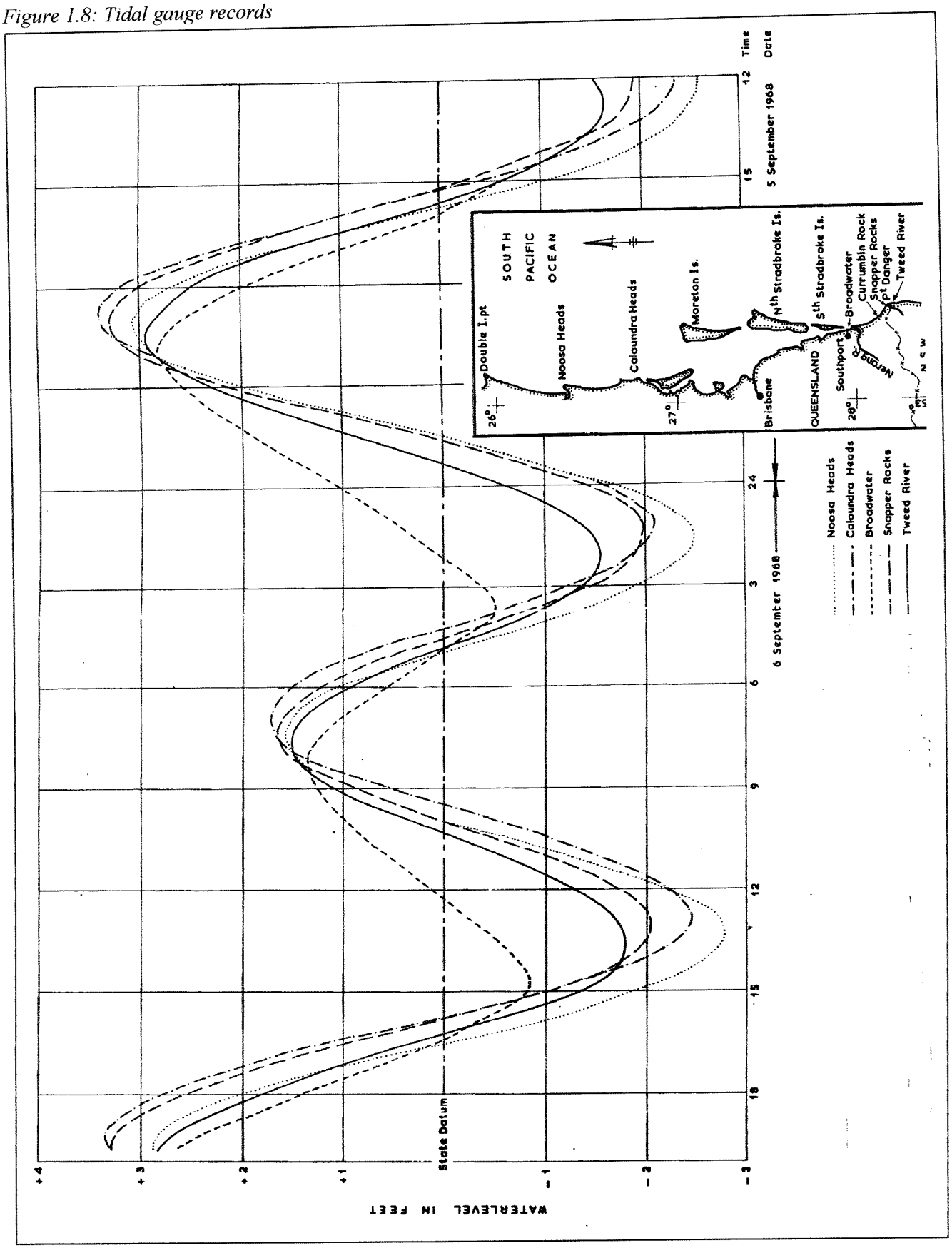

(From: Delft, 1970)

Entrance, water flows into the Broadwater. This continues until some time after high water. After high water the ocean water level starts to fall until it reaches the basin water level. This causes a relatively long high water period inside the basin. When the trough of the tidal wave passes, low water will be higher inside the Broadwater so ebb flow continues during the initial phase of the following flood. Looking at Figure 1.8 it is obvious that the ebb duration is longer and the head difference across the Nerang River Entrance is greater.
Figure 1.9 shows that the tidal range (measured between high and low water) exceeded during 50% of the time inside the Broadwater approximately 0,75 m. At Snapper Rocks (near Tweed River) the 50% exceedance tidal range is approximately 1m, with a low water level of State Datum -0,4 m. The maximum was assumed to be State Datum +1,3 m and minimum water level State Datum -1,0 m. Table 2 gives the tidal characteristics based on the classical method of tidal analysis.

Table 2: Tidal characteristics

	Snapper Rock	Broadwater
Median Level of all high waters	+ 0.61 m	+ 0.58 m
Median Level of all low waters	- 0.49 m	- 0.15 m
Median tidal range	1.04 m	0.75 m
Mean High Water Spring Tide Level	+ 0.75 m	+0.69 m
Mean Low Water Spring Tide Level	- 0.67 m	- 0.24 m
All levels relative to State Datum		

As mentioned earlier the Department of Harbours and Marine and the Gold Coast Waterways Authority jointly monitored the tidal water level variations in the Broadwater/Nerang River system. These monitoring took place prior to training and after the construction of the Gold Coast Seaway and the related upgrading of the navigational channels in the Broadwater. The results of these measurements were published in "Water level monitoring report the Broadwater/Nerang River Entrance 1987". Figure 1.10 shows the locations and water level monitoring gauge sites. Appendix B gives the results of these measurements. Appendix B Table 1 gives the mean tidal planes and Table 2 gives the Average time difference.

The water level variation in the Broadwater/Nerang River system prior to the improvement can be evaluated using the simple bay/inlet system described in section 2.2.2.3. of Volume I Figure 1.9 shows that for mean tidal conditions (50% time tidal range is exceeded) a tidal range inside the Broadwater is 0.70 m with an ocean tide of approximately 1.0 m seem reasonable values. Figure 1.11 shows the tidal discharges through the Nerang River Entrance with respect to the tidal range inside the Broadwater. With a tidal range inside the Broadwater of approximately 0.70 m the tidal discharges through the entrance is $P= 2.25*10^7$ m^3 / half-tidal cycle.

The cross-sectional area of the Nerang River entrance was measured relative to State Datum +1.3 m in the year 1969 (1860 m^2) and 1973 (1930 m^2). However using the simple bay/inlet system the cross-sectional area is defined relative to mean sea level (=State Datum). The inlet width varies between 600 and 700 m so the cross-sectional area (A_c) to be used in the bay/inlet system is roughly 1000 m^2. The bay area can be roughly determined using the measurements which were carried out in October 1974 (Table 4). Looking at the values presented in Table 4 it shows that more water is flowing in during rising tide than that is flowing out during falling tide. This can be explained by the fact that the tidal range measurements during rising tide was significantly larger than during the measurement at falling tide. Another explanation of this difference is that some water is being transported to the north were the inlet Jumpinpin is located. Also a difference in tidal volumes is present between the total measured tidal volume and the volumes measured at the Nerang River

Figure 1.9: Probabilty of exceedence of tidal range

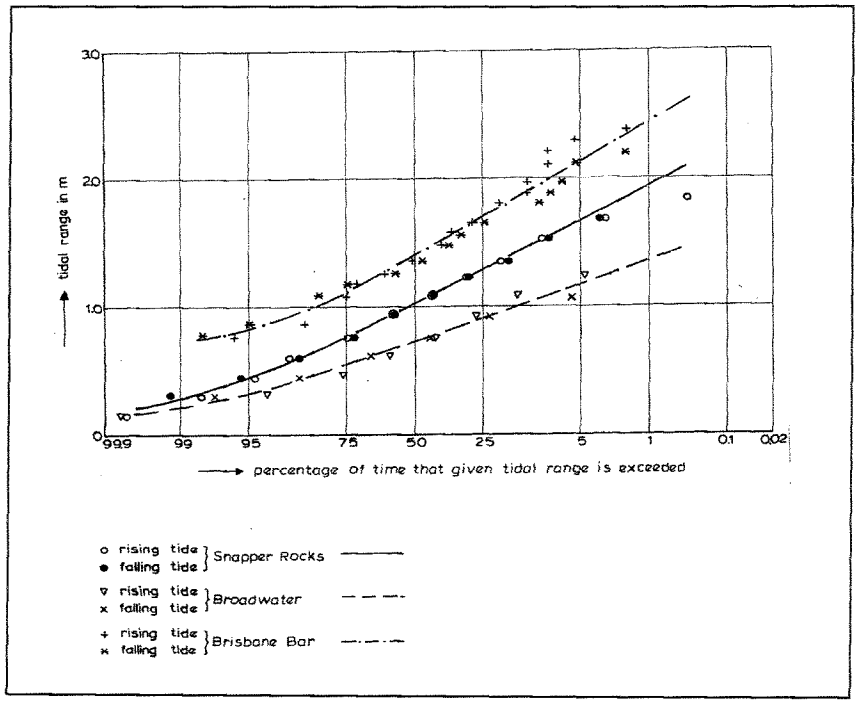

(From: Delft 1971)

Figure 1.10: Location and water level monitoring gauging sites

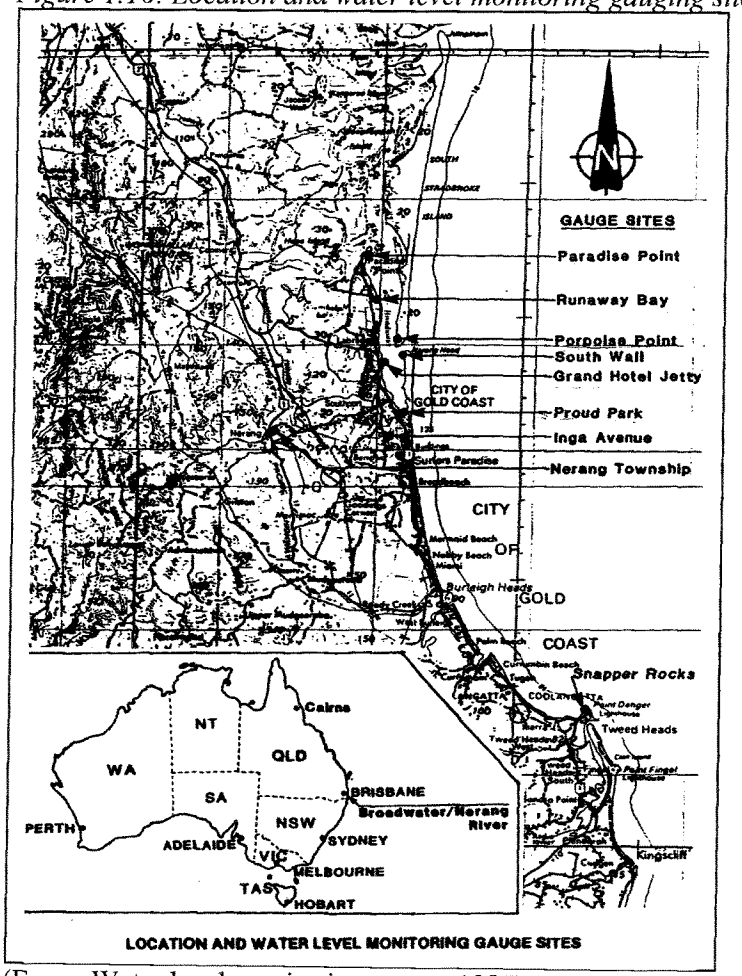

(From: Water level monitoring report, 1987)

Entrance. This is probably caused by measurement errors. However, assuming a uniformly fluctuating bay water level, the bay area can be computed with the values of Table 4.

Table 4: Tidal current measurements 1974

location	falling tide (ebb)		rising tide (flood)	
	tidal volume (m^3)	tidal range (m)	tidal volume (m^3)	tidal range (m)
Broadwater (Anglers' Paradise)	9.62×10^6	0.7	14.94×10^6	1.1
Highway Bridge	2.52×10^5	0.5	4.16×10^6	0.9
Storage area	4.74×10^5	with 0.6	7.89×10^5	with 1.0
Grande Hotel Jetty		0.5		0.9
Predicted ocean tide, Snapper Rocks		0.9		1.3
Predicted tide, Brisbane Bar		1.2		1.7
total	16.88×10^6		26.99×10^6	
Nerang River Entrance	18.32×10^6		26.16×10^6	

(From: Delft, 1976)

For rising tide: (Ocean tidal range: 1.3 m):

$$A_b = \sum \frac{P}{2 \cdot a_0} = \frac{14.94 \cdot 10^6}{1.1} + \frac{4.16 \cdot 10^6}{0.9} + \frac{7.89 \cdot 10^6}{1.0} = 2.61 * 10^7 m^2$$

For falling tide (Ocean tidal range: 0.9 m):

$$A_b = \sum \frac{P}{2 \cdot a_0} = \frac{9.62 \cdot 10^6}{0.7} + \frac{2.52 \cdot 10^6}{0.5} + \frac{4.74 \cdot 10^6}{0.6} = 2.67 * 10^7 m^2$$

From the above computed basin areas it is obvious that the basin area does not vary considerably with the ocean tidal range. The basin area for mean tidal conditions is roughly: $A_b = 2.65 * 10^7$ m^2. The tidal period is determined using actual water level measurements inside the Nerang River Entrance. T_{tide} = 12.4 hrs. The inlet length (L_c) is roughly determined by measuring the inlet length from Figure 1.12 and Figure 1.13: L_c= 800 m.

The Nerang River Entrance depth varies considerable between 3 m in the year 1969 and 8 m in 1974 (reference level unknown). Karssen and Wang (1990) relate the inlet depth to the tidal volume (Equation 18c; Volume I). This relationship gives in this case a water depth relative to mean sea level of h = 4,2 m which seems to agree rather well with the depth contours of 1953 (Figure 1.12) and 1973 (Figure 1.13) as well as some observed depths in the model. Volume I shows a relationship between the width at the throat at mean sea level and the mean depth below mean sea level for some untrained tidal inlets along the USA coast. The Nerang River Entrance fits rather well in the case W= 650 m (2000 ft) and h = 4.2 m (14 ft). The Chezy value can be calculated with the following empirical relationship proposed by Bruun and Gerritsen (1960).

$$C = 30 + 5 \cdot \mathrm{Log}(A_c) \qquad (1)$$

In which: C = Chezy value [$m^{1/2}/s$]
A_c = Cross-sectional area below mean sea level[m^2]

Figure 1.11: Tidal discharges through Nerang River Entrance

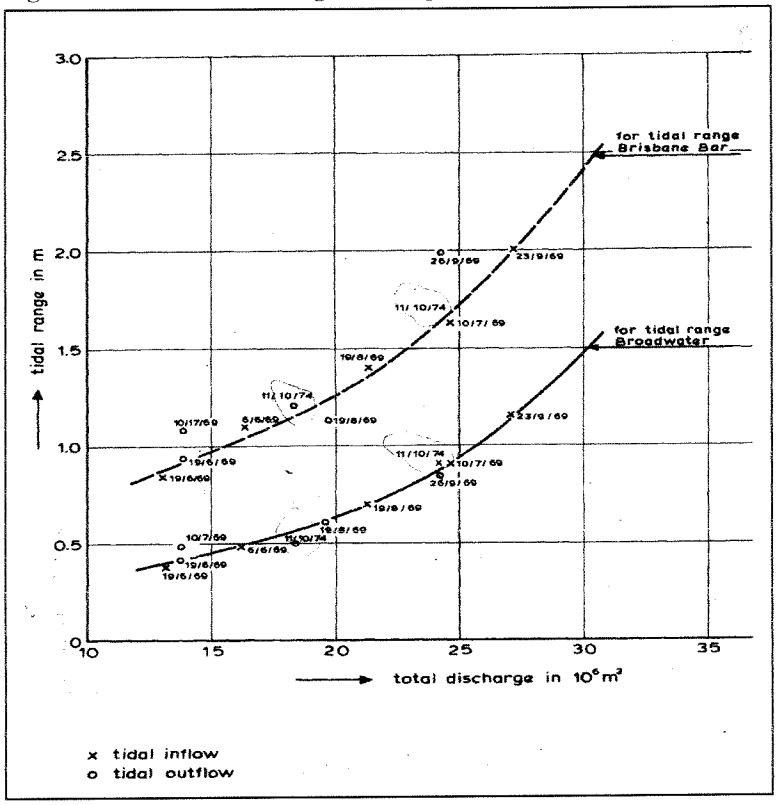

(From: Delft, 1970)

Figure 1.12: Depth contours 1953

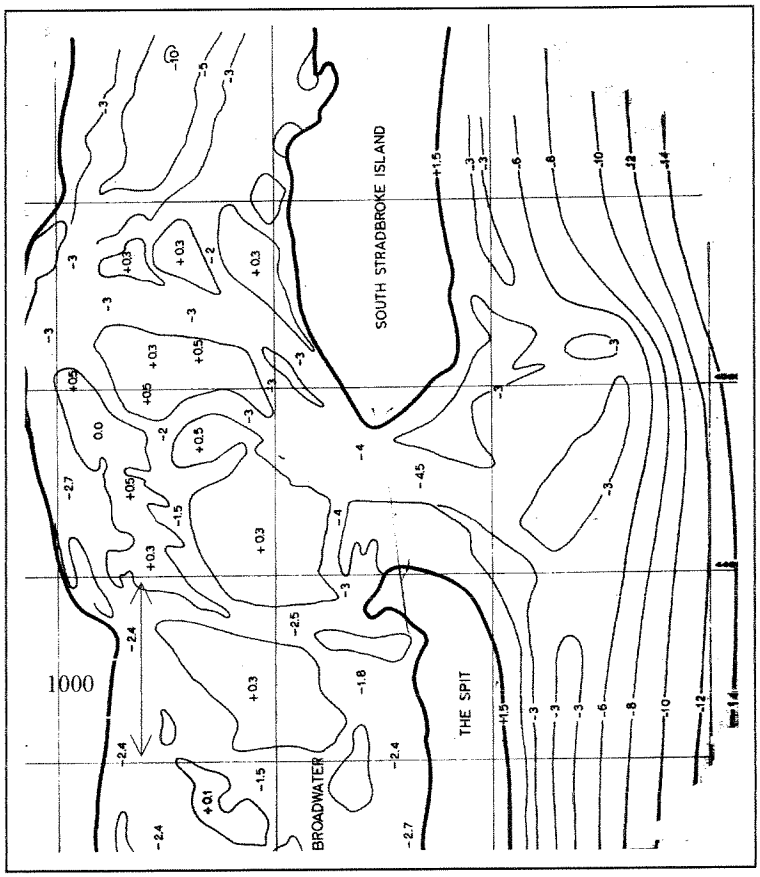

(From: Delft 1976)

This yields: C = 45 $m^{1/2}/s$. The ocean amplitude/bay amplitude ratio (R) and the tidal phase lag (E) can now be calculated using the simple algorithm proposed by Mehta and Özsoy (1978). For more information of this algorithm is referred to section 2.2.2.3. Volume I. For the calculation of the parameters in Table 5 reference is made to Appendix C. The calculations in yields to the following results:

Table 5: Resume of the calculations in Appendix C

Parameter	Equation(*	Value
F (Friction loss coefficient)	(2)	2.9
G (Dimensionless tidal frequency)	(3a)	0.20
B (Dimensionless damping coefficient)	(3c)	24.1
M (Coefficient)	(3b)	1.75
R (ratio ocean waterl./bay waterl.)	(3)	0.83
E (phase lag, degrees)	(4)	37.3
V_{max} (King, 1974), m/s	(10)	1.42
V_{max} (Drapeau, 1988), m/s	(11)	1.43

(The numbers between brackets refer to equations discussed in Volume I)

Comparing the measured average time difference (Appendix B, Table 2) with the calculated time differences it turns out that the calculated phase lag agrees rather well with the observed phase lag for Grand Hotel Jetty which is located directly opposite of the entrance (Figure 1.10). It is noted that the average time differences and phase lag are measured relative to high and low water at Brisbane Bar.

The measured time difference in September 1974 for location Grand Hotel Jetty was –0.15 minutes. The average time difference for high water relative to the Snapper Rock observed time was (85 min - 15 min) = 70 minutes phase lag between Snapper Rock observed time and the observed time difference at location Grand Hotel Jetty. This 70 minutes phase lag means, assuming a tidal period of 12.4 hrs, a phase lag of (70*360/12.4*60 =) 33,9 degrees, which is close to the calculated 37.3 degrees. The difference between the observed time differences and the calculated time differences is approximately 7 min for high water conditions.

The calculated ratio between the ocean water level and the bay water level shows some difference with the observed ratio. For the average mean high water level relative to A.H.D. the ratio becomes: $R_{obs\ high\ water} = \frac{0.51}{0.46} = 0.91$ which is higher than the calculated ratio (R = 0,83). High values of R indicates that the Broadwater water level can easily follow the ocean water level variations. In this case the flow restricting effect of the entrance is low, which means that the cross-sectional area is almost sufficient for the tidal prism to enter the Broadwater. Values of R about unity means that the cross-sectional area of the entrance is large enough for the whole tidal prism entering the basin.

However the measured mean low water level (relative to A.H.D.), compared with the mean low water level at Snapper Rock (Ocean tide) gives much lower values of R. For location Grand Hotel Jetty for instance the average mean low water level is approximately -0.20 m and the average ocean mean low water level is -0.52 m. So value $R_{obs\ low\ water} = 0.38$ which means that the Nerang River cross-sectional area is relatively small for ebb flow. Or in other words the cross-sectional area of the Nerang River Entrance during ebb was too small for the whole ebb tidal prism. Looking at the inlet morphology in the year 1953 (Figure 1.12) and the inlet morphology in the year 1973 (Figure 1.13), this assumption seems to agree. The inlet gorge in both bathymetries is rather small for low water levels compared to the inlet width.

Figure 1.13: Depth contours 1973

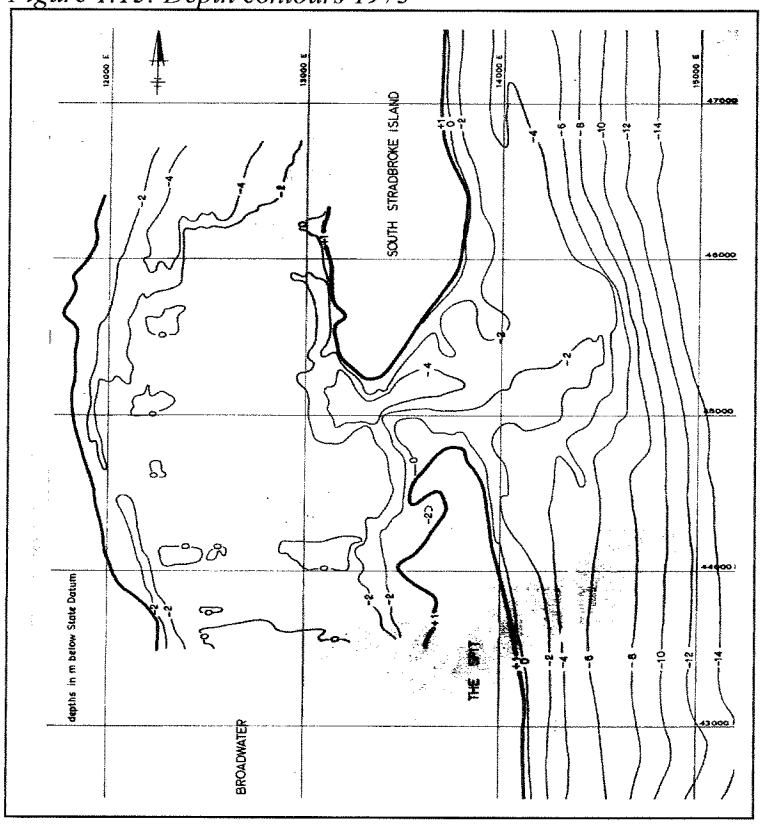

(From: Delft 1976

Figure 1.14: Probability of exceedance of tidal volume

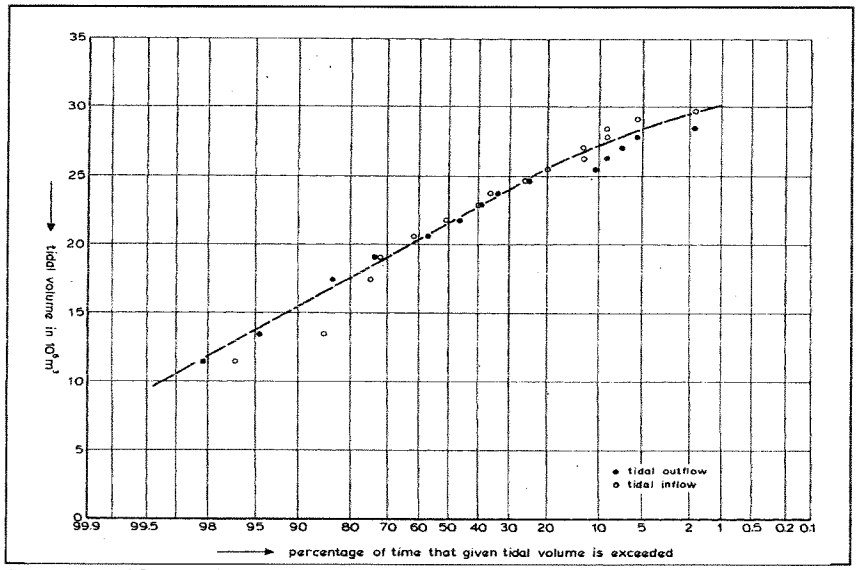

(From: Delft 1976)

Another explanation for the difference between the observed and the calculated values of R can be explained by the fact that the cross-sectional area of the simple bay/inlet system is idealised and in this case significantly different compared to the actual and unstable Nerang River cross-sectional area.

The above described also explains the large differences between measured maximum velocities and calculated maximum velocities, which will be discussed in the next section. The simple bay/inlet system also assumes a uniformly fluctuating basin water level. Table 6 gives the observed water levels at different locations inside the Broadwater area (see also Figure 1.10 and Appendix B, Table 1).

Table 6: Observed water levels Nerang River Entrance

Location Broadwater area								
[-]= not available	Grand Hotel Jetty		Proud Park		Runaway Bay		Paradise Point	
	M.H.W.L	M.L.W.L	M.H.W.L	M.L.W.L	M.H.W.L	M.L.W.L	M.H.W.L	M.L.W.L
September 1974	*+0.50*	-0.27	*+0.51*	-0.28	-	-	-	-
August 1983	*+0.33*	-0.34	-	-	-	-	*+0.33*	-0.37
April 1985	*+0.34*	-0.15	*+0.32*	-0.15	*+0.44*	-0.18	*+0.41*	-0.29

Table 6 shows clearly that not much difference occurs in the observed water levels. So the assumption of an uniformly fluctuating Broadwater water level agrees rather well for the Nerang/Broadwater system. However for April 1985 the location Runaway Bay and Paradise Point show some differences.

Due to the construction of the Gold Coast Seaway and dredging operations inside the Broadwater area in potential modifies the above-described tidal regime. The modifications on the tidal regime due to the construction of the Gold Coast Seaway will be described in section 3.2.2.

1.4.3.4. Horizontal tides

Water level variations outside the Gold Coast Seaway cause hydraulic gradients along the entrance channel. These hydraulic gradients are the driving force for the ebb and flood currents through the entrance channel. Currents through the entrance channels in general are very important for the morphology of the Nerang River Entrance. The relationship between the predicted tidal range at Brisbane Bar and the measured tidal volume passing through the Nerang River Entrance, during rising and falling tide was illustrated in Figure 1.11. The probability of exceedance of the tidal volume though the Nerang River Entrance is shown in Figure 1.14. From this figure can be seen that the tidal volume passing the untrained Nerang River Entrance varies between $P = 10 * 10^6 m^3$ *and* $P = 30 * 10^6 m^3$.

Tidal current measurement in 1973 carried out at the Nerang River Entrance showed that the ratio between the maximum and mean discharge rate through the entrance equals 1,33 for ebb flow and 1,43 for flood flow. Similar measurements were carried out in 1974. These results were already shown in Table 4. In Delft (1976) this table was used to determine the discharges passing through the location Gold Coast Bridge to the south and the discharges passing through the north. Figure 1.15 shows where the measurement took place. The ratio of discharge through the south and the north was approximately 0,26 for falling tide and 0,28 for rising tide. The same distribution was found for the current measurement in 1969, 0,23 for falling tide and 0,21 for rising tide. The tidal flow towards and from the Nerang River is about one-third of the total flow through the Nerang River Entrance. Canal development along the

Figure 1.15: Location current measurements in the Broadwater area

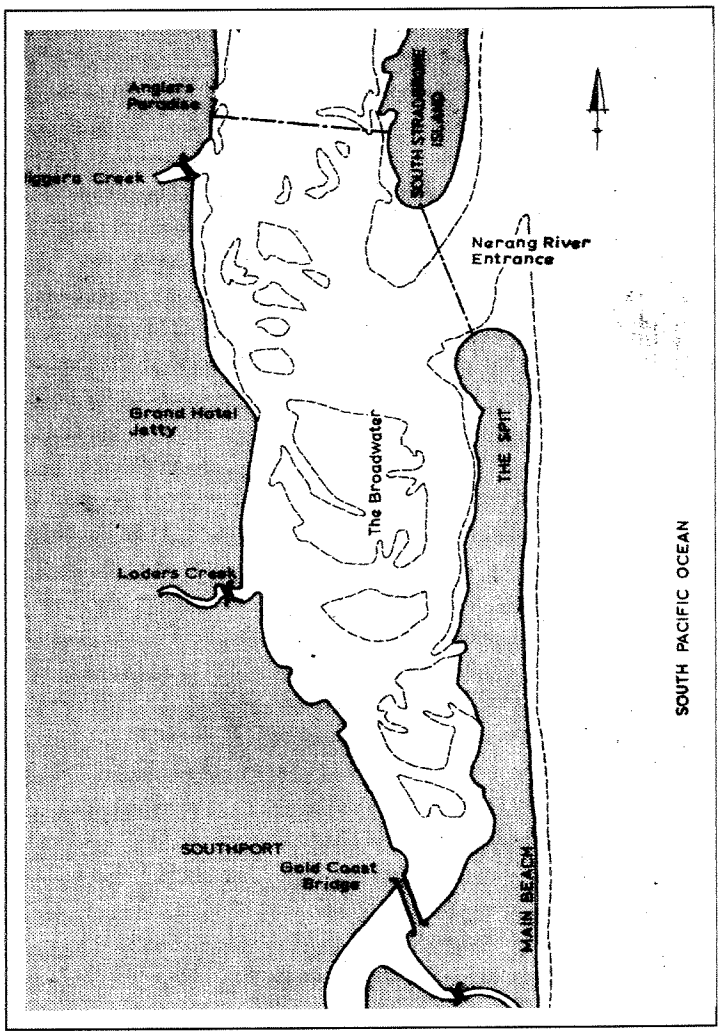

(From: Delft, 1976)

Nerang River leads to an increase of the tidal flow through the Nerang River Entrance. Before the stabilization this was approximately 15 % of the total tidal flows through the entrance. It was expected that the canal development would increase this by less than 10%.

The magnitude of inlet velocities prior to the construction of the Gold Coast Seaway were measured during experiments of 23 and 26 September 1969 (inflow and outflow tide). The total discharges through the Nerang River Entrance at this date was approximately $24*10^6$ m^3/half tidal cycle. This is somewhat higher than the tidal prisms used in the calculations with the simple bay inlet system in Appendix C. The velocities inside the entrance can be calculated using Equation 10 and the solutions curves of King (1974). Equation 11 can also be used to calculate the entrance velocities (Drapeau, 1988). For a description of these equations is referred to section 2.3.5. Volume I. The results of the measurements and calculations are presented in Table 7.

Table 7: Measured versus calculated inlet velocities

Measured (V_{max})	1.83 m/s - 2.13 m/s
King (1974) (V_{max})	1.42 m/s
Drapeau (1988) (V_{max})	1.36 m/s

1.4.4. Ocean Currents

Currents on the ocean can be split up into three categories, depending on their origin:

*1. **Ocean currents***, related to the East Australian Coast Current, and drift currents caused by local winds. Delft (1970) gives average current velocities for different locations. For the model investigations an average drift velocity is taken of 0.10 ***m/s*** and assumed to be directed northward for SE-waves and southward for NE-waves. However Delft (1992) ignores this current because of the little impact on the sediment movement along the coast.

*2. **Tidal currents***, oscillatory with a period of approximately 12.4 hours. All reports concluded that the tidal currents in the Gold Coast region are of negligible importance and therefore ignored. This is due to the fact that in the Gold Coast region tidal waves approach in general perpendicular to the coast

*3. **Wave generated currents***. Wave generated currents are confined to the breaker zone and some small distance seaward of the breaker line, and related to the dominant wave direction. Wave generated currents are very important for the longshore transport rate. In Delft (1970) comparison was made between measured longshore current velocities and computations from Eagleson formula. It showed that the computed longshore velocities always exceeded the observed velocities. In Delft (1976) preference is given to the formula of Longuet-Higgens which is based on principles of radiation stress. For a full description of the formula, reference is made to Delft (1976). The velocities computed by the Longuet-Higgens formula was used for the computations of the littoral drift used in the model experiments.

1.4.5. Nerang River discharges and sediment transport

The Nerang River Entrance discharge was described in Delft (1970). It shows that the total annual discharge is extremely variable. In the period 1919-1967 it varied between $30*10^6$ m^3/year and $500*10^6$ m^3/year. The distribution of high annual discharges was also varied. Delft (1970) showed that the highest discharges per month are likely to occur in the months January to March and, June and July. Delft (1976) showed a detailed analysis of the highest

discharge in each month. The discharges were usually associated with the presence of a cyclone in the adjacent area.

1.4.6. Sediment budget Nerang River Entrance

According to Delft (1970) the average annual sediment load of the Nerang River was 9,000 m^3. Keeping the discharge distributions in mind, these sediment quantities will be delivered at erratic intervals. Delft (1976) determines the sediment transport through the Nerang River Entrance by computation. The results of these computations are given in Figure 22 and Figure 23 of Delft (1976). The conclusions of these computations were a sediment transport in seaward direction during ebb of 710,000 m^3/year. Sediment transport in landward direction during flood was 815,000 m^3/year. And the sediment transport during Nerang River flood runoff is approximately 10,000 m^3/year. So the net annual sediment volume entering the Broadwater was 115,000 m^3/year.

The migration rate in the period 1955-1973 is approximately 37 m/year. Delft (1976) stated that this migration rate leads to a volumetric growth rate of The Spit of 72,000 m^3/ year and erosion of South Stradbroke Island of 86,000 m^3/ year.

According to Delft (1970) the Bureau of Mineral Recourses measured the near surface temperature and vertical profiles of temperature variation in January to February 1967. These measurements indicated the presence of (24.5 - 25 °) river water flowing eastward and southeastward from the Nerang River mouth. Near the coast, immediately south from Nerang River entrance slightly cooler (23 - 24,5 °) water masses were located. The minor temperature variation observed from the profiles, show no evidence of important stratification; the temperature decreases slowly from surface to bed. Near the Nerang River mouth some density difference was found, about 0,5 kg/m^3, which was restricted to the upper layer of about 0.6 m. Looking at these values it may be concluded that there are no density currents which could influence the transport of sediment along the coast.

1.4.7. Severe weather conditions in the Gold Coast Region

The wave data recording program, (Gold Coast 1987-1997) recorded the major meteorological events in the Gold Coast region. These recordings show that besides cyclones also pressure systems (severe storm) occur and are responsible for severe wave action. For example: The highest significant wave height (H_{sig} = 7.0 m) and maximum wave height (H_{max} = 12.0 m) in this period were recorded during a high pressure system over the Tasman Sea and a low pressure system over south-east Queensland on 3 May 1996.

A general description of the influence of severe weather conditions like cyclones was already given in Volume I. For the investigation in Delft (1976) cyclone data up to 1974 were obtained. Figure 1.7 already showed the number of cyclones per year in the Gold Coast region in the period 1870-1975. In the period 1987 - 1997, 13 cyclones exceeded the storm wave threshold of 2 m. In the Gold Coast region cyclones occur mostly in the months January to March. Cyclones have the following hydrological effects on the Gold Coast Seaway:

*1. **Surge levels;*** It has been estimated that the pressure gradients between the low central pressures and the higher outer pressures can contribute approximately 0.3 m to the storm surge, however, a surge of 0.9 m was measured during cyclones in 1967. (Mc Grath, 1967)

*2. **Wave action;*** An increase in wave heights leads to a more than linear increase in sediment transport. Severe wave action from the southeast during a cyclone can induce a sediment

Figure 1.16: Sand samples

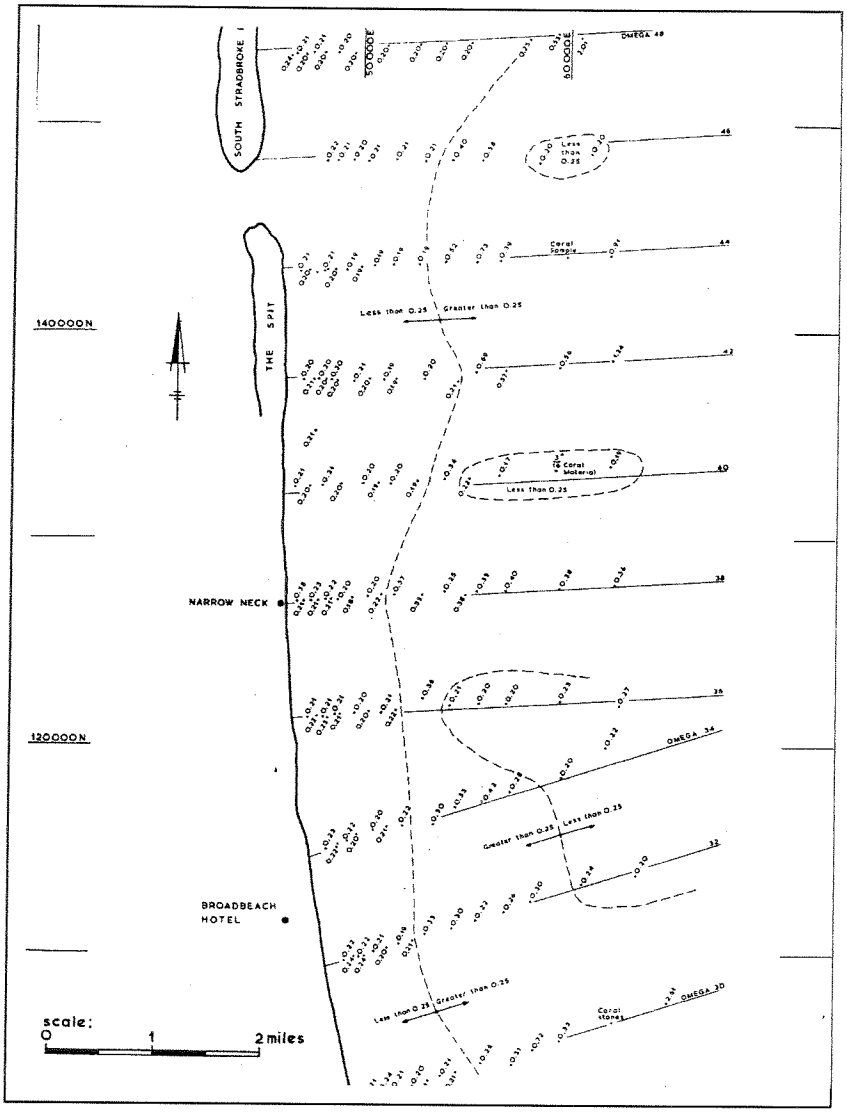

(From: Delft 1976)

transport of 100,000 m^3/week in northward longshore direction. A result of this large sediment transport is a narrowing of the untrained entrance channel. The trained entrance may suffer of some sediment being transported along the southern training-wall into the entrance.

*3. **Nerang River discharges;*** Associated with cyclones high rainfall in the catchment area of the Nerang River leads to peak runoffs. The high river discharges has a consequence to the ratio between the river discharges from the Nerang River and the Broadwater north of the entrance. The peak runoff in the Nerang River is always somewhat delayed with respect to the high wave action during and shortly after the passing of the cyclone. It is normal for the high runoff to reach the entrance about 5 days after the passing of the cyclone. The peak runoff has an important influence on the morphology of the bed at the entrance. The Nerang River Entrance appeared to be very unstable. So a large amount of sediment along the Gold Coast after passing of a cyclone tries to close the inlet by silting it up. However the increased discharges from the Nerang River results in higher inlet velocities which keeps the Nerang River Entrance from silting up.

1.4.8. Composition of the seabed

The composition of the seabed was determined by sampling the bed material around various sounding lines during the 1970 investigations. The bed material is mainly sand with a high quartz content (> 90%) and includes some shell rests. As can be seen from Figure 1.16 , the median particle diameter in the area up to approximately 2500 m (1 mile = 1.609 km) from the waterline is fairly uniform in The Spit area being approximately 0.2 mm. Delft (1976) report showed that a study of Figure 1.16 reveals that up to approximately 600 m from the baseline the following grading of bed material can be assumed:

- $D_{90} = 0.45$ *mm.*
- $D_{50} = 0.23$ *mm.*
- $D_{10} = 0.17$ *mm.*

For the model investigations a ***D_{50} of approximately 0.23 mm*** was used. For the sediment transport computations a ***$D_{35} = 0.2$ mm*** was used. The grading of the Nerang River is, according to Delft (1976), comparable with that of the offshore gradings (only slightly coarser).

1.5. Sediment transport

1.5.1. Introduction

The stability criterion of Bruun (1978) shows that the development and stability of tidal inlets in general depends mainly on the earlier described discharges through the entrance (tidal prism) and the total annual littoral drift ($r = P/M_{total}$). For more information about the stability criterion is referred to section 4.2.4. in Volume I.

The cross-shore sediment transport is mainly caused by wave action and plays also an important role. Wave breaking on the ebb tidal delta near tidal inlets stir up sand which is transported into the inlet system by flood and, depending on the inlet and wave characteristics deposited inside the lagoon or returned to the ebb tidal delta where it is lost either to the deeper parts outside the ebb tidal delta or transported in longshore direction into the littoral drift. Cross-shore transport can be onshore or offshore. The direction of cross-shore transport in general depends on the deep-water wave characteristics. Johnson (1953) found a critical

Figure 1.17: Mean Profiles: The Spit

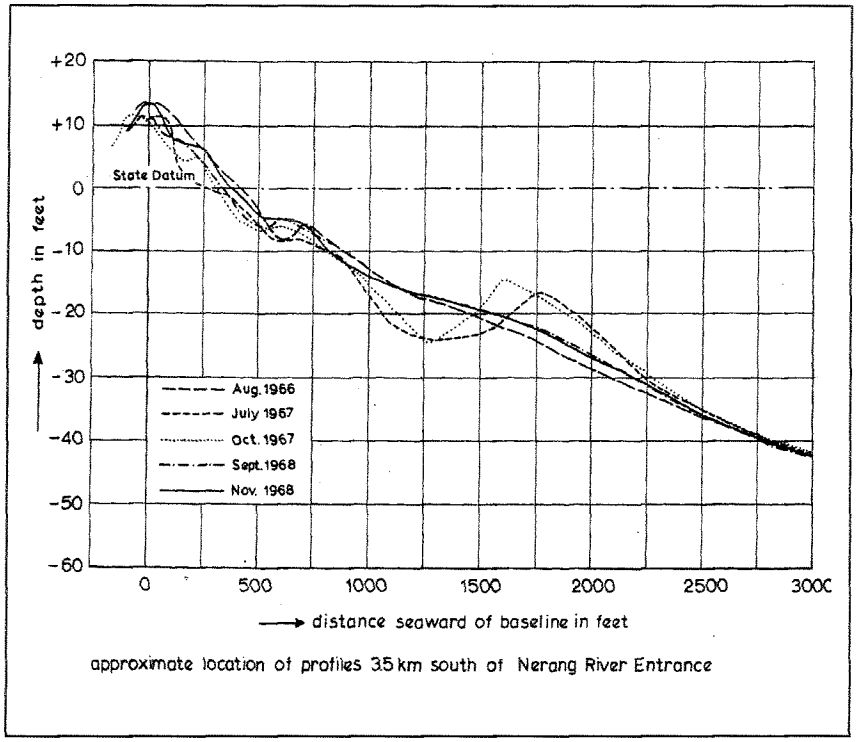

(From: Delft 1976)

Figure 1.18: Distribution of longshore transport across coastal profile

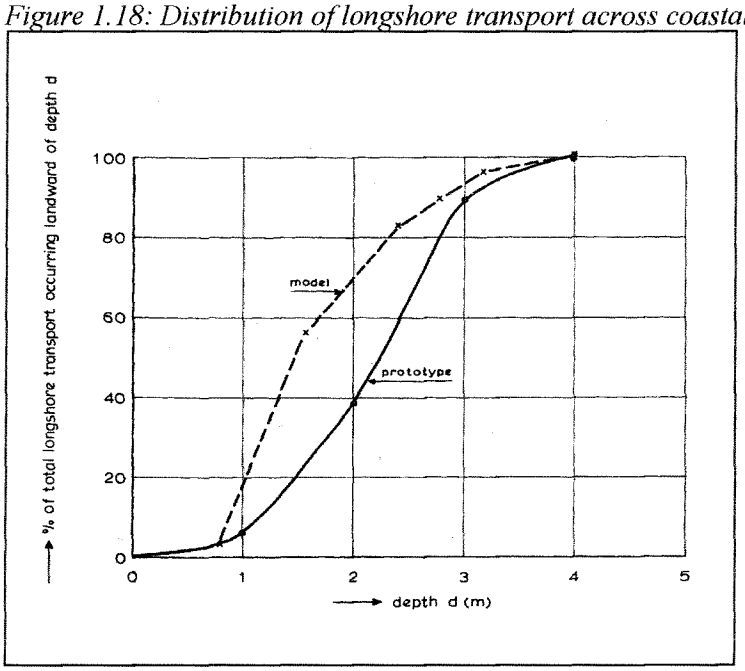

(From: Delft 1976)

wave steepness, which determined whether the transport is directed onshore or offshore. When the deep water wave steepness (H_0/L_0) reaches the value of approximately 0.03, it changes the direction of cross-shore transport (Van der Velden, 1995). The higher values indicate an offshore-directed sediment transport and the lower values an onshore directed transport. Over a year the above described wave characteristic change, especially during stormy seasons. Not only the deep water wave steepness determines the cross-shore transport of sediment. There are some other phenomena that determines the direction and amount of cross-shore sediment transport.

1.5.2. Cross-shore transport in the Gold Coast region

Looking at the beach profiles of The Spit near the Nerang River Entrance showed that the major changes occur landward of the position of the -14 m depth line. This is illustrated in Figure 1.17. Cross-shore sediment transport at greater depths is rather small and therefore not important for profile changes.

1.5.3. Longshore transport in the Gold Coast region

Longshore sediment transport or littoral drift is mostly concentrated in the breaker zone. Figure 1.18 gives the distribution of the longshore transport across the coastal profile. From this figure can be seen that there is no longshore transport below the level of State Datum -4,0 m. The current velocity outside the breaker zone was, as already described before as 0.10 m/s. However it is concluded that these large scale currents don't have much influence because these currents and current gradients are rather weak in areas where significant bottom changes occur.

The Delft (1970) study uses the Bijker equation for the prediction of the longshore sediment transport. For the model experiments the equation of Ackers and White was used because of the more reliable results. The longshore current velocity for the Bijker- and the Ackers and White equation was calculated according to the theory of Longuet-Higgens. Delft (1992) estimated the longshore transport using several longshore transport equations and also by calculating the equilibrium coastline. It turned out that with a transport rate of approximately 550,000 m^3/year, the predicted equilibrium coastline was very similar to the existing coastline. This is illustrated in Figure 1.19. In Delft (1992) the longshore transport rate was computed with the CERC equation using the wave climate of the British Meteorological Office Hindcast Model. The applied coefficient was a factor 3.4 less than recommended by the Coastal Research Centre.

A summary, until 1992, of these longshore transport computations are given below (Location Spit):

Table 8: Summary longshore transport

Wave Data until	Theory	net longshore transport m^3/year
1970	Bijker	485,000
1976	Ackers and White	500,000
1981	CERC	530,000
1981	Equilibrium coastline	550,000

The Beach Protection Authority operates COPE (Coastal Observation Programme Engineering) stations at Currigee on South Stradbroke Island and at a number of other Gold Coast beaches. The recorded COPE data (Appendix D) can be used to give an assessment of

Figure 1.19: Existing coastline versus computed equilibrium coastline

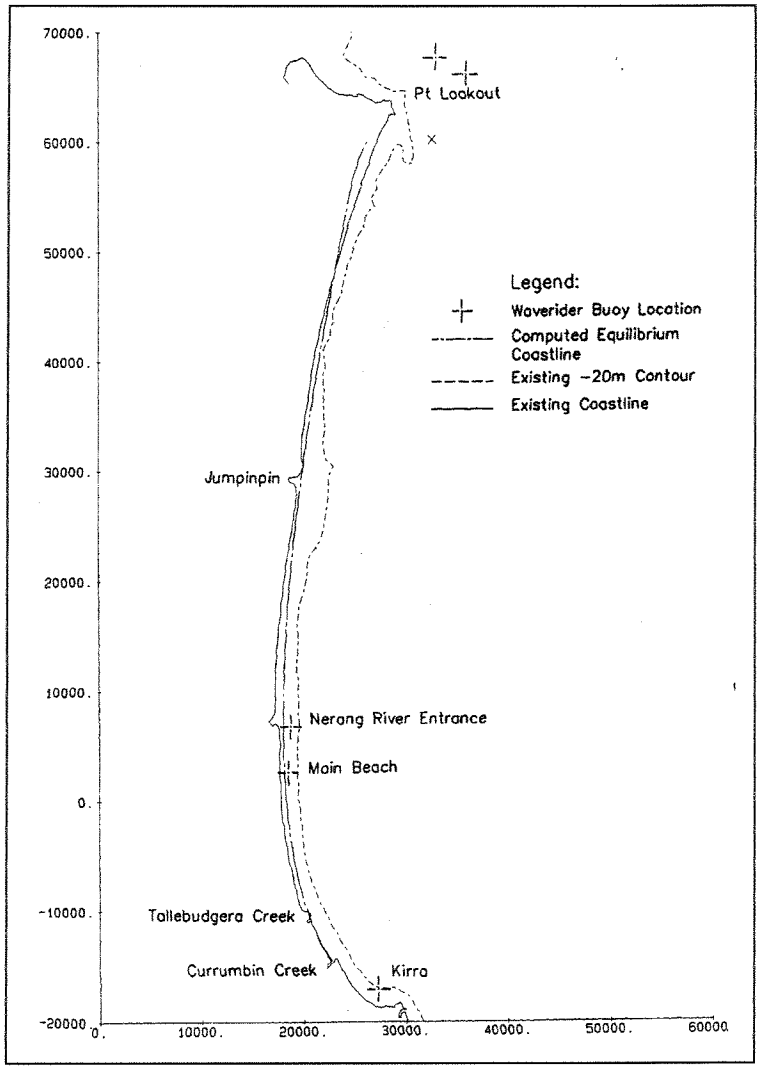

(From: Delft, 1992)

the rate of longshore sand transport and to compare this with the sand bypassing volumes and morphological changes of the Gold Coast Seaway area. Volunteer observers at these stations record information daily on wave height at the outer edge of the breaker zone and the average longshore current inside the breaker zone. As pointed out earlier, major meteorological events like cyclones usually are associated with high transport rates. The average velocity (av. vel.) mentioned in Appendix D is recorded from direct observation of a dye path released into the breaker zone. The longshore transport rates are calculated using adaptation of the CERC formula (i.e. $S = K \cdot H^2_{average} \cdot V_{average}$). The sand transport rates are calculated for a limited number of days. The values in Table 9 are calculated by taking the average of the original estimate based on the limited number of days and the corrected monthly average values. This results in the following values.

Table 9: Predicted longshore transport rates

Transport direction	[m^3/year]
North	1,038,000
South	-400,000
Net	638,000
Total	1,438,000

1.5.4. Nerang River Entrance configuration

1.5.4.1. Introduction

Three morphological units can be identified for tidal inlets on littoral drift shores:

- Ebb tidal delta
- Flood tidal delta
- Entrance channel (incl. gorge)

Each of these units has its own specific developments, which mainly depend on the relative importance of tides and waves. In the following sections the bathymetry of these three units are briefly described. The bathymetry of the 1953 situation of the Nerang River Entrance is illustrated in Figure 1.12. Figure 1.13 shows the situation in 1973. Comparing these figures it is clearly shown that the Nerang River Entrance has migrated northward. The shape of the ebb tidal delta shows some similarity in both situations. However, all morphological units show a very complex and extremely variable bathymetry. Both bathymetries were used as a base in the model investigations.

1.5.4.2. Classification and stability of the Nerang River Entrance

Classification of the Nerang River Entrance provides a tool to analyse the system and detect the parameters representative to the processes at work and to compare the Nerang River Entrance with inlets in similar situations. The classification of tidal inlets was already described in detail in section 1.2 in Volume I. Figure 1.9 shows that the tidal range exceeded 50 % of time outside the Nerang River Entrance were 1,0 m (for Snapper Rock) and 1,4 m (for Brisbane Bar). According to Davies (1969) these tidal ranges are classified as microtidal (0 - 2 m). Later Heyes et al. (1979) modified the earlier classification by Davies. According to Heyes et al. (1979) the Nerang River tidal ranges are classified as Low mesotidal (1,0 - 2,0 m).

Tidal inlets can also be classified with the help of yearly average significant wave height (H_S). By looking at the different wave climates (Appendix A and Table 1), in the Gold Coast region, it can be concluded that for the prevailing south-east wave direction the H_S exceeds 1,5 m which means 'High Wave energy'.

The general the stability criterion defined by Bruun (1978): $r = \frac{P}{M_{total}}$ Where: P = tidal prism or tidal volume at spring tide and M_{total} = Total annual sediment transport (north- and south going). Low values ($r < 100$) indicate a unstable situation whereas large values ($r > 150$) indicate stable situations. Generally the following situation was present before training of the Nerang River Entrance: Figure 1.14 gives the probability of exceedance of the tidal volume though the entrance. The tidal volume at spring tide (with a percentage of exceedance of ≈ 6%), is approximately: $P = 30*10^6$ m^3 and M_{total}= 1,438,000 m^3/year (Table 9).

$$r = \frac{30 \cdot 10^6}{1{,}438{,}000} = 21 \qquad (2)$$

This ratio indicates an unstable inlet. Looking at the migration rate of the Nerang River Entrance as illustrated in Figure 1.4 this instability is not a surprise. Comparing the Nerang River Entrance with the stability criterion shows that the instability of the Nerang River Entrance generally fits within numerous investigated tidal inlets all over the world. Increasing migration rates indicate more instability of the entrance and therefore a lower value of "r". Increasing discharge (P) through the entrance increases the stability and therefore decreases the migration rate. Cyclones are responsible for higher discharges through the entrance but also strongly increase the longshore transport rate in a relatively short period of time therefore increasing the inlet migration rate.

1.5.4.3. Nerang River Entrance ebb tidal delta

The nearshore bathymetry around the Nerang River Entrance is rather regular, with an average beach slope between +1 m bed contour and the -14 m bed contour of approximately ***1:60***. The bathymetry directly outside the entrance forms an exception. Every tidal inlet on littoral drift shores, improved or not, tends to build an offshore bar to bypass a part of the littoral drift across the entrance. Wave action prevents an extensive bar growth. Section 1.2.3. (Volume I) described the ebb tidal delta classification by Oertel (1988). Sketch C from Figure 1.9 in Volume I shows a situation quite similar to the Nerang River Entrance situation. Tidal waves approach the Gold Coast beaches at more or less right angles with a predominant southeast wave climate. Compare sketch C with the Nerang River Entrance ebb tidal delta bathymetry in 1953 and 1973 and it is evident that the ebb tidal delta asymmetry and orientation show some similarities.

Oertel (1988) stated that the channel orientation and ebb tidal delta asymmetry is caused by different magnitudes of inlet migration and sand bypassing (see 4.3. Volume I). Oertel (1988) compared the stability criterion by Bruun (1978) with the natural inlet jet field (SLjf) and the adjacent littoral zone (SLlz). The 1953 ebb delta morphology shows that the Nerang River Entrance fits in between Type B and Type C inlets. The entrance channel orientation in downdrift direction of Type B and C inlets can also be recognised in the 1973 bathymetry.

According to Delft (1976), the ocean bar at the Nerang River Entrance has been fully developed with an area of approximately $A_{bar} = 0{,}5\ km^2$ with an average height of 2 m higher than the surrounding bed profiles. The volume of the sediment in the bar is approximately $V_{bar} = 1*10^6\ m^3$.

Section 4.2.5.1. in Volume I described the empirical relationships by Walton and Adams (1976) for equilibrium ebb delta volumes. The Gold Coast region is exposed to high wave energy. According to Walton and Adams (1976) the following relationship is valid:

$$V = 1.95 \cdot 10^{-4} \cdot P^{1.23} \Leftrightarrow = 1.95 \cdot 10^{-4} \cdot \left(28 \cdot 10^{6}\right)^{1.23} = 0.3 * 10^{6}\ m^3 \qquad (3)$$

This value is much lower than the $1 \cdot 10^6$ m^3 by Delft (1970, 1976). This can be explained by the fact that the empirical equilibrium ebb delta relationships are probably not valid in cases of migratory inlets with low tidal prisms and high longshore transport rates (unstable inlets). Inlets with volumes trapped in the ebb delta who fall above the predicted value by Walton and Adams (Shore Protection Manual, 1984) might be considered as poor bar-bypassers, but efficient sediment sinks. Due to the unstable character of the Nerang River Entrance, the entrance is not able to create a bar with sufficient height in order to become a bridge for sediment to naturally bypass the entrance. However on the other hand much sand is trapped in the delta due to the migratory character of the Nerang River Entrance.

1.5.4.4. Nerang River Entrance flood tidal delta

The Nerang River Entrance flood tidal delta is called Southport or Broadwater. Sediment from the littoral drift is brought in by flood flows and part of it is deposited in the less exposed lagoon. It is obvious that this shoaling has a great influence on the sand balance along the coast and therefore has an effect on the downdrift beaches north of the entrance. Due to the northward migration of the entrance a continuing shoaling of the lagoon took place. Also a considerable siltation by the Nerang River took place. Navigation during this period was very difficult because of the complex and continuously changing bathymetry. According to Delft (1970), there is only one suitable survey of the siltation rates available: from November 1967 to February 1968. The survey area extended from Jubilee Bridge to Crab Island. The Broadwater was split up in three sections as shown in Figure 1.3.

Delft (1970) assumed that the sections I and II had originally the same depth as section III. With this assumption, and several others, an average shoaling of the Broadwater was found for the period 1900 to 1970: 140.000 m^3/year. There is more information on this subject in Delft (1970).

1.5.4.5. Nerang River Entrance channel

Tidal prism, littoral drift and the Nerang River Entrance configuration determine mainly the cross-sectional area of the Nerang River Entrance. The average cross-sectional area measured relative to State Datum +1,3 m (maximum water level) according to Delft (1976) were:

- 1969 $\rightarrow A_{cross} = 1860\ m^2$
- 1973 $\rightarrow A_{cross} = 1930\ m^2$
- 1974 $\rightarrow A_{cross} = 2325\ m^2$

The average cross-sectional area (relative to M.W.L.):

$$A_{average} = \frac{1860 + 1930 + 2325}{3} - 1.3 \cdot 700 = 1128\ m^2 \qquad (4)$$

Already mentioned, the cross-sectional area differs from a relatively shallow main channel (3 m) in 1969 to a relatively deep main channel (8 m) in 1974. The width of the entrance varied

between 600 and 700 m, and depends to a large extent on the wave climate during the previous months.

In order to get a first estimate of the Nerang River Entrance stability, the theory originally presented by Escoffier (1940) and later improved by Van de Kreeke (1990) is used.

The so-called closure curve can be calculated using Equation (32), (34) and (29) in Volume I. The entrance channel cross-sectional area must be used as the variable parameter. The Broadwater surface area, hydraulic radius, tidal period, energy losses, tidal amplitude and tidal prism are assumed to be constant. The curve is calculated with cross-sectional areas from 0 m^2 to 2500 m^2 by substituting the parameters into:

$$K = \frac{T}{2 \cdot \pi \cdot \eta_0} \cdot \frac{A_c}{A_b} \cdot \sqrt{\frac{2 \cdot g \cdot R \cdot \eta_0}{m \cdot R + 2 \cdot F \cdot L}} \tag{5}$$

After the repletion coefficient is known the values C (K) and sinγ(K) are determined with the curves illustrated in Figure 4.5 in Volume I. The tidal maximum of the cross-sectional averaged velocity and the actual bottom shear stress is then calculated with the following expressions:

$$V = C(K) \cdot \sin\gamma(K) \cdot \frac{2\pi A_b a_0}{A \cdot T} \tag{6}$$

$$\tau_b = \rho \cdot \frac{g}{C^2} \cdot V|V| \tag{7}$$

The equilibrium shear stress curve follows by making use of Equation (6), (7) and an empirical relationship between the tidal prism and the cross-sectional area. These emperical relations were already discussed in section 4.2.2.1. (Volume I). However the Nerang River Entrance is not a stable tidal inlet. This means that the empirical relationships between the cross-sectional area and the tidal prism are generally not valid in these particular cases. Bruun (1978) and Van de Kreeke (1990) stated that the cross-sectional critical velocity in most cases is about 1 m/s. Van de Kreeke (1990) suggested that the critical shear stress (or equilibrium shear stress) could be determined in terms of the cross-sectional area using the following expression:

$$\tau_{cr} = B \cdot F\left[C(K) \cdot A_c^{\,D}\right]^2 \tag{8}$$

Parameters B and D must be determined using an empirical relationship between the cross-sectional area and the tidal prism.

Van de Kreeke (1990) used the following empirical relationship for stable inlets along the West Coast of Florida:

$$A_c = 1.175 \cdot 10^{-4} \cdot P^{0.97} \tag{9}$$

The latter empirical relationship is not valid in the case of the Nerang River Entrance. This means that an empirical relationship valid for the Nerang River Entrance must be found. Making use of the measured cross-sectional areas (equation 4). This yields to the following empirical relationship valid for the Nerang River Entrance.

$$A_c = 6.302 \cdot 10^{-3} \cdot P^{0.97} \tag{10}$$

The expression for the critical shear stress then becomes:

$$\tau_{cr} = \rho \cdot f \cdot V^2 \qquad (11) \quad \text{Critical Shear stress}$$

$$P = 2 \cdot A_b \cdot \hat{\eta}_0 \sin\varphi \qquad (12) \quad \text{Tidal Prism}$$

$$A_c = 6.302 \cdot 10^{-3} \cdot P^{0.97} \quad \longrightarrow \quad P = \left(\frac{A_c}{6.302 \cdot 10^{-3}}\right)^{1.031} \qquad (13) \text{ Dynamic equilibrium cross sectional area.}$$

$$V = C(K) \cdot \sin\gamma \cdot \frac{2 \cdot \pi \cdot A_b \cdot \hat{\eta}_0}{A_c \cdot T} \qquad (14)$$

combining (10) and (12) yields:

$$V = \frac{C(K) \cdot \pi \cdot P}{A_c \cdot T} \qquad (13)$$

combining (13) and (14) yields:

$$V = \frac{C(K) \cdot \pi \cdot \left(\frac{A_c}{6.302 \cdot 10^{-3}}\right)^{1.031}}{A_c \cdot T} = \frac{C(K) \cdot \pi \cdot (A_c)^{1.031}}{\left(6.302 \cdot 10^{-3}\right)} = \frac{C(K) \cdot \pi \cdot (A_c)^{1.031}}{\left(6.302 \cdot 10^{-3}\right)^{1.031} \cdot A_c \cdot T}$$

T= 44,640 s and ρ=1024 kg/m^3

$V = C(K) \cdot A_c^{0.031} \cdot 0.596$ combining this expression with (1) yields:

$$\tau_{cr} = \rho \cdot f \cdot V^2 = 1024 \cdot f \cdot \left(C(K) \cdot A_c^{0.031}\right)^2 \cdot (1.51)^2 \quad \longleftrightarrow$$

$$\tau_{cr} = 2303 \cdot f \cdot \left(C(K) \cdot A_c^{0.031}\right)^2 \quad \text{expression for the critical shear stress curve}$$

The computation of the critical shear stress curve and the closure curve are presented in Appendix E. The resulting closure curve and critical shear stress curves are illustrated in Figure 2 of Appendix E.

From the Escoffier stability analysis may be concluded that the cross-sectional area of the Nerang River Entrance falls within the equilibrium interval as defined by Van de Kreeke (1990). Prior to the training of the Nerang River Entrance a cross-sectional area of approximately 1000 m^2 – 1200 m^2 was measured relative to mean sea level. The Escoffier stability analysis presented in Appendix E; Figure 2 shows that the dynamic equilibrium cross-sectional area is A_S = 1350 m^2 which is higher than the measured cross-sectional area. This means that the entrance cross-sectional in this particular case has the intention to erode until it reaches the "stable point" located at the intersection of the closure curve and the equilibrium shear stress curve. In cases were there is a temporarily large littoral drift after for instance passing a storm, the Nerang inlet cross-sectional area decreases. In order to re-establish its equilibrium cross-sectional area forces are mobilised to scour the entrance until it reaches the "stable point" on the Escoffier closure curve.

Figure 1.20: Possible layouts for improving the Nerang River Entrance

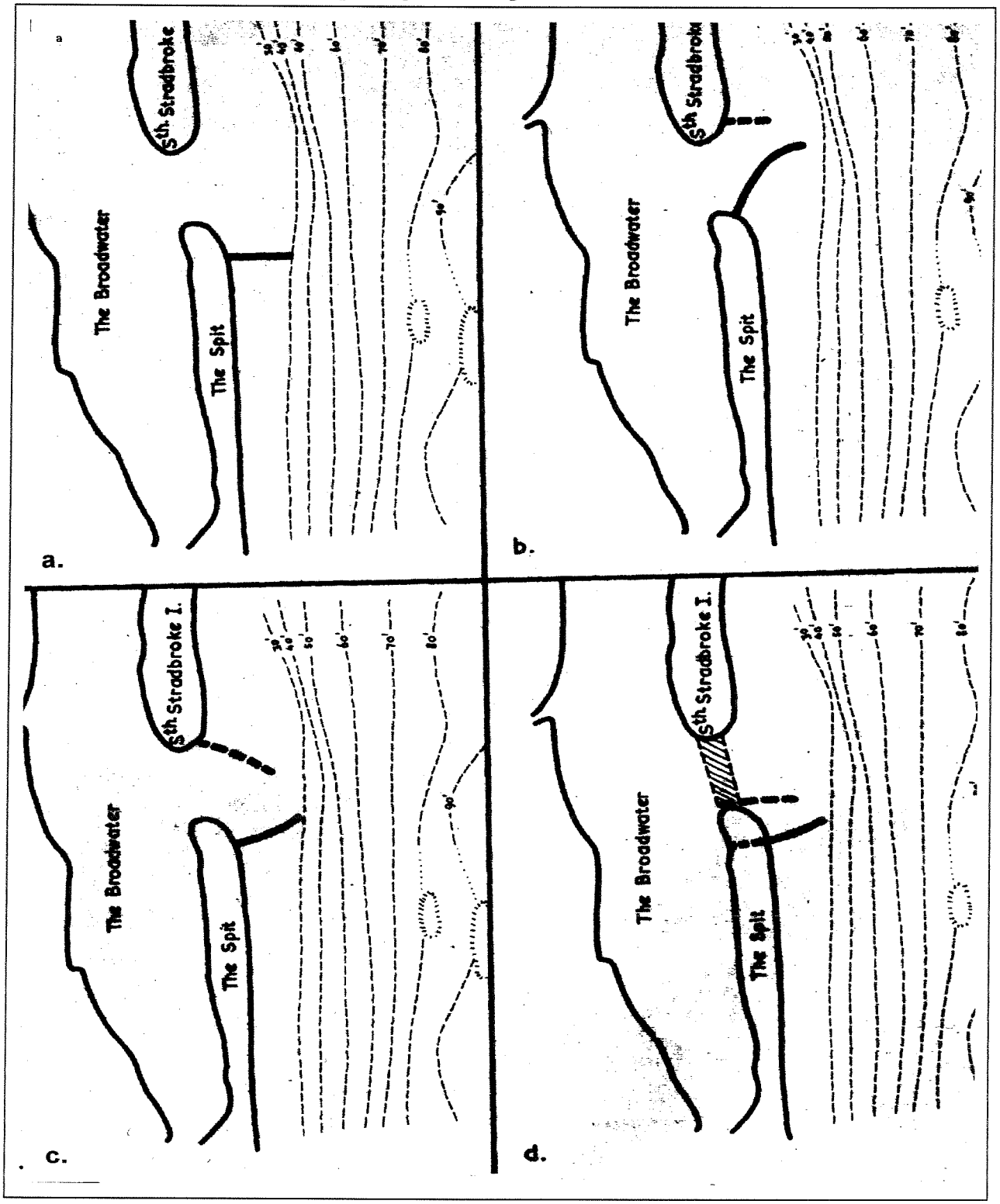

(From: Delft, 1970)

1.6. Improvement of the Nerang River Entrance

1.6.1. Introduction

In order to improve the Nerang River Entrance, several layouts were possible. In the next sections the conclusions and recommendations by Delft (1970), will be described briefly as well as some additional considerations. The final recommendation by the Delft Hydraulic Laboratory for stabilizing the Nerang River Entrance was done after the model investigations and will be shortly described later.

The purpose to improve the Nerang River Entrance was to stabilize the entrance and to provide a safe navigation for small ships like fishing vessels and small coasters. Also the influence of the stabilization works on the adjacent beaches must be taken into account. Therefore sediment coming from the littoral drift has to bypass the entrance in order to prevent the downdrift coastal regions from severe erosion. There are several ways of bypassing sediment, each of them have a significant influence on the layout of the entrance.

Delft (1970) stated that in order to stabilize the Nerang River Entrance, training-walls (breakwaters) should be constructed on both sides of the entrance. Bypassing of the littoral drift is advised to prevent serious erosion of South Stradbroke Island and to guarantee the accessibility of the entrance for navigation. In the following sections some alternative layouts, considered by Delft Hydraulics, will be briefly discussed. These alternatives were the basis for the model experiments and they are illustrative for the improvement of tidal inlets in general.

1.6.2. Possible layouts for improving the Nerang River Entrance

1.6.2.1. General

According to Delft (1970) a training-wall more or less perpendicular to the coast at the northern end of The Spit, in combination with sand nourishment to the beaches, in order to prevent South Stradbroke Island coast from erosion, was considered. The training-wall should at least be reaching to the 7,6 m (25 ft) depth contour. This layout, as shown in Figure 1.20a, is the simplest and economical because of the relative short breakwaters in this situation.

To actually improve the Nerang River Entrance a second training-wall was necessary on the southern end of South Stradbroke Island. This wall will be long and must be built from South Stradbroke Island, which is not accessible directly from the mainland. Therefore this option was unattractive. Figure 1.20b gives a possibility of a shorter training-wall at South Stradbroke Island. The curved wall at the Spit has a rather short effective length perpendicular to the coast with respect to its actual length. The curved wall also crosses the deeper parts of the entrance, thus needs significantly more material. Another option was the layout with a curved training-wall at The Spit as shown in Figure 1.20c. The southern training-wall is mostly located in the shallow areas, which is important for the amounts of material needed, but the training-wall on South Stradbroke Island now needs more equipment and is therefore expensive. Trucks can reach the Spit and to lower the costs, the alternative layout given in Figure 1.20d is possible. The northern as well as the southern training-wall are located on the Spit. After this, it is necessary to close the original entrance. Using the material from the Broadwater and the material from dredging through The Spit can do this. The construction of any training-wall will cause erosion on the beaches of South Stradbroke

Island. Erosion weakens the coastal protection, which may result in a new breakthrough of South Stradbroke Island. This may cause a worsening of the improved Nerang River Entrance and must therefore be prevented. So a very important issue is the continuation of the net northward longshore transport in order to prevent serious erosion of the South Stradbroke Island and sedimentation of the entrance by the large amounts of sediments moving in from the tip of the training-wall into the entrance. In general sand has to be brought from the immediate south of the southern training-wall, and brought to the north of the northern training wall. There are several possibilities to bypass sand from the south of the entrance to the north mechanically. The method of mechanical bypassing determines the layout of the entrance. Delft (1970) advised that the whole net annual littoral drift have to be bypassed.

1.6.2.2. Mechanical sand bypassing

The way of mechanical bypassing of sand across the entrance has a significant influence on the layout of the improved Nerang River Entrance. Delft (1970,1976) both describe some alternative bypassing methods. Delft (1976) described four possibilities of artificial mechanical bypassing of sand, and its effects on the layout of the improved Nerang River Entrance. A description of the possibilities of artificial mechanical bypassing of sediment was already been given in section 5.4. (Volume I.) Only the most important considerations by Delft Hydraulics are briefly summarised in Appendix F.

Figure 2.1: Layout of the model

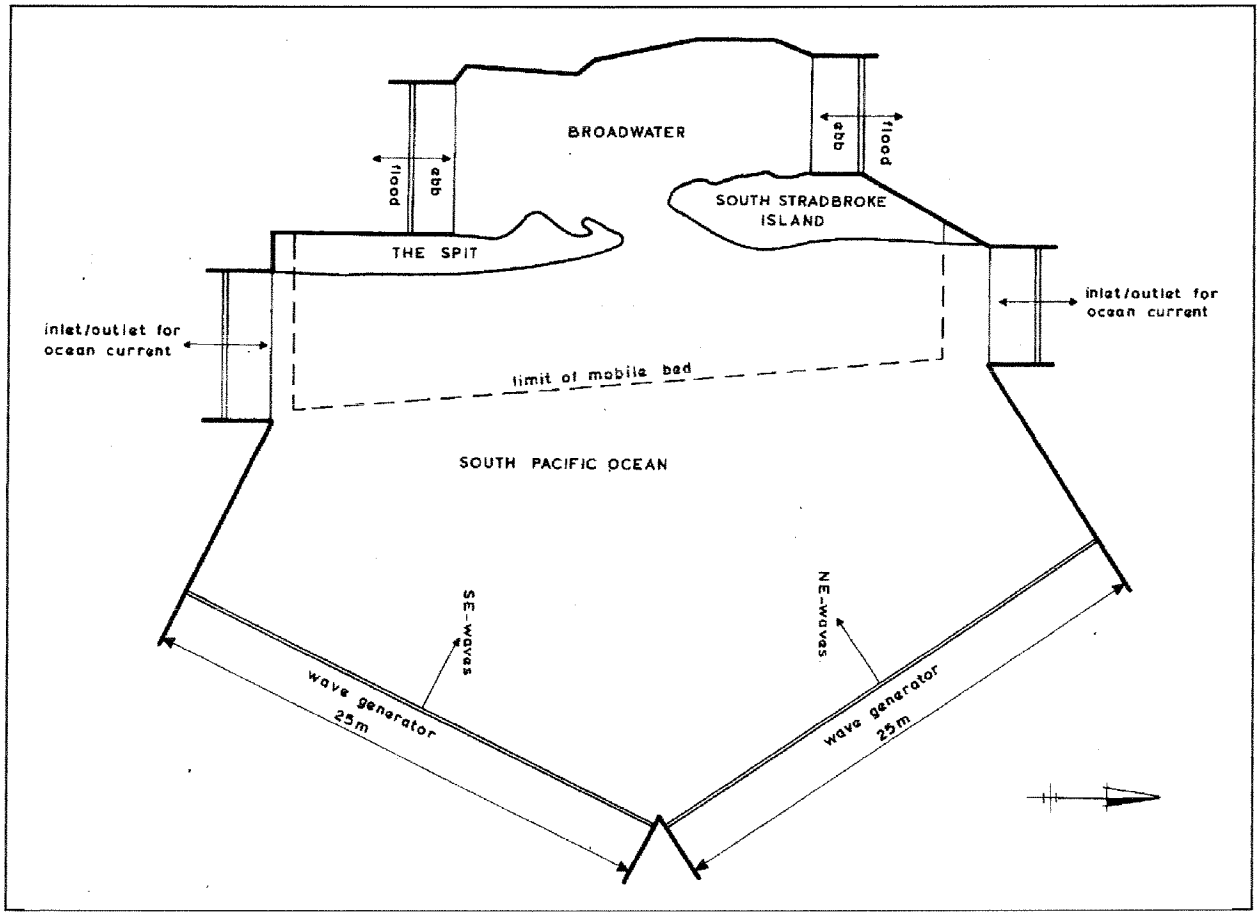

(From: Delft, 1976)

Figure 2.2: Calibration tests

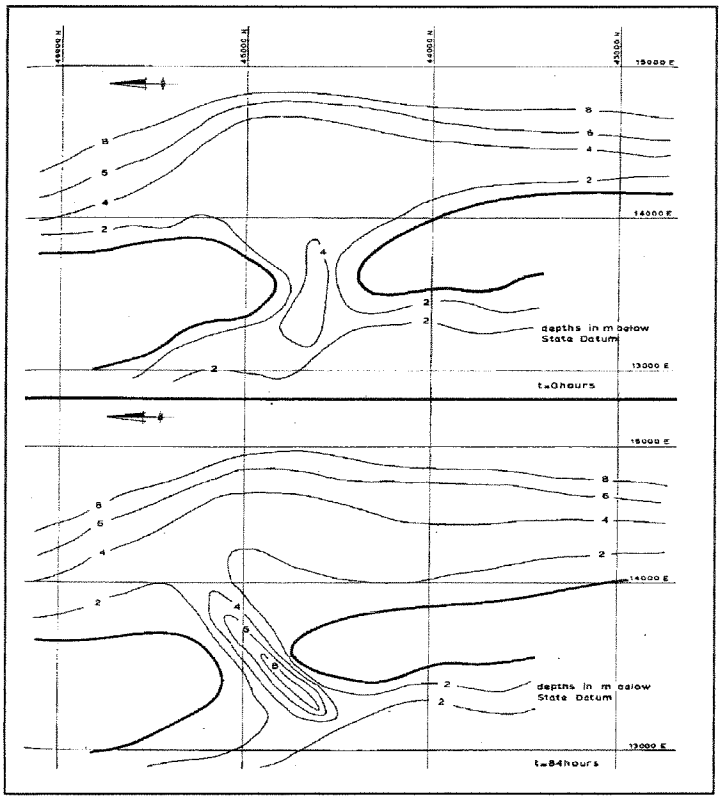

(From: Delft, 1976)

2. Model investigations Nerang River Entrance

2.1. Introduction

Due to the complex morphological behaviour of unstable tidal inlets, three-dimensional morphological model studies can increase the insight of the processes involved on specific cases. In the following sections a brief description of the Nerang River Entrance model tests will be given. The emphasis in this report lies on the morphological behaviour of the different training-wall layouts, the influence of the mechanical bypassing of sediment and its effects on the nearshore bathymetry. Especially the influence of the sand bypassing installation is important, because little information is available on this topic in the literature. In the sections below only the most important and illustrative results of the model tests will be described. More information may be found in Delft (1976).

In general the model tests are necessary to enable a proper design for the works to solve the stabilization problems of the entrance, and to study the effects of the future interventions on the existing non-trained situation. The basis for the determination of the hydraulic boundary conditions for the model study were derived from the 1970-report and updated by information received from the Department of Harbours and Marine and The Dutch Meteorological Institute (KNMI). Figure 2.1 shows the layout of the model.

It is obvious that the reliability of a morphological model is highly dependent on the degree of similarity of the model and the `prototype`. In the prototype the morphological hydrological conditions were very complex. Waves, currents, water level variations and the sediment movement in the nearshore region changed continuously. The sea bed in the prototype consists of sand with varying size distribution and amounts of crushed shells. Therefore this complicated situation had to be drastically schematised in the model. The waves in the model investigations had uniform height and periods and approached from two directions (NE and SE). The tidal movement has been brought back to two phases, which are of importance for the morphological behaviour of the entrance. The bed material in the model had an uniform size distribution at all locations in the model.

2.2. Calibration tests

Because of these schematisations, the model has to be tested in order to meet the real morphological behaviour of the prototype. This was done by calibration of the model, which means that the boundary conditions like waves, currents and water levels were chosen in such a way that the morphology changes in the model agree with the actual developments in the prototype. The calibration of the model was focused on the representation of the Nerang River Entrance behaviour in the period 1955-1973. (see also Figures 1.12 and 1.13) The main criteria used for the calibration tests were:

Longshore transport rates, siltation of the Broadwater and the migration of the entrance.

Bar shape and location.

The hydraulic boundary conditions during the first, of total 7 documented calibration tests, were based on the hydraulic boundary conditions in the prototype. With these hydraulic boundary conditions the Nerang River entrance model was either stable or migrated in a southerly direction. In order to improve the morphological behaviour, a set of experimental boundary conditions had been derived after 90 hours model operation. These boundary

Figure 2.3: Test (T1), with the prototype situation of 1973

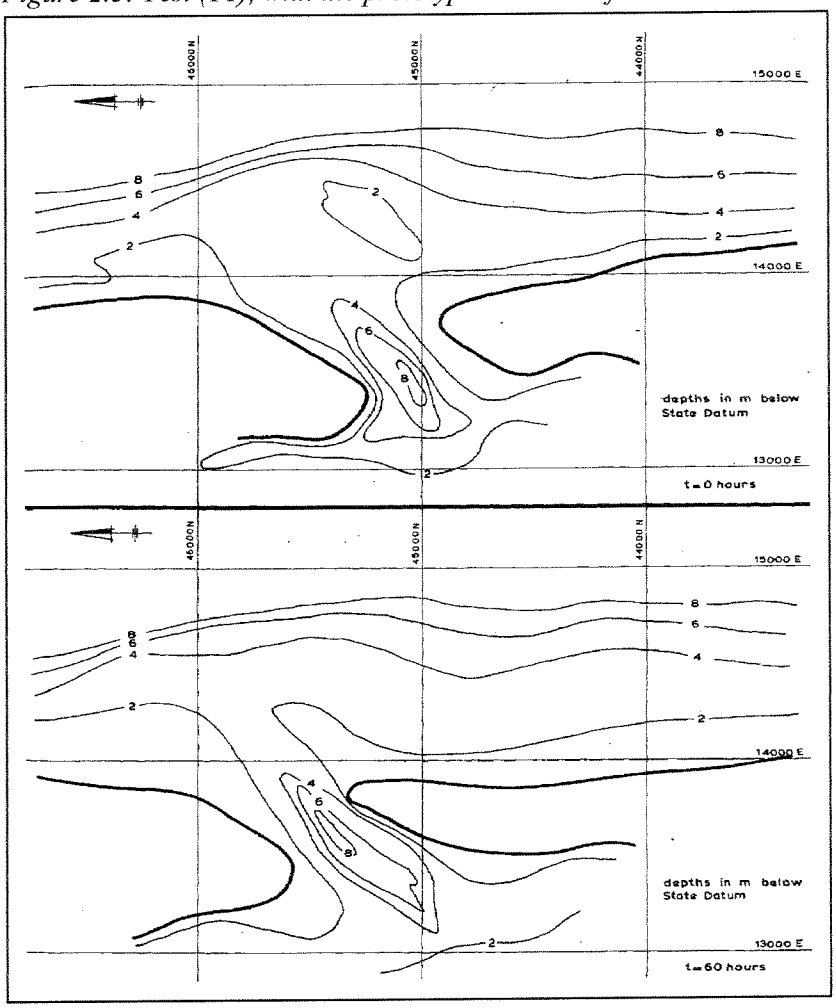

(From: Delft, 1976)

Figure 2.4: Inlet minimum cross-sectional area

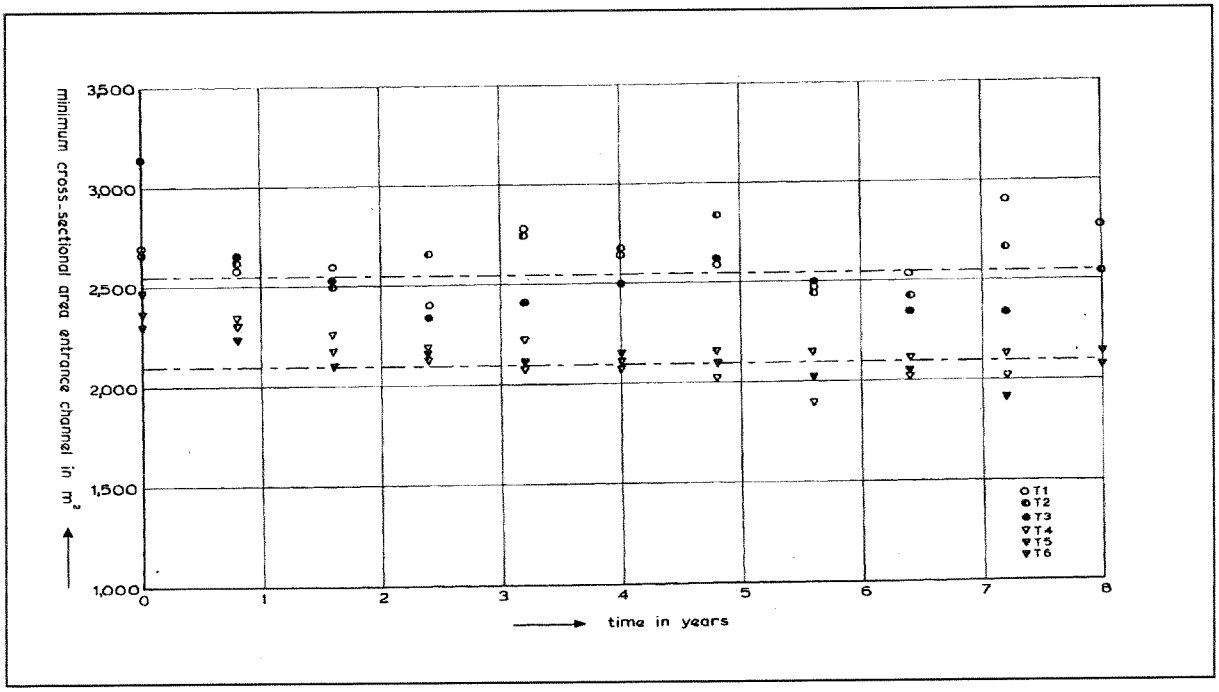

(From: Delft, 1976)

conditions were used in further calibration tests. The morphology of the Nerang River entrance as observed in these tests were practically identical, with a steady northward migration and a morphologic development which was considered satisfactory. The morphological development of the entrance after 84 hours calibration test (7,5 hours ≅ 1 year prototype) of model operation is given in Figure 2.2. The initial situation is also given in Figure 2.2.

2.3. Model tests

2.3.1. Introduction

The actual model test were focused on the location of the trained entrance and the impact of various layouts, with and without mechanical bypassing, on the morphology in the vicinity of the Nerang River Entrance. For the location of the new entrance two alternatives were tested: A new entrance at the 1976 location and a new entrance located on The Spit. In total seven morphological test with various training-wall layouts were performed, and one test in which only the current patterns were measured, in order to determine the optimal alignment of the training-walls. After the calibration tests, a test (T1) was done with the prototype situation of 1973. Figure 2.3 shows the morphological development after 60 hour model testing. With respect to the average morphological time scale (7,5 hours ≅ 1 year prototype) a migration rate of 37 m/year was found for the period 1974-1981. Figure 2.4 shows the development of the minimum cross-sectional area of the Nerang River Entrance. These test results served as a basis for later tests with structures in the vicinity of the Nerang River Entrance. The further tests situations were:

- Retention groins 200 m south of the north end of The Spit. (T2 and T3)
- New entrance through The Spit without mechanical bypassing, and with both training-walls of the same length. (T4)
- New entrance through The Spit with mechanical bypassing, and with both training-walls of the same length. (T5)
- New entrance through The Spit with mechanical bypassing, and training-walls with different length. (T6)
- Current pattern measurement (T7)
- New entrance through The Spit with mechanical bypassing, and training-walls with different length and adapted alignment of the training-walls as a result of T7. (T8)
- New entrance at the present 1976 location with mechanical bypassing, and training-walls with different length and different alignment of the training-walls. (T9)

2.3.2. Retention groins

Two retention groins located at The Spit have been tested, a long groin and a shorter groin. The reason for testing these situations was:

- Study the effect of construction in phases on the morphology near the entrance.

Figure 2.5: Morphological development test T4

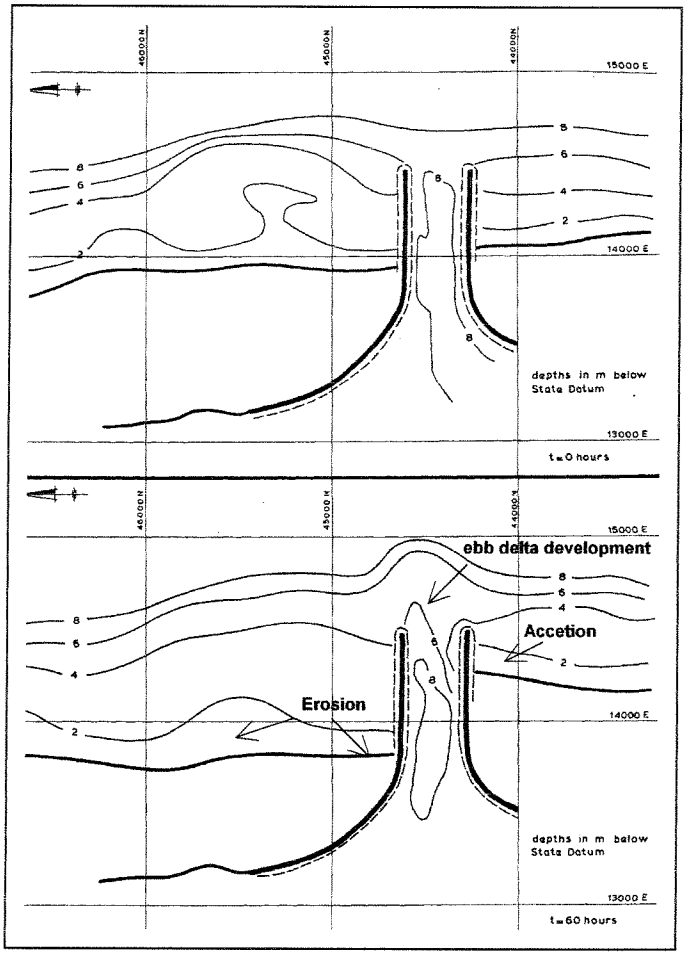

(From: Delft, 1976)

Figure 2.6: Development cross-sectional area

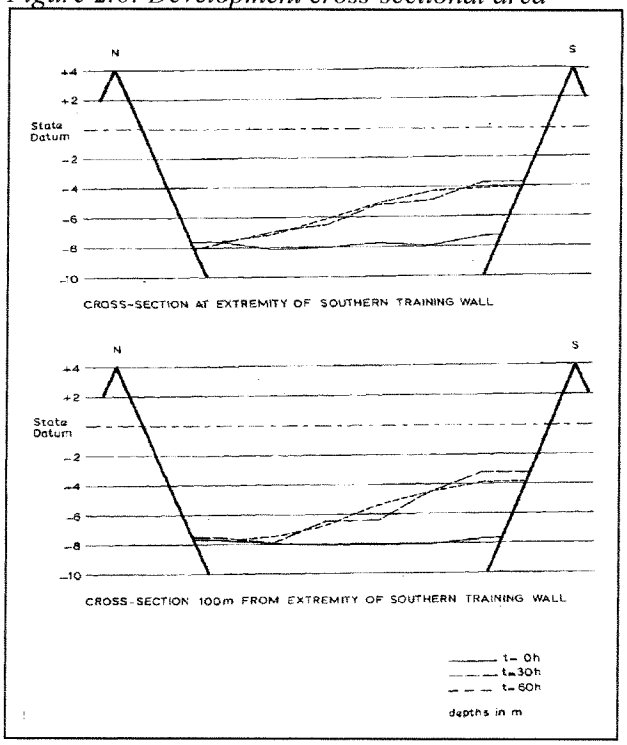

(From: Delft, 1976)

- Study the effects of the structure on the nourished sand on the beaches between Main Beach and Surfers Paradise.

The results of the investigations indicated that the building of a retention groin without replenishment to the immediate south of it, can temporarily lead to a shoaling and widening of the Nerang River Entrance as well as to erosion of the beaches to the north of the location of the groin, both on The Spit and on the southern tip of South Stradbroke Island. Conclusion of the above mentioned tests is that building of a retention groin without beach replenishment to the immediate south of it is not recommended. A combination of a retention groin and beach replenishment, in such a way that sediment will be bypassed, leaves the situation compared to the situation without any action unchanged: The entrance migrates normally and the siltation of the Broadwater stays also unchanged. From the above described situation it can be concluded that retention groin with or without beach replenishment does not keep the entrance from migrating, and is therefore not recommended for entrance stabilization. However, in the model the retention groin was situated approximately 200 m southward from the northern end of The Spit. This was done to be able to study the effects on the nearshore zone by a retention groin, fitting in the training-wall of the improved entrance through The Spit. There is more information on this subject in Delft (1976).

2.3.3. Trained entrance through Spit without sand bypassing (T4)

Figure 2.5 shows a layout, and the morphological development of the trained Nerang River Entrance after 60 hours model operation. (approximately 8 years prototype)

The sediment accumulation to the south of the entrance after 24 hours (3 years prototype) of model operation showed amounts to nearly 100% of the net longshore transport. After this, sediment started bypass the training-walls due to a strong seaward directed current along the southern training-wall (rip-current). This phenomenon was responsible for less accretion than expected. After 60 hours of model operation 60% of the net longshore transport has accumulated to the south of the entrance.

Severe erosion occurred on South Stradbroke Island during the model tests (see Figure 2.5). It can be concluded that considerable erosion of South Stradbroke Island took place in the 8 years after construction.

From the lower section in Figure 2.5 can be concluded that the entrance channel shoaled, especially at the end of the entrance. It seems that sediment is creeping from the updrift side into the entrance channel along the south training-wall. Figure 2.6 shows the cross-sectional area of the entrance. The original depth of the entrance channel was State Datum -8,0 m. Both figures show a reduction of depths near the southern training-wall. The minimum cross-sectional area of the entrance decreased about 20% with respect to the untrained entrance (see also Figure 2.4).

Figure 2.5 also shows that a new offshore bar has formed outside the entrance. The old bar has almost completely eroded.

2.3.4. Entrance through Spit with bypassing (T5)

The previous test was repeated, but now with sand bypassing. The borrow area was located in the surf zone within the 4 m depth contour and approximately 300 m to the south of the southern training-wall. The sand was removed from borrow area at regular intervals during

Figure 2.7: Morphological development with sand bypassing (T5)

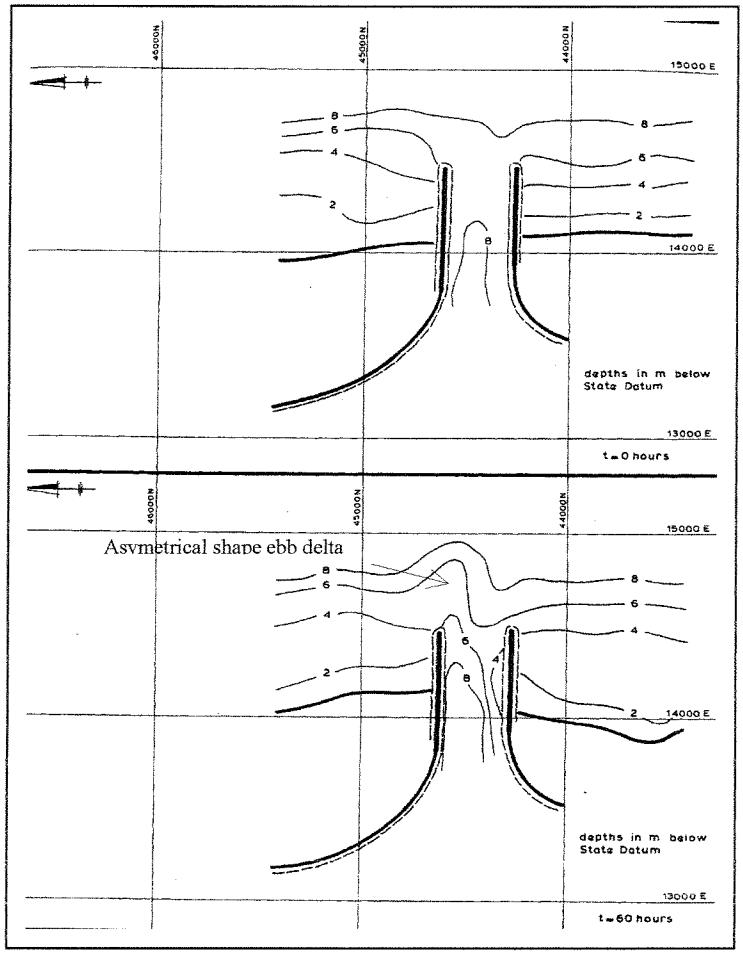

(From: Delft, 1976)

Figure 2.8: Morphological development test (T6)

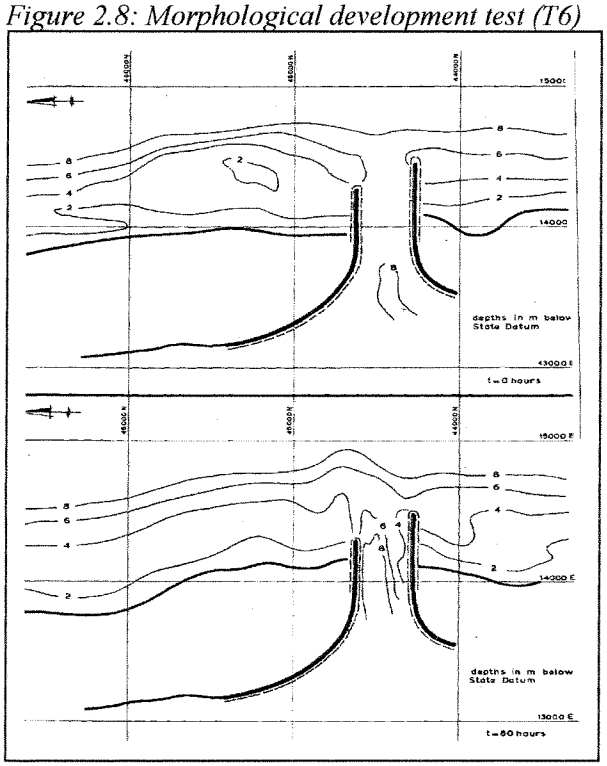

(From: Delft: 1976)

each cycle and dumped directly to the north of the northern training-wall. The bypassed volume was equal to that supplied at the southern boundary of the model. The morphological development after 60 hours (8 years prototype) is shown in Figure 2.7.
The volume of sand accumulated in the immediate south of the training-wall amounts to a 5% decrease of the net northward transport, with respect to the previous test without sand bypassing. From this may be concluded that the amount of bypassed sediment was too high. Although the same amount is bypassed as supplied from the boundaries. A possible explanation for this phenomenon must be sought in the already mentioned seaward directed current (rip current) located to the south of the south training-wall. This was confirmed by visual observations in the model.

Directly north from the northern training-wall accretion took place (10% net northward transport). This can be explained by the fact that the feeder beach partly falls in the shadow of the northern jetty during the prevailing south-easterly waves.

The entrance channel shows a decrease in minimum cross-sectional area, which was similar to the test without bypassing (see also Figure 2.6). However no accretion occurred in the Broadwater area, thus the sediment transported towards the entrance channel must only have been enough to account for the shoaling of the channel. More sediment was not available to be transported into the Broadwater.

The old offshore bar, to the north of the entrance was also eroded. A new offshore bar has formed just outside the entrance channel. The average sedimentation during the test was amounted to approximately 10% of the total net annual longshore transport. The shape of the offshore bar is somewhat different from the previous tests, caused by the sediment bypassing.

2.3.5. Alternative Entrance through Spit with bypassing (T6, T7 and T8)

The previous test were also carried out with the following changes:

- Northern wall was shortened by 200 m
- Reduction of the bypass rate to 80% of the net annual sediment transport.

Figure 2.8 shows the morphological development after 60 hours model operation. Due to smaller bypass rate The Spit accreted slightly. (approximately 10 % net annual transport rate) The accretion of the beach to the north of the training-wall reduced the erosion of the beach at the termination of the outer bar. The entrance shoaling is caused by the longshore transport. The shoaling rate of the Broadwater reached a value of 15% of the net longshore transport.

The purpose of the current measurements (T7) was to study the current patterns in the trained entrance. A general tendency showed for the ebb current to separate from the southern training-wall. The current patterns are illustrated in Figure 2.9. Based on the results the layout was changed by the re-alignment of the southern training-wall. This was tested with 80% bypass rate. The results of these tests (T8) are shown in Figure 2.10. The behaviour of The Spit and South Stradbroke Island did not change compared to the previous tests. The narrowed entrance eroded to some extent to attain its equilibrium cross-sectional area. The amount of sediment transport through the entrance into the Broadwater appeared to be very small (5% net annual transport rate). In these tests also erosion occurred of the existing outer bar and sedimentation in front of the entrance. The sediment deposited on the outer bar originated from the entrance channel. If the entrance had its equilibrium depth at the beginning, seaward shoaling would have been less.

Figure 2.9: Current pattern test T7

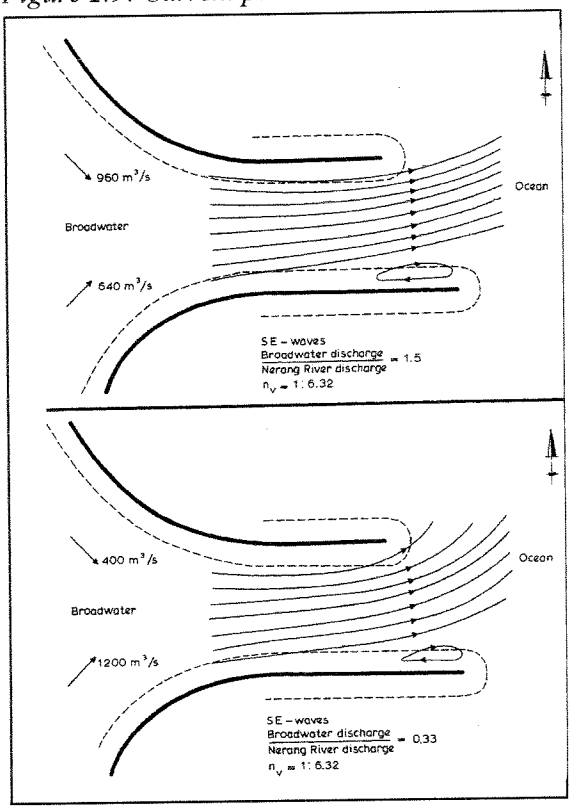

(From: Delft, 1976)

Figure 2.10: Morphological development test T8

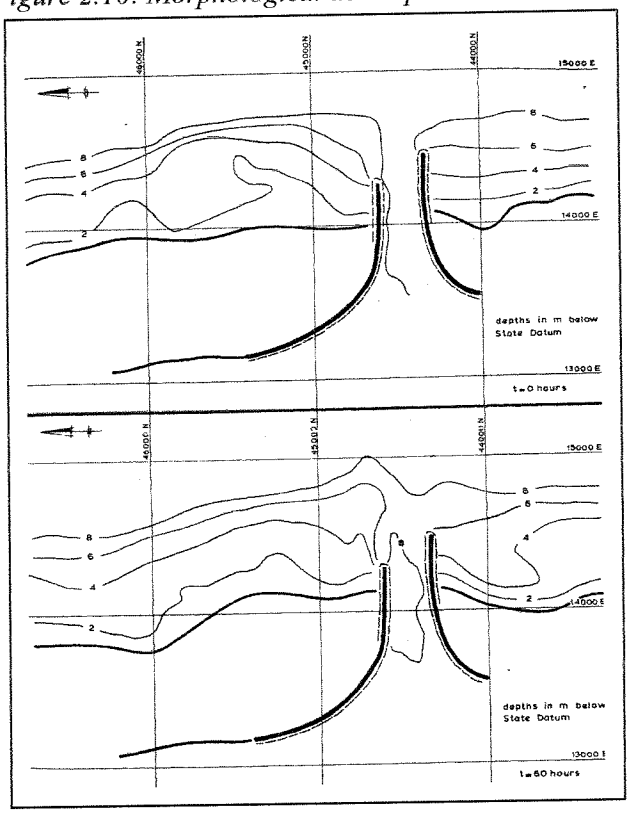

(From: Delft, 1976)

Figure 2.11: Proposed Stabilised Nerang River Entrance through the Spit

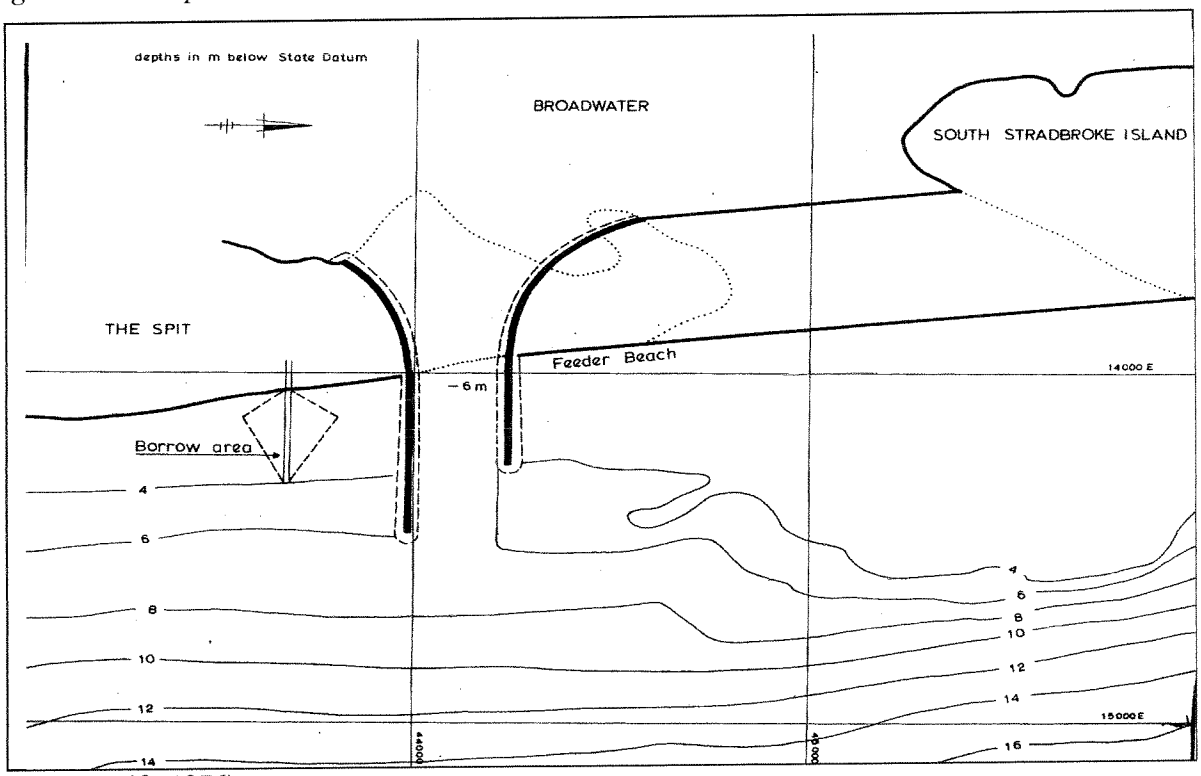

(From: Delft, 1976)

2.3.6. Summary of the most important recommendations

In this section only the most important recommendations and conclusions from the model investigations will be described. This is done to make a comparison of the recommendations by Delft Hydraulics and the actual layout which was built in 1984. The location of the improved entrance was chosen through The Spit because this was the most economic choice. The Delft Hydraulics concluded that the test results (T8) was the most feasible for the training of the entrance. According to Delft Hydraulics, the trained entrance should have the following characteristics:

- The southern wall should extent to the -5,5 m State Datum depth contour, or approximately 500 m to 600 m from LWM to provide navigation requirements.
- The cross-sectional area of the trained entrance should be 1700 m^2, measured relatively to State Datum + 1,3 m.
- The bed level in the channel of -6,0 m State Datum guarantees a minimum depth of State Datum (A.H.D.) -5,5 m or 4,5 m below Low Water Datum, the centre lines of the two training-walls can be approximately 260 m apart, measured at the seaward extremity of the northern wall.
- The northern wall can be shorter by 200 m; since this has no effects on the entrance channel, it is cheaper and its reduces the beach length in the downdrift shadow of the wall, thereby reducing the bypass pumping distance. In addition to this also the natural tidal flow bypassing of sand is returning more easily back into the littoral drift just north of the northern training wall. This reduces the ebb delta growth and probably the erosion of South Stradbroke Island.

The final layout of the improved Nerang River Entrance, recommended by Delft Hydraulics (1976) is illustrated in Figure 2.11.

Figure 3.1: Schematic diagram of the sand bypassing system

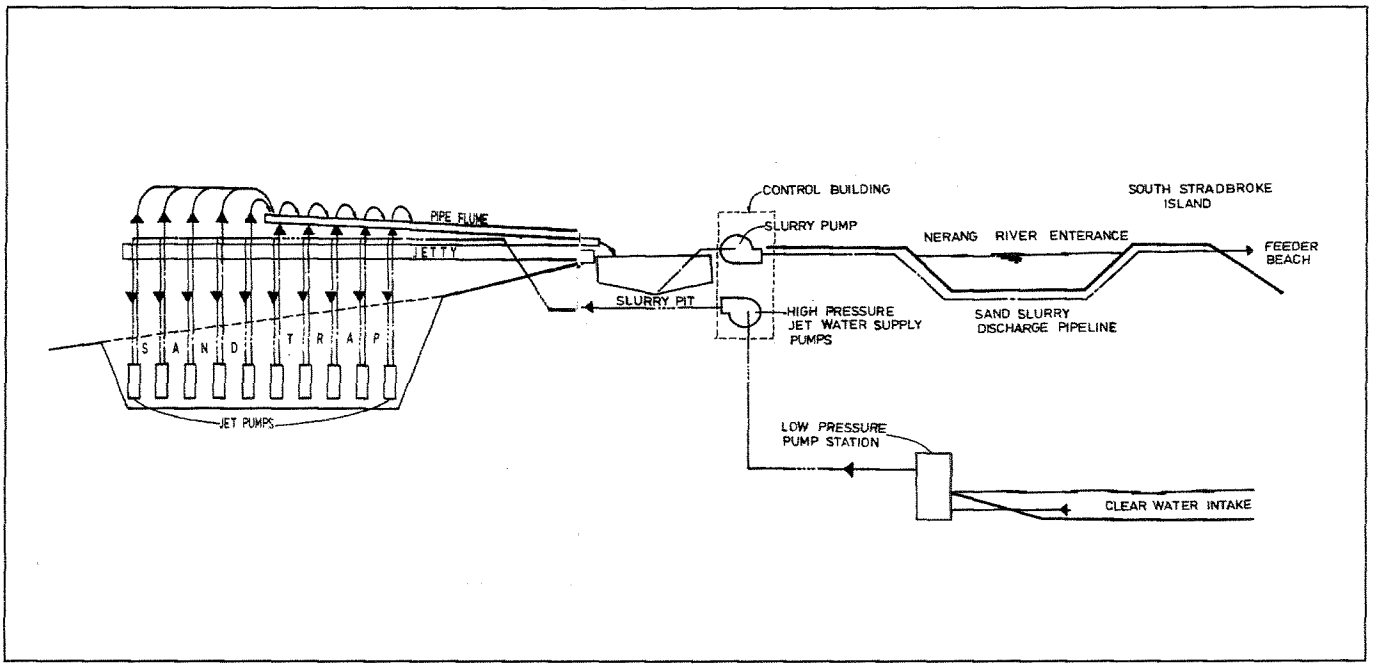

(From: Second Australian Port, Harbour and Offshore Engineering Conference 1988)

Figure 3.2: General Plan of The Gold Coast Seaway

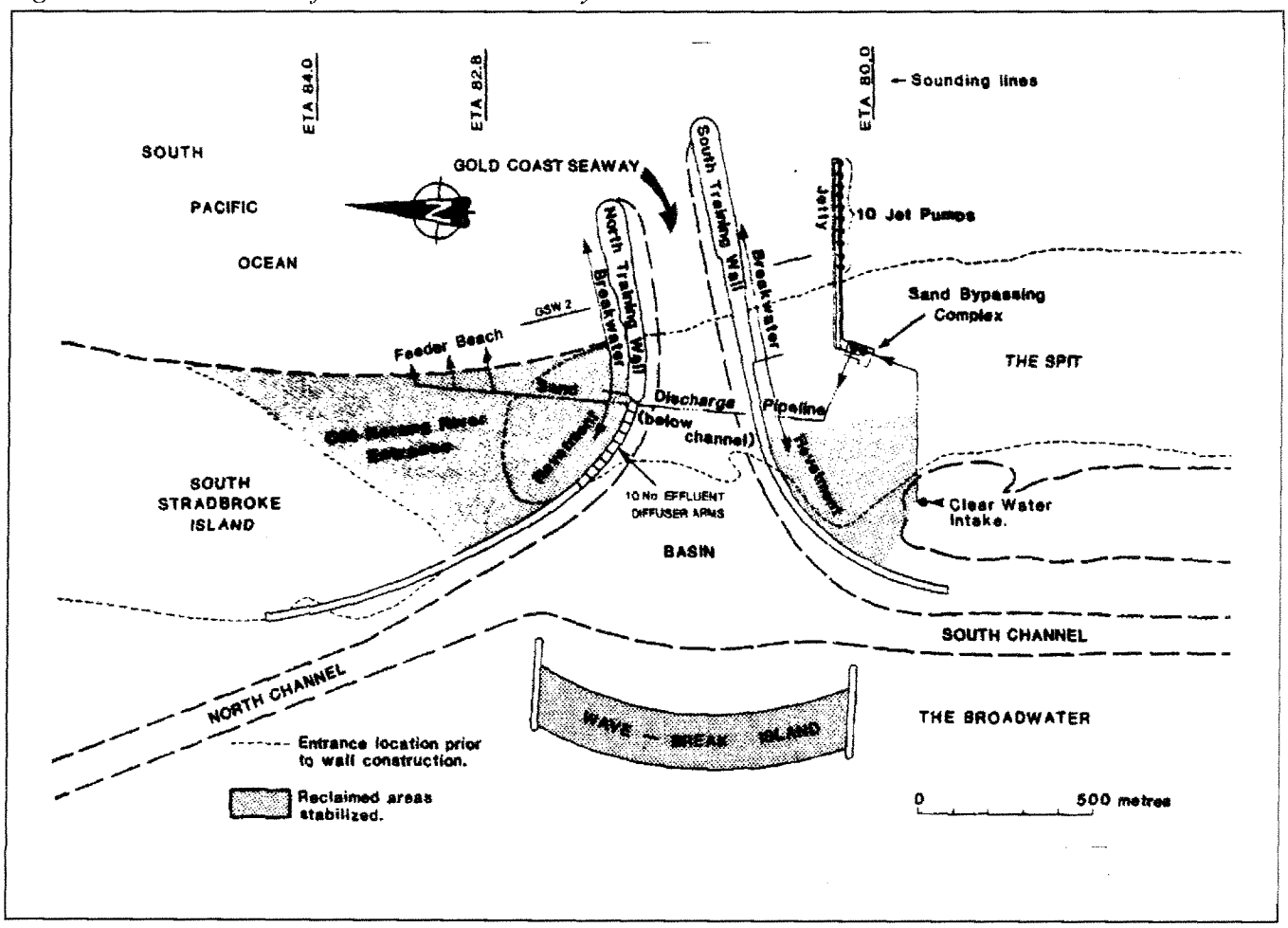

(From: Second Australian Port, Harbour and Offshore Engineering Conference 1988)

3. Gold Coast Seaway

3.1. Introduction

The Delft Hydraulic Laboratory advised on stabilizing of the Nerang River Entrance. The main conclusions from these investigations were described in the previous section. The Department of Harbours and Marine in Australia provided detailed engineering advise on the proposed training works. They undertook fixed bed modelling of the design of the breakwater heads as well as wave penetration into the Broadwater. The design of the training works was based on the recommendations by Delft Hydraulics (1976), but modified to suit the requirements of the Australian Waterways Authority. The training-walls were oriented 15 degrees north of east rather than due east and shifted slightly north of the location recommended by Delft.

The wave penetration through the trained entrance was expected to be greater than through the untrained entrance. This was due to the fact that a trained entrance channel is deeper than a non-trained entrance, so more waves passing the entrance can travel without breaking into the Broadwater area. In addition to this, dredging of the Broadwater leads to an increase in wave energy on the west side of the Broadwater because the shoals no longer dissipate the wave energy. A wave penetration model was constructed by The Department of Harbours and Marine to study this problem. The conclusion was that a wave-break island opposite the trained entrance would be the best way to control wave penetration through the new entrance. The actual construction of the Nerang River Entrance involved two major training walls about 320 m apart just south of the existing entrance. The southern training-wall extends approximately 600 m out to sea while the northern training-wall extends 400 m seaward. The new entrance channel through the Spit and the access channels in the Broadwater area involved 4.5 million m^3 dredging of sand. The sand from the dredging operations was used to close the old entrance and to construct the wave-break island. In order to prevent erosion of the wave-break island, The Spit and South Stradbroke Island, revegetation by local plant species was undertaken.

For the design of the bypassing system, the Beach Protection Authority commissioned the Delft Hydraulic Laboratory to further investigate the sand bypassing system. The chosen system was similar to the one recommended by Delft Hydraulics (1976). The sand bypassing system contents of ten jet pumps suspended from and spaced about 30 metres apart along a trestle extending 490 m into the sea. The trestle is located some 250 m south of the southern training wall. The jet pumps are submerged approximately 10 m below the normal seabed and their operation creates a trench or sand trap at right angels to the beach. The sand moving from the south inside the trench is pumped through a pipeline under the entrance to the northern beach. The clear water intake was located inside the Broadwater. The system has the capacity to pump either 335 or 585 m^3/hour. The sand bypassing system is expected to operate 5 days a week and can operate unattended overnight. Under storm conditions, it operates continuously at peak capacity. (Nerang River Entrance Stabilization, 1986) The sand bypassing system has been designed to handle the average northward longshore sand transport of 500,000 m^3/year although it has reserve capacity to handle higher peak transport rates during cyclones. The system can operate during severe weather conditions, 24 hours a day if necessary. Figure 3.1 shows the schematic diagram of the sand bypassing system. The whole project was completed in May 1986 at a total coast of approximately A$ 50 million. From this time the stabilized Nerang River Entrance is officially renamed The Gold Coast Seaway. Figure 3.2 shows the general plan of the Gold Coast Seaway.

An essential part of the project was monitoring the effectiveness and the impact of the entire Nerang River Entrance training project. The Australian Beach Protection Authority monitored

Figure 3.3: Location ETA lines

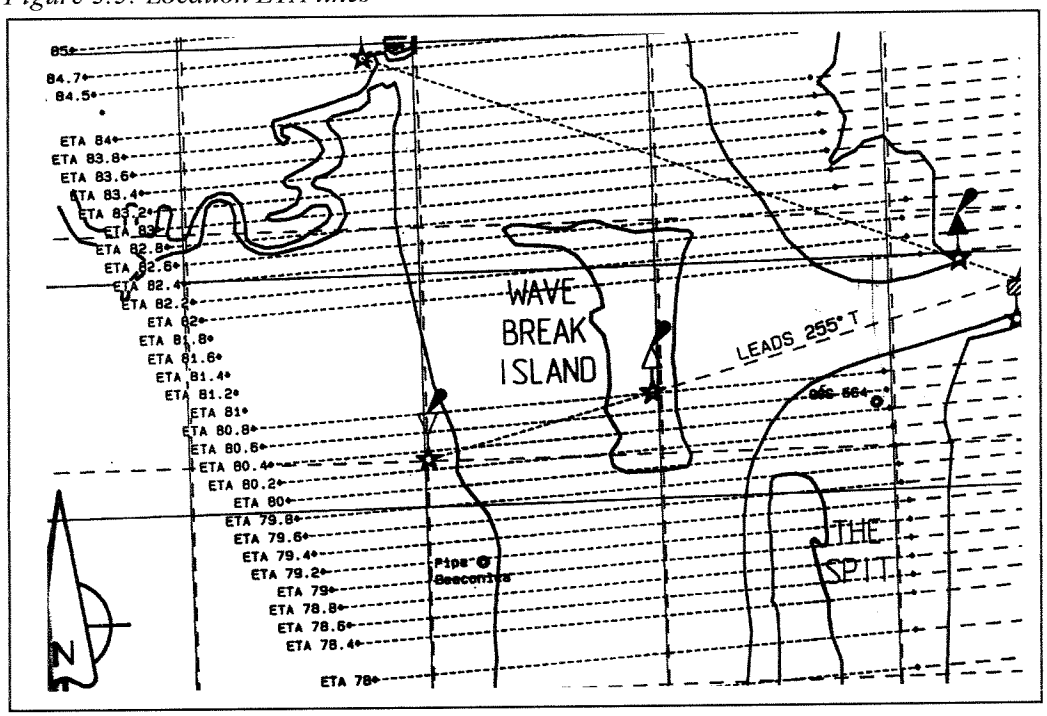

Figure 3.4: Volumetric changes south of the Gold Coast Seaway

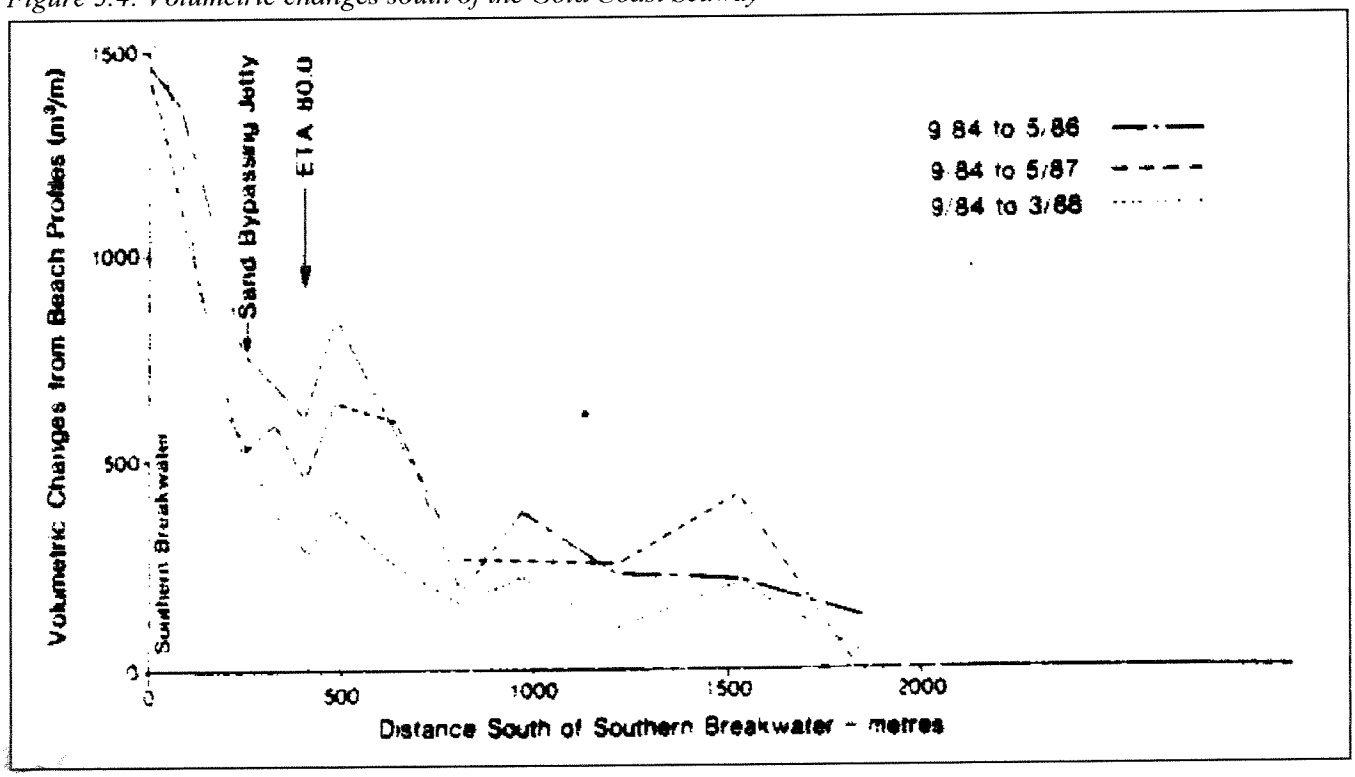

(From: Goughlan and Robinson, 1988)

the beach conditions to ensure that the volume of bypassed sand is sufficient to prevent erosion on either side of the Gold Coast Seaway. The result of these measurements are presented in Appendix G. In this Appendix G the monthly bypassed sand and the predicted total littoral drift (From C.O.P.E. data) are presented in one graphic. The graphic starts in May 1986, the start of the bypassing, until December 1996.

3.2. Impact bypass installation

3.2.1. Introduction

The Gold Coast Seaway project was started with the construction of the breakwaters in September 1984. The whole project was completed within 20 months and was officially opened on 31 May 1986. The impact of the Gold Coast Seaway construction from the completion in 1986 until now is determined using sounding lines (ETA-lines) of the northern and southern Gold Coast Seaway beaches and combined with soundings of the Gold Coast Seaway entrance and ebb tidal delta. Figure 3.3 shows the location of the sounding lines. With these soundings bathymetries are generated using the Delft-quickin program. This program is a user interface for generation of bathymetries by interpolate available soundings on a predefined grid. Appendix H shows which soundings are used to create the bathymetries. In order to determine the changes of the Gold Coast Seaway bathymetry from before the commencement of the works (1985) until now the Gold Coast Seaway bathymetry was divided in five sections (see also Appendix H); Section I is part of the south coast of the Gold Coast Seaway. Section II is the deeper part of the southern beaches. Section III is the ebb tidal delta. Section IV is the entrance channel and section V the northern beaches (feeder beach). By studying the net bathymetrical changes of the separate sections over the past 10 years and compare them to other sections gives an idea how the bypass installation affects the Gold Coast Seaway bathymetry as well as the governing sediment transport distribution. The net bathymetrical changes are determined for each section by calculation of the volume changes by subtracting generated bathymetries for each year of available soundings. (i.e. 1986 - 1985). The results of this bathymetry subtraction for each section of the Gold Coast Seaway are discussed in the next sections. The available sounding lines are located within approximately 1000 m in the vicinity of the Gold Coast Seaway. However the bathymetrical changes caused by the Gold Coast Seaway construction extents over a longer distance. Figure 3.4 clearly shows that the volumetric changes south of the Seaway extent over a much longer distance then the available sounding lines.

However not only the sand volumes are important to study, also the distribution of sediment along bottom profiles gives an idea how the bypass system affects the nearshore zone. Appendix I gives the bottom profiles ETA 80, location The Spit. Appendix J gives the bottom profiles at the Gold Coast Seaway ebb tidal delta (ETA 80.8). Appendix K gives the bottom profiles at the Feeder beach, the location were the bypassed sand is transported back into the active system (ETA 84). Appendix L gives the bottom profiles just north of the northern breakwater (ETA 82.8). For all bottom profiles it turned out that not much changes occur below the –10 m AHD line (see the large scale bottom profiles, Appendix I). The changes in the bottom profiles and volumes are discussed for each part in sections 3.2.3. , 3.2.4. and 3.2.5.

3.2.2. Effects Gold Coast Seaway on the water level variation

Appendix B shows the water level variations inside the Broadwater before and after the construction of the Gold Coast Seaway. The water level variation inside the Broadwater, prior to training, is already discussed in section 1.4.3.

The water level variations inside the Broadwater are significantly influenced by the construction of the Gold Coast Seaway, wave break island and dredging operations. Navigation channels were dredged along the eastern side of The Broadwater to the north and south of the Seaway. By November 1984 a bund, for construction access between the southern training wall and the wave break island, had been completed. The South Channel was dredged from Sea World north to this bund. On April 17, 1985 the bund was breached and the South Channel was re-established with an improved hydraulic efficiency. The wave break basin and the North Channel was completed during May 1986. (Water Level Monitoring Report, 1987).

Before the construction of the Gold Coast Seaway the Broadwater tidal amplitude was significantly decreased due to the flow restricting effect of the entrance channel. The Broadwater tidal range was approximately 60 % of the ocean tidal range.

As a result of the construction of the Gold Coast Seaway the attenuation of the ocean tide decreases. Appendix B clearly shows this effect. After the construction of the Gold Coast Seaway the Broadwater tidal range reaches to 90% of the ocean tidal range. The water level variation inside the Broadwater follows more easily the ocean tide because more water is able to enter the Broadwater through the enlarged and stabilised Gold Coast Seaway entrance channel. The high tides are slightly higher (0.1 m). The most changes occur at low tides they have become significantly lower. (0.25 m) The highest tides remain unchanged. The changes of the low tides can be explained by the fact that due to the increased depth and cross-sectional area of the entrance channel at low water, more water is able to flow through the entrance channel.

Due to the construction of the breakwaters the littoral drift was partly blocked, and therefore the transported littoral drift through the entrance channel was significantly reduced with respect to the situation prior to training. The new dredged entrance channel scours it self until a dynamic equilibrium cross-sectional area has reached. As a result of this the cross-sectional area of the Gold Coast Seaway increases and therefore also the tidal prism. Both reduction of the littoral drift inside the entrance channel and the increased tidal prism eventually results in a stable entrance channel. (Stability criterion by Bruun, 1976)

3.2.3. Effects of the sand bypass installation on the southern beaches

The effects of the bypass installation on the southern beach is analysed using the ETA-80 bottom profiles as well as the calculated volumetric changes and the available data of the measured bypass rates. The effects of the bypass installation extend further than the available data. This means that only hypothetical conclusions can be drawn. However some information was available about the impact of the bypass installation on the beaches further to the south. Coughlan and Robinson (1988) stated that before the commencement of the sand bypassing 970,000 m^3 sand had accumulated south of the entrance as a direct result of the construction of the southern breakwater. The construction of the southern breakwater started in September 1984 and was finished in May 1986. During this period (20 months) a longshore transport between 750,000 m^3 and 1,000,000 m^3 occurred (Coughlan and Robinson, 1988). This volume favours the accumulated volumes south of the entrance however some sand would have naturally bypassed the southern breakwater while it was being constructed. (Coughlan and Robinson, 1988). Most of the sand trapped south of the entrance occurred above the -10 m A.H.D. level:

- 390,000 m^3 above -1.0 m A.H.D. (approximately Low Water Datum)
- 570,000 m^3 from -1.0 m A.H.D. to -10.0 m A.H.D.
- 10,000 m^3 below -10.0 m A.H.D.

Figure 3.5 ETA 80 bottom profiles from September 1984 until May 1987

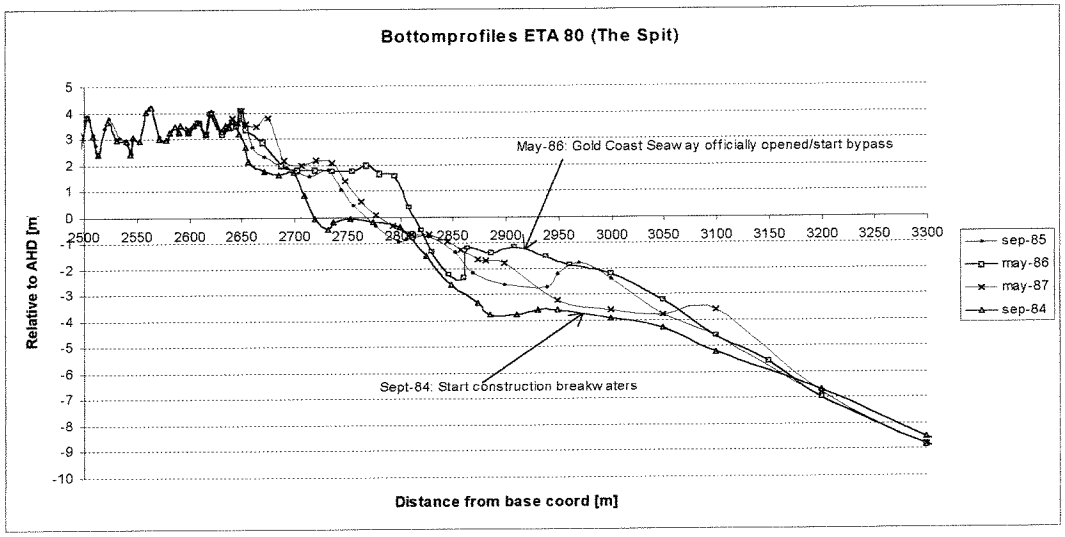

Figure 3.6: Cumulative volumes southern beaches versus bypass rates

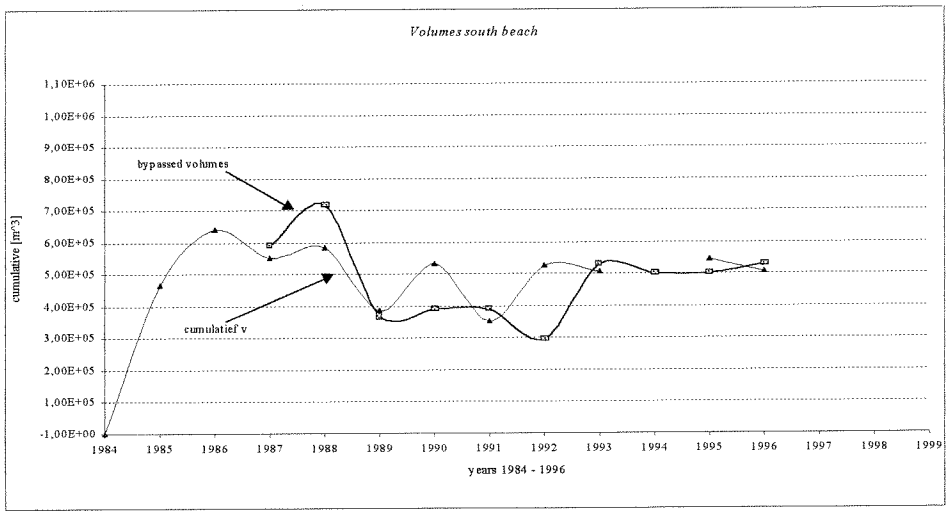

Figure 3.7 Cumulative volumes southern beaches deeper part

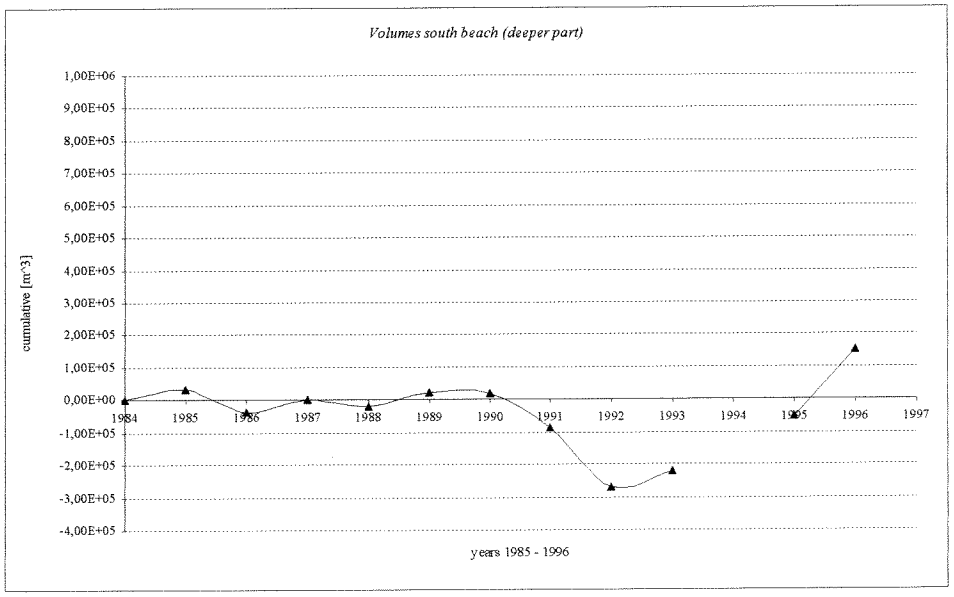

Sand accumulation below -10.0 m A.H.D. all occurred 1 kilometre or further south of the entrance. There was a loss of 6,000 m^3 below -10.0 m A.H.D. along the 1 kilometre section of the coastline immediately south of the entrance (Coughlan and Robinson, 1988).

The bypass quantities were measured monthly from the start in May 1986 until October 1997. The sand bypass system was designed to pump the amount of sand coincide with the net longshore transport rate (approximately 500,000 m^3/year) for the Gold Coast Seaway. As already described above, an accumulation of sand occurred during the first period of operation. This was the result of an unexpected time lag between the construction of the breakwaters and the start of the sand bypassing. Figure 3.5 shows the bathymetrical changes in the period during construction of the breakwaters. The difference between the bottom profiles at the start of the construction of the breakwaters in September 1984 and the officially opening of the Gold Coast Seaway in May 1986 shows that a large accumulation occurred during this period. The accumulation was mostly concentrated over approximately 350m (3200-2850 m relative to base coord) length along the ETA 80 bottom profile. The depth at a distance 2900m relative to base coord was reduced in this period from –3,8 m in September 1984 to –1,2m in May 1986.

In general the accumulation of sand during the period of construction caused a coastline change in the seaward direction. These changes resulted in shoaling in the vicinity of the southern jetty. According to Coughlan and Robinson (1988) a net accumulation of between 570,000 m^3 to 670,000 m^3 of sand occurred along two to three kilometres south of the Gold Coast Seaway beaches up to the end of March 1988. This accumulation affected the entrance and the part on the immediate seaward side of the southern jetty. Some leakage of sand occurred at the end of the southern jetty. This leakage of sand caused in the 1986 entrance survey that the depth on the immediate side of the southern jetty was reduced to -4.2 m A.H.D. which was less than the required -5.5 m A.H.D. minimum design depth for navigation. The latter illustrates that it is important to start bypassing directly from the start of the construction of the breakwaters.

The results of the bypass measurements, the cumulative volumetric changes and the assessed littoral drift are presented in the Appendix H. Table 10 shows the yearly bypassed volumes over the last ten years.

Table 10: Bypassed sand volumes

Year	Bypassed volumes [m3/year]
1987	590,000
1988	715,000
1989	370,000
1990	390,000
1991	390,000
1992	295,000
1993	530,000
1994	500,000
1995	500,000
1996	530,000

In the first year of operation approximately 590,000 m^3 was bypassed. In this same period a longshore transport rate between 270,000 m^3 and 300,000 m^3 was assessed (from the COPE data). As a result of this a reduction between 150,000 m^3 and 190,000 m^3 occurred south of the Seaway. The bottom profiles from May 1986 to November 1986 (Appendix I) show erosion as a result of the excessive bypass rates during the first period of bypassing. This erosion took

Figure 3.8. Major Meteorological events

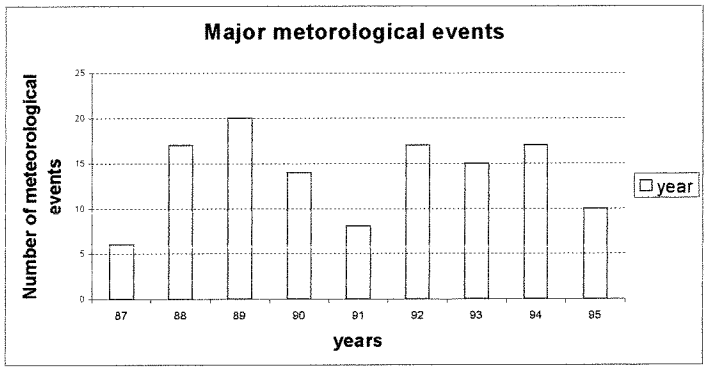

Figure 3.9 Bottom profiles Nerang River Entrance

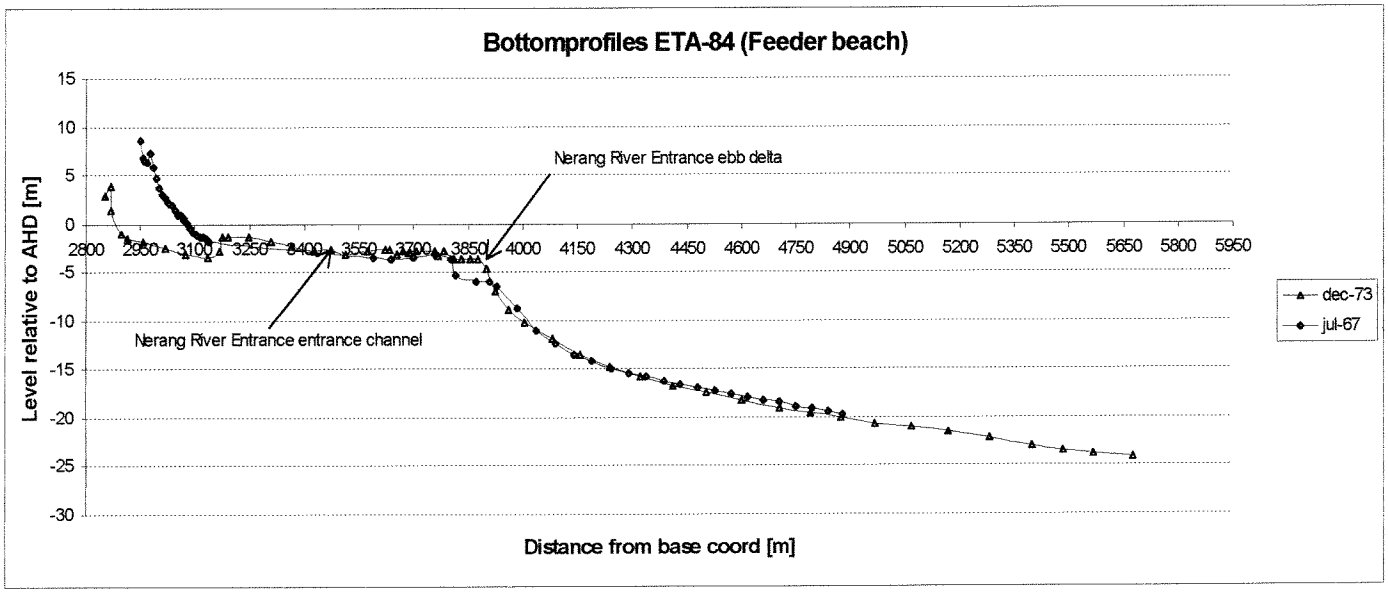

Figure 3.10 Bottom profiles Northern beaches (Feeder beach)

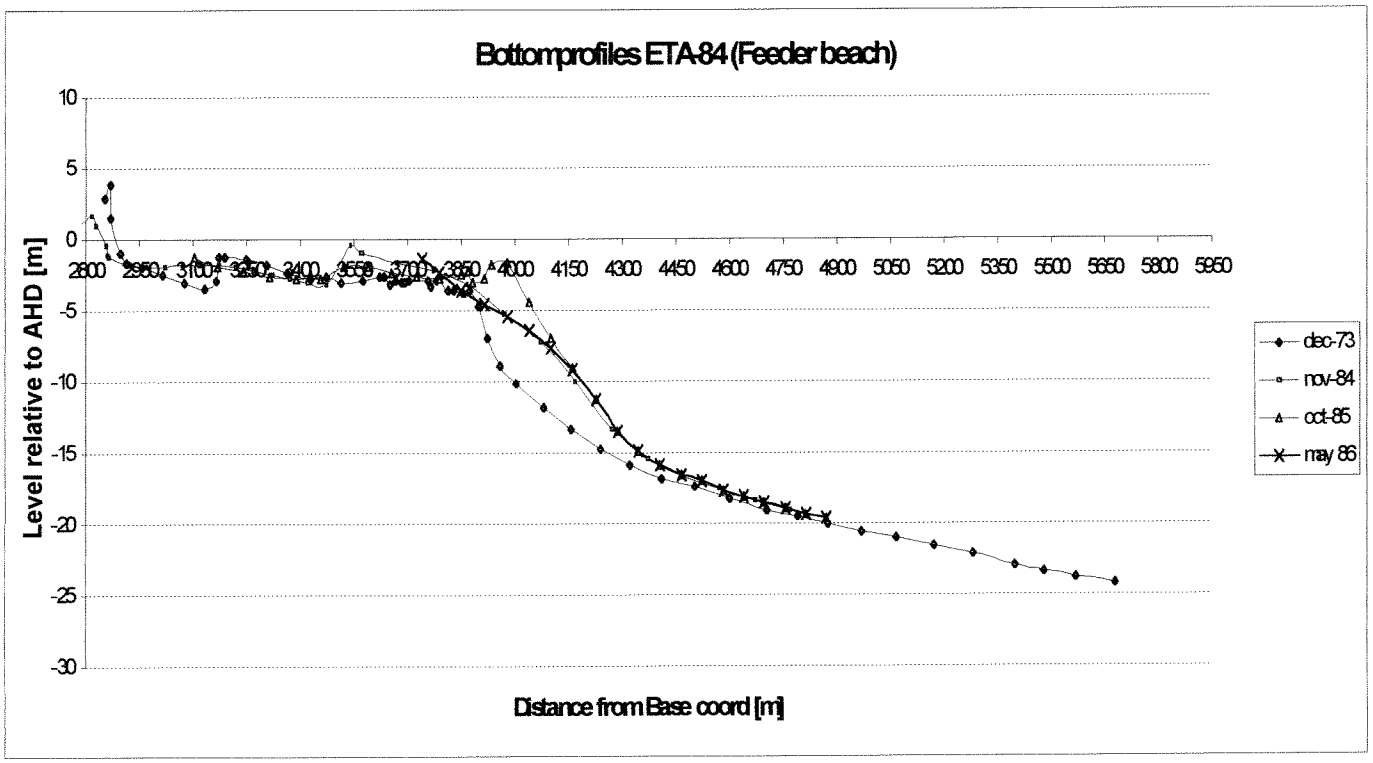

place in the same area as the accretion prior to training. The sand bypassing rates were continued in excess of the net annual longshore transport rate in order to reduce the accumulation on the south side of the Gold Coast Seaway to return the beaches back to the non-trained September 1984 condition.

The impact of the bypass rates on the sediment distribution along the ETA 80 sounding line prior to training and after the commencements of the works is illustated in Appendix I. For the period May 1987 to March 1988, a total of 460,000 m^3 of sand was bypassed compared with a net average longshore transport rate of 370,000 m^3. Bottom profiles ETA 80 shows the erosion during this period. The bottom profiles of September 1984 and March 1988 shows that the accretion during the first stages of construction was successfully reduced to the September 1984 condition. The bottom profiles ETA 80 from November 1988 to March 1991 show that no dramatic changes occur during this period. The profiles from March 1991 until November 1993 show the same tendency. The bottom profiles from November 1993 until December 1996 and the bottom profile from September 1984, prior to training, shows that the southern beaches have accreted with respect to the September 1984 situation, and it shows that they are in state of dynamic equilibrium.

Analysing the bottom profiles (ETA 80) for location The Spit and, comparing them with the Volumetric changes of the southern Gold Coast Seaway beaches (Appendix I), shows that the southern beaches have eroded and accreted in the period 1984 to 1989. In this period net erosion occurred of approximately 256,000 m^3 (464,600-390,000) as a result of the higher bypass rates during the first years after construction. After this erosion it appears that the southern beaches are more or less in dynamic equilibrium. Figure 3.6 illustrates clearly that after some time the volumetric changes follow bypass rates. From 1991 until 1996 the average bypassed sand is slightly higher than the 500,000 m^3/year which was the design bypass rate.

Figure 3.7 shows the cumulative volumetric changes in the deeper section of the southern beaches. This deeper section is located outside the zone were the southern breakwater extents. Looking at the volumetric changes, in the first years of operation, it shows that the deeper parts of the southern beaches do not change. However after some years from the start of the bypassing, erosion took place between 1989 and 1995. Looking at the bottom profile (ETA 80) from November 1988 until March 1991 and compare them to the bottom profiles from March 1991 until November 1993 shows that relative much differences occur in the deeper parts of the bottom profiles, from November 1988 until March 1989. These differences can be explained by looking at the major meteorological events that took place in that period. Figure 3.8 shows the major meteorological events over the last ten years. In the year 1989 twenty (!) major meteorological events took place. These events are probably the reason for the beach erosion of the deeper part of the southern beaches. After this erosion again accretion took place in order to re-establish the dynamic equilibrium.

3.2.4. Effects of the sand bypass installation on the northern beaches

The beaches at the northern side of the Gold Coast Seaway are also interesting to analyse. In this part of the beach the bypassed sand is transported back into the active system by the bypass installation. Therefore this part of the Gold Coast Seaway is called Feeder beach. Appendix K shows bottom profiles ETA 84. The ETA 84 sounding line is located at some distance from the northern breakwater. Appendix L shows the bottom profiles ETA 82.8, which are located just north of the northern breakwater. The bottom profiles from July 1967 and December 1973 (ETA 84) shows the old Nerang River Entrance ebb delta and entrance channel. The depth at the ebb delta and entrance channel varied between –1,3m A.H.D. inside the entrance channel and –3,6m A.H.D. at the outer edge of the ebb delta. It is obvious that these depths are dangerous for navigation. Figure 3.9 illustrates these bottom profiles from July 1967 and December 1973.

Figure 3.11: Bottom profiles ETA 82.8 Construction phase Gold Coast Seaway

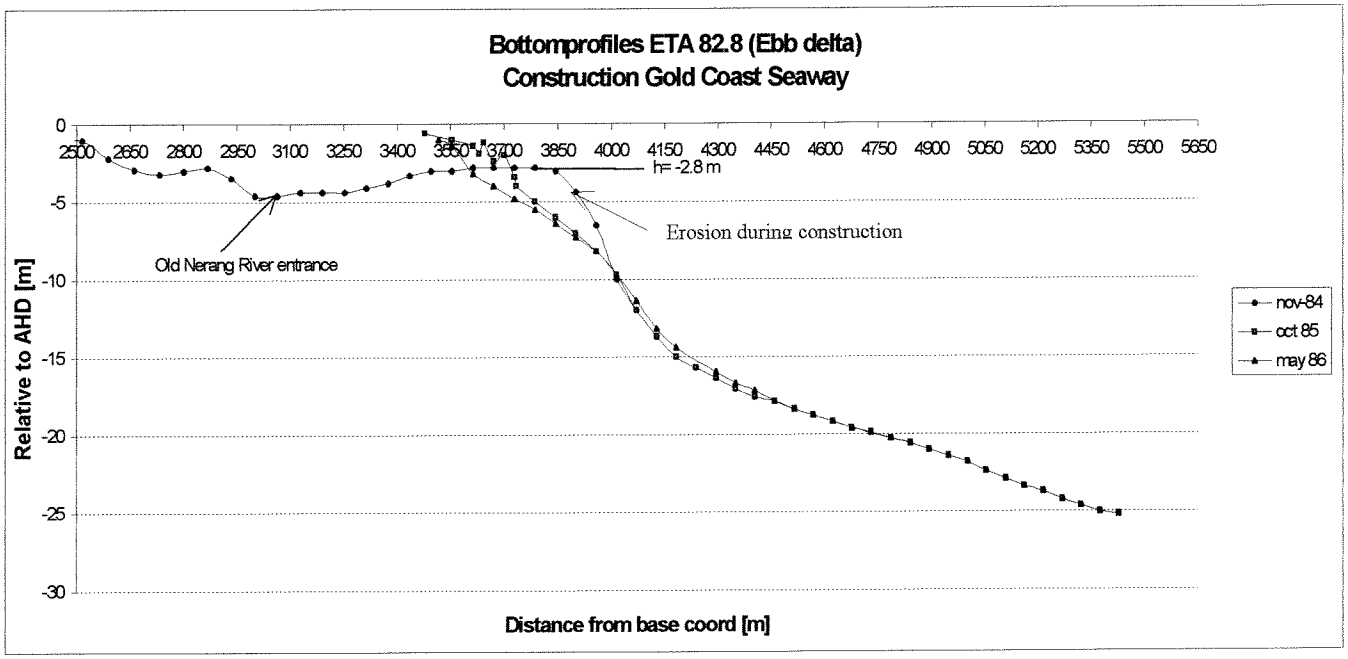

Figure 3.12: Aerial photographs prior and after stabilisation

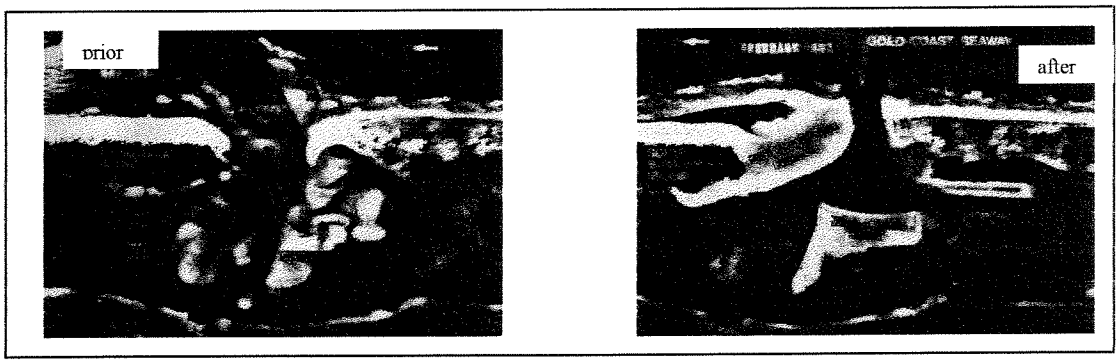

(From: Coughlan and Robinson, 1988)

Figure 3.13: Cumulative volumetric changes northern beaches (Feeder beach)

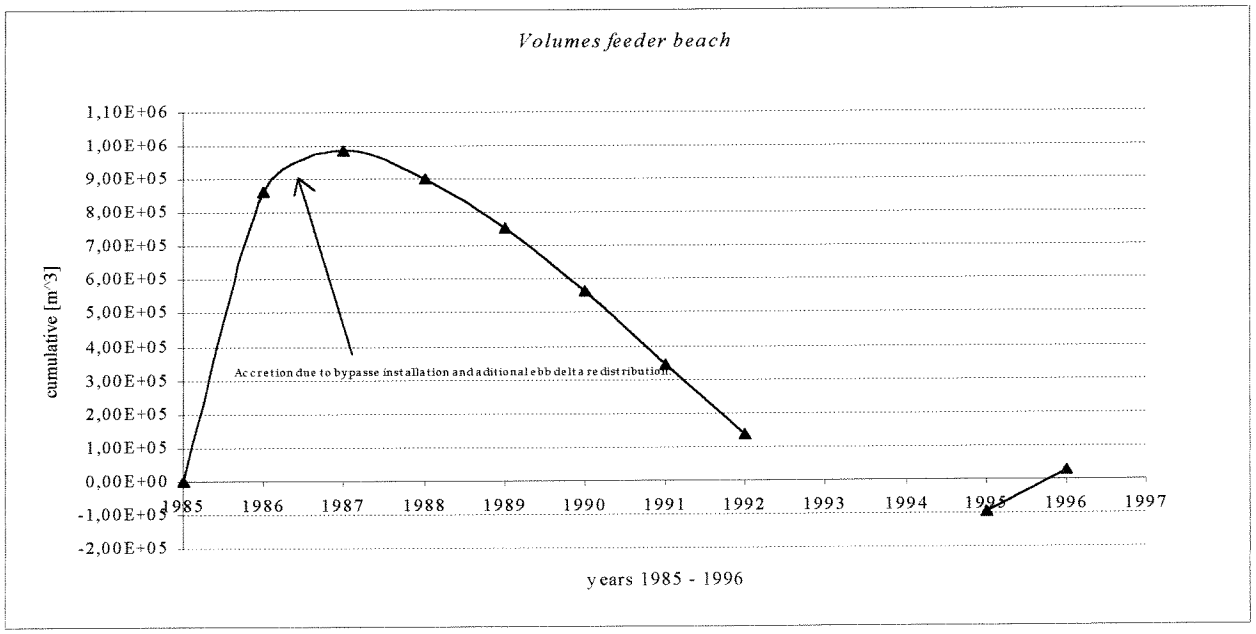

The new Gold Coast Seaway entrance was dredged through The Spit. During the construction of the training walls and the following year the old entrance remained open. The closure of this entrance was undertaken in November and December 1985. The construction of the training walls and the closure of the old entrance resulted in a lag of sand supply towards the northern beaches. As a result of this the part of the of the old Nerang ebb tidal delta just north of the northern breakwater eroded under the prevailing wave condition. This is clearly visible in Figures 3.11. Looking at the bottom profiles at some distance from the northern breakwater (Figure 3.10, ETA 84) it shows that in the same period accretion took place. So during the construction phase of the Gold Coast Seaway redistribution of sand from the old Nerang delta took place. This additional redistribution of sand from the old ebb tidal delta was sufficient to compensate the accretion of the southern beaches prior to the start of the bypassing system. (See also Figure 3.13)

Aerial photography of the Gold Coast Seaway showed, in Figure 3.12, the developments of the northern beaches after the construction of the training-walls and the start of sand bypassing. These photographs show that a new beach above mean sea level developed and a lagoon was formed between the new beach and the reclaimed area of the old Nerang River Entrance. Initially all bypassed sand was discharged directly into this lagoon area which was not part of the active longshore transport system. The lagoon has decreased in depth and size as a result of these sand discharges. However for a successful operation of the sand bypass system the sand has to be discharged into the active intertidal zone where it is transported northward in order to prevent erosion of the northern Stradbroke Island. A consequence of the sand discharges into the lagoon, instead of the intertidal zone, was erosion between 150,000 m^3 and 200,000 m^3 of the northern beaches in the period May 1986 until April 1988. The accretion in the first period after commencement of the works and the erosion due to sand discharges into the lagoon is clearly visible in Figure 3.13. Figure 3.14 shows the bottom profiles from 1986 until 1992. The erosion was concentrated above the –10 m A.H.D line. Below this line no significant changes occurred. Figure 3.15 shows the sand bypass into the lagoon (Bottom profiles: ETA 84).

3.2.5. Ebb tidal delta evolution of the Gold Coast Seaway

The ebb delta evolution from the start of the construction of the breakwaters until the year 1996 can be analysed by calculation of the volume changes over the past ten years. The sediment distribution can be studied by the bottom profile ETA 82.8. The ETA line 82.8 is located at the old Nerang River Entrance on the north side of the Gold Coast Seaway (South Stradbroke Island). The ETA 82.8 lines from November 1984 until December 1996 are presented in Appendix L. The new Gold Coast Seaway ebb tidal delta has an asymmetrical shape with respect to the orientation of the Seaway entrance. This asymmetrical shape of the ebb tidal delta also appeared in the model tests (Figure 2.7 and 2.10). The outer edge of the ebb tidal delta is therefore slightly shifted to the north and located on this line. Figure 3.11 shows a cross-section of the old Nerang River entrance and ebb tidal delta in November 1984 just before the start of the construction of the breakwaters. In November 1984 the old Nerang River ebb tidal delta extends approximately 3850m seaward (relative to base coord.) The minimum water depth at that point is approximately –2.8 m. The old entrance channel of the Nerang River Entrance is also clearly present. The old entrance shows a variation in depths along the ETA 82.8 line. The bottom profiles along the cross section of the old Entrance shows that the depth varies between –2.8 m at the outer edge of the ebb tidal delta to approximately –4.6 m inside the entrance channel. As pointed out before, accretion on the southern beaches of the Seaway took place in the first stages of construction from November 1984 to May 1986. As a result of this accretion, the old ebb tidal delta eroded.

The new Gold Coast Seaway with bypass installation opened in May 1986. Bottom profiles from May 1986 until December 1986 clearly shows a ebb delta is formed and grows in seaward direction. The new ebb delta grows in a period from August 1986 to December 1986

Figure 3.14 Erosion of the Feeder beach from 1986 until 1992

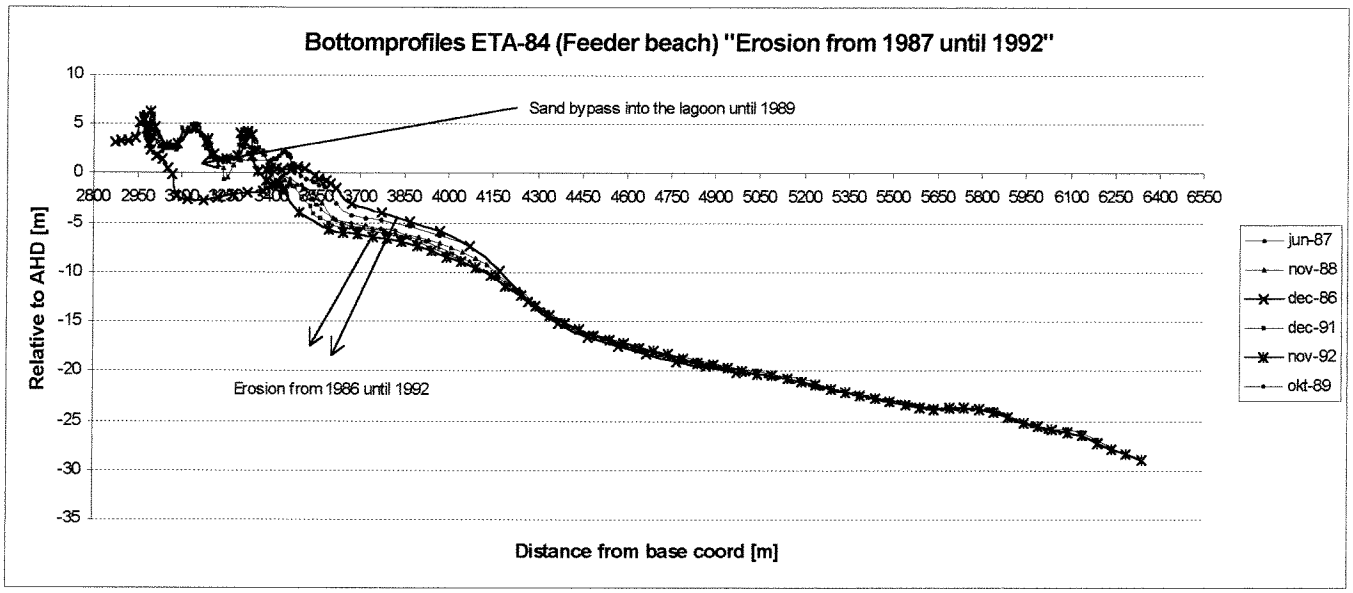

Figure 3.15: Sand Bypass in the lagoon (ETA 84)

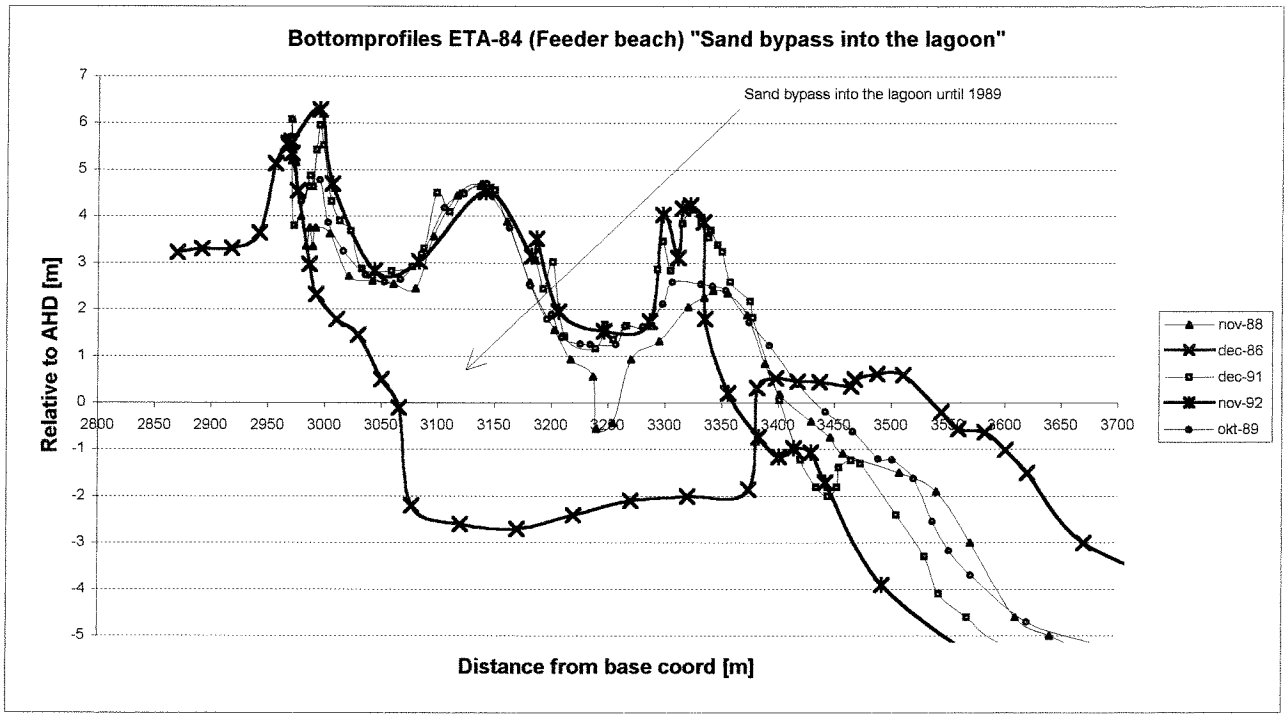

approximately 130 m in seaward direction. The depth at the outer edge of the ebb delta was approximately –4.2 m A.H.D. in August 1986 and increased to –4.6 m A.H.D. in December 1986. At the outer edge of the ebb delta the depth drops steeply from –4.4 m to –12.6 m A.H.D. with a slope 1:14.

The bottom profiles from December 1986 to March 1988 show clearly an offshore sand bar is created in front of the entrance and this new ebb delta continues to move in seaward direction. In this period the ebb delta has moved approximately 150m seaward. The ebb delta has become deeper with a level change from -4.4 m A.H.D. in December 1986 to -6.0 m A.H.D. March 1988. From March 1988 to November 1992 the delta had moved some 260m further seawards with an increase depth from –6.1 m A.H.D. in March 1988 to –6.8 m in November 1992.

Figure 3.16 illustrates the increase of the ebb delta length over the past ten years. This figure shows that the ebb delta moved approximately 600 m in seaward direction over the first ten years of operation. Looking at Figure 3.16 it may be concluded that not much increase in length is expected in the future. Figure 1.17 shows the minimum depth (at the outer edge of the ebb tidal delta) over the last ten years. From this figure it is clear that the minimum depth increased from –4.2 in August 1986 to –7.4m in July 1996, witch is below the minimum –5.5 m A.H.D. required depth for navigation.

Looking at the depth variation along the rest of the ETA 82.8 line (Appendix N) from 3400m to 4300m, relative to base coord, shows that during the first years of operation, the depth varies significant. This variety continues until 1988. The lines from October 1989 until December 1996 show not much variety. However the ebb delta still grows in this period. Below the line –20m A.H.D. no significant changes occurred over the last ten years.

The volumetric growth of the ebb tidal delta (section III) is calculated with the Delft-quickin program. The calculations shows a sand accumulation of 657,000 m^3 in the period August 86 - May 87. This accumulation agrees rather well with the 650,000 m^3 determined by Coughlan and Robinson (1988). The same procedure was used to calculate the ebb delta evolution from 1986 until 1997. Table 11 gives the results of the ebb delta calculations.

Table 11: Volumetric growth ebb delta

Year	Volumetric growth [m^3]
1985	0
1986	945,000
1987	657,000
1988	335,000
1989	315,100
1990	380,000
1991	252,000
1992	153,000
1993	No data available
1994	No data available
1995	470,400
1996	-76,440
1997	13,390

From the calculations can be concluded that the ebb delta is still growing. In order to get an estimate on the longterm equilibrium of the ebb delta the following linear differential equation can be used to calculate the equilibrium ebb delta volume:

Figure 3.16: Cumulative ebb delta growth

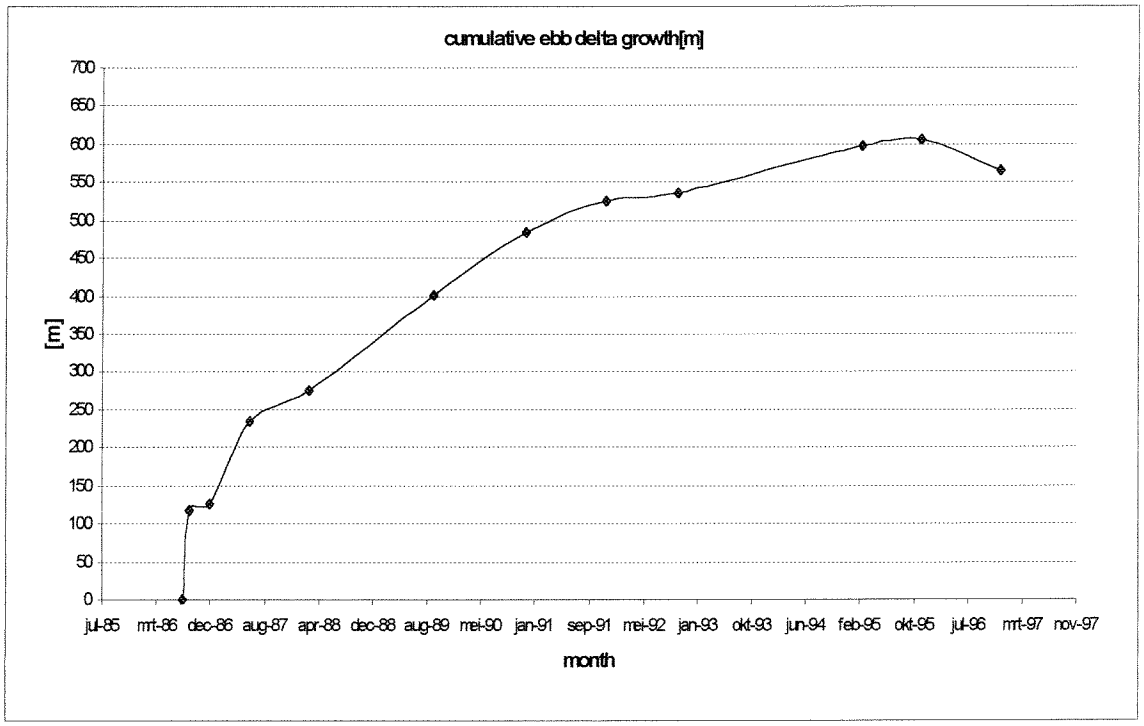

Figure 3.17: Depth edge ebb tidal delta

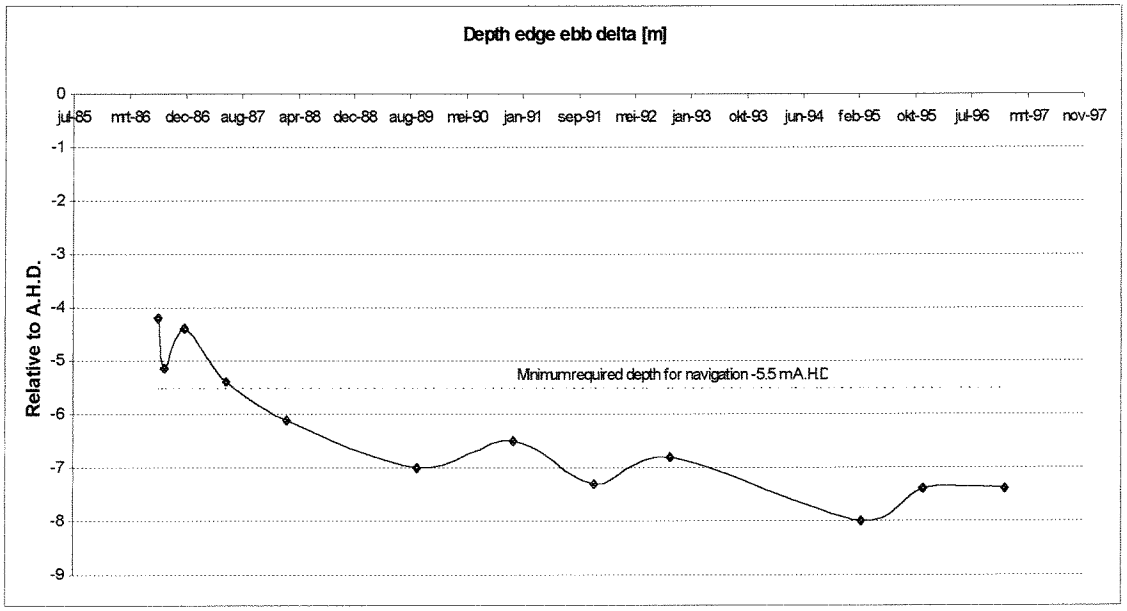

$$\frac{\partial S}{\partial t} = -\tau \cdot (S - S_e) \Leftrightarrow \frac{\partial S}{S - S_e} = \frac{dt}{-\tau} \Leftrightarrow \partial \ln(S - S_e) = \frac{dt}{-\tau} \Leftrightarrow \ln(S - S_e) = -\frac{t}{\tau} + C \Leftrightarrow \quad S - S_e = C \cdot e^{\frac{-t}{\tau}}$$

For $t = 0 \Leftrightarrow S = 0 \Leftrightarrow C = -S_e \Leftrightarrow S = S_e \cdot \left(1 - e^{\frac{-t}{\tau}}\right)$

In which:

$\tau = \frac{\partial V(t=0)}{\partial S(t=0)}$: The τ-value can be regarded, as the time required obtaining the new equilibrium situation in case the initial adjustments remain constant in time.

$\partial V(t=0)$ = new longterm equilibrium situation.
$\partial S(t=0)$ = initial sedimentation
$\partial S(t)$ = annual morphological response after time t.
$S(t=0)$ = initial morphological response
$S(t)$ = total morphological response after time t

This function of the Gold Coast Seaway ebb delta evolution is determined by trial and error in order to fit within the calculated ebb delta evolution. The exponential function for the equilibrium ebb delta volume then becomes:

$$S(t) = S(t=0) + 3.65 \cdot 10^6 \cdot \left(1 - e^{\left(\frac{-t}{3.8}\right)}\right)$$

in which: $S(t=0)$ → Ebb delta volume in the year 1986 (initial ebb delta volume)
t = Time in years. (t=0 = 1986)

The long term equilibrium ebb delta growth can now be calculated as follows:

$$S(t=\infty) = 3.65 \cdot 10^6 \cdot \left(1 - e^{\left(\frac{-t_{end}}{3.8}\right)}\right)$$

in which: t_{eind} = Required time to reach the equilibrium ebb delta volume [years].

Figure 3.18 shows that the exponential decay function is almost horizontal after 20 years measured relative from the opening of the Gold Coast Seaway in the year 1986, which means that an equilibrium condition is reached in the year 2005. The equilibrium ebb delta growth then becomes:

$$\Delta S(t_{end}) = 4 \cdot 10^6 m^3$$

3.2.6. Changes of the entrance channel cross-sectional area

The new entrance channel was dredged through The Spit. The minimum navigational channel depth was -5.5 m A.H.D. The dredging of the entrance channel was undertaken to -6.0 m A.H.D. Surveys indicated that the entrance channel adopted a asymmetrical cross-section with scouring along the southern breakwater to -13.0 m A.H.D. and shoaling along the northern breakwater to -3.5 m A.H.D. Model tests show the same tendency. Figure 3.6 illustrated the development of the cross-sectional area with sand bypass.

Figure 3.18: Ebb delta decay function

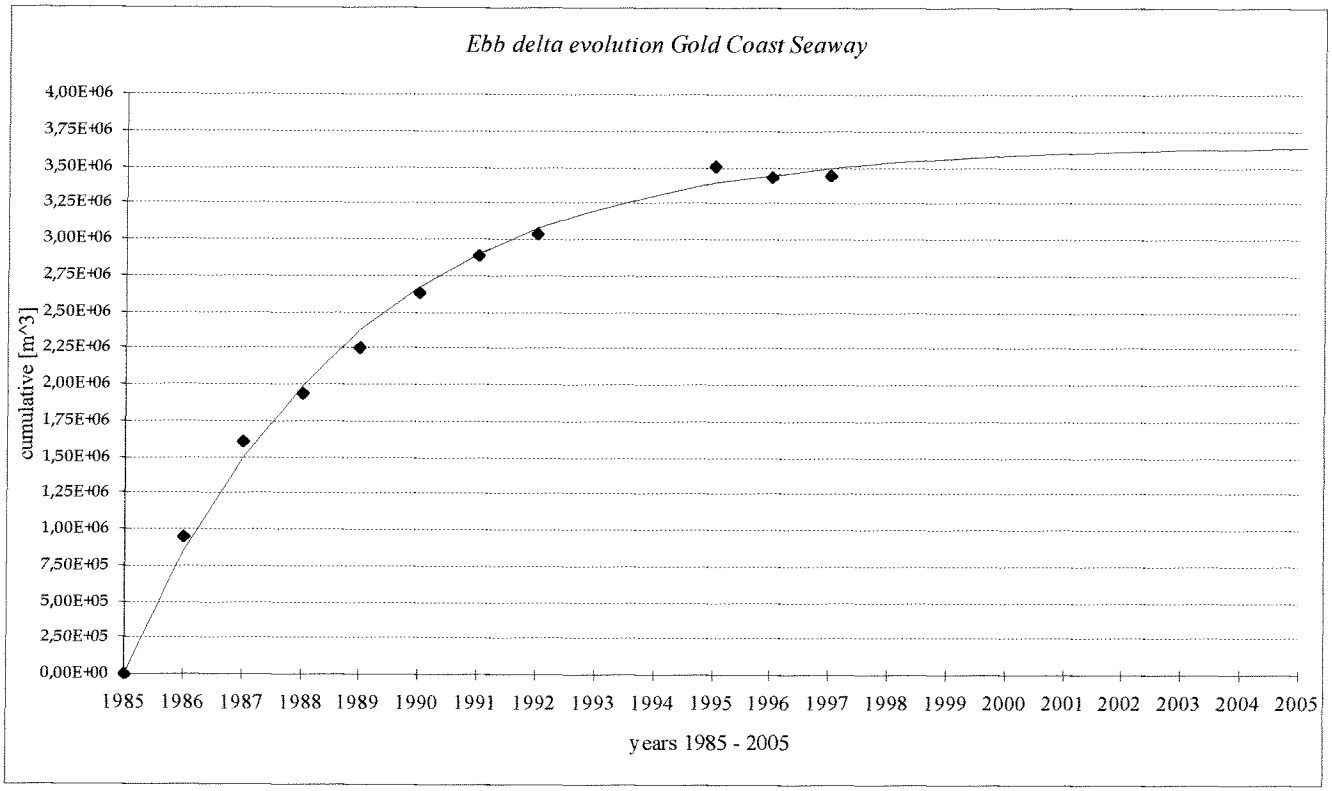

Surveys showed that the entrance depth increased over its entire length in the period May 1986 until April 1988 with a significant scouring along the southern breakwater.
Since the opening of the Gold Coast Seaway in May 1986, there have been two occasion where shoaling above design depth occurred in the seaward part of the entrance. In September 1986, and April 1988 as a result of a series of storms some leakage of sand passing the jetty occurred. However the Gold Coast Seaway project provided a safe navigation for recreational crafts without much adverse effects on the adjacent coastline.

4. Conclusions

Looking at the ebb delta evolution and the effects of the bypass installation on the development of the southern and northern beaches of the Gold Coast Seaway the following can be concluded.

The sand bypass installation combined with the training works had a positive effect on the morphological behaviour of the Gold Coast Seaway. Prior to training the Nerang River Entrance was very unstable which was dangerous for navigation. However not much data was available on the entrance channel itself but it is clear that the cross-sectional area increased after the stabilisation of the Nerang River Entrance. Only at a limited number of times and after severe weather conditions some deposition of sand occurred at the tip of the southern breakwater. This caused a local and temporarily excedance of the minimum required depth for navigation. The increase of the Seaway cross-sectional area was a direct result of the construction of the jetties but also as a result of the bypass of sand across the entrance. The strong decrease in littoral drift through the entrance channel probably caused a strong increase of the cross-sectional area. The increase of the inlets cross-sectional area probably continuos until the inlet currents are lower then the threshold of particle motion.

The bypass installation prevented massive accretion of the southern beaches and also severe erosion of the northern beaches. The increase of ebb delta volume over the last ten years was not dangerous for navigation. The ebb delta until now still grows but will be in dynamic equilibrium after 20 years of operation. During this time the minimum depth over the ebb delta increases slowly, probably over the same amount of time as the ebb delta needs to reach its dynamic equilibrium.

In general it can be concluded that the stabilisation of the Nerang River Entrance with jetties and a mechanical bypass installation was successfully.

5. Recommendations

Because of the limited information available of the Gold Coast Seaway entrance channel it was not possible to get a clear picture of the morphological changes of the entrance channel over the first ten years after the commencement of the bypass installation. The entrance channel probably plays an important role in the sediment supply towards the ebb delta. There was sufficient information available for the sections just north and south of the Gold Coast Seaway. But to get a clear picture of the sand distribution of the Gold Coast Seaway morphological system more monitoring is needed which extend further to the south and to the north of the Gold Coast Seaway.

This case study needs further investigation. With the data presented in this report and the theory described in Volume I another graduate student is able to get quickly insight in the most important processes at work. Not only in this particular case but also for tidal inlets in general. In order to get a better understanding of the morphological changes due to the bypass installation a model should be made to simulate the Gold Coast Seaway system. This can be done with the use of the program DELFT3D-MOR from Delft Hydraulics.

References (Volume I and II)

Aubrey , David G. , Weishar, Lee (Editors) , 1988, Hydrodynamics and sediment Dynamics of Tidal Inlets
Section: "Shoreline erosional-depositional processes associated with tidal inlets"
Springer-Verlag, New York, USA

Beach Protection Authority Queensland, Australia
Nerang River Entrance Stabilization, 1986

Bruun, Per , 1978
Stability of tidal inlets (Theory and Engineering)
Development in geotechnical engineering; volume 23
Elsevier scientific publishing company, Amsterdam -The Netherlands.

Bruun, Per , 1978, Gerritsen, F. , 1960
Stability of Coastal inlets
Coastal Engineering Laboratory, University of Florida, Gainsville
North-Holland Publishing Company, Amsterdam -The Netherlands.

Coughlan, P.M. ; Robinson, D.A. ; 1988
Gold Coast Seaway-Its impact on the Adjacent Coast
Second Australian Port, Harbour and Offshore Engineering Conference 1988
Brisbane, 25-27 October 1988.
Brisbane Australia.

Delft Hydraulics Laboratory, 1970.
Gold Coast, Queensland, Australia
Coastal erosion and related problems
Volume I ; Conclusions and recommendations, I - R 257 (I)
Delft; The Netherlands.

Delft Hydraulics Laboratory, 1970.
Gold Coast, Queensland, Australia
Coastal erosion and related problems
Volume II , part I, Investigations (Text and Tables) , I - R 257 (IIa)
Delft; The Netherlands.

Delft Hydraulics Laboratory, 1970.
Gold Coast, Queensland, Australia
Coastal erosion and related problems
Volume II , part II, Investigations (Figures) , I - R 257 (IIb)
Delft; The Netherlands.

Delft Hydraulics Laboratory, 1976.
Nerang River Entrance Stabilization
Report on model investigations ; M 1259
Delft; The Netherlands.

Delft Hydraulics Laboratory, 1992.
Gold Coast, Queensland, Australia
Southern Gold Coast littoral sand supply
Final Report, Volume II
Delft; The Netherlands.

Department of Harbours and Marine and the Gold Coast Waterways Authority, Australia
Water level monitoring report the Broadwater/Nerang River Entrance 1987
Tide section, Department of Harbours & Marine August 1987

Di Lorenzo, J.L., 1988
The overtide and filtering Responce of Small Inlet Bay Systems
Aubrey, D.G. and Weishar, L. , 1988; pp 24 - 53

Dombrowski, Michael R. , Mehta, Ashish J. , 1996
Ebb delta evolution of coastal inlets
Coastal Engineering 1996 Volume 3 ; chapter 253 (Edited by Billy L. Edge)
Proceedings of the twenty-fifth international conference ; American Society of Civil Engineering - New York

Drapeau, Georges, 1988
University of Quebec, Canada
Lecture notes on Coastal and Estuarine Studies, Volume 29.

Escoffier, Francis F. , 1940
United States Engineer Office. Mobile, Alabama
Stability of Tidal Inlets
Shore and Beach, October 1940 pag.114-115

FitzGerald, Duncan M. , 1988
Department of Geology, Boston University
Lecture notes on Coastal and Estuarine Studies, Volume 29.

Huis in `t Veld, J.C. ; Stuip, J. ; Walther, A.W. ; van Westen, J.M. , 1987
The Closure of Tidal Basins; part: Environmental Conditions; D. Smith
Delft University Press, Delft - The Netherlands.

Jonsson, I.G., 1978
Stability of tidal inlets (Theory and Engineering); part: Combinations of waves and currents
Development in geotechnical engineering; volume 23
Elsevier scientific publishing company, Amsterdam -The Netherlands.

Karssen, B and Wang, Z.B. , 1991
Morphological modelling in estuaries and tidal inlets
Part: I A literature survey Z473
Delft Hydraulic Laboratory ; Delft - The Netherlands

Kana and Mason, 1988
Department of Geology, Boston University
Lecture notes on Coastal and Estuarine Studies, Volume 29.

King, D.B. (1974)
The dynamics of inlets and bays
Tech. Rep. 2, Coast. and Ocean. Eng. Lab. ; University of Florida

Keulegan, G., 1950
Tidal flow in entrances. Water level fluctuations of basins in communication with seas.
Techn. Bull. Nr. 4 , Committee on tidal hydraulics, USCE, Waterways Experiment Station, Vicksburg, Miss.

Kreeke, J. van de , 1990
Stability analysis of a two-inlet bay system
Coastal Engineering Nr. 14 pp 481-497
University of Miami

Loo, van L.E. , 1976
Coastal Engineering Vol. I Introduction ; part Coastal Formations
Faculty of Civil Engineering , Delft University of Technology ; Delft - The Netherlands

Matsunaga, N.; Hashida, M. ; Kawakami, H. , 1996
Wind Induced Waves and Currents in a Nearshore Zone
Coastal Engineering 1996 Volume 3 ; chapter 260 (Edited by Billy L. Edge)
Proceedings of the twenty-fifth international conference ; American Society of Civil Engineering - New York

Manual on the use of Rock in Hydraulic Engineering, CUR Report 169, 1994
Centre of Civil Engineering Research and Codes; Rijkswaterstaat/ Department of Public Works
Gouda - The Netherlands.

Marino, James N., (Coastal Engineering Research Centre) and Mehta, Ashish J. (Coastal and Oceanographic Engineering Department, University of Florida), 1988
Lecture notes on Coastal and Estuarine Studies, Volume 29.

Mehta, A.J. and Özsoy , 1978
Stability of tidal inlets (Theory and Engineering), Per Bruun, Chapter 3 , Inlet Hydraulics
Development in geotechnical engineering; volume 23
Elsevier scientific publishing company, Amsterdam -The Netherlands.

Niemeyer, H.D. , 1990
CM5 Morphodynamics of Tidal Inlets
Course: Coastal morphology; Stichting Postak. Onderwijs Civiele Techniek en bouwtechniek, Delft

Nortier, I.W., 1989
Toegepaste vloeistof mechanica. hydraulica voor waterbouwkundigen
Educaboek BV, Culemborg - The Netherlands.

O`Brian, M.P. 1969
Equilibrium Flow areas of inlets on sandy coasts
Journal of the waterways and harbours Div. , ASCE, Nr. WWI; pp 43 - 52

O`Brian, M.P. and Dean, R.G. , 1972
Hydraulics and sedimentary stability of coastal inlets
Proc. 13th. Coastal Engineering Conf., ASCE, New York; pp 761-780

Oertel, G.F., 1975
Ebb tidal deltas o9f Georgia estuaries
Cronin, L.E.

Oertel, G.F., 1988
Processes of Sediment Exchange Between Tidal Inlets, Ebb deltas and Barrier Islands
Aubrey, D.G. and Weishar, L.

Sha, L.P., 1990
Sedimentological studies of the ebb tidal deltas along the West Frisian islands, The Netherlands

Ph.D. thesis; publication nr. 64, Geologica Ultraiectina, University of Utrecht, Utrecht, the Netherlands

Shore Protection Manual, Volume I and II (Second Printing, Fourth Edition), 1984
Coastal Engineering Research Centre
US Army Corps of Engineers, Washington DC - USA.

Silvester, Richard , Hsu, John R.C. , 1993
Coastal Stabilization Innovative Concepts
Department of Civil and Environmental Engineering , The University of Western Australia
New Jersey USA.

Steijn, R.C. , 1991
Some considerations on tidal inlets; Literature Survey H 840.45
Delft Hydraulics ; Delft - The Netherlands

Technische Adviescommissie voor de Waterkeringen, 1995
Basisrapport Zandige Kust (Behorend bij de Leidraad Zandige Kust)

Velden, E.T.J.M. van der; 1995
Coastal Engineering
Faculty of Civil Engineering , Delft University of Technology
Delft - The Netherlands

Wang, Xu , Lin, Lihwa , Wang , Hsiang, 1996
Laboratory Mobile Bed Studies on Ebb Tidal Shoal Evolution
Coastal Engineering 1996 Volume 3 ; chapter 255 (Edited by Billy L. Edge)
Proceedings of the twenty-fifth international conference
American Society of Civil Engineering - New York

Appendix A

(Directional wave climate at the 10 m depth contour)

(Number of pages: 2)

Representative Offshore H_s-Values

T_p (s) dirn. (deg)	2.00	4.00	6.00	8.00	10.00	12.00	14.00
15.00	0.00	0.92	1.30	1.31	1.25	1.24	0.00
45.00	0.00	1.18	1.26	1.40	1.40	1.03	0.00
75.00	0.00	1.09	1.41	1.66	2.42	1.79	0.00
105.00	0.00	1.07	1.63	1.03	2.51	2.30	1.75
135.00	0.00	1.05	1.51	1.10	2.00	2.09	1.67
165.00	0.25	1.10	1.58	1.78	1.76	1.85	2.79

No. of Days Per Year

T_p (s) dirn. (deg)	2.00	4.00	6.00	8.00	10.00	12.00	14.00
15.00	0.00	4.84	11.32	17.48	14.04	4.22	0.00
45.00	0.00	0.60	2.11	8.63	7.91	1.31	0.00
75.00	0.00	0.30	2.93	18.10	9.17	0.58	0.00
105.00	0.00	0.26	5.38	27.86	18.34	7.75	0.15
135.00	0.00	0.56	7.91	32.65	22.14	4.97	0.25
165.00	0.11	1.74	10.24	36.04	50.15	11.18	0.56
All	0.11	8.30	39.89	140.76	121.75	30.01	0.96

Refracted Directions (Unibest Definition) For Coast Orientation 0.00 Degrees

T_p (s) dirn. (deg)	2.00	4.00	6.00	8.00	10.00	12.00	14.00
15.00			-55.50	-39.00	-34.00	-29.00	
45.00			-38.00	-31.00	-25.00	-21.00	
75.00			-13.20	-11.00	-9.30	-7.60	
105.00			12.80	10.50	8.40	6.60	
135.00			37.50	30.10	24.10	20.20	
165.00			50.00	40.00	30.80	27.60	

Refracted H_s-Values Plus Correction with Factor 0.88

T_p (s) dirn. (deg)	2.00	4.00	6.00	8.00	10.00	12.00	14.00
15.00	0.00	0.00	0.69	0.65	0.61	0.61	0.00
45.00	0.00	0.00	0.94	1.09	1.10	0.84	0.00
75.00	0.00	0.00	1.16	1.32	2.13	1.65	0.00
105.00	0.00	0.00	1.29	1.73	2.22	2.14	0.00
135.00	0.00	0.00	1.16	1.63	1.55	1.75	0.00
165.00	0.00	0.00	0.14	0.31	0.48	0.78	0.00

Directional Wave Climate at 10 m Depth Contour - The Spit (Based on British Meteorological Office Directions and Brisbane Waverider Buoy)

Refraction Coefficients

T_p (s) dirn. (deg)	2.00	4.00	6.00	8.00	10.00	12.00	14.00
15.00			0.87	0.85	0.93	0.95	
45.00			0.91	0.94	1.00	1.23	
75.00			0.90	0.92	0.97	1.07	
105.00			0.72	0.74	0.76	0.78	
135.00			0.15	0.30	0.40	0.48	
165.00		0.00	0.00	0.00	0.15	0.20	

Refracted Directions

T_p (s) dirn. (deg)	2.00	4.00	6.00	8.00	10.00	12.00	14.00
15.00			20.60	28.00	30.00	33.00	
45.00			46.10	48.10	48.00	48.00	
75.00			72.40	69.60	67.90	64.00	
105.00			95.00	87.60	81.60	78.50	
135.00			100.00	92.80	87.80	83.50	
165.00					89.40	82.90	

Table 3.5.1 Refraction Coefficients and Refracted Directions for 10 m line - Tugun

Refraction Coefficients

T_p (s) dirn. (deg)	2.00	4.00	6.00	8.00	10.00	12.00	14.00
15.00			0.60	0.56	0.56	0.56	
45.00			0.85	0.89	0.89	0.92	
75.00			0.93	0.90	1.00	1.05	
105.00			0.90	0.97	1.00	1.06	
135.00			0.87	0.88	0.88	0.95	
165.00		0.00	0.10	0.20	0.31	0.48	

Refracted Directions

T_p (s) dirn. (deg)	2.00	4.00	6.00	8.00	10.00	12.00	14.00
15.00			34.50	51.00	56.00	61.00	
45.00			52.00	59.00	65.00	69.00	
75.00			76.80	79.00	80.70	82.40	
105.00			102.80	100.50	98.40	96.60	
135.00			127.50	120.10	114.10	110.20	
65.00			140.00	130.00	120.80	117.60	

Refraction Coefficients and Refracted Directions for 10 m line - The Spit

Appendix B

(Tidal planes and average time differences, Nerang River Entrance and Gold Coast Seaway)

(Number of pages: 2)

Place	Date	M.H.W.L. m A.H.D.	M.L.W.L. m A.H.D.	M.Ra m	L.W.L. m A.H.D.
Grand Hotel Jetty	Dec 1967	+0.45	-0.15	0.60	N.A.
	Apr 1970	+0.54	-0.21	0.75	-0.48
	Apr 1973	+0.56	-0.19	0.75	N.A.
	Sept 1974	+0.50	-0.27	0.77	-0.44
	Jun 1978	+0.52	-0.09	0.61	-0.43
	Aug 1983	+0.33	-0.34	0.67	-0.52
	Apr 1985	+0.34	-0.15	0.49	-0.23
	Apr 1986	+0.53	-0.34	0.87	-0.55
	Mar 1987	+0.49	-0.41	0.90	-0.74
Proud Park (Jubilee Br.)	Sept 1974	+0.51	-0.28	0.79	-0.34
	Apr 1985	+0.32	-0.15	0.47	-0.18
	Apr 1986	+0.54	-0.33	0.87	-0.53
	Mar 1987	+0.48	-0.43	0.91	-0.75
Inga Ave (Near Cronin Is)	Sept 1974	+0.47	-0.22	0.69	-0.22
	Apr 1985	+0.35	-0.07	0.42	-0.10
	Apr 1986	+0.50	-0.26	0.76	-0.42
	Mar 1987	+0.45	-0.31	0.76	-0.64
Nerang Township	Sept 1974	+0.55	-0.15	0.70	-0.22
	Apr 1985	N.A.	N.A.	N.A.	N.A.
	Apr 1986	+0.60	-0.22	0.82	-0.31
	Mar 1987	+0.53	-0.27	0.80	-0.54
Runaway Bay	Jan 1979	+0.48	-0.21	0.69	-0.40
	Apr 1985	+0.44	-0.18	0.62	-0.35
	Apr 1986	+0.54	-0.30	0.84	-0.53
	Mar 1987	+0.46	-0.41	0.87	-0.68
Paradise Point	Aug 1983	+0.33	-0.37	0.70	-0.60
	Apr 1985	+0.41	-0.29	0.70	-0.46
	Apr 1986	+0.58	-0.33	0.91	-0.52
	Mar 1987	+0.44	-0.41	0.85	-0.64
Snapper Rocks		0.51	-0.52	1.03	-0.78

Table 1 - Mean Tidal Planes for Selected Dates

Place	Date	Average Time Difference	
		High Water H.M.	Low Water H.M.
Grand Hotel Jetty	Sept 1974	-0 15	+0 35
	Aug 1983	-0 03	+0 29
	Apr 1985	+0 16	+0 34
	Apr 1986	-0 41	-0 28
	Mar 1987	-0 41	-0 41
Proud Park (Jubilee Br)	Sept 1974	-0 00	+1 00
	Apr 1985	+0 33	+1 05
	Apr 1986	-0 41	-0 28
	Mar 1987	-0 47	-0 41
Inga Ave (Near Cronin Is)	Sept 1974	+0 30	+1 15
	Apr 1985	+1 05	+1 34
	Apr 1986	-0 07	+0 09
	Mar 1987	-0 24	-0 10
Nerang Township	Sept 1974	+1 20	+2 20
	Apr 1985	+1 55	+2 38
	Apr 1986	+1 00	+1 30
	Mar 1987	+0 49	+1 18
Runaway Bay	Jan 1979	-0 15	+0 05
	Apr 1985	+0 08	+0 28
	Apr 1986	-0 07	+0 03
	Mar 1987	-0 27	-0 22
Paradise Point	Aug 1983	+0 20	+0 37
	Apr 1985	+0 23	+0 34
	Apr 1986	+0 10	+0 18
	Mar 1987	+0 03	+0 10
Snapper Rock (Ocean Tides)	- -	-1 25	-1 31

Base Time is the Observed Time of High and Low Water at the Brisbane Bar.

Table 2 - Average Time Differences for Selected Dates

Appendix C

(Inlet calculations)

(Number of pages: 2)

Tidal inlet computations

The formulas used in these computations are decribed and presented in section 2.2.2.3 of Volume I

Input

Tidal prism	P=	2,25E+07	m^3/half tidal cycle
Basin area	A_b =	2,65E+07	m^2
Cross-sectional area	A_c =	1000	m^2
Lenght inlet channel	L =	800	m
Tidal amplitude	η_0 =	0,5	m
Darcy-Weisb. coeff.	f =	0,0388	[-]
$K_{en}+K_{ex}$	m =	1,05	[-]
gravitational acceleration	g =	9,81	m/s^2
T_{tide}	T =	12,4	hrs
water depth	R =	4,16	m
Chezy	C =	45	$m^{1/2}/s$
water density	ρ_w=	1024	kg/m^3

Friction loss coefficient: $$F = K_{en} + K_{ex} + \frac{f \cdot L_b}{4 \cdot R} \Longleftrightarrow F = 2{,}92$$

Dimensionless damping coefficient: $$B = \frac{F}{2L_c} \cdot \frac{A_b}{A_c} \cdot H_0 \Longleftrightarrow B = 24{,}14$$

Dimensionless tidal frequency: $$G = \sqrt{\frac{L_c A_b}{g A_c}} \cdot \frac{2\pi}{T_{tide}} \Longleftrightarrow G = 0{,}21$$

Coefficient: $$M = \frac{16BG^2}{3\pi} \Longleftrightarrow M = 1{,}75$$

Amplitude ratio: $$R = \frac{a_b}{a_0} = \sqrt{\left\{\frac{\sqrt{\left(\left(1-G^2\right)^4 + M^2\right)} - \left(1-G^2\right)^2}{0.5M^2}\right\}} \Longleftrightarrow R = 0{,}83$$

Repletion coefficient: $$K = \frac{T}{2 \cdot \pi \cdot \eta_0} \cdot \frac{A_c}{A_b} \cdot \sqrt{\frac{2 \cdot g \cdot R \cdot \eta_0}{m \cdot R + 2 \cdot F \cdot L}} \Longleftrightarrow K = 0{,}98$$

Functions C (K) and sin γ (K) according to van de Kreeke

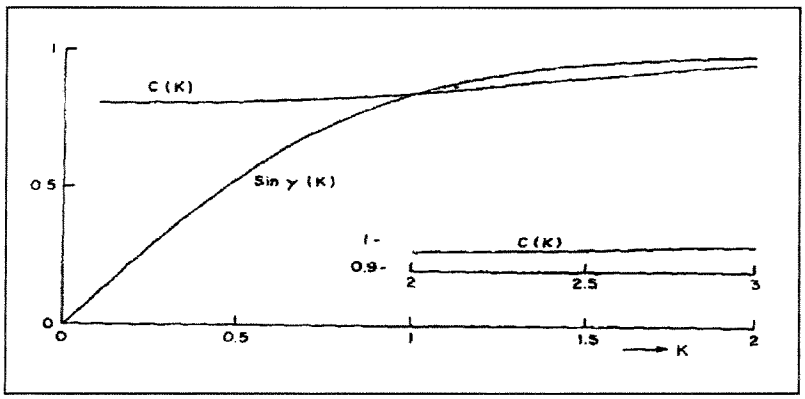

Repletion coefficient: K = 0,98 <==> C(K) 0,87
<==> sin(k) 0,90

Angle of phase lag: $E = TAN^{-1}\left[\frac{MR}{2(1-G^2)}\right]$ <==> E = 37,30 degrees

Maximum velocity: $V_{max} = \sqrt{\frac{2 \cdot g \cdot \eta_0 \sin(E)}{F}}$ <==> V_{max} = 1,43 m/s

Velocity $V = C(K) \cdot \sin\gamma(K) \cdot \frac{2\pi A_b a_0}{A \cdot T}$ <==> V = 1,46 m/s

Bottom shear stress: $\tau_{cr} = \rho \cdot f \cdot V^2$ <==> τ_d = 10,58 N/m^2

Appendix D

(Assessed sediment transport from COPE data)

(Number of pages: 3)

Longshore transport derived from COPE observations									
Station: Currigee (South Stradbroke Island)									
# = Major meteorological event									
month	**net**	**no.d**	**cor.net**	**gross N**	**cor. gr N**	**gross S**	**cor.gr S**	**N+S**	**corr. N+S**
may-86	63947	21	**79172**	71033	86254	-7086	-8773		
jul-86	35140	22	**42328**	51647	61037	-16507	-19883		
aug-86	43791	20	**55834**	56383	70479	-12592	-16055		
sep-86	26502	22	**31923**	32096	37932	-5595	-6739		
oct-86	-4648	22	**-5599**	5983	7071	-10631	-12806		
nov-86	22763	19	**29951**	31749	40940	-8986	-11824		
dec-86	-14981	21	**-18548**	13670	16599	-28651	-35473		
	172.514		***215.061***	**262.561**	**320.312**	**-90.048**	**-111.553**	***352.609***	***431.864***
jan-87	25582	17	**36116**	53861	74455	-28279	-39923		
feb-87	12221	19	**16080**	23969	30907	-11748	-15458		
march-87	39974	21	**49492**	42552	51670	-2578	-3192		
apr-87	17534	20	**22356**	34303	42879	-16769	-21380		
may-87	45265	19	**59559**	47564	61333	-2299	-3025		
jun-87	1647	21	**2039**	11699	14206	-10052	-12445	# (Blanche)	
jul-87	-7973	23	**-9360**	10369	11947	-18343	-21533	##	
aug-87	-2921	20	**-3724**	22058	27573	-24979	-31848	#	
sep-87	21972	21	**27203**	29889	36294	-7917	-9802		
oct-86	14089	22	**16971**	31934	37740	-17844	-21494		
nov-87	95475	21	**118207**	98874	120061	-3398	-4207		
dec-87	33364	21	**41308**	50347	61136	-16983	-21027	#	
	296.229		***376.247***	**457.419**	**570.200**	**-161.189**	**-205.335**	***618.608***	***775.535***
jan-88	9668	18	**13159**	52802	70403	-43134	-58710	## (Agi)&(Delilah)	
feb-88	70936	21	**87826**	90354	109716	-19418	-24041	(Charlie)	
march-88	31950	22	**38485**	63174	74660	-31224	-37611	##	
apr-88	245431	17	**346491**	278042	384352	-32611	-46039	##	
may-88	76450	21	**94652**	81634	99127	-5184	-6418	#	
jun-88	88733	21	**109860**	113103	137339	-24370	-30172	#	
jul-88	-53099	21	**-65742**	63838	77518	-116937	-144779	##	
aug-88	29941	23	**35148**	42496	48963	-12556	-14740		
sep-88	21859	21	**27064**	44975	54613	-23117	-28621	#	
oct-88	-4118	21	**-5098**	9479	11510	-13597	-16834		
nov-88	64760	22	**78006**	117836	139261	-53075	-63931	#	
dec-88	68685	19	**90375**	116920	150765	-48235	-63467	##	
	651.196		***850.226***	**1.074.653**	**1.358.226**	**-423.458**	**-535.365**	***1.498.111***	***1.893.591***
jan-89	7759	20	**9893**	91955	114944	-84196	-107350	###	
feb-89	110122	19	**144897**	138253	178274	-28131	-37014	## (Harry)	
march-89	17136	21	**21216**	69540	84441	-52404	-64881	#	
apr-89	-54033	15	**-82851**	96208	144312	-150241	-230370	##(Aivu)	
mei-89	52644	22	**63412**	78968	93326	-26324	-31708	#(Meena & Ernie)	
jun-89	42748	21	**52926**	54637	66345	-11889	-14720	###	
jul-89	79149	21	**97994**	99583	120922	-20434	-25299	#	
aug-89	-811	23	**-952**	64332	74122	-65143	-76472	#	
sep-89	41743	20	**53222**	71690	89613	-29947	-38182		
oct-89	90961	22	**109567**	110617	130729	-19656	-23677		
nov-89	74350	22	**89558**	97560	115298	-23210	-27958		
dec-89	91886	19	**120903**	127837	164842	-35951	-47304	# (Felicity)	
	553654		***679785***	**1101180**	**1377168**	**-547526**	**-724935**	***1648706***	***2102103***
jan-90	148570	21	**183944**	151741	184257	-3171	-4681	(Nancy-90)	
month	**net**	**no.d**	**cor.net**	**gross N**	**cor. gr N**	**gross S**	**cor.gr S**	**N+S**	corr. N+S

feb-90	58654	20	**74784**	86089	107611	-27436	-34981	##	
march-90	7315	22	**8811**	54154	64000	-46838	-56419	###(Hilda & Ivor)	
apr-90	12045	17	**17005**	33521	46338	-21476	-30319	#	
mei-90	121633	22	**146512**	144992	171354	-23359	-28137	##	
jun-90	103351	20	**131773**	113132	141415	-9781	-12471	#	
jul-90	19254	22	**23192**	29100	34391	-9845	-11859		
aug-90	52226	23	**61309**	60547	69761	-8321	-9768		
sep-90	40054	20	**51069**	57411	71764	-17358	-22131		
nov-90	59280	21	**73394**	96314	116953	-37034	-45852	#	
dec-90	-61699	16	**-90620**	7796	11207	-69495	-102071	(Joy)	
	560683		***681172***	**834797**	**1019050**	**-274114**	**-358688**	***1108911***	***1377738***
jan-91	-17285	22	**-20821**	41526	49076	-58811	-70841	##	
feb-91	-26470	20	**-33749**	45474	56843	-71943	-91727	(Kelvin)	
march-91	14261	20	**18183**	64795	80994	-50534	-64431	#	
apr-91	13340	18	**18157**	55013	73351	-41673	-56722	#	
mei-91	44883	16	**65922**	69919	100509	-25035	-36770	#(Lisa)	
jun-91	31975	18	**43522**	58848	78464	-26873	-36577		
jul-91	75625	22	**91094**	78753	93072	-3128	-3768		
aug-91	14710	20	**18755**	28589	35736	-13880	-17697		
sep-91	22127	21	**27395**	55810	67769	-33683	-41703		
oct-91	49889	22	**60094**	60176	71117	-10287	-12391		
nov-91	15422	20	**19663**	28945	36181	-13523	-17242		
dec-91	-111484	16	**-163742**	13559	19491	-125043	-183657	#	
	126993		**144472**	**601407**	**762602**	**-474413**	**-633525**	***1075820***	***1396127***
								#(Mark, Betsy & Nina)	
feb-92	160974	20	**205242**	203484	254355	-42509	-54199	##(Daman & Esau)	
march-92	225356	18	**306735**	234748	312997	-9392	-12784	#(Fran)	
apr-92	45186	20	**57612**	63802	79753	-18616	-23735	#	
may-92	10433	20	**13302**	22663	28329	-12230	-15593		
jun-92	37090	21	**45921**	76965	93458	-39875	-49369	#	
			0					#	
			0					#	
sep-92	23892	20	**30462**	35584	44480	-11692	-14907		
okt-92	117656	22	**141722**	123133	145521	-5477	-6597	#	
nov-92	-10192	21	**-12619**	38845	47169	-49037	-60712	##	
dec-92	87860	18	**119587**	99790	133053	-11931	-16239		
	698255		***907964***	**899014**	**1139114**	**-200759**	**-254137**	***1099773***	***1393251***
jan-93	-18104	19	**-23821**	21332	27507	-39436	-51889	(Rewa)	
feb-93	7476	20	**9532**	42539	53174	-35062	-44704	#(Oliver & Polly)	
march-93	245386	22	**295579**	270679	319893	-25294	-30468	##(Roger)	
apr-93	48644	19	**64005**	52068	67140	-3424	-4505		
mei-93	97842	13	**165579**	103931	171886	-6088	-10303	#	
jun-93	125781	20	**160371**	126434	158043	-654	-834		
jul-93	25058	20	**31949**	64694	80868	-39636	-50536	#	
aug-93	70789	21	**87644**	76244	92582	-5455	-6754	#	
sep-93	12643	22	**15229**	52048	61511	-39405	-47465	##	
oct-93	10863	20	**13850**	52534	65668	-41671	-53131	#	
nov-93	92030	22	**110854**	105028	124124	-12998	-15657	#	
dec-93	62819	19	**82657**	82734	106683	-19915	-26204	#	
	781227		***1013427***	**1050265**	**1329078**	**-269038**	**-342449**	***1319303***	***1671528***
jan-94	-82134	20	**-104721**	54705	68381	-136839	-174470	##(Sadie)	
feb-94	-43998	19	**-57892**	31006	39981	-75003	-98688	#(Theodore)	
march-94	1180	22	**1421**	55444	65525	-54264	-65363	###	

month	net	no.d	cor.net	gross N	cor. gr N	gross S	cor.gr S	N+S	corr. N+S
apr-94	42704	18	**58125**	61172	81563	-18468	-25137	#	
may-94	75956	21	**94041**	76794	93250	-838	-1038	#	
jun-94	129710	19	**170671**	134500	173434	-4789	-6301	##	
jul-94	97907	21	**121218**	100454	121980	-2548	-3155	#	
aug-94	99003	23	**116221**	105757	121850	-6754	-7929		
sep-94	201849	21	**249908**	214516	260484	-12667	-15683	#	
oct-94	65006	21	**80484**	81964	99528	-16958	-20996	#	
nov-94	-2327	22	**-2803**	45354	53600	-47681	-57434	#	
dec-94	-31572	21	**-39089**	40452	49120	-72024	-89173	#	
	553284		**687584**	**1002118**	**1228696**	**-448833**	**-565366**	***1450951***	***1794062***
jan-95	62968	20	**80284**	96040	120050	-33072	-42167		
feb-95	83542	20	**106516**	134421	168026	-50879	-64871	##	
march-95	102735	22	**123749**	112808	133319	-10073	-12133	##(Violet)	
apr-95	69566	17	**98211**	76225	105370	-6659	-9401	#(Agnes-95)	
may-95	96132	22	**115795**	100329	118571	-4197	-5055	#	
jun-95	81186	20	**103512**	83392	104240	-2206	-2813		
jul-95	80112	21	**99186**	87788	106600	-7676	-9504		
aug-95	33181	23	**38952**	64527	74346	-31346	-36797	#	
sep-95	35932	20	**45813**	41657	52071	-5725	-7299		
oct-95	48294	22	**58172**	61258	72396	-12963	-15615		
nov-95	103055	22	**124134**	127345	150499	-24290	-29258		
dec-95	12095	16	**17765**	45642	65610	-33547	-49272	#	
	808798		***1012090***	**1031432**	**1271097**	**-222633**	**-284186**	***1254065***	***1555283***
jan-96	21837	21	**27036**	30802	37402	-8965	-11100	#(Barry & Celeste)	
feb-96	350036	21	**433378**	355563	431755	-5527	-6843	##(Dennis)	
march-96	141014	20	**179793**	148955	186194	-7941	-10125	##(Ethel)	
apr-96	35327	19	**46483**	50367	64947	-15039	-19788		
may-96	134723	20	**171772**	206661	258326	-71937	-91720	##	
jun-96	76552	18	**104196**	85947	114596	-9396	-12789	#	
umber of days:					20,27	days			
transport rate:					***656.803***	m^3/year			
transport rate:					***1439108***	m^3/year			
transport rate:					***1.037.554***	m^3/year			
transport rate:					***-401.554***	m^3/year			

Appendix E

(Escoffier stability analysis Nerang River Entrance)

(Number of pages: 3)

Escoffier stability analysis Nerang River Entrance

In this appendix the Escoffier closure curve and critical shear stress curve are calculated
First a calculation is presented for one point of the critical shear stress curve and the closure curve

Inlet characteristics:

Tidal prism	P=	2,25E+07	m^3/half tidal cycle	
Basin area	A_b =	2,65E+07	m^2	
Cross-sectional area	A_c =	1000	m^2	
Lenght inlet channel	L =	800	m	
Tidal amplitude	η_0 =	0,5	m	F=g/C^2
Darcy-Weisb. coeff.	f/8 =	0,0048		f = 8*g/C^2
K_{en}+K_{ex}	m =	1,05		
grav.	g =	9,81	m/s^2	
Ttide	T =	12,4	hrs	
h	R =	4,16	m	
Chezy	C =	45		
water density	ρ_w=	1024	kg/m^3	

Repletion coefficient "K":

K =	0,98	
C(K) =	0,87	(Figure 1)
sinγ(K) =	0,90	(Figure 1)

Used equations for the calculations of the curves:

(For describtion of the theory reference is made to section: 4.2.3 in Volume I)

$$\tau_{cr} = 2303 f \cdot \left(C(K) \cdot A_c^{0.031}\right)^2$$

$$V = C \cdot \sin\gamma \cdot \frac{2\pi A_b a_0}{A \cdot T} \qquad \tau_d = \rho \cdot F \cdot V|V|$$

$$K = \frac{T}{2 \cdot \pi \cdot \eta_0} \cdot \frac{A_c}{A_b} \cdot \sqrt{\frac{2 \cdot g \cdot R \cdot \eta_0}{m \cdot R + 2 \cdot F \cdot L}}$$

With the use of the above described equations the calculation yields to the following results:

V =	1,46	m/s
τ_{cl} =	10,60	N/m^2
V_{cr} =	1,24	m/s
τ_{cr} =	7,64	N/m^2

Figure 1: Functions C (K) and sin γ (K) according to van de Kreeke

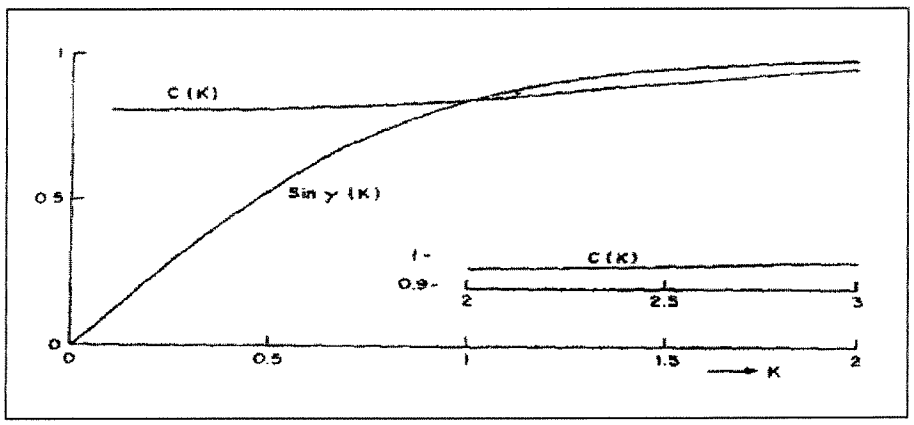

A_c [m2]	K	C(K)	sinγ(K)	V [m/s]	τ_{cl} [N/m^2]	τ_{cr} [N/m^2]	V_{cr} [m/s]
25	0,02	0,81	0	0,00	0,00	7,47	1,23
30	0,03	0,81	0,01	0,50	1,26	7,48	1,23
35	0,03	0,81	0,02	0,86	3,70	7,48	1,23
40	0,04	0,81	0,03	1,13	6,37	7,49	1,23
45	0,04	0,81	0,04	1,34	8,94	7,49	1,23
50	0,05	0,81	0,05	1,51	11,32	7,50	1,23
100	0,10	0,81	0,12	1,81	16,30	7,53	1,23
150	0,15	0,81	0,2	2,01	20,12	7,55	1,23
200	0,20	0,81	0,26	1,96	19,13	7,56	1,23
250	0,25	0,81	0,31	1,87	17,41	7,57	1,24
300	0,30	0,81	0,38	1,91	18,16	7,58	1,24
350	0,34	0,81	0,43	1,86	17,09	7,59	1,24
400	0,39	0,81	0,5	1,89	17,69	7,60	1,24
450	0,44	0,81	0,53	1,78	15,70	7,60	1,24
500	0,49	0,82	0,58	1,77	15,61	7,61	1,24
550	0,54	0,82	0,63	1,75	15,22	7,61	1,24
600	0,59	0,83	0,67	1,72	14,64	7,62	1,24
650	0,64	0,83	0,72	1,71	14,58	7,62	1,24
700	0,69	0,83	0,74	1,64	13,28	7,62	1,24
750	0,74	0,85	0,76	1,61	12,80	7,63	1,24
800	0,79	0,86	0,81	1,62	13,08	7,63	1,24
850	0,84	0,86	0,84	1,59	12,46	7,63	1,24
900	0,89	0,86	0,86	1,53	11,65	7,64	1,24
950	0,93	0,86	0,86	1,45	10,46	7,64	1,24
1000	0,98	0,87	0,9	1,46	10,58	7,64	1,24
1050	1,03	0,88	0,91	1,42	10,04	7,64	1,24
1100	1,08	0,89	0,93	1,40	9,77	7,64	1,24
1150	1,13	0,90	0,94	1,37	9,34	7,65	1,24
1200	1,18	0,91	0,95	1,34	8,95	7,65	1,24
1250	1,23	0,91	0,96	1,30	8,43	7,65	1,24
1300	1,28	0,92	0,96	1,27	7,96	7,65	1,24
1350	1,33	0,93	0,97	1,25	7,70	7,65	1,24
1400	1,38	0,94	0,975	1,21	7,32	7,66	1,24
1450	1,43	0,94	0,98	1,18	6,96	7,66	1,24
1500	1,48	0,94	0,985	1,15	6,57	7,66	1,24
1550	1,52	0,95	0,99	1,13	6,35	7,66	1,24
1600	1,57	0,96	0,99	1,10	6,02	7,66	1,24
1650	1,62	0,96	0,99	1,07	5,72	7,66	1,24
1700	1,67	0,96	0,99	1,04	5,39	7,67	1,24
1750	1,72	0,96	0,99	1,01	5,09	7,67	1,24
1800	1,77	0,96	0,99	0,98	4,81	7,67	1,24
1850	1,82	0,96	0,99	0,96	4,55	7,67	1,24
1900	1,87	0,96	0,99	0,93	4,32	7,67	1,24
1950	1,92	0,96	0,99	0,91	4,10	7,67	1,24
2000	1,97	0,96	0,99	0,89	3,90	7,67	1,24
2050	2,02	0,96	0,99	0,86	3,71	7,67	1,24
2100	2,07	0,96	0,99	0,84	3,53	7,68	1,24
2150	2,11	0,96	0,99	0,82	3,37	7,68	1,24
2200	2,16	0,96	0,99	0,81	3,22	7,68	1,24
2250	2,21	0,96	0,99	0,79	3,08	7,68	1,24
2300	2,26	0,96	0,99	0,77	2,95	7,68	1,24
2350	2,31	0,96	0,99	0,75	2,82	7,68	1,24
2400	2,36	0,96	0,99	0,74	2,71	7,68	1,24
2450	2,41	0,96	0,99	0,72	2,60	7,68	1,24
2500	2,46	0,96	0,99	0,71	2,49	7,68	1,24

Appendix E; Figure 2

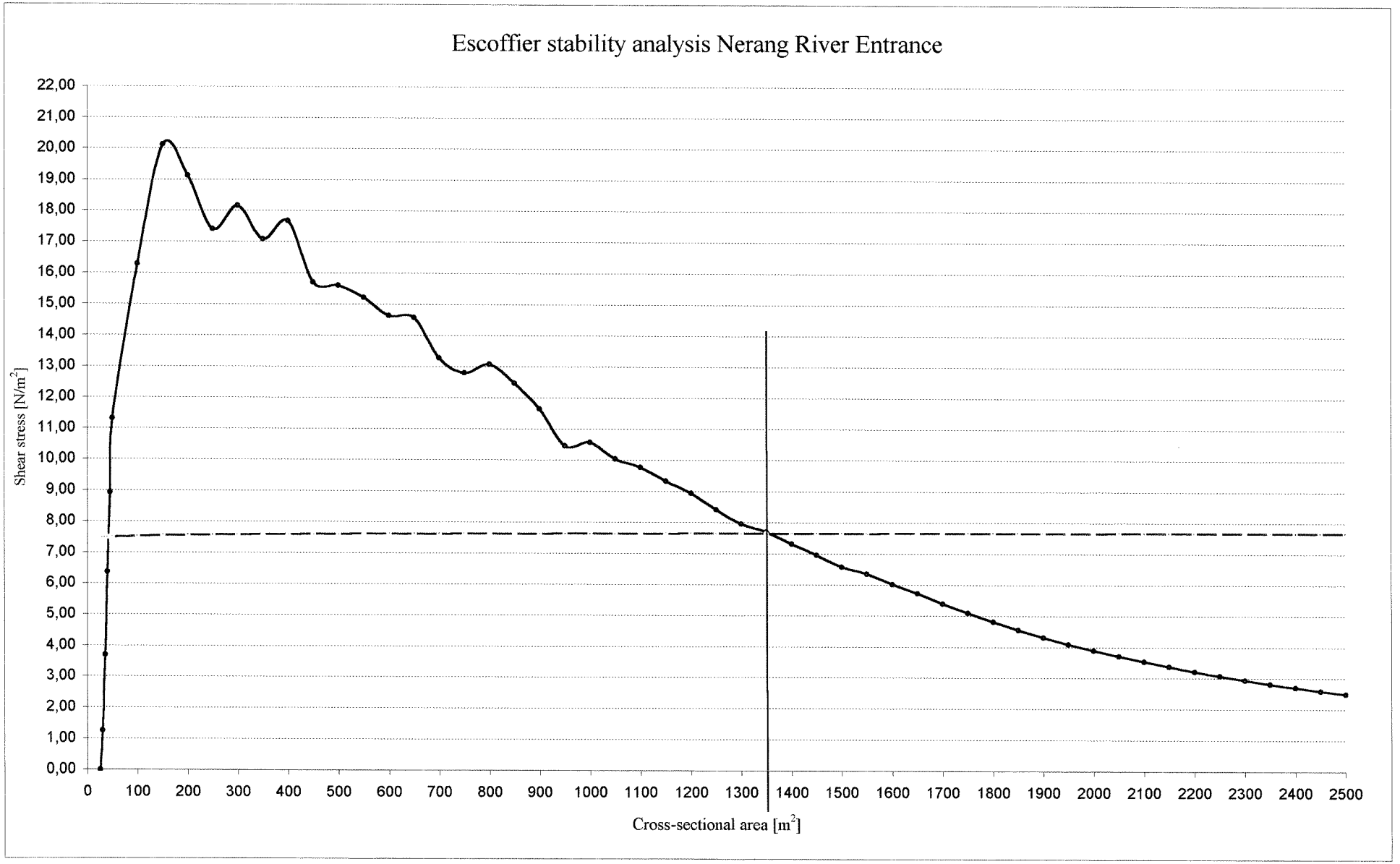

Appendix F

(Possibilities of Mechanical sand bypassing at the Nerang River Entrance)

(Number of pages: 2)

Possibilities of Mechanical sand bypassing at the Nerang River Entrance

The four possible improvements were:

- Low-weir section
- Offshore breakwater
- Fixed land-based dredge
- Mobile land-based dredge

The effect on the layout of the improved Nerang River Entrance using mechanical sand bypassing systems is illustrated in Figure F1 t/m 4.

Advantages of a *low-weir section (Figure F1)* are that maintenance dredging of the entrance channel and dredging operations in the Broadwater can be done with one floating dredge, and the required long training walls offer a good protection against wave penetration into the Broadwater. Some disadvantages of this solution are that floating dredges must operate in relatively calm water. During periods of higher wave action dredging is not possible. The construction of the southern training-wall is expensive because it is inaccessible from the mainland. Maintenance of the seaward part of the southern training-wall is difficult because of the low weir section.

The *offshore breakwater (Figure F2)* concept appeared to work satisfactory in other locations. Due to the predominant southeast wave direction, the offshore breakwater must extent over a significant length, in order to create sufficient shelter in these conditions. Extension in northward direction reduces wave action towards the Broadwater, which is favourable for navigation and dredging operation. The extension of the southern training-wall may be relatively short. In periods of relatively low wave action, the dredge can be used for maintenance dredging of the entrance channel and the Broadwater. However the costs of such a relatively long offshore parallel breakwater are high because it must be built in rather deep water. Also maintenance of the offshore breakwater is difficult because it is inaccessible from the land.

The third alternative is a *fixed land-based dredge. (Figure F3)* A suction dredge can be constructed on the southern training-wall or on an independent foundation, from were the sand is intercepted moving within the reach of the plant. The wave climate has no influence on the dredging operation in normal conditions. The position of such a plant must be in the surfzone and some considerable distance offshore in order to prevent landlocking. The southern training-wall can be kept short, and is therefore relatively cheap, to prevent large accumulations of sediment on the south side of the training-wall, which results in severe erosion on the South Stradbroke Island. On the other hand, short training-wall offers little protection for navigation and may cause more wave penetration into the Broadwater. Another disadvantage of this solution is that not the whole littoral drift can be bypassed and there is no buffer area for storage of sand during severe weather conditions. This results in a shoaling of the entrance channel.

An other solution, according to Delft (1976), than a fixed dredge is to construct a *moveable dredge on a trestle (FigureF4)* normal to the coastline in the area to the south of the training-walls. The sand can be continuously dredged in the area along the trestle; in order to form a trench were the sand moving along could accumulate. During excessive southeasterly wave

conditions part of the sand can pass over the trench and form a temporarily accumulation against the southern training-wall. In order to avoid sedimentation of this sand in the entrance channel the southern training-wall should be rather long, which in turn offer a good protection against wave penetration into the Broadwater. The sand dredged from the trench can be bypassed to the north of the entrance. Also this alternative appeared to be rather cheap in similar other cases. However a trestle has to be constructed which can withstand cyclones and permits the dredging of a deep trench in its immediate surroundings.

For the actual design of the bypassing system, the Beach Protection Authority commissioned the Delft Hydraulic Laboratory to further investigate the sand bypassing system.

Figure F1 t/m 4: Sand by-passing techniques

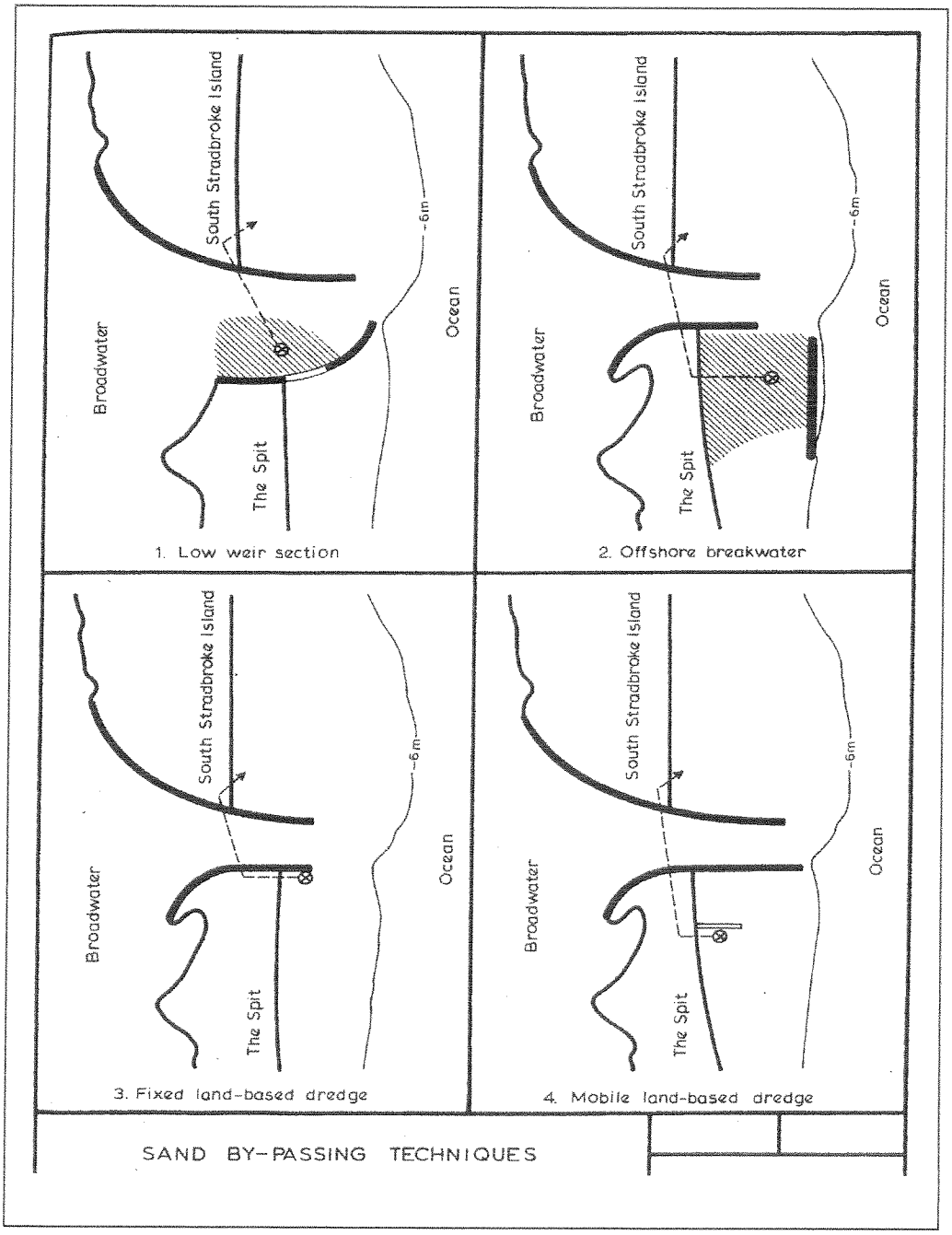

(From: Delft, 1970)

Appendix G

(Monthly bypass rates and predicted littoral drift)

(Number of pages: 7)

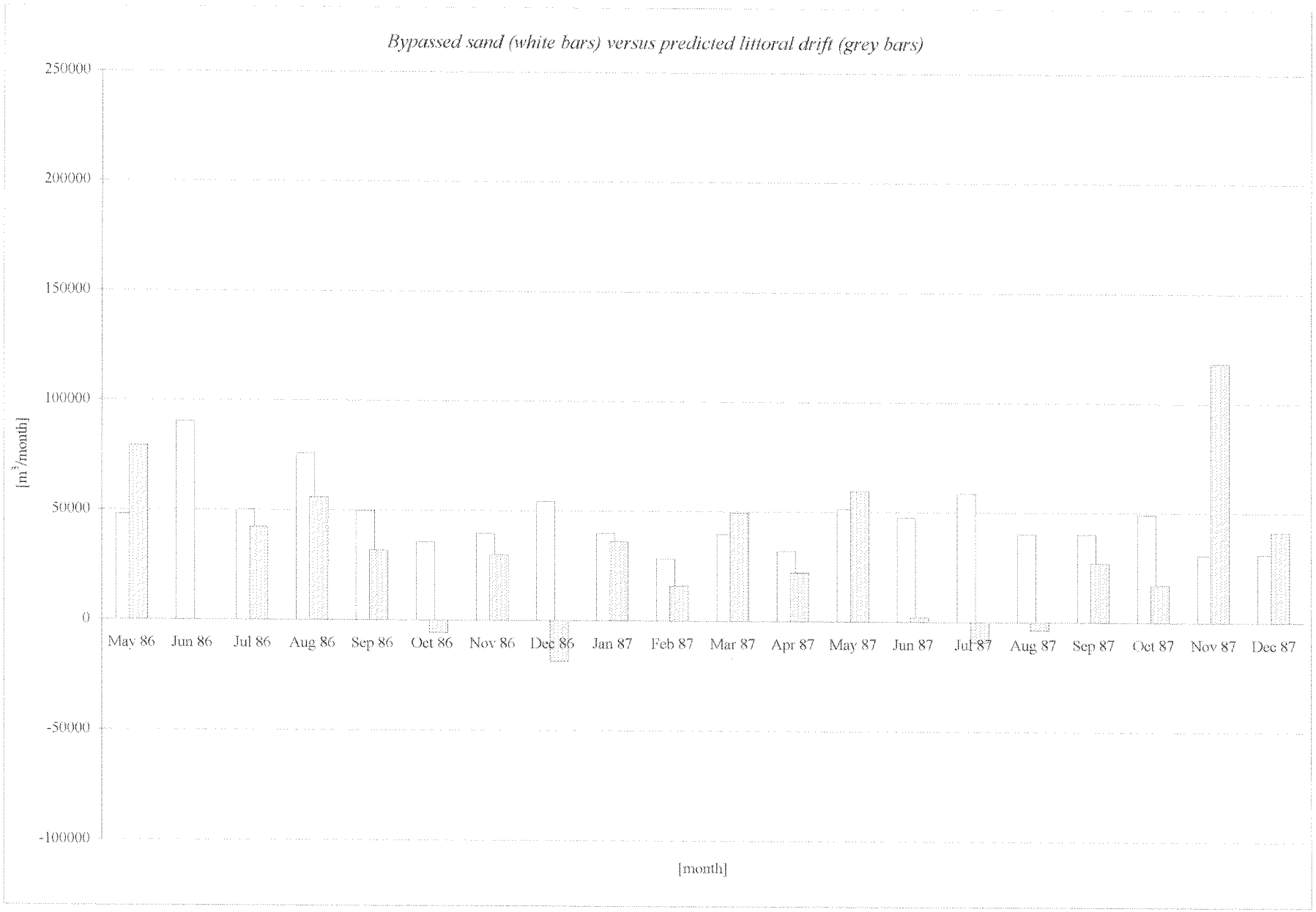
Bypassed sand (white bars) versus predicted littoral drift (grey bars)
250000
200000
150000
100000
50000
0
-50000
-100000
[m3/month]
May 86
Jun 86
Jul 86
Aug 86
Sep 86
Oct 86
Nov 86
Dec 86
Jan 87
Feb 87
Mar 87
Apr 87
May 87
Jun 87
Jul 87
Aug 87
Sep 87
Oct 87
Nov 87
Dec 87
[month]

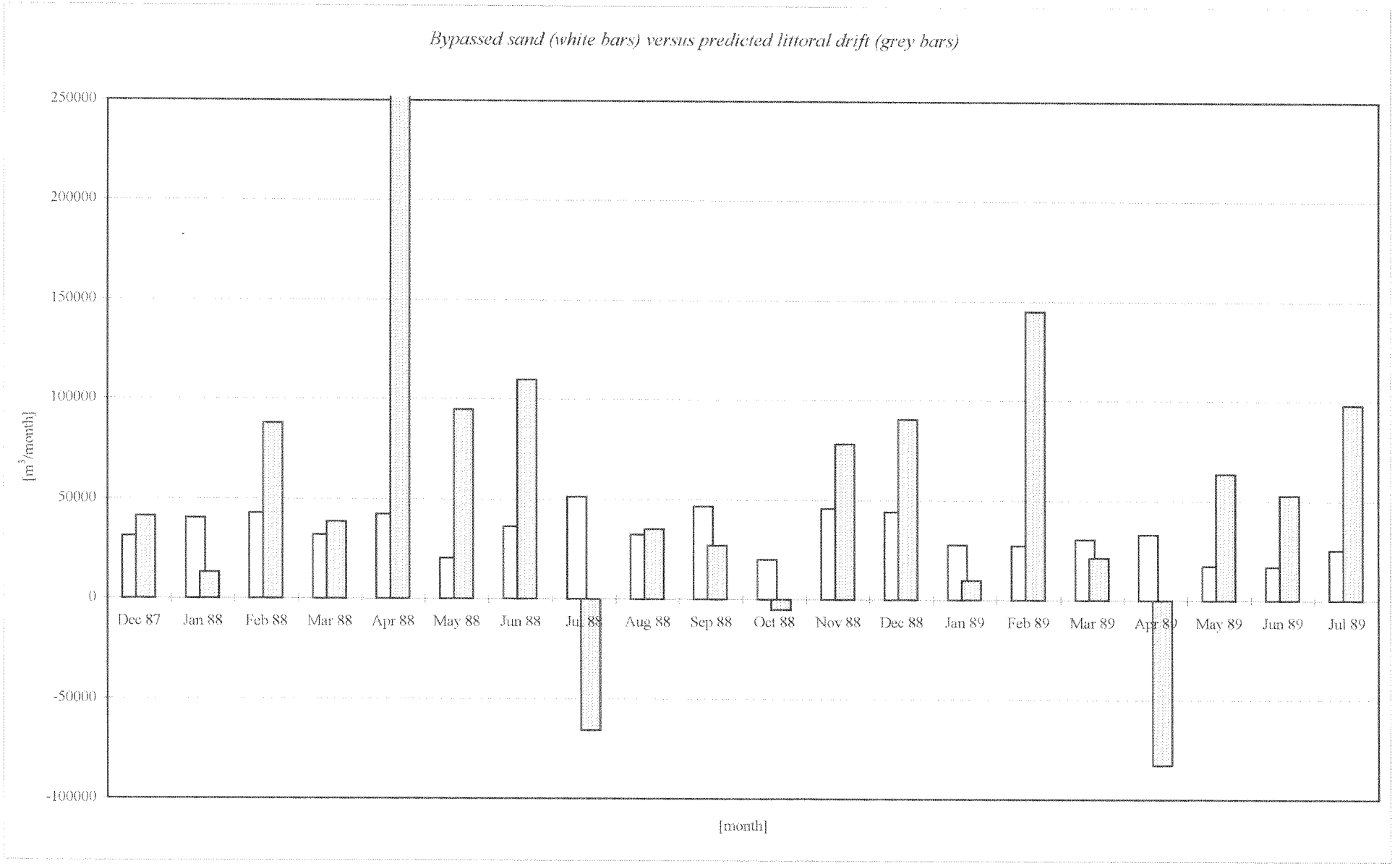
Bypassed sand (white bars) versus predicted littoral drift (grey bars)
250000
200000
150000
100000
50000
0
-50000
-100000
[m³/month]
Dec 87
Jan 88
Feb 88
Mar 88
Apr 88
May 88
Jun 88
Jul 88
Aug 88
Sep 88
Oct 88
Nov 88
Dec 88
Jan 89
Feb 89
Mar 89
Apr 89
May 89
Jun 89
Jul 89
[month]

Bypassed sand (white bars) versus predicted littoral drift (grey bars)

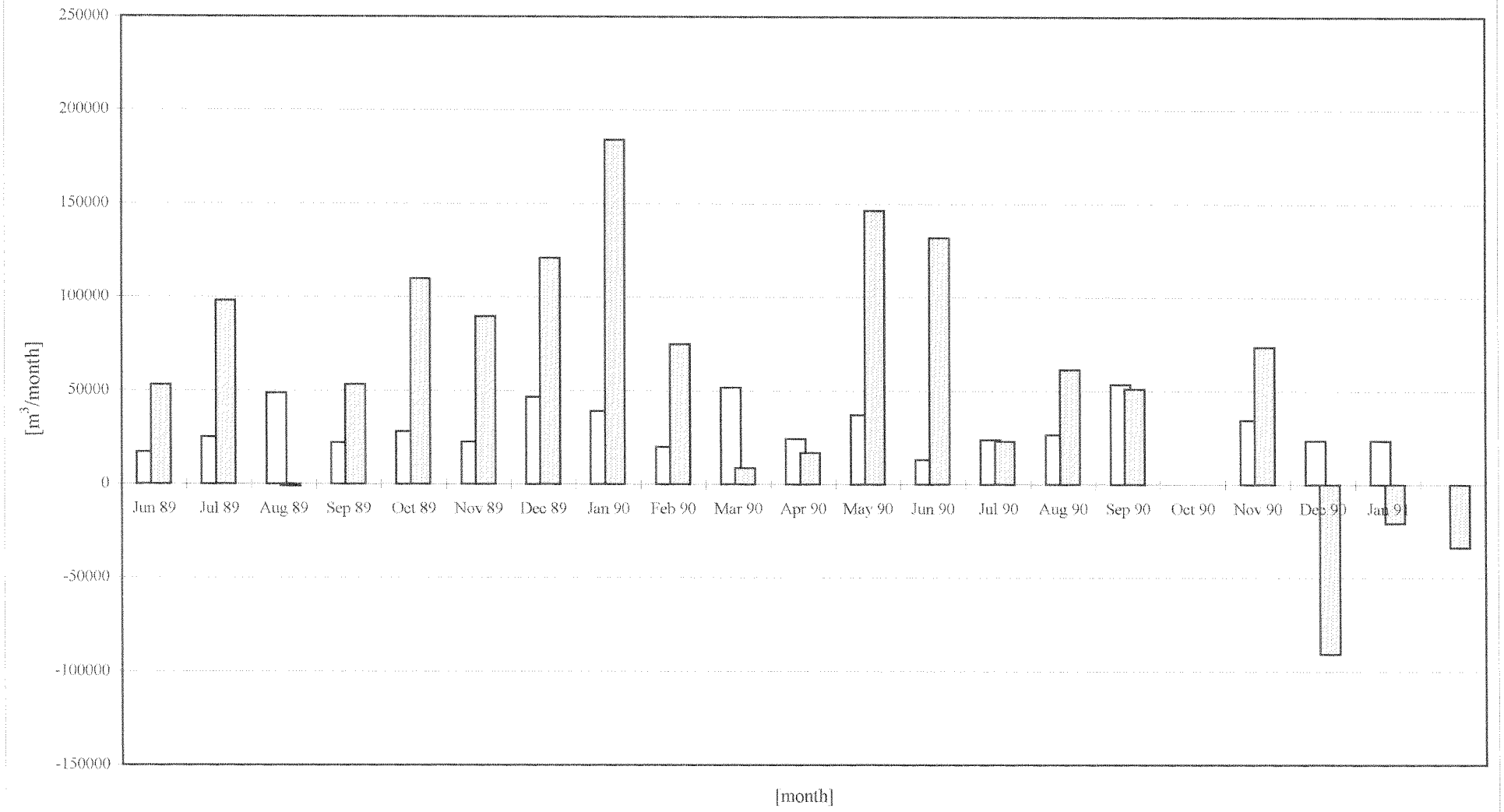

Bypassed sand (white bars) versus predicted littoral drift (grey bars)

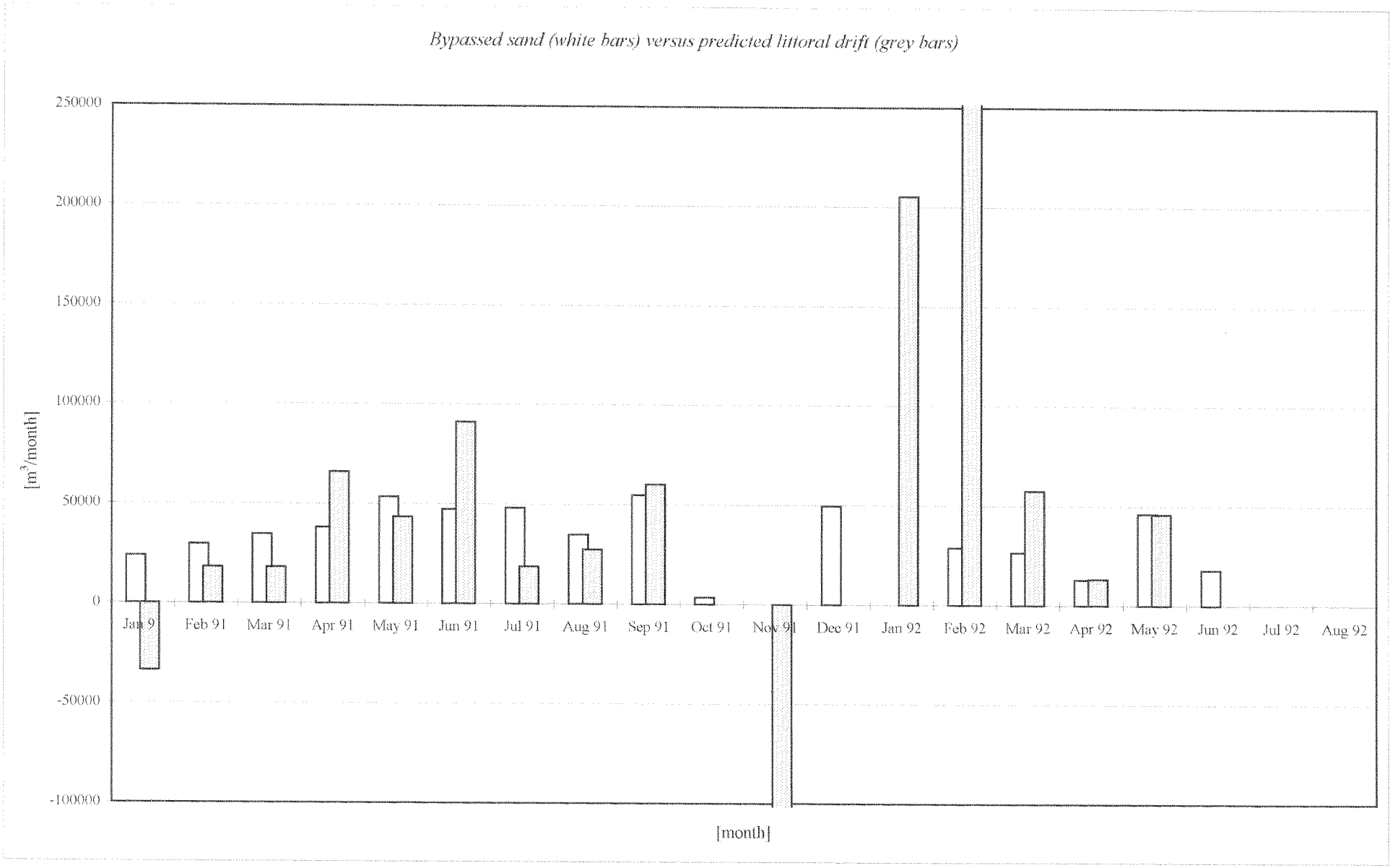

Bypassed sand (white bars) versus predicted littoral drift (grey bars)

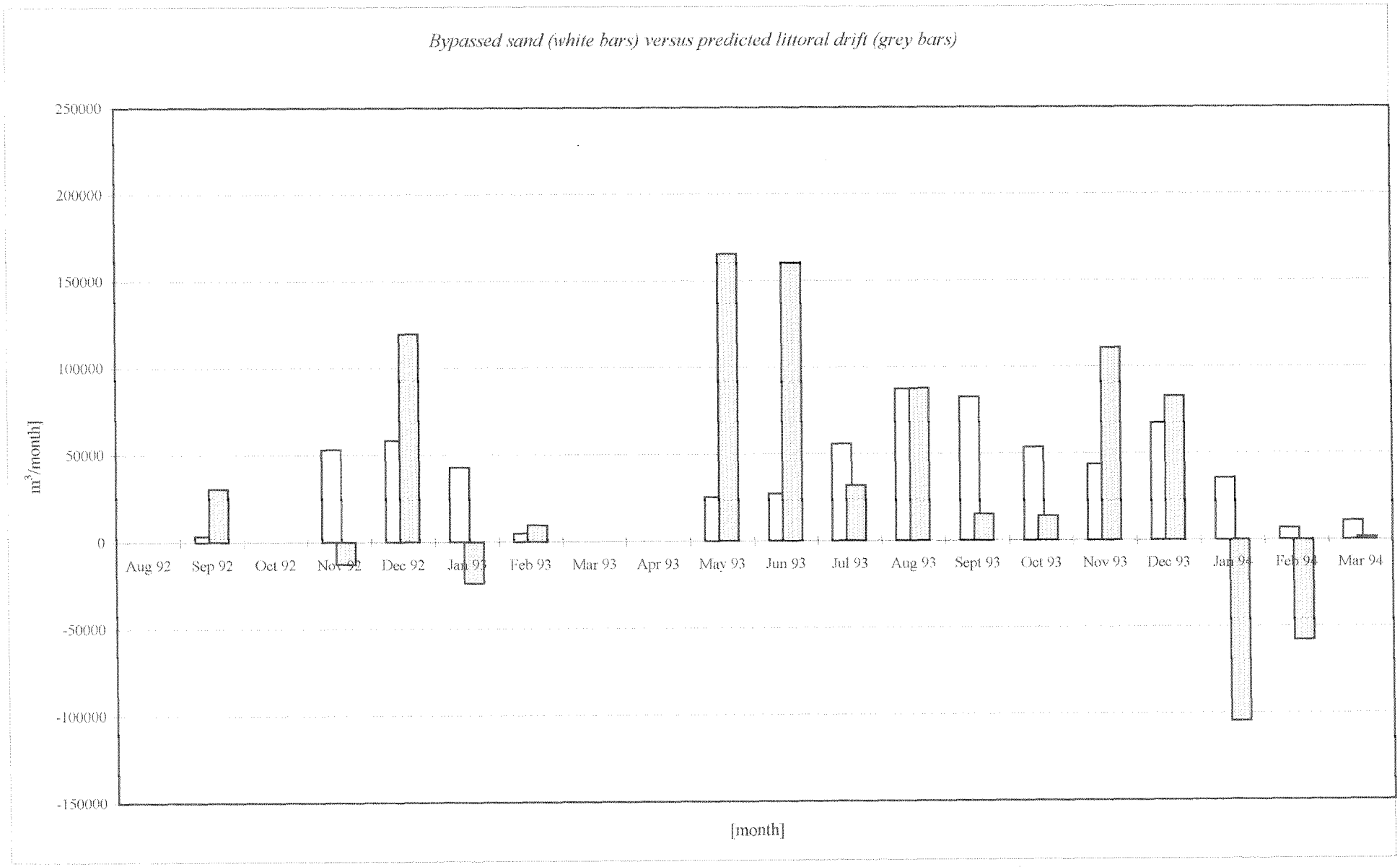

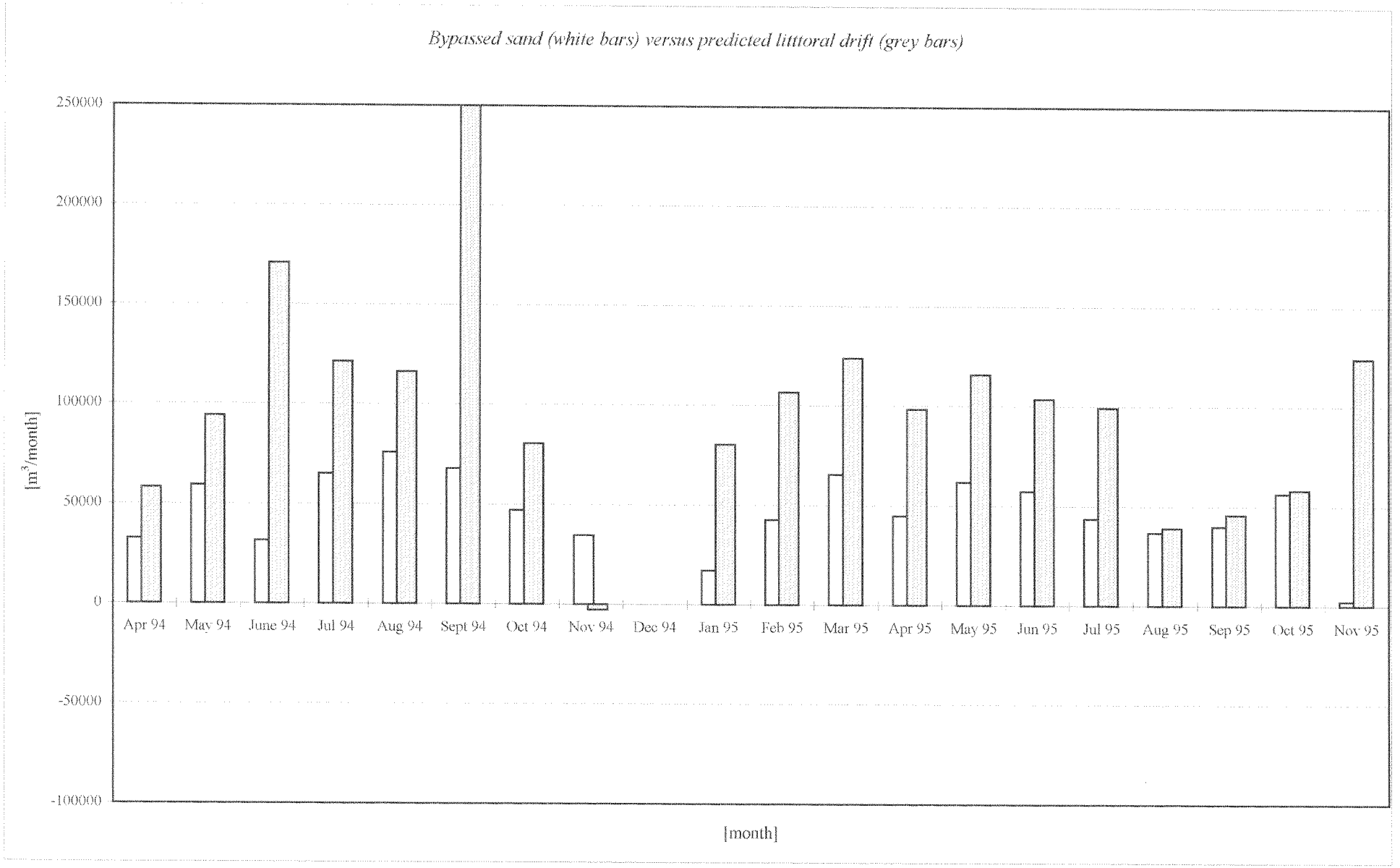
Bypassed sand (white bars) versus predicted litttoral drift (grey bars)
250000
200000
150000
100000
50000
0
-50000
-100000
[m3/month]
Apr 94
May 94
June 94
Jul 94
Aug 94
Sept 94
Oct 94
Nov 94
Dec 94
Jan 95
Feb 95
Mar 95
Apr 95
May 95
Jun 95
Jul 95
Aug 95
Sep 95
Oct 95
Nov 95
[month]

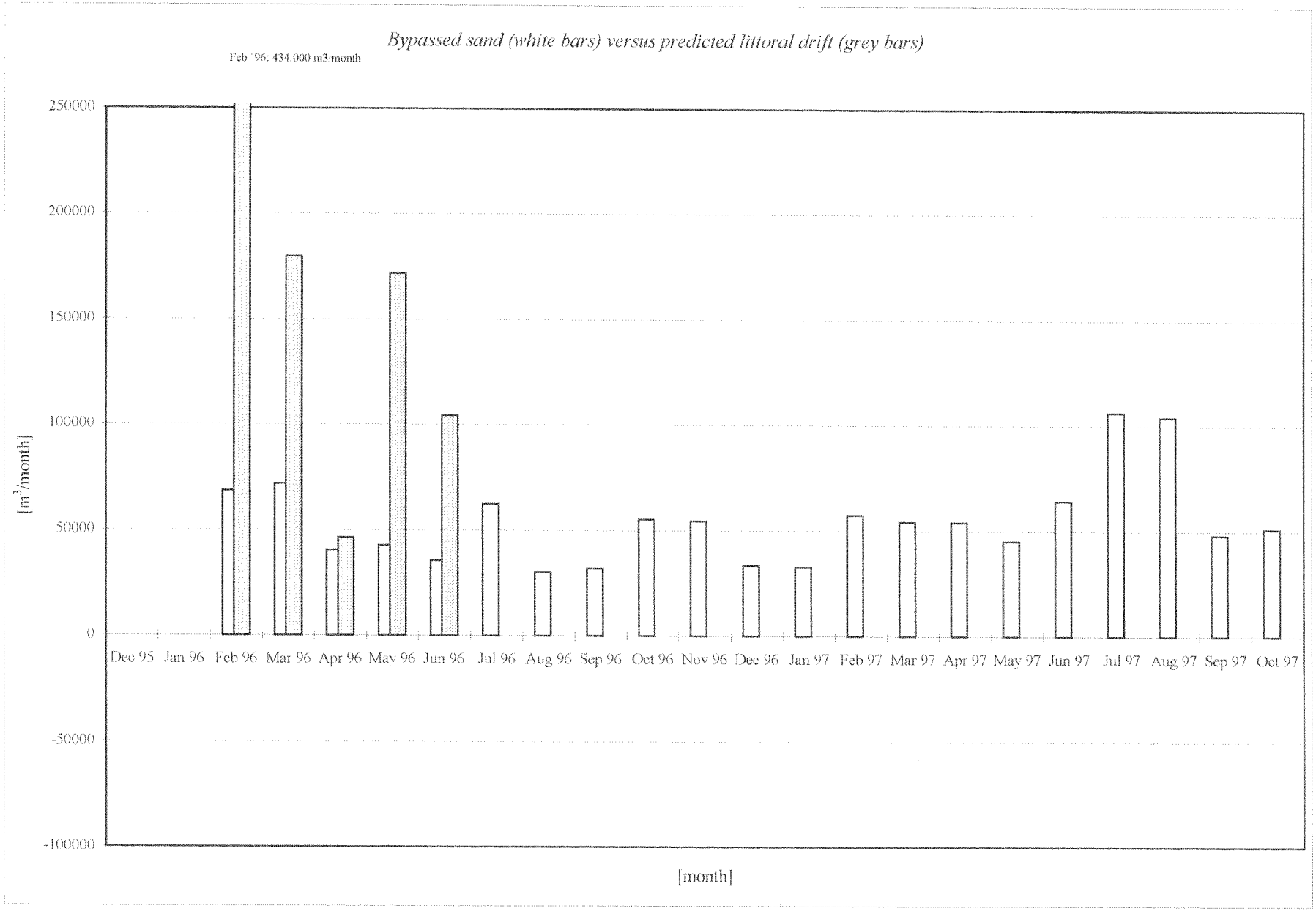
Bypassed sand (white bars) versus predicted littoral drift (grey bars)
Feb '96: 434,000 m3/month
250000
200000
150000
100000
50000
0
-50000
-100000
[m3/month]
Dec 95
Jan 96
Feb 96
Mar 96
Apr 96
May 96
Jun 96
Jul 96
Aug 96
Sep 96
Oct 96
Nov 96
Dec 96
Jan 97
Feb 97
Mar 97
Apr 97
May 97
Jun 97
Jul 97
Aug 97
Sep 97
Oct 97
[month]

Appendix H

(Used soundings in bathymeries and a schematic view of the sections)

(Number of pages: 3)

Calculated sections Gold Coast Seaway

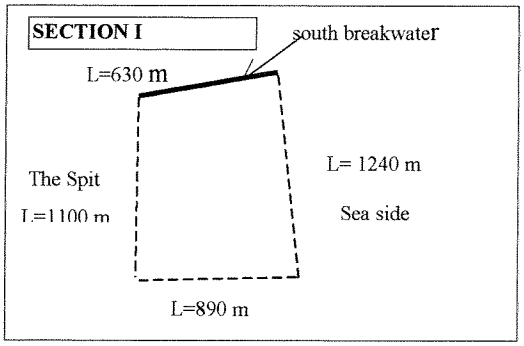

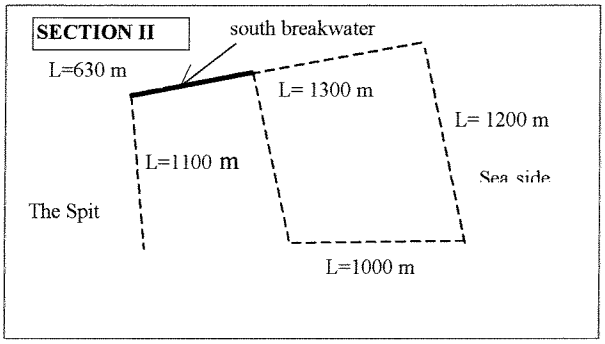

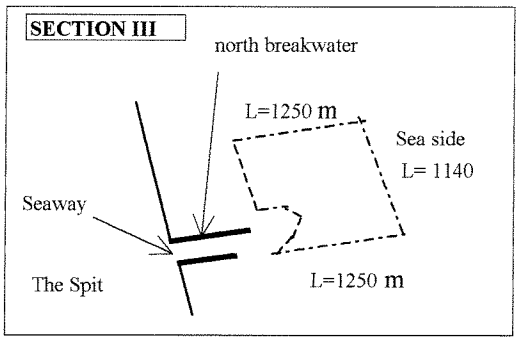

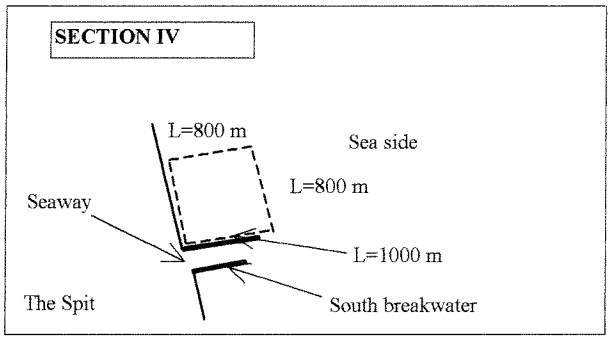

Information bathymetries Gold Coast Seaway

1984:	**Map reference**	***1985:***	**Map reference**
Used bottom profiles	D013-013	*Used bottom profiles*	D013-013
Sept: 78.0-80.6		Sept: 79.2-80.6	
Oct: 80.8-82		Oct: 80.8-84	
Nov: 82.2-84		Aug: 78.4-79	
Used data file:	Non	*Used data file entrance channel:* Nov 88 - Feb 89	D013014
1986:		***1987:***	
Used bottom profiles	D013-013	*Used bottom profiles*	D013-013
Aug: 82.6-84		May: 78.0-84	
Sept: 78.0-84		Jun: 78.0-84	
Oct: 78.0-78.4			
Nov: 78.4-81.8			
Dec: 82-84			
Used data file entrance channel:	Non	*Used data file entrance channel:*	Non
1988:		***1989:***	
Used bottom profiles	D013-013	*Used bottom profiles*	D013-013
Nov: 78.0-84		Oct: 78.0-80.6	
		Nov: 81.0-81.6	
Used data file entrance channel: (Nov 1980 - Febr 1989)	D013014	Oct: 81.8-83.8	
		Used data file entrance channel:	Non
1990:		***1991:***	
Used bottom profiles	D013-013	*Used bottom profiles*	D013-013
Nov: 78.0-80.2		Nov: 78.0-80.2	
Dec: 80.4-83.8		Dec: 80.4-83.8	
Used data file entrance channel:	Non	*Used data file entrance channel:*	Non
1992:		***1993:***	
Used bottom profiles	D013-013	*Used bottom profiles*	D013-013
Vertical datum A.H.D.			
Nov: 78.0-84		Nov: 78.0-81	
		Dec: 81.2-81.8	
Used data file entrance channel:	D013024		
Vertical datum: L.W.D. (RL 5.615 L.W.D.) A.H.D. = L.W.D. + 0.7 (Nov 1992)		*Used data file entrance channel:*	Non

1994: No data available	***1995:*** *Used bottom profiles* D013-013 Dec: 78.0-84 *Used data file entrance channel:* D013024 (Nov-Dec 1995)
1996: *Used bottom profiles* D013-013 Dec: 78.0-84 *Used data file entrance channel:* D013026 (Sept-Oct 1996)	***1997:*** *Used bottom profiles* Non *Used data file entrance channel:* D013027 (May 1997)

Appendix I

(Bottom profiles ETA 80; location The Spit)

(Number of pages: 9)

Appendix I (Large scale)

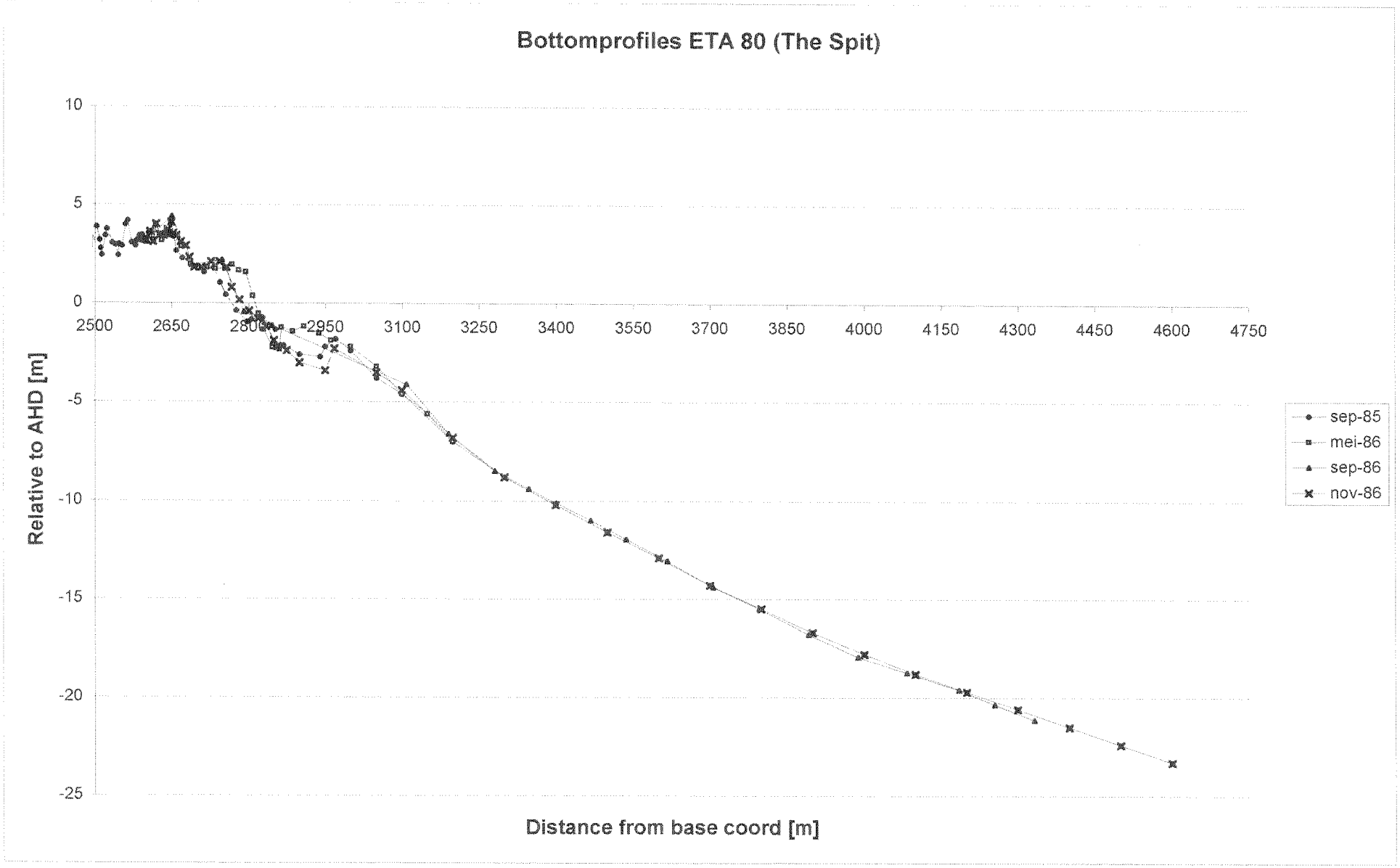

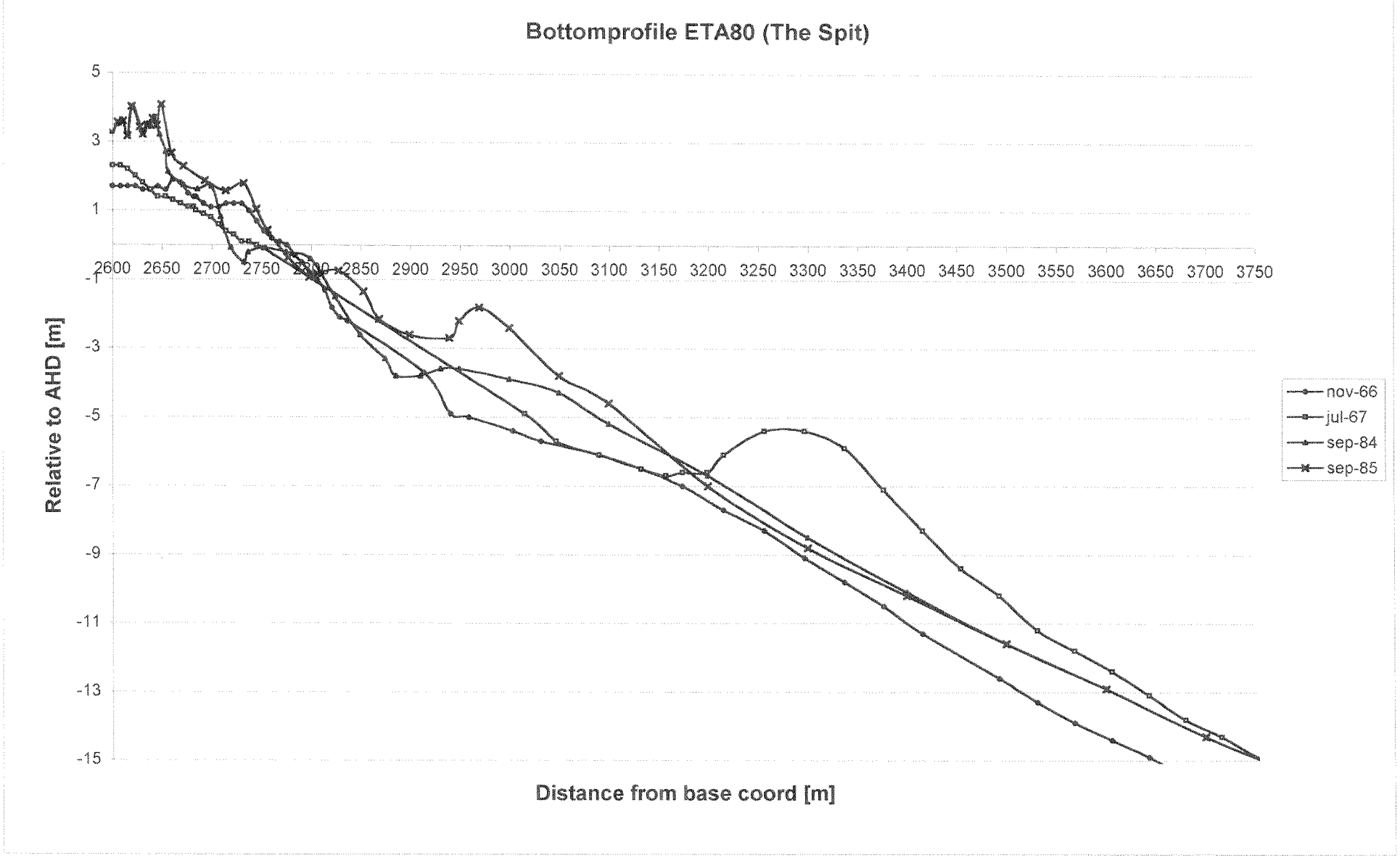
Bottomprofile ETA80 (The Spit)
Relative to AHD [m]
5
3
1
-1
-3
-5
-7
-9
-11
-13
-15
2600 2650 2700 2750 2800 2850 2900 2950 3000 3050 3100 3150 3200 3250 3300 3350 3400 3450 3500 3550 3600 3650 3700 3750
Distance from base coord [m]
nov-66
jul-67
sep-84
sep-85

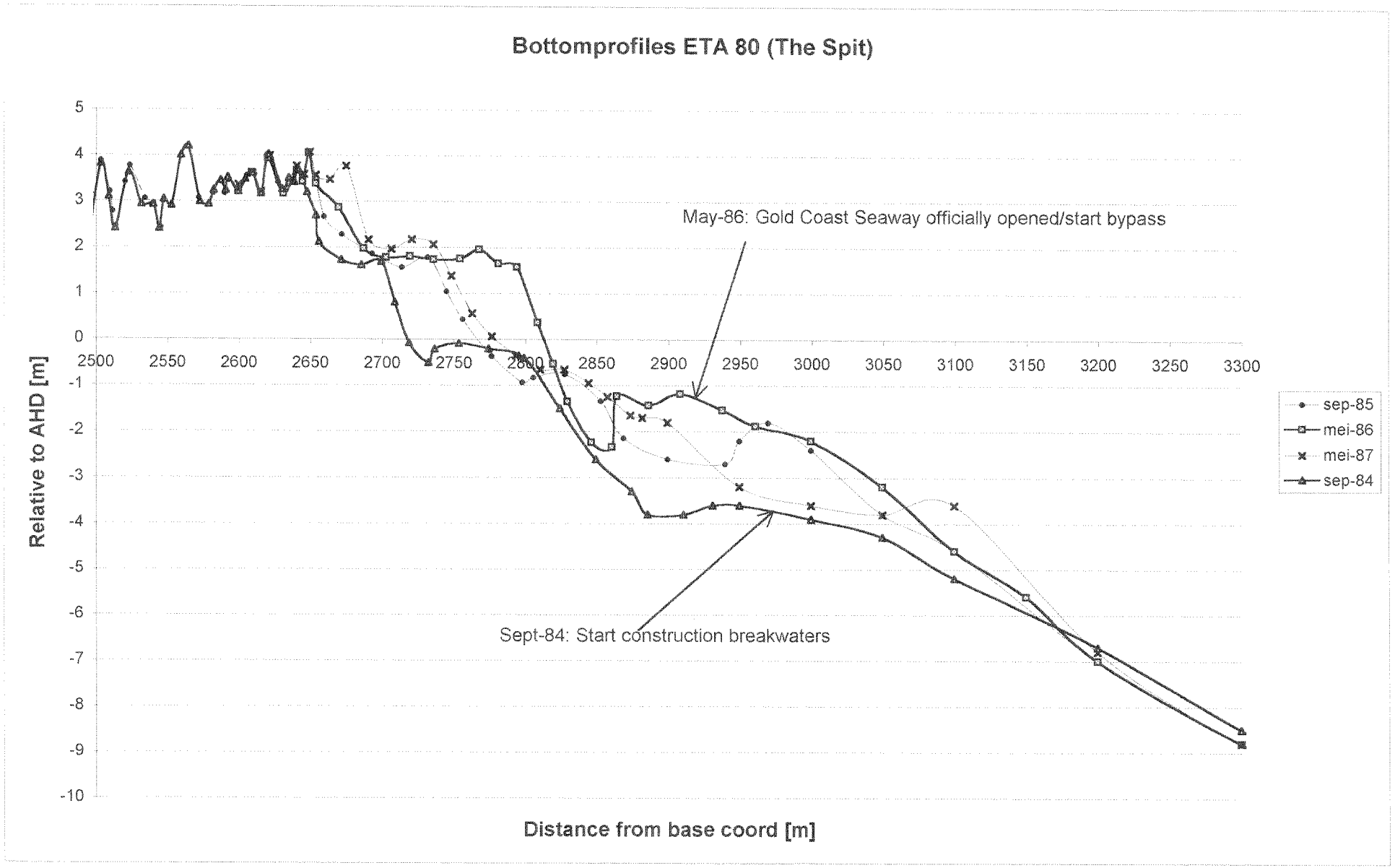
Bottomprofiles ETA 80 (The Spit)
Relative to AHD [m]
Distance from base coord [m]
May-86: Gold Coast Seaway officially opened/start bypass
Sept-84: Start construction breakwaters
sep-85
mei-86
mei-87
sep-84
5
4
3
2
1
0
-1
-2
-3
-4
-5
-6
-7
-8
-9
-10
2500
2550
2600
2650
2700
2750
2800
2850
2900
2950
3000
3050
3100
3150
3200
3250
3300

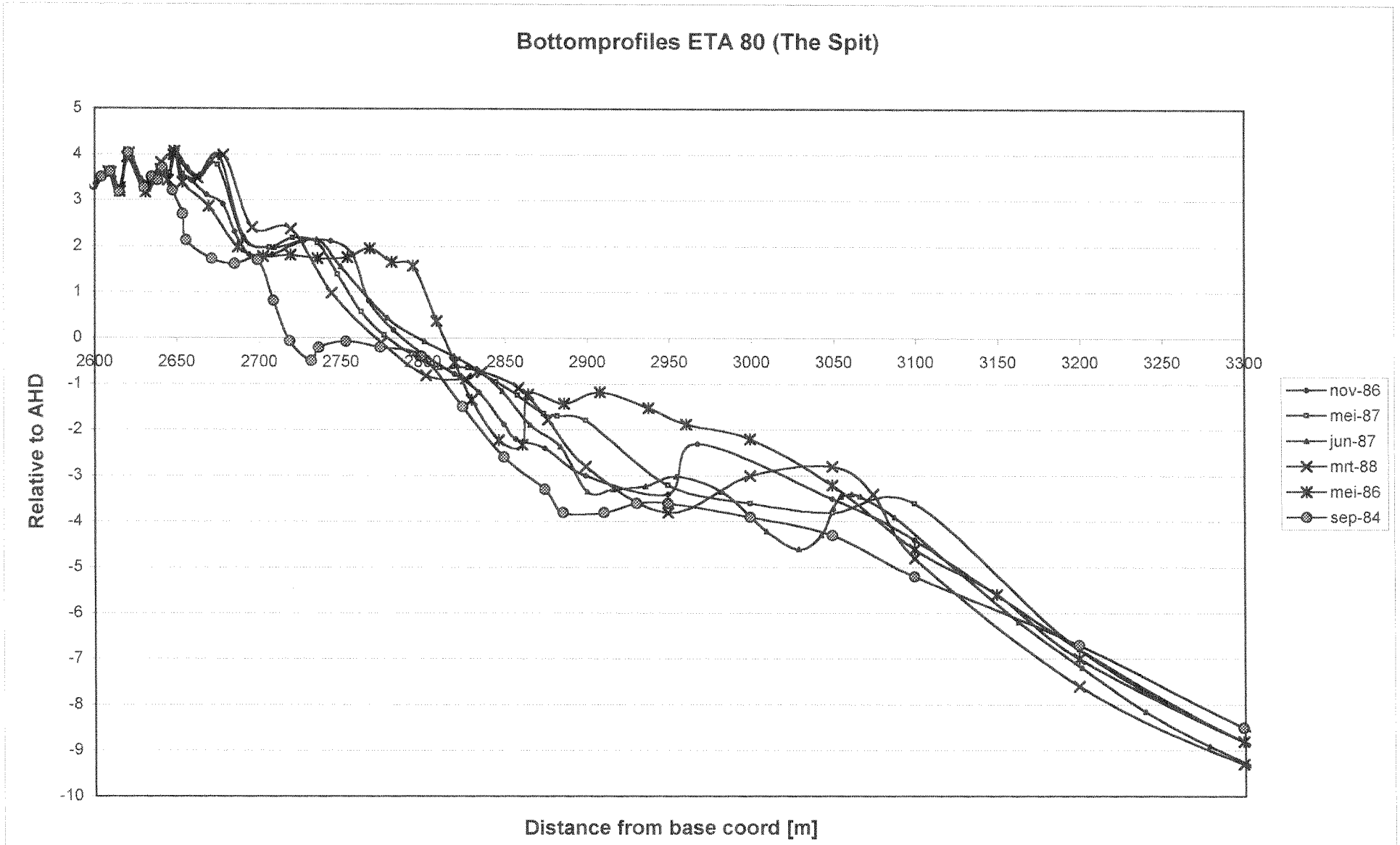
Bottomprofiles ETA 80 (The Spit)
Relative to AHD
5
4
3
2
1
0
-1
-2
-3
-4
-5
-6
-7
-8
-9
-10
2600
2650
2700
2750
2800
2850
2900
2950
3000
3050
3100
3150
3200
3250
3300
Distance from base coord [m]
nov-86
mei-87
jun-87
mrt-88
mei-86
sep-84

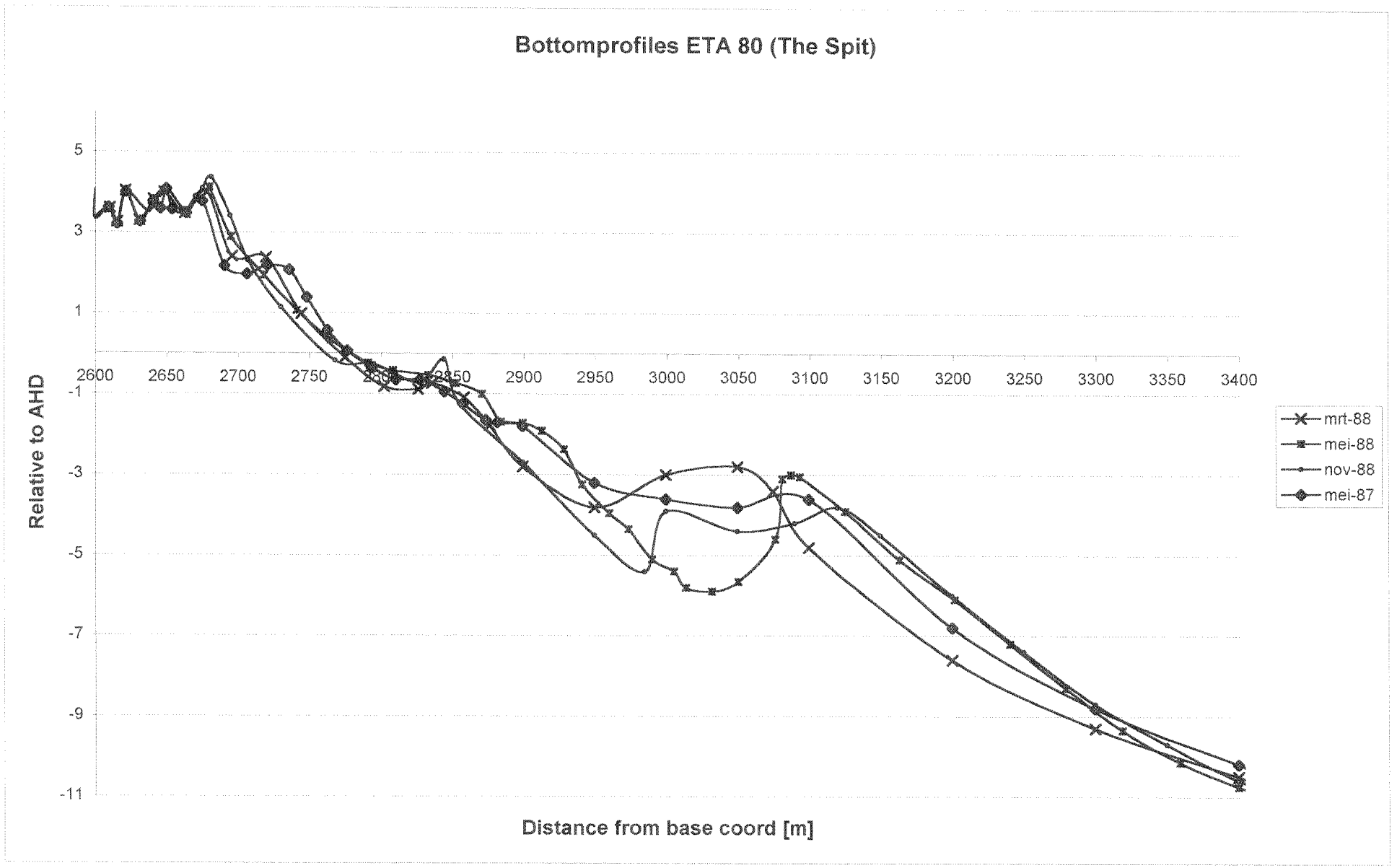
Bottomprofiles ETA 80 (The Spit)
Relative to AHD
5
3
1
-1
-3
-5
-7
-9
-11
2600
2650
2700
2750
2850
2900
2950
3000
3050
3100
3150
3200
3250
3300
3350
3400
Distance from base coord [m]
mrt-88
mei-88
nov-88
mei-87

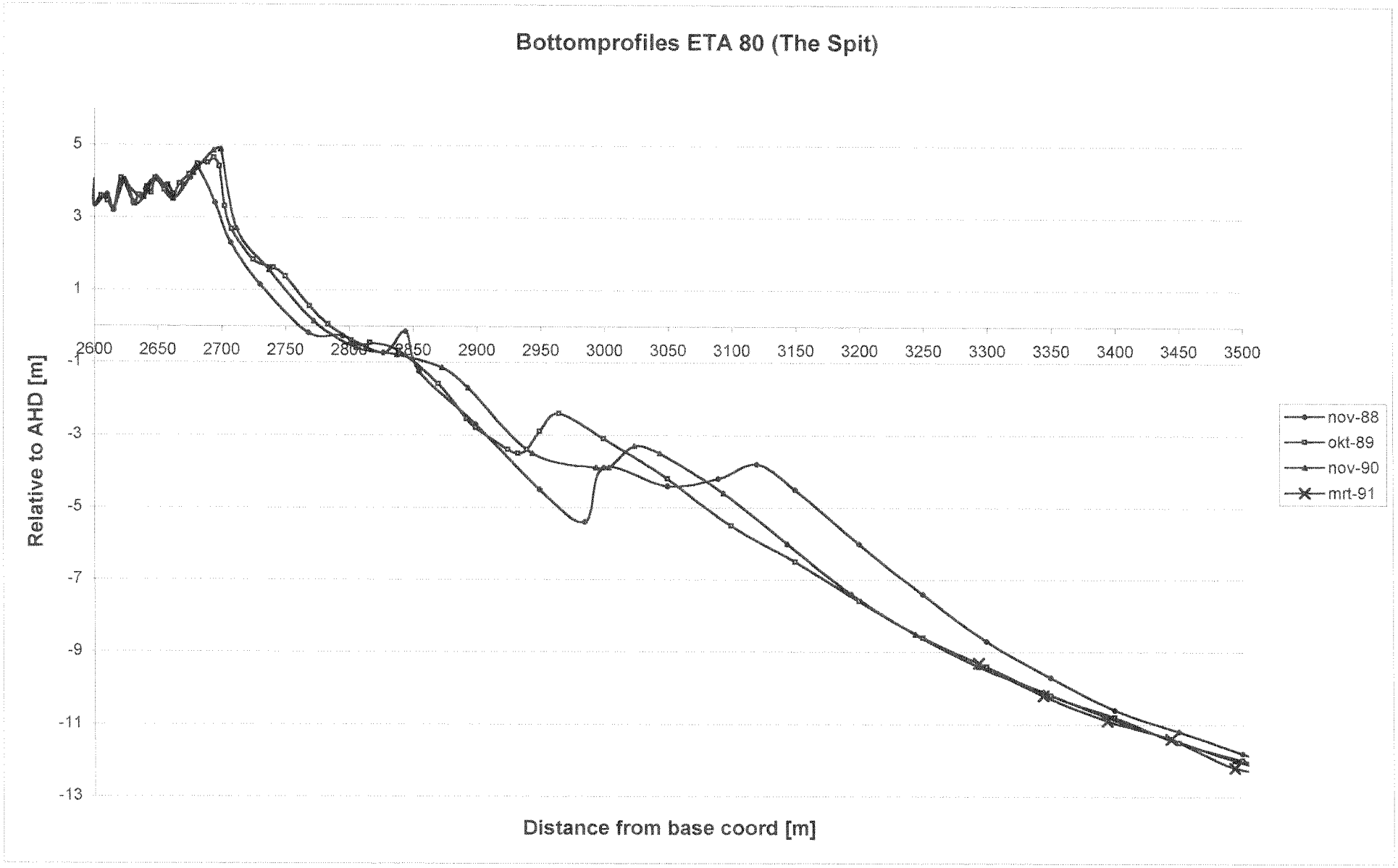
Bottomprofiles ETA 80 (The Spit)
Relative to AHD [m]
5
3
1
-1
-3
-5
-7
-9
-11
-13
2600
2650
2700
2750
2800
2850
2900
2950
3000
3050
3100
3150
3200
3250
3300
3350
3400
3450
3500
Distance from base coord [m]
nov-88
okt-89
nov-90
mrt-91

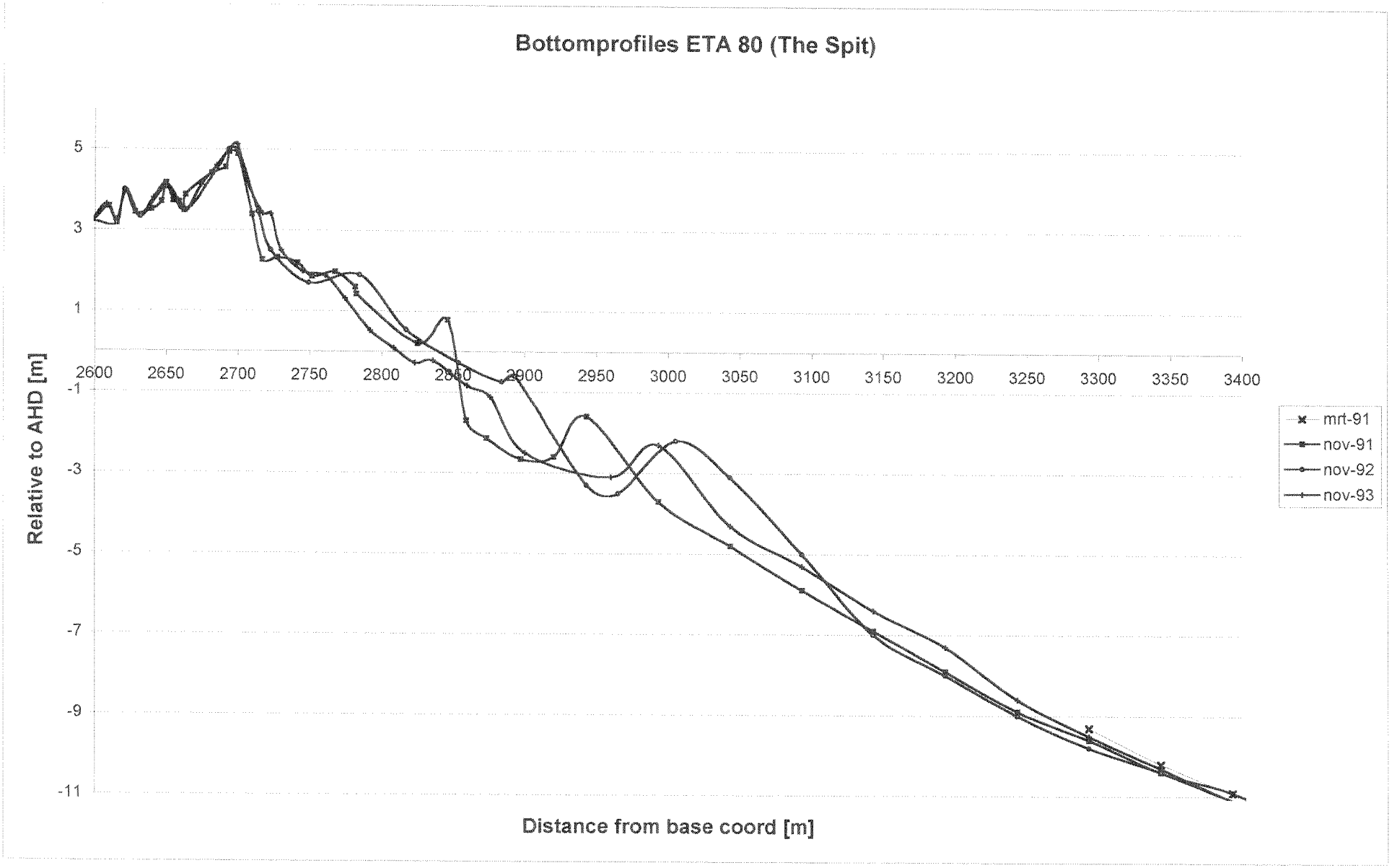
Bottomprofiles ETA 80 (The Spit)
Relative to AHD [m]
5
3
1
-1
-3
-5
-7
-9
-11
2600
2650
2700
2750
2800
2850
2900
2950
3000
3050
3100
3150
3200
3250
3300
3350
3400
Distance from base coord [m]
mrt-91
nov-91
nov-92
nov-93

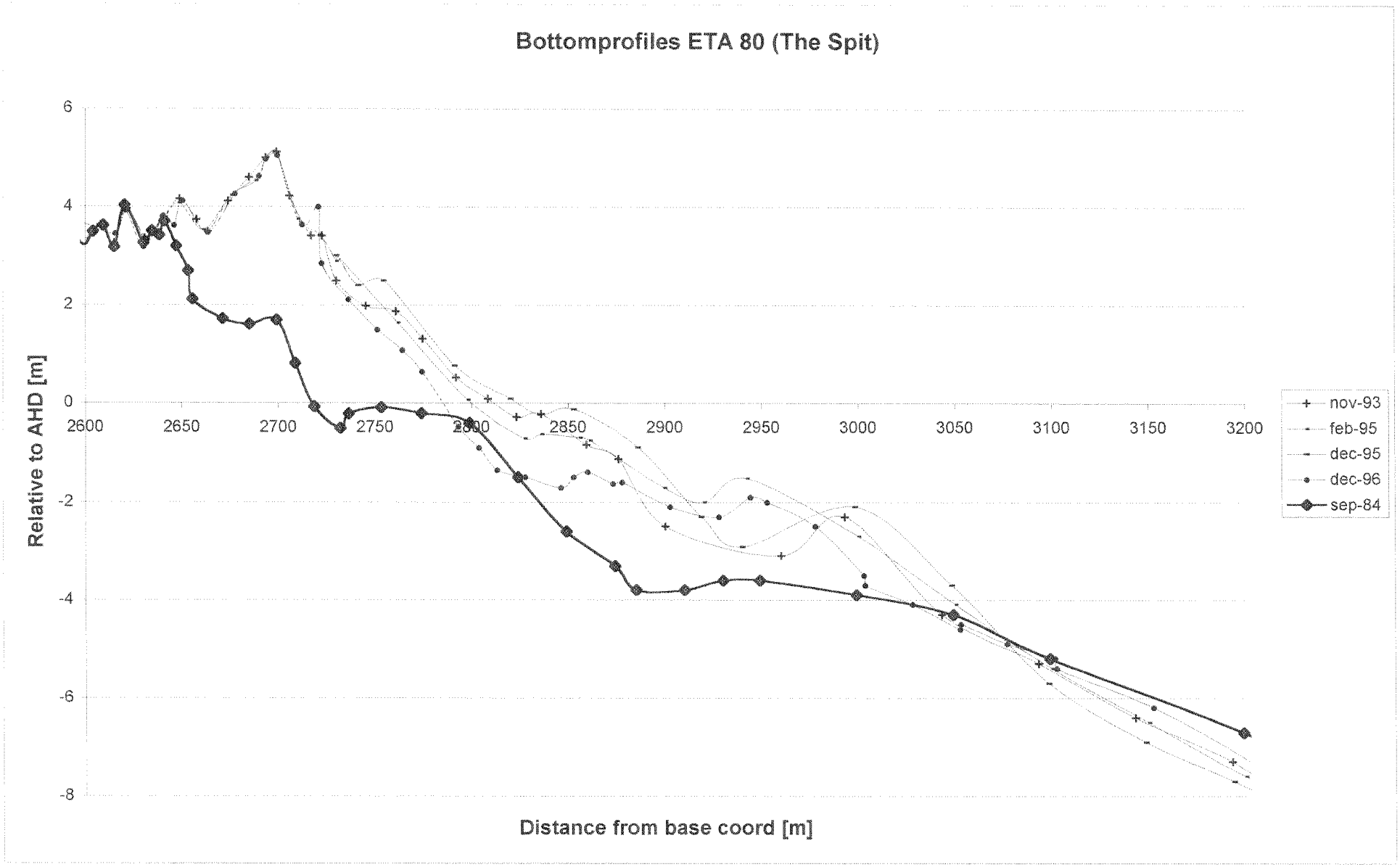
Bottomprofiles ETA 80 (The Spit)
Relative to AHD [m]
6
4
2
0
-2
-4
-6
-8
2600
2650
2700
2750
2800
2850
2900
2950
3000
3050
3100
3150
3200
Distance from base coord [m]
nov-93
feb-95
dec-95
dec-96
sep-84

Appendix J

(Bottom profiles ETA 80.8: Gold Coast Seaway ebb tidal delta)

(Number of pages: 6)

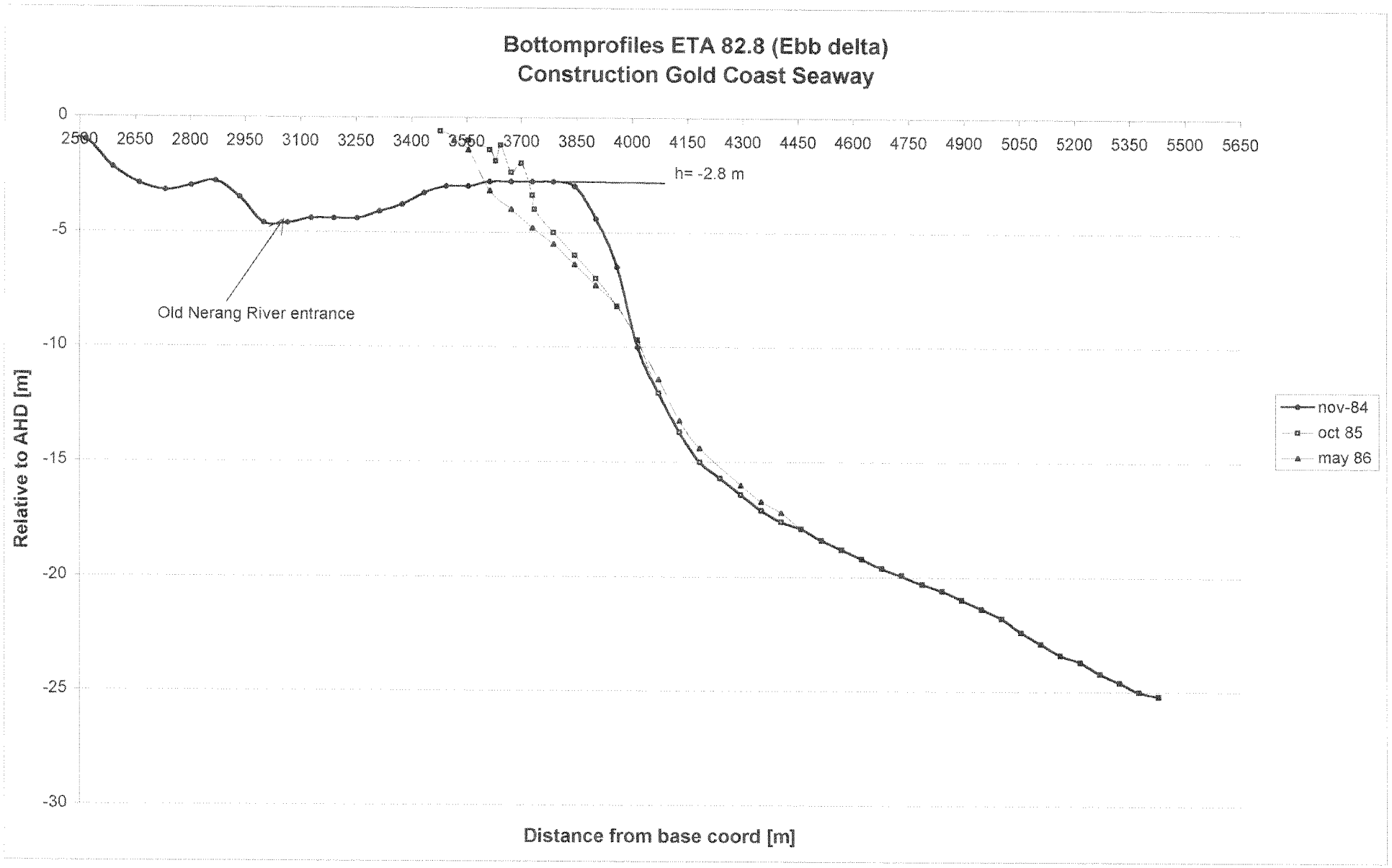
Bottomprofiles ETA 82.8 (Ebb delta)
Construction Gold Coast Seaway
0
-5
-10
-15
-20
-25
-30
2500 2650 2800 2950 3100 3250 3400 3550 3700 3850 4000 4150 4300 4450 4600 4750 4900 5050 5200 5350 5500 5650
h= -2.8 m
Old Nerang River entrance
Relative to AHD [m]
Distance from base coord [m]
nov-84
oct 85
may 86

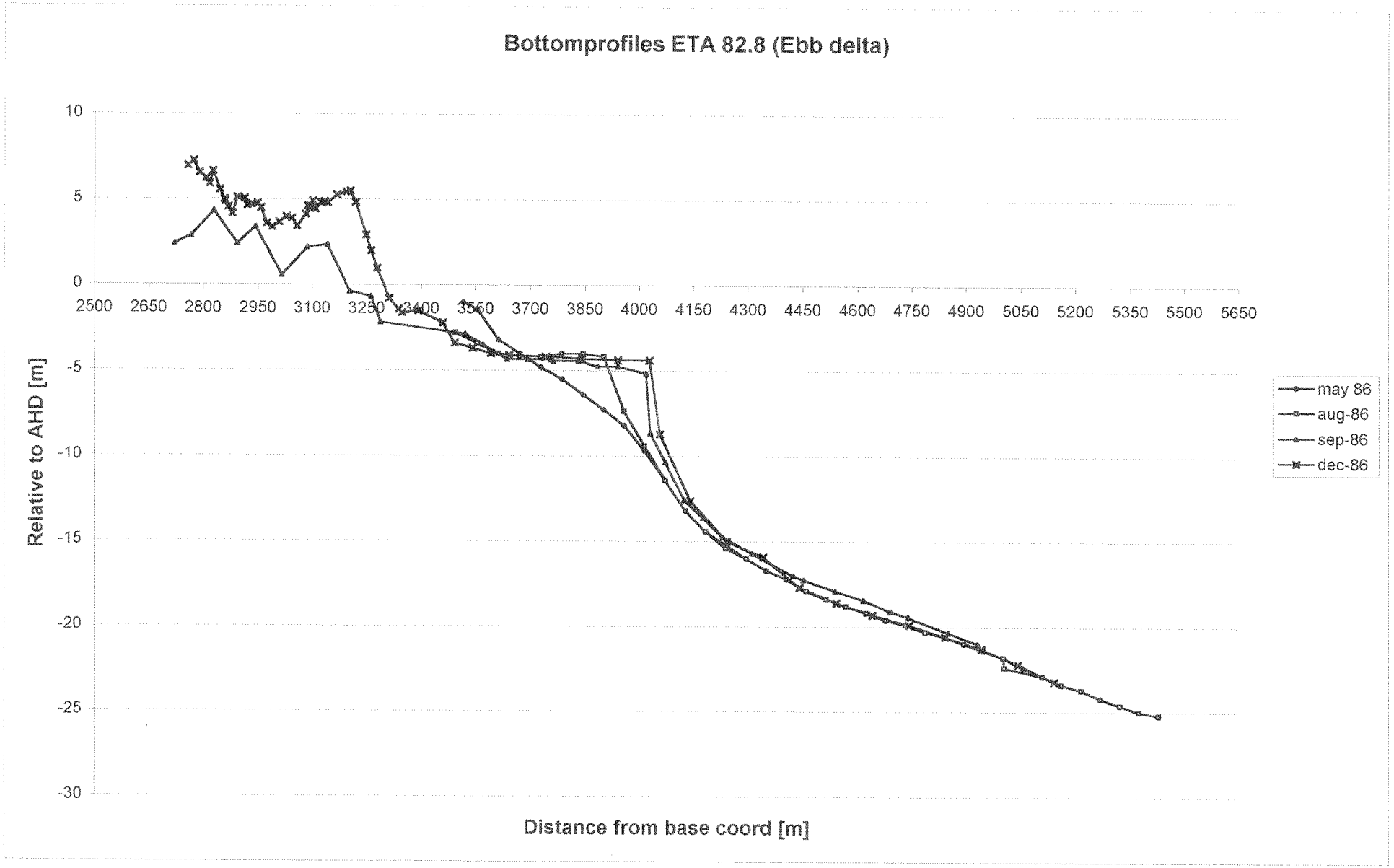
Bottomprofiles ETA 82.8 (Ebb delta)
Relative to AHD [m]
10
5
0
-5
-10
-15
-20
-25
-30
2500 2650 2800 2950 3100 3250 3400 3550 3700 3850 4000 4150 4300 4450 4600 4750 4900 5050 5200 5350 5500 5650
Distance from base coord [m]
may 86
aug-86
sep-86
dec-86

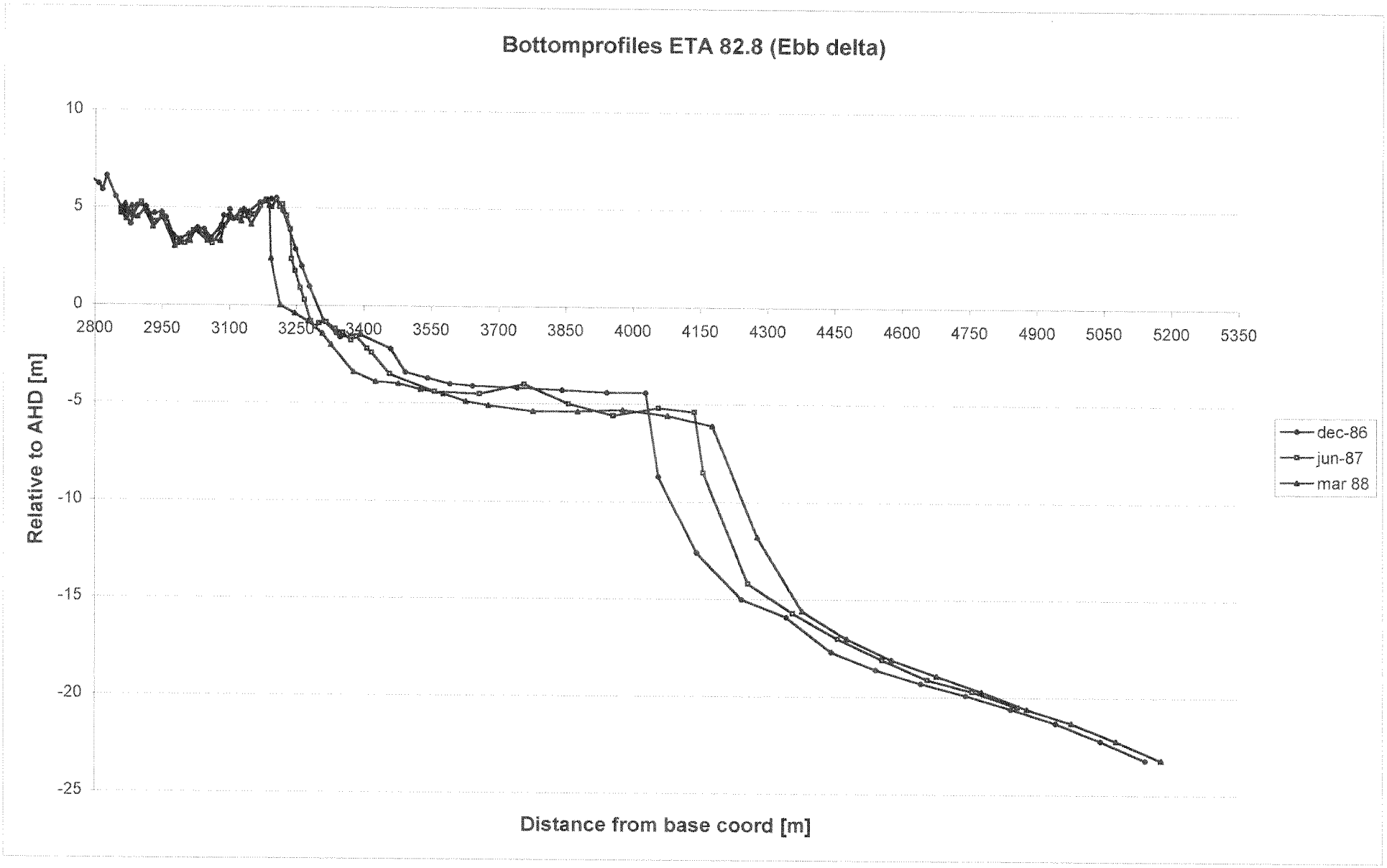
Bottomprofiles ETA 82.8 (Ebb delta)
Relative to AHD [m]
10
5
0
-5
-10
-15
-20
-25
2800
2950
3100
3250
3400
3550
3700
3850
4000
4150
4300
4450
4600
4750
4900
5050
5200
5350
Distance from base coord [m]
dec-86
jun-87
mar 88

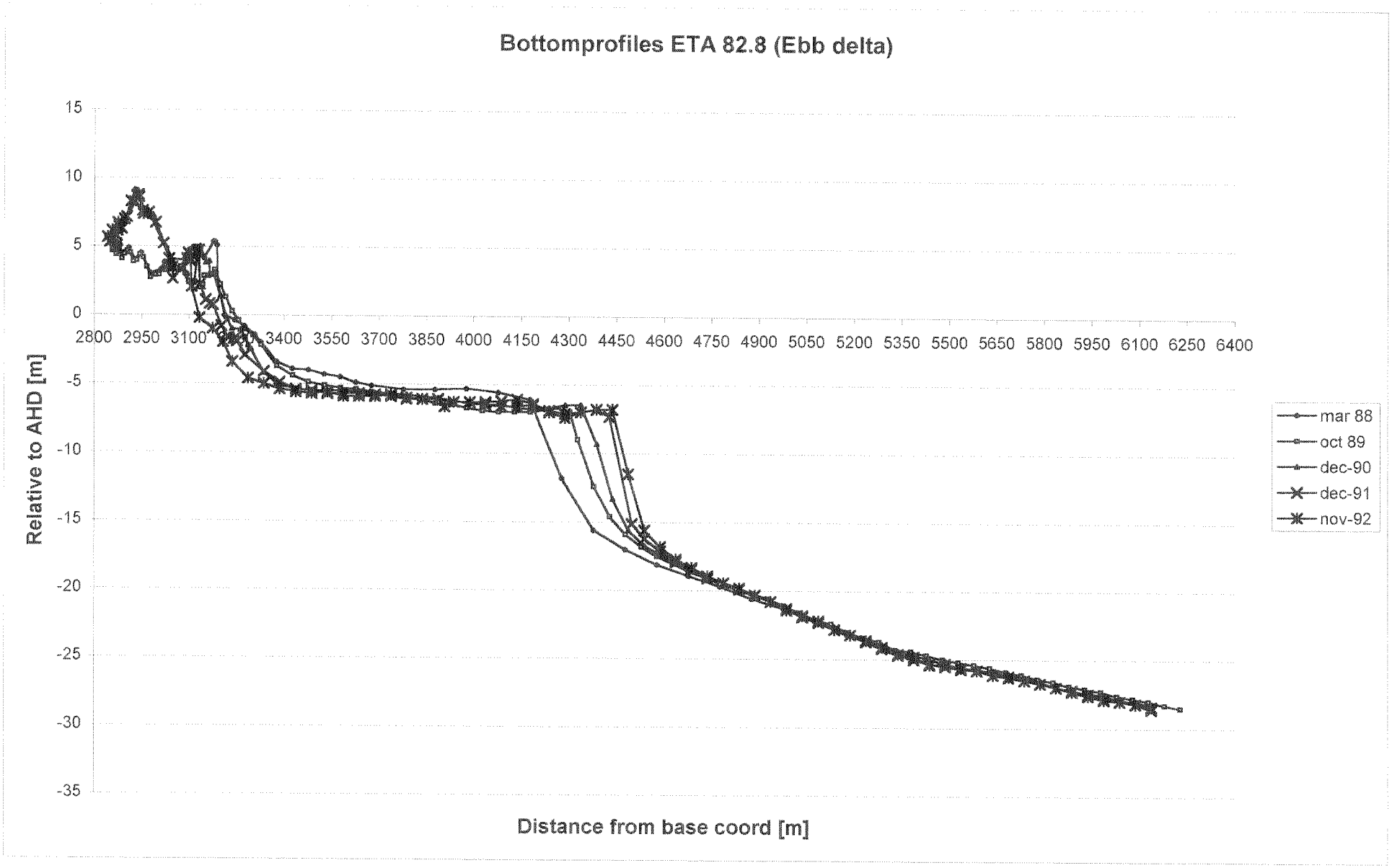
Bottomprofiles ETA 82.8 (Ebb delta)
Relative to AHD [m]
15
10
5
0
-5
-10
-15
-20
-25
-30
-35
2800 2950 3100 3400 3550 3700 3850 4000 4150 4300 4450 4600 4750 4900 5050 5200 5350 5500 5650 5800 5950 6100 6250 6400
Distance from base coord [m]
mar 88
oct 89
dec-90
dec-91
nov-92

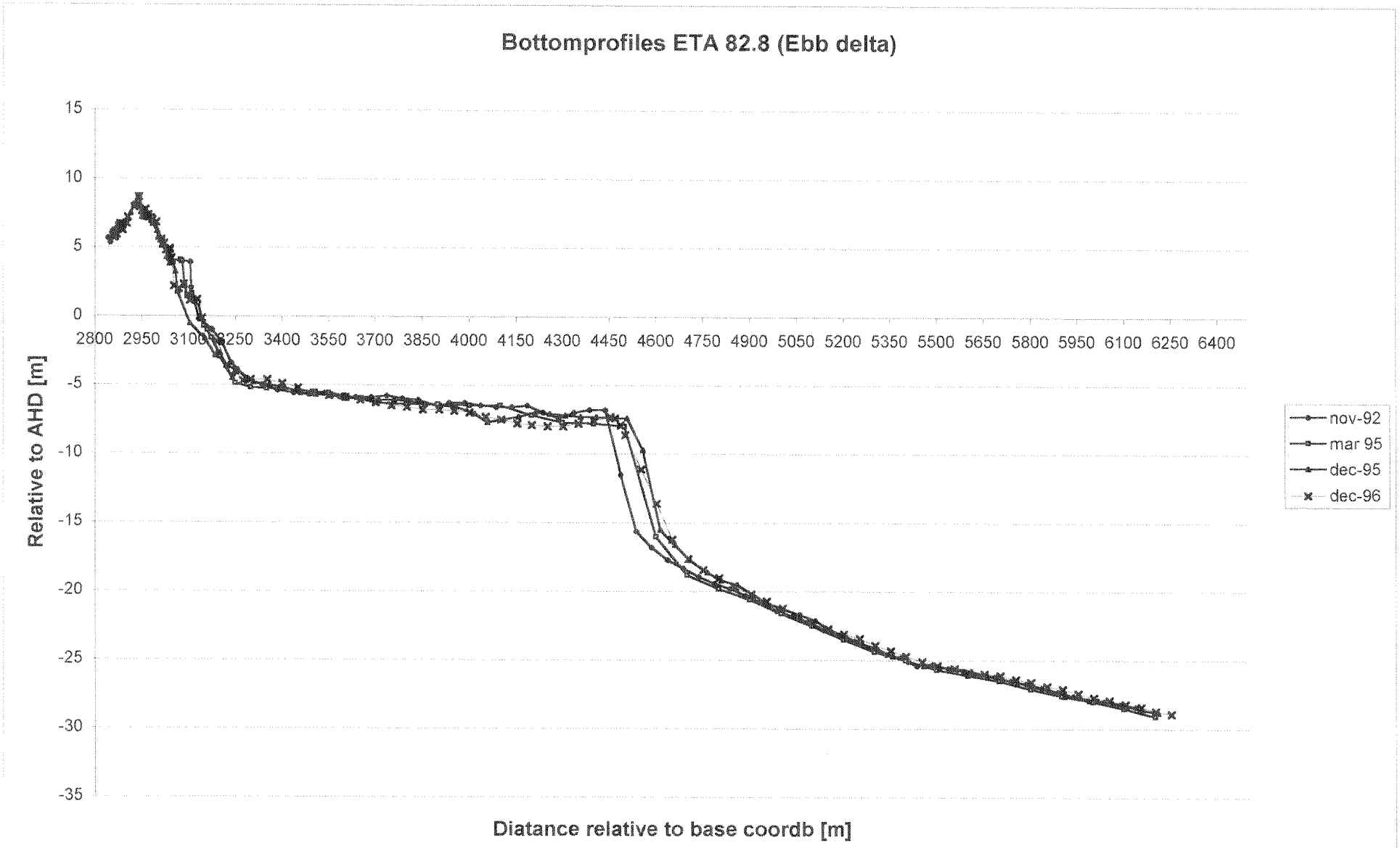
Bottomprofiles ETA 82.8 (Ebb delta)
15
10
5
0
-5
-10
-15
-20
-25
-30
-35
2800 2950 3100 3250 3400 3550 3700 3850 4000 4150 4300 4450 4600 4750 4900 5050 5200 5350 5500 5650 5800 5950 6100 6250 6400
Relative to AHD [m]
Diatance relative to base coordb [m]
nov-92
mar 95
dec-95
dec-96

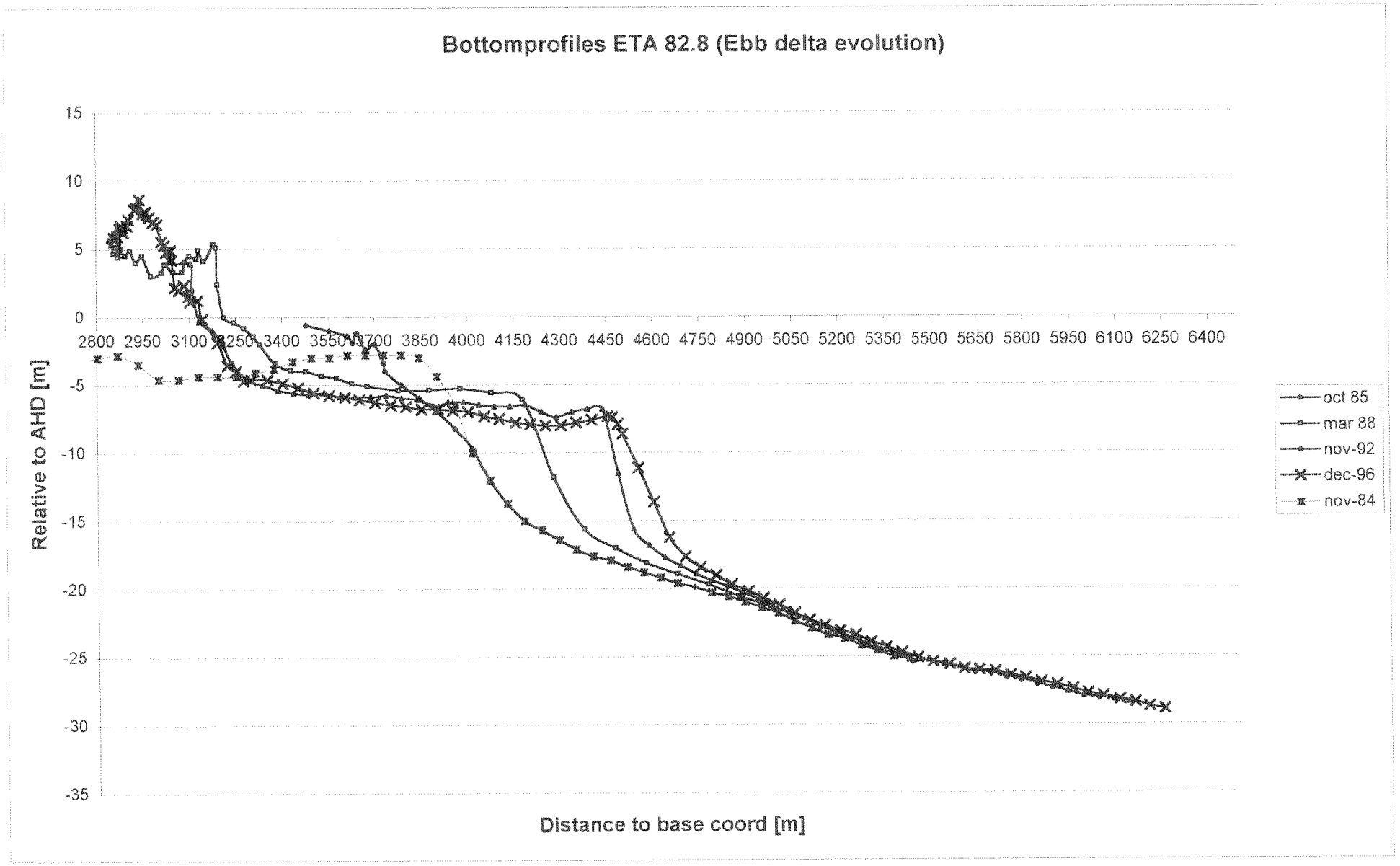
Bottomprofiles ETA 82.8 (Ebb delta evolution)
Relative to AHD [m]
15
10
5
0
-5
-10
-15
-20
-25
-30
-35
2800 2950 3100 3250 3400 3550 3700 3850 4000 4150 4300 4450 4600 4750 4900 5050 5200 5350 5500 5650 5800 5950 6100 6250 6400
Distance to base coord [m]
oct 85
mar 88
nov-92
dec-96
nov-84

Appendix K

(Bottom profiles ETA-84 Feeder beach)

(Number of pages: 8)

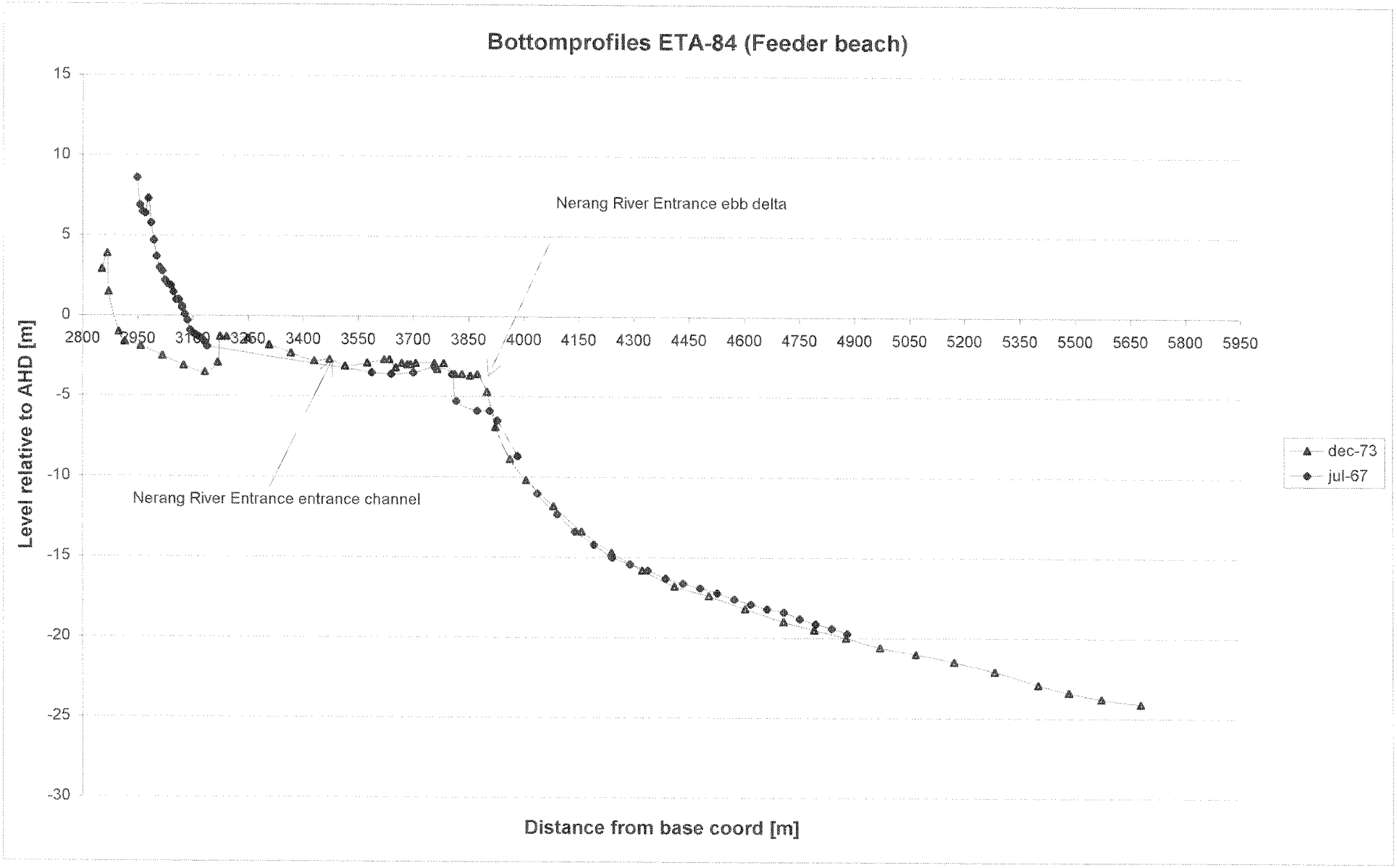
Bottomprofiles ETA-84 (Feeder beach)
Level relative to AHD [m]
15
10
5
0
-5
-10
-15
-20
-25
-30
2800
2950
3100
3250
3400
3550
3700
3850
4000
4150
4300
4450
4600
4750
4900
5050
5200
5350
5500
5650
5800
5950
Nerang River Entrance ebb delta
Nerang River Entrance entrance channel
dec-73
jul-67
Distance from base coord [m]

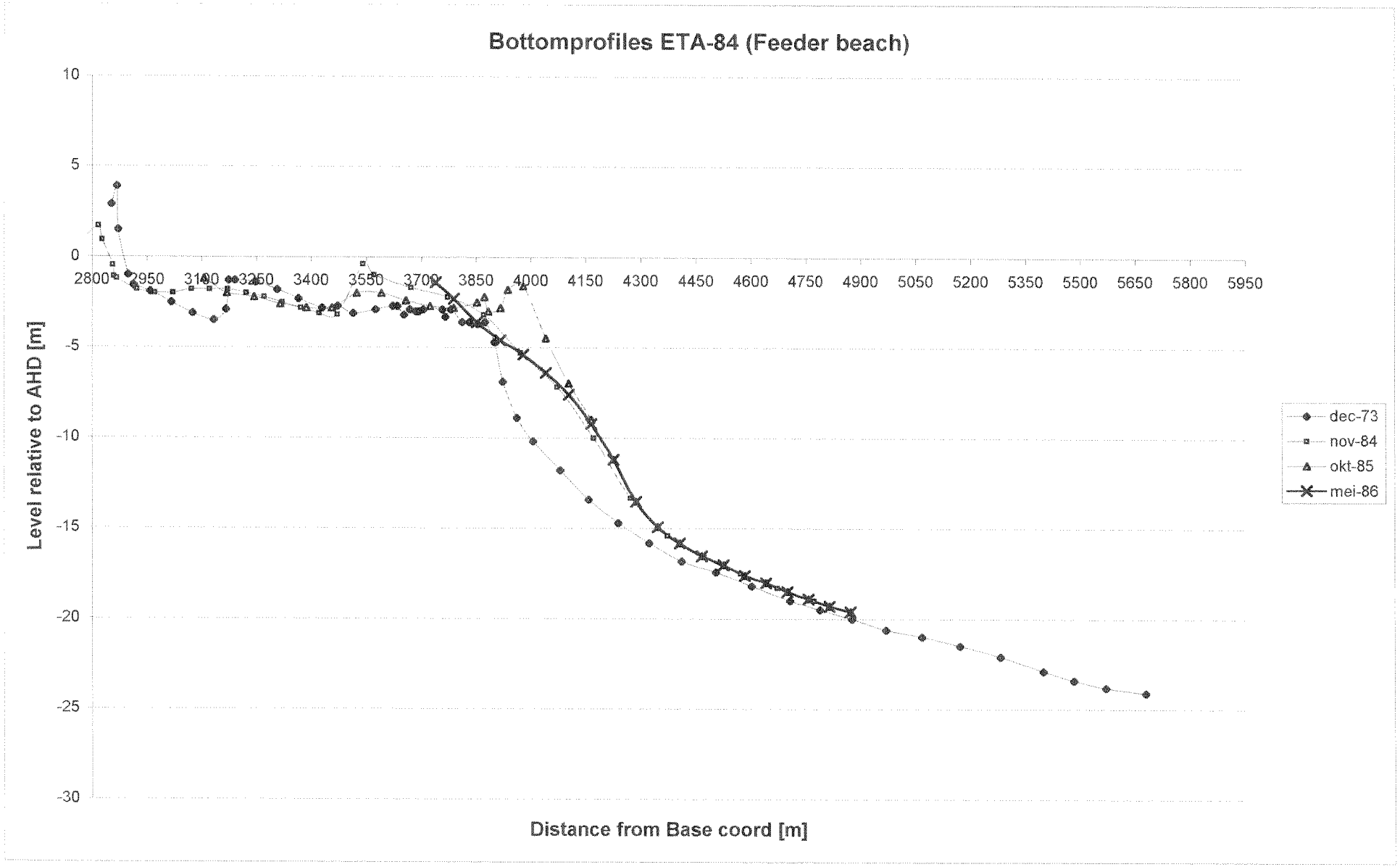
Bottomprofiles ETA-84 (Feeder beach)
Level relative to AHD [m]
10
5
0
-5
-10
-15
-20
-25
-30
2800
2950
3100
3250
3400
3550
3700
3850
4000
4150
4300
4450
4600
4750
4900
5050
5200
5350
5500
5650
5800
5950
Distance from Base coord [m]
dec-73
nov-84
okt-85
mei-86

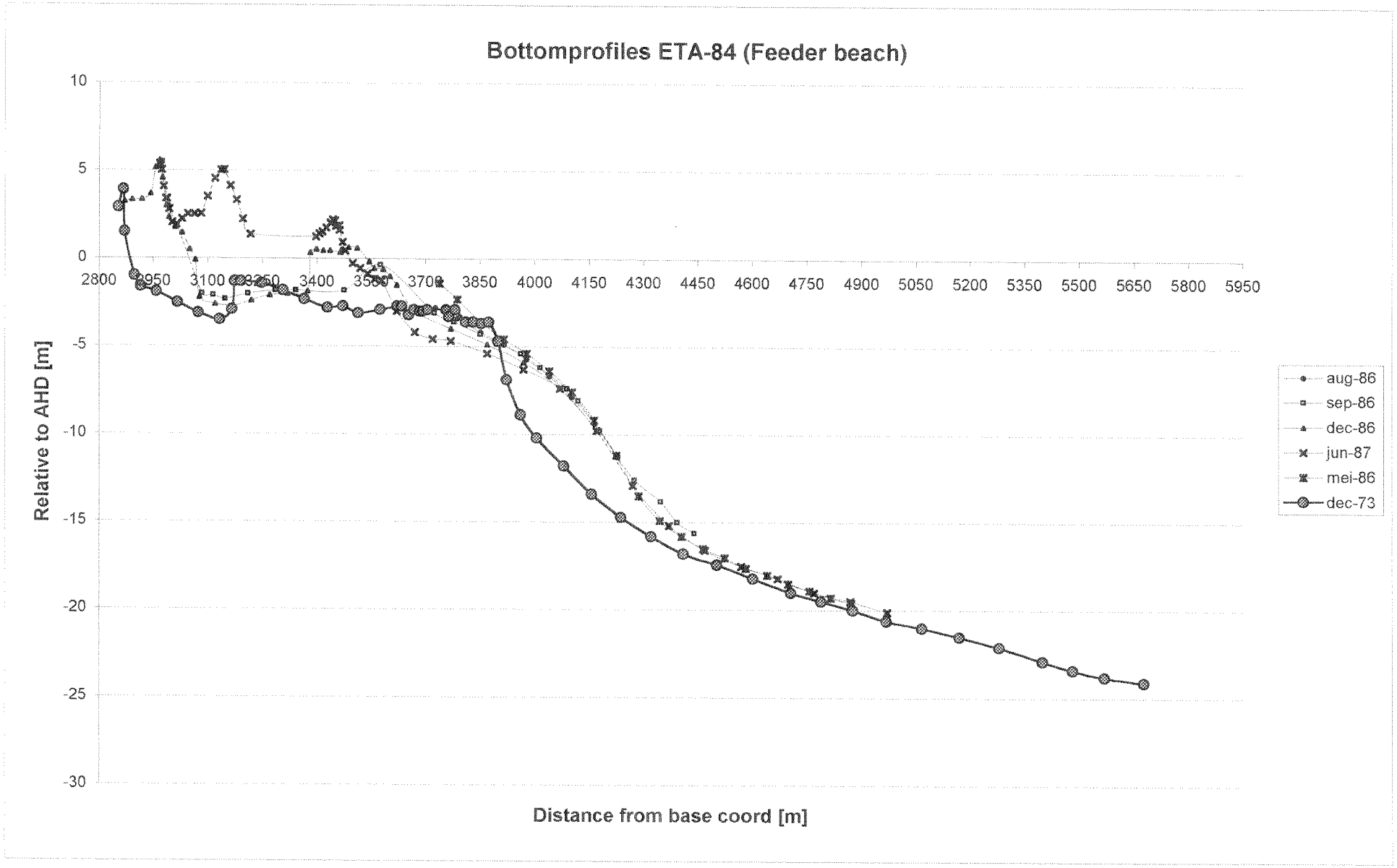
Bottomprofiles ETA-84 (Feeder beach)
Relative to AHD [m]
10
5
0
-5
-10
-15
-20
-25
-30
2800
2950
3100
3250
3400
3550
3700
3850
4000
4150
4300
4450
4600
4750
4900
5050
5200
5350
5500
5650
5800
5950
Distance from base coord [m]
aug-86
sep-86
dec-86
jun-87
mei-86
dec-73

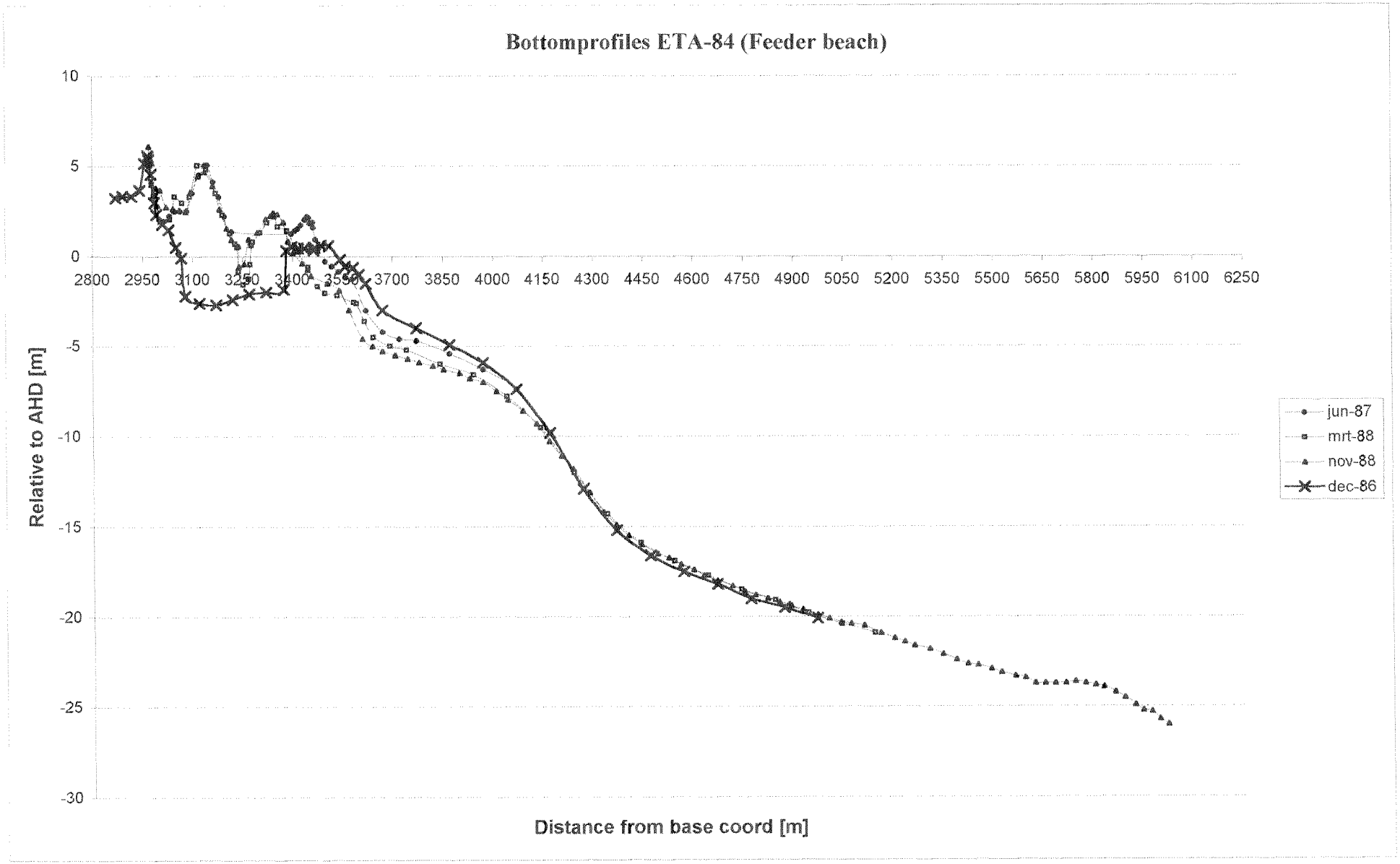
Bottomprofiles ETA-84 (Feeder beach)
Relative to AHD [m]
10
5
0
-5
-10
-15
-20
-25
-30
2800 2950 3100 3250 3400 3550 3700 3850 4000 4150 4300 4450 4600 4750 4900 5050 5200 5350 5500 5650 5800 5950 6100 6250
Distance from base coord [m]
jun-87
mrt-88
nov-88
dec-86

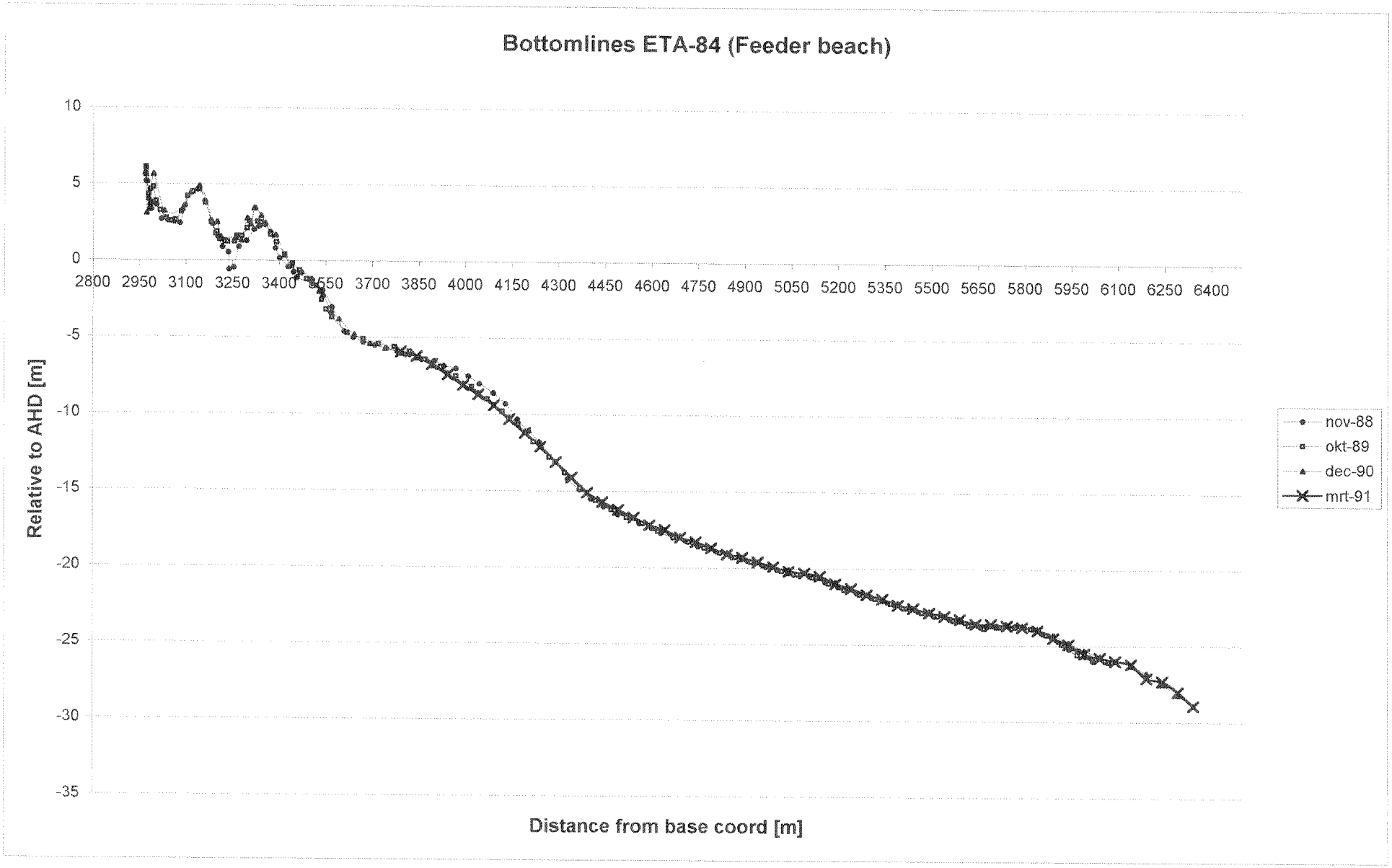
Bottomlines ETA-84 (Feeder beach)
Relative to AHD [m]
10
5
0
-5
-10
-15
-20
-25
-30
-35
2800 2950 3100 3250 3400 3550 3700 3850 4000 4150 4300 4450 4600 4750 4900 5050 5200 5350 5500 5650 5800 5950 6100 6250 6400
Distance from base coord [m]
nov-88
okt-89
dec-90
mrt-91

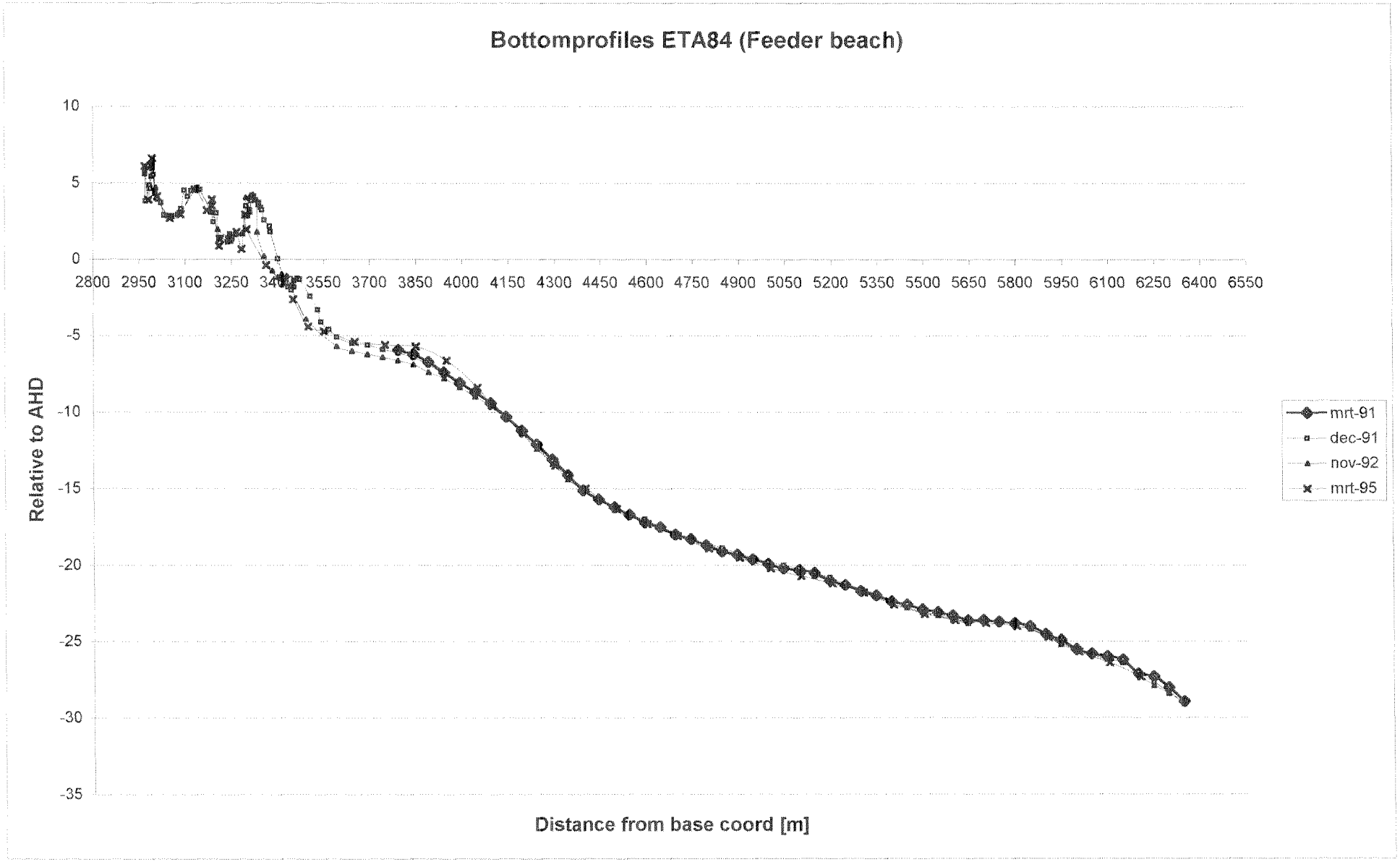
Bottomprofiles ETA84 (Feeder beach)
10
5
0
-5
-10
-15
-20
-25
-30
-35
2800 2950 3100 3250 3400 3550 3700 3850 4000 4150 4300 4450 4600 4750 4900 5050 5200 5350 5500 5650 5800 5950 6100 6250 6400 6550
Relative to AHD
Distance from base coord [m]
mrt-91
dec-91
nov-92
mrt-95

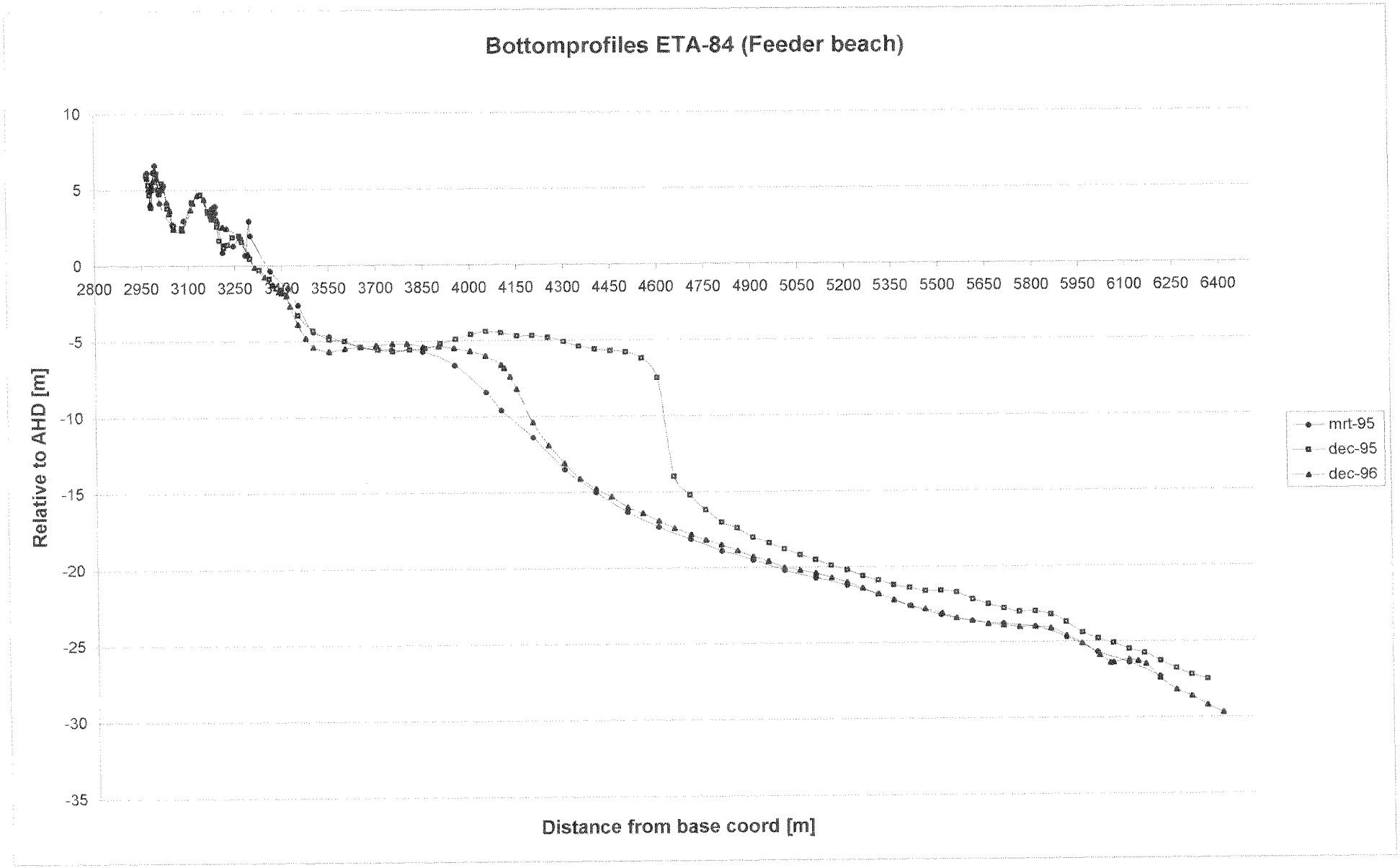
Bottomprofiles ETA-84 (Feeder beach)
Relative to AHD [m]
10
5
0
-5
-10
-15
-20
-25
-30
-35
2800 2950 3100 3250 3400 3550 3700 3850 4000 4150 4300 4450 4600 4750 4900 5050 5200 5350 5500 5650 5800 5950 6100 6250 6400
Distance from base coord [m]
mrt-95
dec-95
dec-96

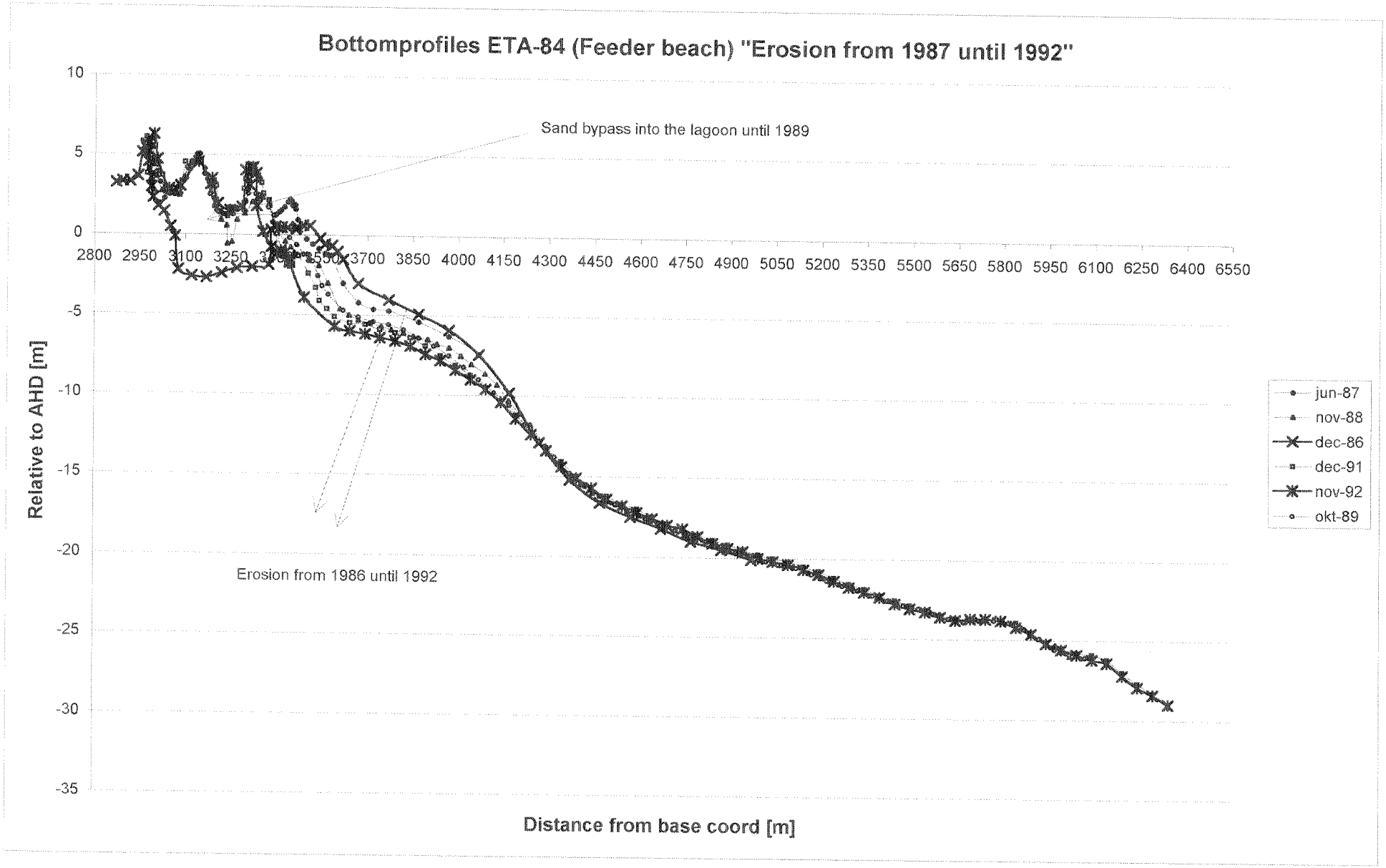
Bottomprofiles ETA-84 (Feeder beach) "Erosion from 1987 until 1992"
Sand bypass into the lagoon until 1989
Erosion from 1986 until 1992
Relative to AHD [m]
Distance from base coord [m]
10
5
0
-5
-10
-15
-20
-25
-30
-35
2800 2950 3100 3250 3700 3850 4000 4150 4300 4450 4600 4750 4900 5050 5200 5350 5500 5650 5800 5950 6100 6250 6400 6550
jun-87
nov-88
dec-86
dec-91
nov-92
okt-89

Appendix L

(Bottom profiles ETA-82.8: location north side feeder beach)

(Number of pages: 6)

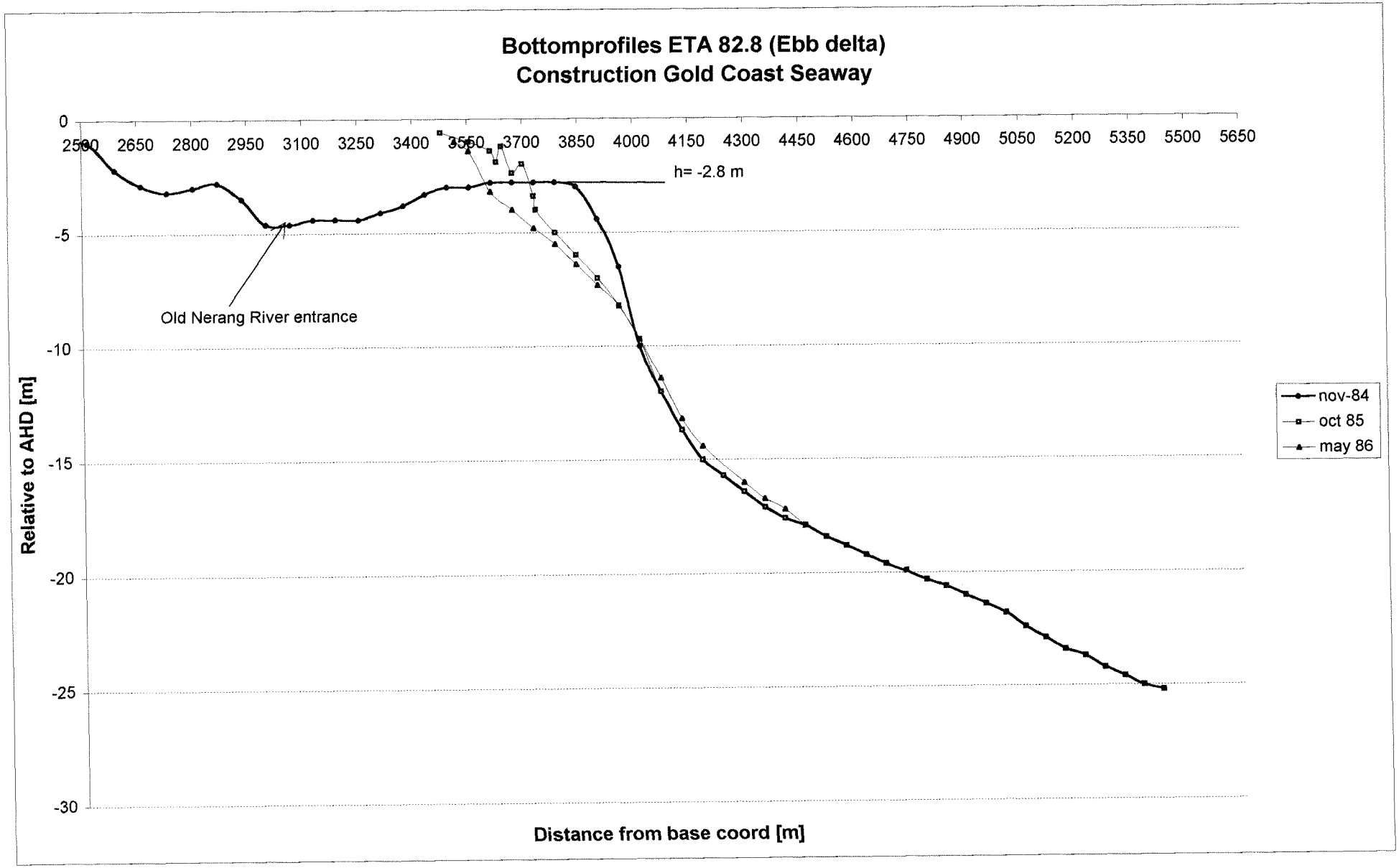
Bottomprofiles ETA 82.8 (Ebb delta)
Construction Gold Coast Seaway
0
-5
-10
-15
-20
-25
-30
2500
2650
2800
2950
3100
3250
3400
3550
3700
3850
4000
4150
4300
4450
4600
4750
4900
5050
5200
5350
5500
5650
h= -2.8 m
Old Nerang River entrance
Relative to AHD [m]
Distance from base coord [m]
nov-84
oct 85
may 86

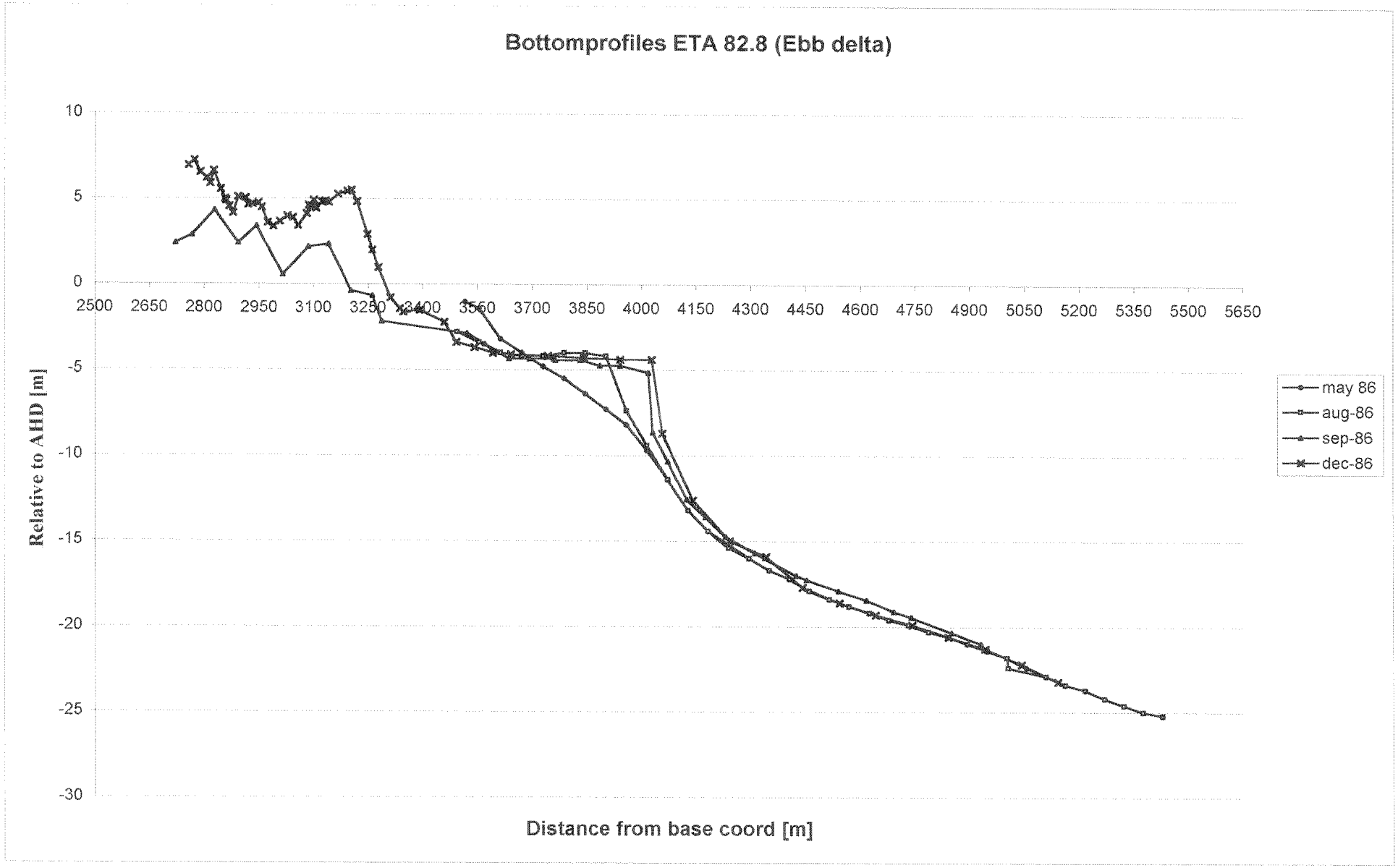
Bottomprofiles ETA 82.8 (Ebb delta)
Relative to AHD [m]
10
5
0
-5
-10
-15
-20
-25
-30
2500
2650
2800
2950
3100
3250
3400
3550
3700
3850
4000
4150
4300
4450
4600
4750
4900
5050
5200
5350
5500
5650
Distance from base coord [m]
may 86
aug-86
sep-86
dec-86

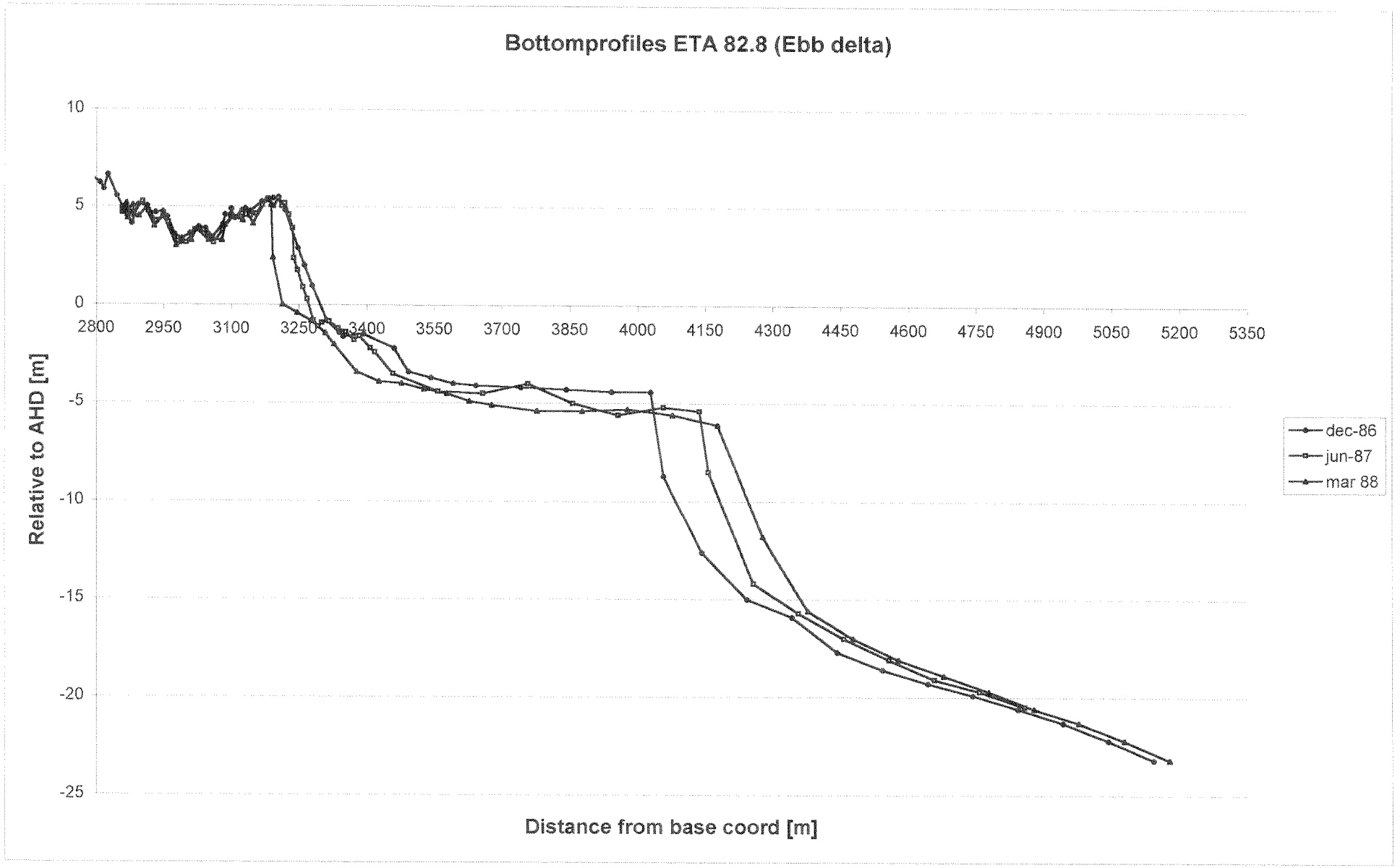
Bottomprofiles ETA 82.8 (Ebb delta)
Relative to AHD [m]
10
5
0
-5
-10
-15
-20
-25
2800
2950
3100
3250
3400
3550
3700
3850
4000
4150
4300
4450
4600
4750
4900
5050
5200
5350
Distance from base coord [m]
dec-86
jun-87
mar 88

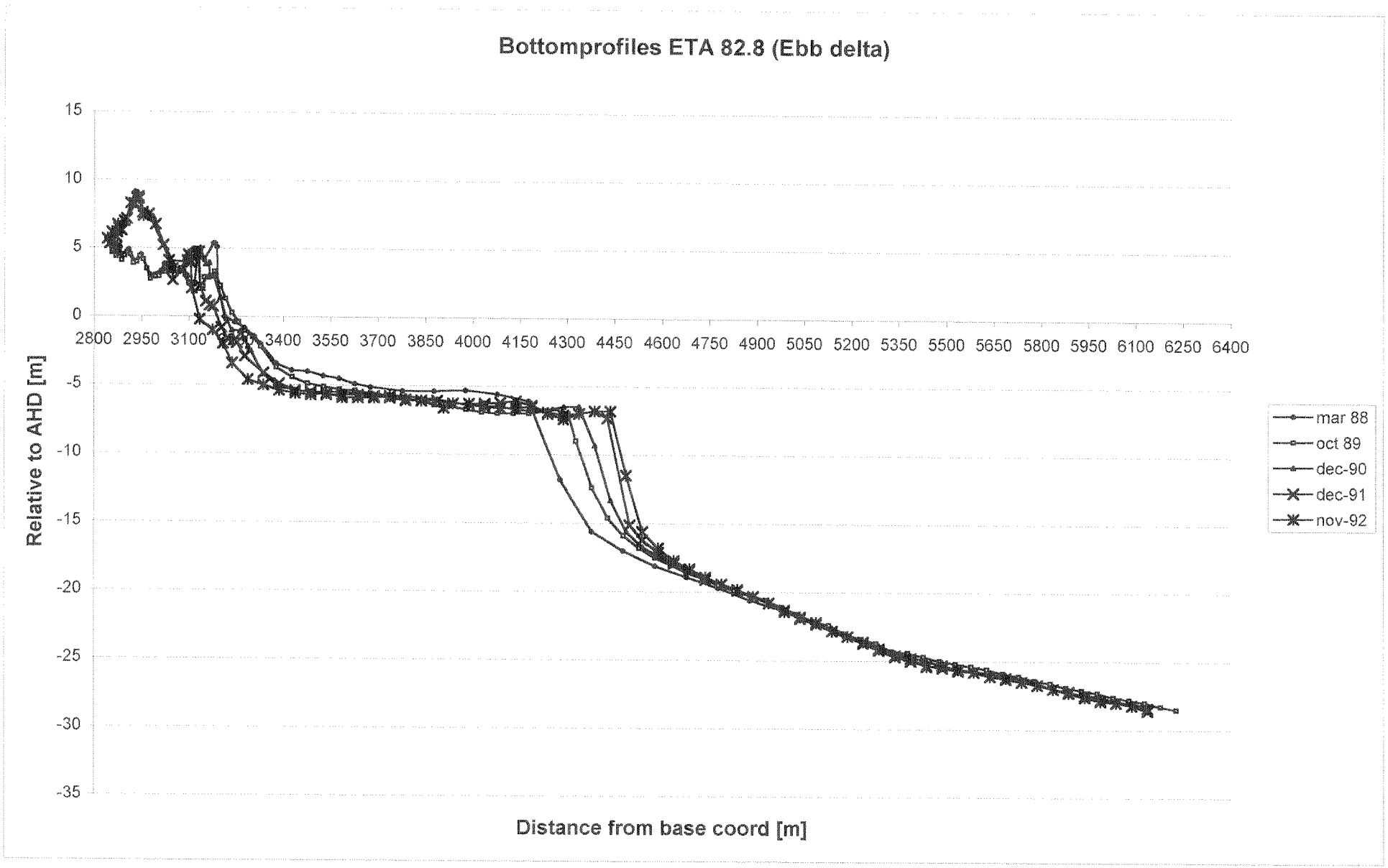
Bottomprofiles ETA 82.8 (Ebb delta)
Relative to AHD [m]
15
10
5
0
-5
-10
-15
-20
-25
-30
-35
2800 2950 3100 3400 3550 3700 3850 4000 4150 4300 4450 4600 4750 4900 5050 5200 5350 5500 5650 5800 5950 6100 6250 6400
Distance from base coord [m]
mar 88
oct 89
dec-90
dec-91
nov-92

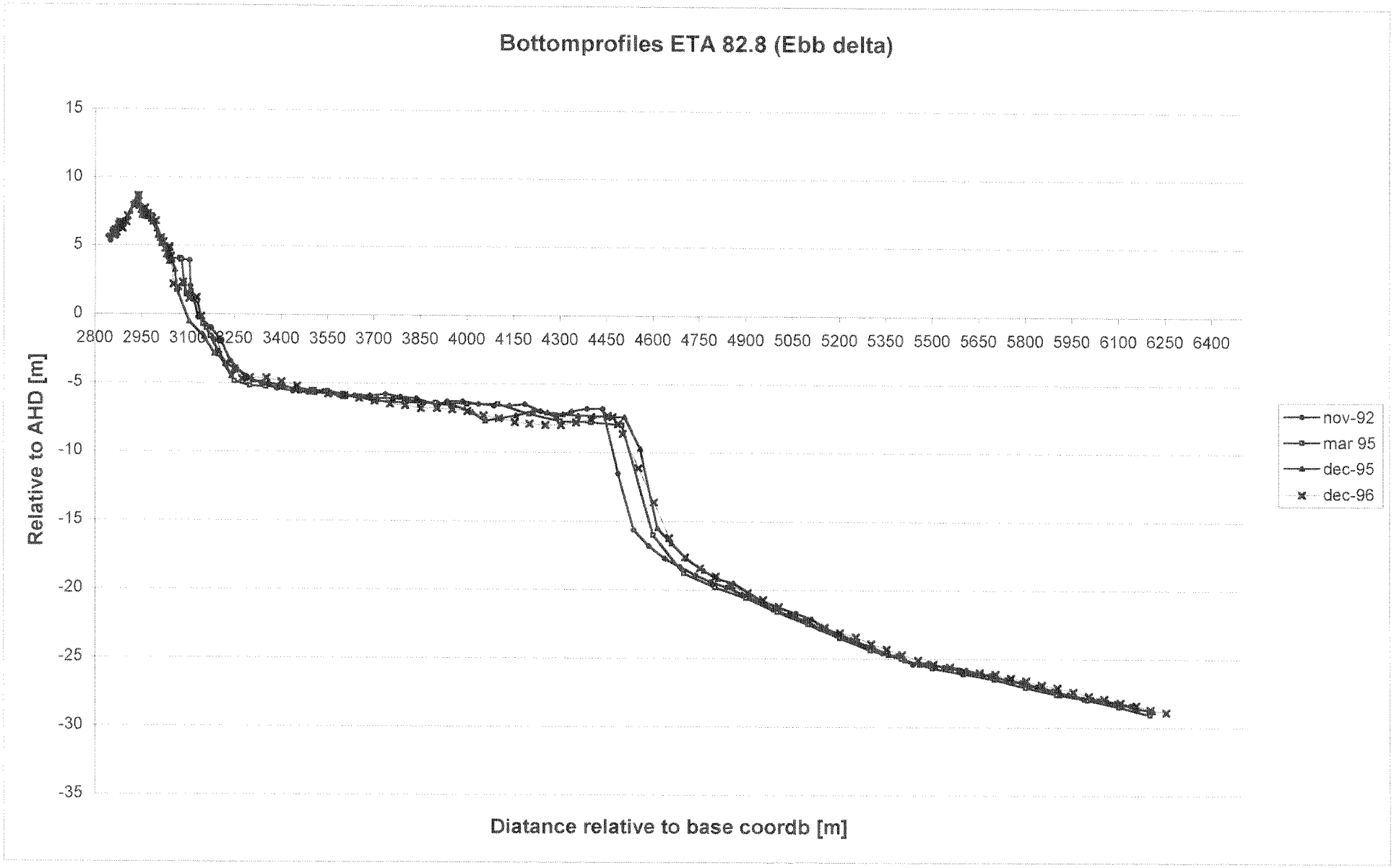
Bottomprofiles ETA 82.8 (Ebb delta)
Relative to AHD [m]
15
10
5
0
-5
-10
-15
-20
-25
-30
-35
2800 2950 3100 3250 3400 3550 3700 3850 4000 4150 4300 4450 4600 4750 4900 5050 5200 5350 5500 5650 5800 5950 6100 6250 6400
Diatance relative to base coordb [m]
nov-92
mar 95
dec-95
dec-96

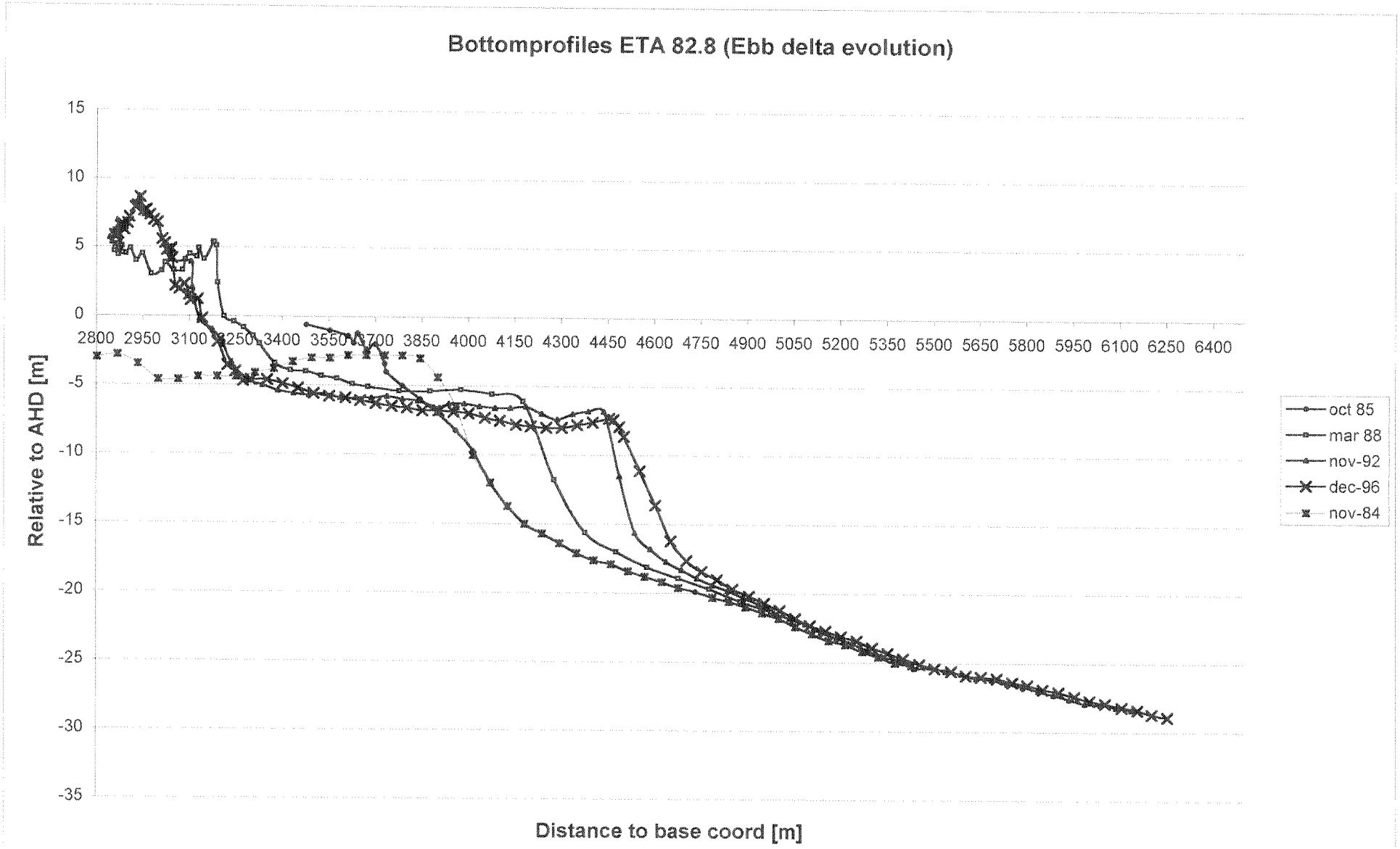
Bottomprofiles ETA 82.8 (Ebb delta evolution)
Relative to AHD [m]
15
10
5
0
-5
-10
-15
-20
-25
-30
-35
2800 2950 3100 3250 3400 3550 3700 3850 4000 4150 4300 4450 4600 4750 4900 5050 5200 5350 5500 5650 5800 5950 6100 6250 6400
Distance to base coord [m]
oct 85
mar 88
nov-92
dec-96
nov-84